

A SEQUENCE STRATIGRAPHIC APPROACH
TO THE DEPOSITIONAL HISTORY ANALYSIS OF
THE UPPER EOCENE SEDIMENTARY SUCCESSION,
NORTHWEST OF THE THRACE BASIN, TURKEY

A THESIS SUBMITTED TO
THE GRADUATE SCHOOL OF NATURAL AND APPLIED SCIENCES
OF
MIDDLE EAST TECHNICAL UNIVERSITY

BY

MEHMET AKİF SÜNNETÇİOĞLU

IN PARTIAL FULFILLMENT OF THE REQUIREMENTS
FOR
THE DEGREE OF DOCTOR OF PHILOSOPHY
IN
GEOLOGICAL ENGINEERING

FEBRUARY 2008

Approval of the thesis:

A SEQUENCE STRATIGRAPHIC APPROACH TO THE DEPOSITIONAL HISTORY ANALYSIS OF THE UPPER EOCENE SEDIMENTARY SUCCESSION, NORTHWEST OF THE THRACE BASIN, TURKEY

submitted by **MEHMET AKİF SÜNNETÇİOĞLU** in partial fulfillment of the requirements for the degree of **Doctor of Philosophy in Geological Engineering Department, Middle East Technical University** by,

Prof. Dr. Canan Özgen
Dean, Graduate School of **Natural and Applied Sciences** _____

Prof. Dr. Vedat Doyuran
Head of Department, **Geological Engineering** _____

Prof. Dr. Demir Altınır
Supervisor, **Geological Engineering Dept., METU** _____

Examining Committee Members:

Prof Dr. Ali Koçyiğit
Geological Engineering Dept., METU _____

Prof. Dr. Demir Altınır
Geological Engineering Dept., METU _____

Prof. Dr. Berkan Ecevitoğlu
Geophysical Engineering Dept., Ankara Univ. _____

Assoc. Prof. Dr. Bora Rojay
Geological Engineering Dept., METU _____

Assist. Prof. Dr. Ömer Yılmaz
Geological Engineering Dept., METU _____

Date: 07.02.2008

I hereby declare that all information in this document has been obtained and presented in accordance with academic rules and ethical conduct. I also declare that, as required by these rules and conduct, I have fully cited and referenced all material and results that are not original to this work.

Name, Last name: MEHMET AKİF SÜNNETÇİOĞLU

Signature :

ABSTRACT

A SEQUENCE STRATIGRAPHIC APPROACH TO THE DEPOSITIONAL HISTORY ANALYSIS OF THE UPPER EOCENE SEDIMENTARY SUCCESSION, NORTHWEST OF THE THRACE BASIN, TURKEY

SÜNNETÇİOĞLU, Mehmet Akif

Ph.D., Department of Geological Engineering

Supervisor: Prof. Dr. Demir Altıner

February 2008, 262 pages

This study investigates the depositional history of the Late Eocene sedimentary record in the northwest of the Thrace Basin in a sequence stratigraphic approach and estimates the contribution of regional tectonics, basin physiography and eustasy.

Late Eocene sedimentary succession was analyzed in two third-order sequences based on two major data sets; seismic reflection and well data sets. Depositional Sequence-1, represented by progradational stacking patterns, comprises the coarse-grained "Hamitabat" turbidite system. The base of the Sequence-1 was defined as the base of channel fill deposits in the northern shelf setting and the base of slope fan deposits in the slope setting. This boundary separates Lower-Middle and Upper Eocene

sediments. In the slope setting, the “Hamitabat” turbidite system was analyzed in three major depocenters; Western, Northwestern and Northeastern depocenters respectively.

“Hamitabat” turbidite system was controlled by the interaction of regional tectonics, basin physiography and eustatic fluctuations in the Late Eocene. This study highlighted the role of the regional variables; tectonic influence and basin morphology on the submarine canyon formation. The facies distribution was controlled by the high subsidence rate of sea-floor dominantly instead of eustasy.

Depositional Sequence-2, represented by mostly retrogradational stacking patterns, is a clastic-carbonate mixed system. Depositional Sequence-2 was subdivided into three higher-order sequences. The lower sequence boundaries were induced by the rapid relative sea-level rise. The upper boundary of the Depositional Sequence-2 was defined as the termination of clastic-carbonate mixed system and a candidate for the Eocene-Oligocene contact.

Key words: The Thrace Basin, slope fans, sequence stratigraphy, clastic-carbonate mixed system, retrogradation.

ÖZ

ÜST EOSEN YAŞLI SEDİMAN TOPLULUĞUNUN İSTİF STRATİGRAFI YAKLAŞIMI İLE ÇÖKELİM TARİHÇESİ ANALİZİ KUZEYBATI TRAKYA, TÜRKİYE

SÜNNETÇİOĞLU, Mehmet Akif

Doktora, Jeoloji Mühendisliği Anabilim Dalı

Tez Yöneticisi: Prof. Dr. Demir Altınır

Şubat 2008, 262 pages

Trakya Havzası'nın kuzeybatısında, üst Eosen yaşlı sedimanter kayaların çökelim tarihçesi ve bölgesel tektonizma, havza fizyografisi, global deniz seviyesi gibi değişkenlerin sedimanter kayda olan etkileri istif stratigrafi yaklaşımı ile incelenmiştir.

Üst Eosen yaşlı sedimanter istif, sismik ve kuyu veri setleri kullanılarak iki farklı üçüncü dereceden istife bölünerek incelenmiştir. Çökelim istifi-1 havzaya doğru ilerleyen fasiyesleri ile, kaba taneli "Hamitabat" turbidit sistemini ve onun karasal eşleniklerini kapsamaktadır. Çökelim istifi-1'in alt sınırı kuzeydeki şelf alanında kanal dolgusu çökellerinin tabanı, yamaç ortamında ise yamaç çökellerinin tabanı olarak belirlenmiştir. Bu seviye Alt-Orta Eosen çökelleri ile Üst Eosen çökellerini ayırmaktadır.

Yamaç çökelim ortamında, “Hamitabat” turbidit sistemi batı, kuzeybatı ve kuzeydoğu olmak üzere üç ana depolanma merkezinde incelenmiştir.

Bu çalışma “Hamitabat” turbidit sisteminin Geç Eosen’deki bölgesel tektonik, basen fizyografisi ve global deniz seviyesindeki değişimlerin karşılıklı etkileşimleri sonucu kontrol edildiğini kanıtlamıştır. Tektonik kontrollü denizaltı kanyon gelişimi, güneydoğu-kuzeybatı doğrultulu temel ilişkili normal faylar ve normal faylarla ilişkili kalınlık değişimleri bu dönemdeki fasiyes dağılımının global deniz seviyesindeki değişimler yerine basendeki yüksek çökme miktarı ile kontrol edildiğine işaret etmektedir.

Çökelim istifi-2 karaya doğru gerileyen fasiyesleri ile kırıntılı-karbonat karışık bir istiften oluşmaktadır. Bu sistem daha yüksek dereceli (dördüncü veya beşinci) üç farklı sekansa bölünmüştür. Sekansların alt sınırları göreceli deniz seviyesindeki hızlı yükselme ile tetiklenmiş olan transgresif çökellerin tabanı olarak belirlenmiştir. Çökelim istifi-2’nin üst sınırı kırıntılı-karbonat karışık sistemin sona ermesi ve muhtemel Eosen-Oligosen sınırı olarak belirlenmiştir.

Anahtar kelimeler: Trakya Havzası, yamaç çökelleri, istif stratigrafisi, kırıntılı-karbonat istif, retrogradasyon.

ACKNOWLEDGEMENTS

First of all, I would like to express my gratitude to my adviser, Prof. Dr. Demir Altınar and the committee members; Prof. Dr. Ali Koçyiğit, Prof. Dr. Berkan Ecevitöğlü, Assoc. Prof. Dr. Bora Rojay and Assist. Prof. Dr. Ömer Yılmaz for their contribution and support.

The data base of the study was supported by Turkish Petroleum Corporation. I am grateful to TPAO, Exploration Group Management for giving me the great opportunity to accomplish the thesis.

I owe special thanks to Kerem Ali Bürkan for the field trip, which can not be accomplished without his guidance and Muzaffer Siyako for his permanent advising.

I would specifically like to thank my friends and colleagues Zeynep Elif Yıldız, Özgür Sipahioğlü and Hasan Güney for their invaluable comments.

Additionally, I should emphasize the benefits of the countless discussions made with the members of the Thrace Basin Project, in Exploration Group.

TABLE OF CONTENTS

ABSTRACT	iv
ÖZ	vi
ACKNOWLEDGEMENTS	viii
TABLE OF CONTENTS	ix
LIST OF TABLES	xiii
LIST OF FIGURES	xiv
CHAPTERS	
1. INTRODUCTION	1
1.1 Purpose and Scope	1
1.2 Location of the Study Area	2
1.3 Data Sets	4
1.4 Research Methods	7
1.5 Hydrocarbon Exploration Activities in the Thrace Basin	8
2. GEOLOGY OF THE STUDY AREA	10
2.1 Introduction	10
2.2 Origin of the Thrace Basin in Global Tectonic Concept	12
2.3 Structural Setting	17
2.3.1 Seismic Expression of the Strike-Slip Thrace Fault	
System	18
2.3.1.a Terzili Fault Zone	19

2.3.1.b	Kuzey Osmancık Fault Zone	23
2.3.2	Results of the Study	26
2.4	Stratigraphic Setting	33
2.4.1	Lower Eocene-Middle Eocene Interval	37
2.4.1.a	Karaağaç Formation	37
2.4.1.b	Fıçitepe Formation	40
2.4.1.c	Gaziköy Formation	42
2.4.1.d	Keşan Formation	45
2.4.1.e	Hamitabat Formation	49
2.4.2	Middle Eocene-Lower Miocene Interval	53
2.4.2.a	Koyunbaba Formation	53
2.4.2.b	Soğucak Formation	56
2.4.2.c	Ceylan Formation	58
2.4.2.d	Mezardere Formation	60
2.4.2.e	Osmancık Formation	63
2.4.2.f	Danişmen Formation	71
3.	PRINCIPLES OF RESEARCH METHODS	75
3.1	Seismic Reflection Principles	75
3.1.1	Resolution	82
3.1.2	Synthetic Seismogram Concept	84
3.2	Seismic Stratigraphy	90
3.2.1	Reflection Termination Patterns	90
3.2.2	Seismic Facies Analysis	95

3.3	Well-Logging Principles	98
	3.3.1 Gamma-ray Logging	100
	3.3.2 Sonic Logging	101
3.4	Vertical Trend Analysis in Well-Logs	102
3.5	Sequence Stratigraphic Terminology	104
4.	A SEQUENCE STRATIGRAPHIC APPROACH TO THE DEPOSITIONAL HISTORY ANALYSIS OF THE UPPER EOCENE TURBIDITE SYSTEM	
4.1	Introduction	114
4.2	“Hamitabat” Turbidite System	116
	4.2.1 Western Depocenter	119
	4.2.2 Northwestern Depocenter	131
	4.2.3 Northeastern Depocenter	139
4.3	Results of the Analysis: The Comparison of the Characteristics of the Major Depocenters	150
5.	A SEQUENCE STRATIGRAPHIC APPROACH TO THE DEPOSITIONAL HISTORY ANALYSIS OF THE UPPER EOCENE CLASTIC-CARBONATE MIXED SYSTEM	
5.1	Introduction	164
5.2	Carbonate and Marl Dominated Deposition as Response to Relative Sea-Level Changes	167
5.3	Late Eocene Basin Physiography in Northwest of the Thrace Basin	172

5.4	Sequence Stratigraphic Analysis	177
5.5	Results of the Analysis	202
6.	REGIONAL AND GLOBAL VARIABLES IN LATE EOCENE SEDIMENTARY RECORD	
6.1	Introduction	209
6.2	Regional Tectonics	211
6.3	Basin Physiography	220
6.4	The Analysis of Mesozoic and Cenozoic Sequence Chronostratigraphic Chart of European Basins	224
6.5	Results of the Analysis	228
7.	SUMMARY AND CONCLUSIONS	234
	REFERENCES	242
	CIRRICULUM VITAE	263

LIST OF TABLES

TABLES

Table 1.1 The summary of 2D seismic acquisition parameters	5
Table 3.1 Major elements of seismic facies analysis	97
Table 3.2 The abbreviations in sequence stratigraphic terminology	107
Table 3.3 Orders of cyclicity and basic stratigraphic units of different sequence stratigraphic studies	111
Table 4.1 The characteristic features of three major depocenters of the "Hamitabat" turbidite system	155
Table 6.1 Important regional and global variables on the architecture of sedimentary basin fill	210

LIST OF FIGURES

FIGURES

Figure 1.1 Location map of the study area in the northwest of the Thrace Basin	3
Figure 1.2 Location map of the well and 2D seismic data	6
Figure 2.1 Geology map of the Thrace Basin	11
Figure 2.2 The Turkish orogenic collage with major tectonic divisions of the Pontides	13
Figure 2.3 The Intra-Pontide Suture Zone	14
Figure 2.4 A geological cross-section, showing major structural features of the Thrace Basin	16
Figure 2.5 Location map of well and 2D seismic data, used in Chapter-2	19
Figure 2.6 Major structural features of the study area	21
Figure 2.7 Line-SN-6 (interpreted)	22
Figure 2.8 Line-SN-1 (interpreted)	24
Figure 2.9 Line-SN-2 (interpreted)	25
Figure 2.10 Line-SN-3 (interpreted)	27
Figure 2.11 Line-SN-4 (interpreted)	28
Figure 2.12 Line-SN-5 (interpreted)	29
Figure 2.13 A-A' cross-section from the Kuleli-Babaeski paleohigh to the northern paleoshelf	31

Figure 2.14 B-B' cross-section from the central basin to the northern paleoshelf	32
Figure 2.15 Generalized chronostratigraphic section of the Tertiary sediments in the Thrace Basin	35
Figure 2.16 Generalized chronostratigraphic chart of the Tertiary sediments	36
Figure 2.17 Stratigraphic column of the Early-Middle Eocene units	38
Figure 2.18 Type locality of the Karaağaç Formation in Saz Limanı, Gelibolu Peninsula	39
Figure 2.19 A complete Bouma (1962) sequence in turbiditic section from the Karaağaç Formation in Saz Limanı, Gelibolu Peninsula	41
Figure 2.2 A view from the Fıçitepe Formation near Mecidiye	43
Figure 2.21 Simplified stratigraphic section through the Gaziköy and Keşan Formations, north of the Ganos Fault	44
Figure 2.22 A view from the Gaziköy Formation near Uçmakdere in the northern coast of Marmara Sea	46
Figure 2.23 A view of the Keşan Formation from the Işıklar Mountain	47
Figure 2.24 Base of massive sandstone beds in a turbiditic sequence of the Keşan Formation	48
Figure 2.25 Three-dimensional depositional model of the Hamitabat Formation	51
Figure 2.26 Core photo from the Hamitabat Formation in the KY-2 well	52
Figure 2.27 Simplified stratigraphic section of the Upper Eocene	

sedimentary succession through the northern shelf	54
Figure 2.28 A view from Koyunbaba Formation near Hacıfakılı village	55
Figure 2.29 Generalized stratigraphic column of the Middle Eocene- Late Oligocene units of the Gelibolu Peninsula	57
Figure 2.30 A view from the Soğucak Formation near Çatalca	59
Figure 2.31 A view from the Ceylan Formation near Tayfur village, in Gelibolu Peninsula	61
Figure 2.32 Soft sediment deformation from the Ceylan Formation near Tayfur village, in Gelibolu Peninsula	62
Figure 2.33 Simplified measured stratigraphic section through the Mezardere, Osmançık and Armutburnu formations	64
Figure 2.34 A view from the Mezardere Formation, near western exit of Barbaros village	65
Figure 2.35 A view from the Osmançık Formation in the south of Paşaköy village	67
Figure 2.36 A close view from distributary channels of the Osmançık Formation	68
Figure 2.37 A view from typical fluvial-deltaic coarsening upward trend in the Osmançık Formation, near coast of Marmara Ereğlisi	69
Figure 2.38 Seismic section represents progradational character of deltaic parasequences of the Osmançık Formation	70
Figure 2.39 A view showing an angular unconformity overlain by the Ergene Formation ..	72

Figure 2.40 A view from the Danişmen Formation	73
Figure 3.1 The summary of key definitions of seismic reflection methods	76
Figure 3.2 Diagnostic gamma-ray, sonic and density logs of the different lithologies	78
Figure 3.3 Minimum and maximum phase wavelet types used in seismic data processing	80
Figure 3.4 Different seismic reflection data display types; wiggle, variable area and variable density	81
Figure 3.5 The comparison of well, outcrop and seismic scale resolution	83
Figure 3.6 Representative frequency spectrum of 2D seismic reflection data chosen from the study area	85
Figure 3.7 Sonic log data from the DG-3 well	86
Figure 3.8 Generation of synthetic seismogram	88
Figure 3.9 Synthetic seismogram of KZ-1 well	89
Figure 3.10 Major types of geometric relations between reflection terminations and seismic surfaces	91
Figure 3.11 Representative seismic lines from the study area	93
Figure 3.12 The well-log data template used in the study	99
Figure 3.13 Major vertical trends observed on gamma-ray logs	103
Figure 3.14 Major sequence stratigraphic elements of a depositional sequence	106
Figure 4.1 Generalized stratigraphic section of the Eocene sediments in the Thrace Basin	115

Figure 4.2 Three-dimensional depositional model of the “Hamitabat” turbidite system	118
Figure 4.3 Location map of well and 2D seismic data, used in Chapter-4	120
Figure 4.4 LINE-WE-1 (interpreted), a regional seismic line, representing the confined nature of the “Hamitabat” turbidite system	121
Figure 4.5 LINE-SN-1 (interpreted), seismic line crosses the Western depocenter	123
Figure 4.6 LINE-SN-1 (flatten)	124
Figure 4.7 LINE-WE-1 (zoom-interpreted), the representing the Western depocenter in the “Hamitabat” turbidite system	125
Figure 4.8 The evolutionary stages of the ponded basins	127
Figure 4.9 Three seismic lines demonstrates the changing sea-floor morphology	128
Figure 4.10 HB-2 well gamma-ray and sonic log responses	130
Figure 4.11 LNE-WE-3 (interpreted), representing the Northwestern depocenter	133
Figure 4.12 LNE-SN-2 (interpreted), crossing Northwestern depocenter	134
Figure 4.13a KRK-1 well gamma-ray and sonic log responses	136
Figure 4.13b KRK-1 well core photo	137
Figure 4.14 DG-3 well gamma-ray and sonic log responses	138
Figure 4.15 The correlation of gamma-ray and sonic log responses of the KRK-1 and DG-3 wells	140

Figure 4.16 LINE-WE-4 (interpreted), representing channelized reflection geometry in the northern shelf	141
Figure 4.17 A sketch of isolated incised valley fill in the northern margin of the basin	143
Figure 4.18 KV-6 well gamma-ray and sonic log responses	144
Figure 4.19 LINE-SN-2 (interpreted), crossing Northeastern depocenter	146
Figure 4.20 KY-2 well gamma-ray and sonic log responses	147
Figure 4.21 CL-2 well gamma-ray and sonic log responses	149
Figure 4.22 LINE-WE-5 (interpreted), crossing Northeastern depocenter	151
Figure 4.23 KV-6, CL-2 and TT-1 well-log correlation	152
Figure 4.24 Map of three major depocenters of the “Hamitabat” turbidite system	154
Figure 4.25 The sketch, representing the Northeastern and Northwestern physiography in Late Eocene	157
Figure 4.26 Growth fault model of the Northwestern depocenter	159
Figure 4.27 Mitchum (1993) growth fault sequence stratigraphic model	161
Figure 5.1 Generalized stratigraphic section of Eocene sediments in the Thrace Basin	165
Figure 5.2 Three dimensional depositional model of Late Eocene clastic-carbonate mixed system	166
Figure 5.3 Location map of well and 2D seismic data	168
Figure 5.4 Characteristic responses of carbonates as response to specific phases of relative sea-level	170

Figure 5.5a Line-SN-1 (interpreted), representing major physiographic features in the northwestern part of the basin	173
Figure 5.5b Line-SN-1 (flatten)	174
Figure 5.6 Line-SN-1 (zoom-interpreted), representing the shelf-slope margin in Late Eocene	176
Figure 5.7 A view shows gradual transition from shallow marine clastics to limestone near Hacifakılı village	180
Figure 5.8 A view shows limestone overlying the basement rocks unconformably near Çatalca	181
Figure 5.9 Characteristic responses of carbonates as response to specific phases of relative sea-level with two sketches	182
Figure 5.10 BY-1 well gamma-ray and sonic log responses and sequence stratigraphic elements	184
Figure 5.11 West to east oriented gamma-ray and sonic log correlations of the wells located along the northern paleoshelf	186
Figure 5.12 DV-4 well gamma-ray and sonic log responses and sequence stratigraphic elements	188
Figure 5.13 KV-6 well gamma-ray and sonic log responses and sequence stratigraphic elements	190
Figure 5.14a Gamma-ray and sonic log correlations of DV-4 and BY-1 wells	191
Figure 5.14.b Gamma-ray and sonic log correlations of KV-6, DV-4, BY-1 wells	192

Figure 5.15 Line-SN-2 (interpreted) represents partial drowning of the carbonate platform and landward shift of carbonate platform	194
Figure 5.16 Holocene sea-level history on a structure contour along the Cat Island shelf, Bahamas	197
Figure 5.17 Line-SN-5 (interpreted) represents marl and limestone dominated intervals	198
Figure 5.18 Line-SN-4 (interpreted) represents the termination of the Late Eocene clastic-carbonate mixed system	200
Figure 5.19 Line-WE-1 (interpreted) represents submarine canyons in the northern part of the Thrace Basin	201
Figure 5.20 Schematic view represents submarine topography with submarine canyons	203
Figure 5.21 A schematic view representing major physiographic features of Late Eocene	204
Figure 5.22 The sketch representing the evolution of the carbonate platform in Late Eocene	207
Figure 6.1 A geological cross-section, showing major structural features of the Thrace Basin	213
Figure 6.2 Line-SN-6 (interpreted) seismic line	214
Figure 6.3 Growth fault model for the Northwestern depocenter	216
Figure 6.4 Map of the basin physiography in Late Eocene	221
Figure 6.5 Major physiographic features of Late Eocene	223
Figure 6.6 Three seismic lines demonstrates the changing	

sea-floor morphology	225
Figure 6.7 A schematic representation of the major physiographic features of Late Eocene	226
Figure 6.8 Cenozoic-Mesozoic sequence chronostratigraphic chart of the European Basins	228
Figure 6.9 Seismic line represents retrogradational stacking patterns in Late Eocene	229
Figure 6.10 The summary of Upper Eocene sedimentary succession	231
Figure 6.11 Major elements of Depositional Sequence-1 and Depositional Sequence-2	232

CHAPTER 1

INTRODUCTION

1.1 Purpose and Scope

This study investigates the depositional history of the Upper Eocene sedimentary succession in a sequence stratigraphic approach in the northwest of the Thrace Basin. The Tertiary sedimentary succession is composed of up to 9000 m thick, mostly siliciclastic deposits. Due to hydrocarbon exploration significance, the Upper Eocene section was subject to this study.

Two major data sets; seismic reflection and well data sets, were used to apply depositional history analysis to the study interval in sequence stratigraphic approach. Third-order depositional sequences (Mitchum et al., 1977) were identified on the basis of reflection termination patterns on seismic sections within the seismic resolution range. Higher-order (fourth or fifth) depositional sequences were delineated using gamma-ray and sonic log responses in conjunction with seismic interpretation results.

Depositional sequences are formed in response to the interaction of eustatic sea-level changes, tectonic activities (subsidence or uplift), sediment supply, accommodation space and paleogeography (Posamentier

and Allen, 1999). The interaction of these variables on the sedimentary record is observed as the relative sea-level change, which controls the facies distribution and stratal architecture.

Two major objectives of the thesis were to reconstruct the depositional history in a sequence stratigraphic approach and to estimate the impacts of global (eustasy) and regional variables (tectonic activities and basin physiography) in the Upper Eocene sedimentary record of the Thrace Basin.

1.2 Location

The Thrace Basin, in the northwestern part of Turkey, extends from west of Istanbul to the Greece and Bulgaria territories. The study area is situated in Kırklareli and Edirne provinces in the northwest part of the Thrace Basin (Figure 1.1). The basin lies from the Greece-Turkey boundary in the west to the Vize County in the east, covering an area of approximately 3000 km².

This area is bounded by two major geological features of the pre-Tertiary basement; the crystalline Istranca-Rodop Massif in the north and the Kuleli-Babaeski paleohigh in the south which lies in the east-west direction as a subsurface extension of the Istranca-Rodop Massif.



Figure 1.1 The Thrace Basin in the northwest of Turkey extends from west of Istanbul to the Greece and Bulgaria territories. The study area is situated in the northwest of the Thrace Basin.

1.3 Data Sets

Two major data sets; seismic and well-log data sets were analyzed and combined in the sequence stratigraphic framework. Most of the seismic reflection and drilling activity in the northwestern part of the Thrace Basin have been carried out by TPAO. The area has been intensely covered by two-dimensional (2D) seismic profiles to investigate the hydrocarbon potential. Seismic surveys have been designed for five seconds recording time which was a sufficient range to perform our study for the Eocene sedimentary sequence. Data quality ranges from normal to good. Table 1.1 summarizes two-dimensional seismic acquisition parameters shot in different years.

The study utilized more than forty wells. Most of the wells have been drilled for Eocene targets so that the Eocene section could be analyzed in the study concept with ease. Well-log data set has been composed of gamma-ray (GR) and sonic (DT) logs. Additionally, well cuttings and cores were used to confirm log analysis results if available. Figure 1.2 shows the basemap of 2D seismic lines and the well locations.

Most of the studies were carried out in Landmark[®] workstation, using the Openworks[®] applications. The Openworks[®] is an exploration and production data management system used in the oil and gas industry. The following Openworks[®] applications were run: Seisworks[®], Stratworks[®], and Syntool[®]. The Seisworks[®] application was run to perform seismic interpretation, the Stratworks[®] application was run for detailed well-log

Table 1.1 2D seismic reflection acquisition parameters shot in different years by TPAO and CGG in the northwest of the Thrace Basin.

Years	2004	1990	1987	1986	1984	1977
Company	TPAO	TPAO	TPAO	TPAO	CGG	TPAO
Source	VibroSeis®	Dynamite	Dynamite	Dynamite	Dynamite	Dynamite
Channels	400	240	192	120	96	48
Record Length (sec)	5	5	4	6	5	4
Sample Rate (msec)	2	2	2	2	2	4
Shot Interval (m)	20	50	100	100	100	100
Station Interval (m)	20	25	25	25	50	50
Filters (Hz)	Out-125	8-125	8-125	8-128	8-128	12-62
Fold	200	60	24	24	24	12

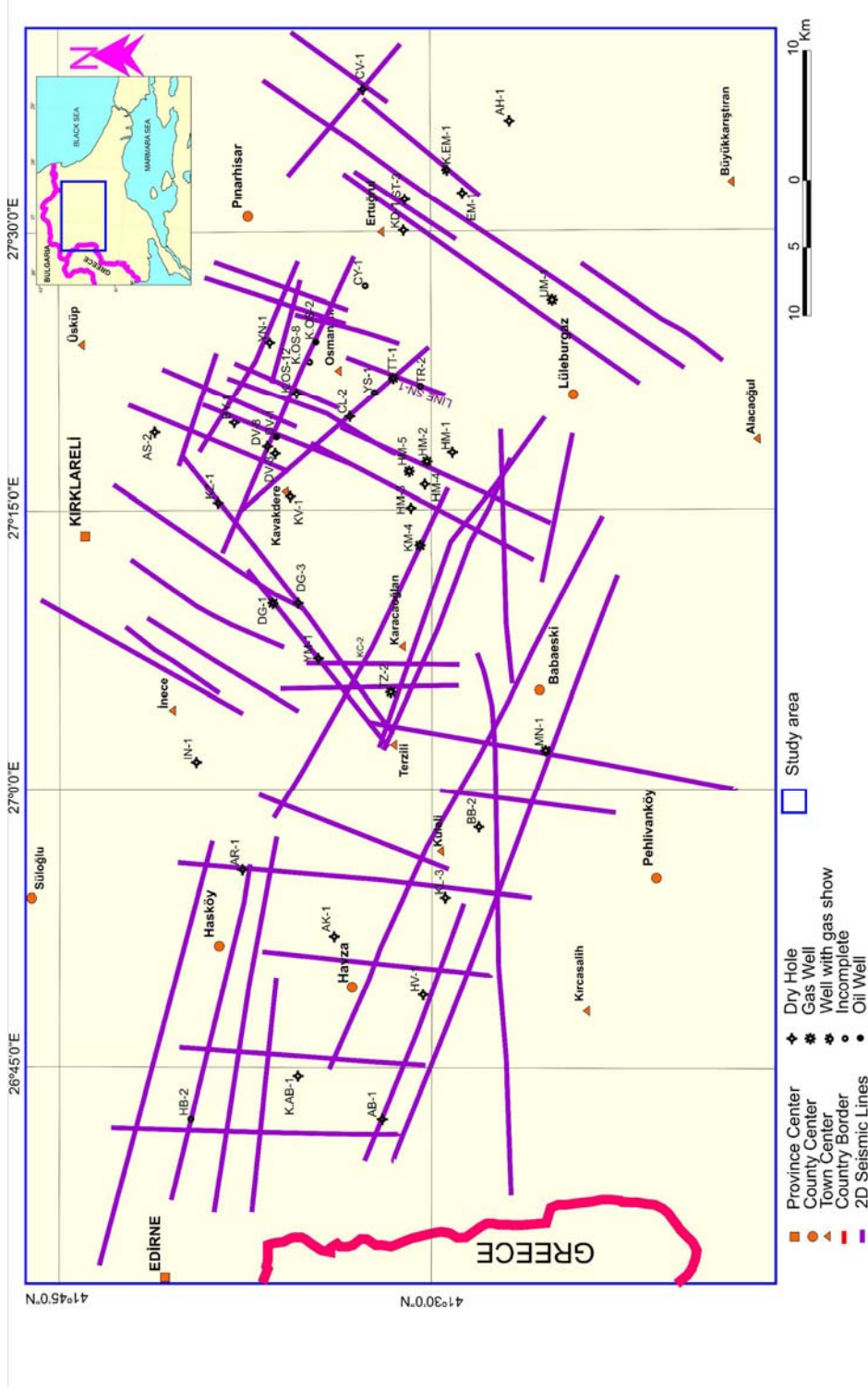


Figure 1.2 The study area is situated in the northwest of the Thrace Basin. The area has been mostly covered by 2D seismic data and drilled intensely for hydrocarbon exploration.

analysis and correlation, and the Syntool[®] application was run to generate synthetic seismograms. Additionally, several PC based software packages such as the Microsoft[®] applications, the CorelDraw[®] etc. were utilized during the study.

1.4 Research Methods

The sequence stratigraphic approach was applied in the following workflow:

1. The study section was subdivided into depositional sequences (Mitchum et al., 1977) and related systems tracts (Van Wagoner et al., 1988) on the basis of geometric relationship between reflection terminations (onlaps, downlaps, truncations, toplaps) and seismic surfaces on 2D seismic sections within seismic resolution range. Then, seismic facies analysis was applied.
2. Basic sequence stratigraphic surfaces (sequence boundaries, maximum flooding surfaces, transgressive surfaces) in time domain were converted to depth domain by synthetic seismograms.
3. Major vertical trends were delineated on gamma-ray and sonic logs. These trends may indicate lithology and stratal architecture (cleaning upward, dirtying upward etc.) and give distinctive responses for a given depositional environment (Coleman and Prior, 1982; Galloway and Hobday, 1983; Pirson, 1983; Cant, 1984; Rider, 1986). The

results were confirmed with cuttings and core data, when they are available.

4. Depositional environments were interpreted on the basis of the log trends and marker lithologies. Additionally, the subsurface interpretations were supported with field observations.
5. Diagnostic seismic and well-log responses of sequences and depositional environments were interpreted in conjunction to finalize depositional history analysis in sequence stratigraphic framework.

1.5 Hydrocarbon Exploration Activities in the Thrace Basin

The Thrace Basin is the most important gas producing basin in the country. Exploration activity in the Thrace Basin goes back to 1890's. First non-commercial oil discovery was made in 1900 by European Petroleum Corporation in Hora well near Mürefte-Tekirdağ. MTA drilled eight wells near Mürefte between 1937 and 1947. After the new petroleum law in 1954, drilling activity has speeded up. TPAO (national oil company), Shell and American Gulf were major oil companies exploring oil and gas.

Since 1890, more than four-hundred wells have been drilled mostly by TPAO. First commercial gas discovery was made by TPAO in 1970 in the Hamitabat Field, which is still one of the largest fields in the basin. Almost a century long exploration activity has resulted in the discovery of twelve gas fields and two major oil fields in the basin. Today, the Thrace

Basin is the main gas producing basin in the country with ten billion cubic meter of gas (proven reserves in place).

In modern exploration concept; turbiditic sandstones of the Upper Eocene Hamitabat Formation, reefal limestones of the Upper Eocene Soğucak Formation and deltaic sandstones of the Oligocene Osmancik Formation are three major targets. The major exploration strategy can be classified into two subjects: concentration on structural traps and reefal bodies using conventional methods, and concentration on both structural and stratigraphic traps using three-dimensional seismic reflection data. Since 1995, three-dimensional seismic data has been effectively used for detecting structural and stratigraphic traps. Direct hydrocarbon indication and paleoenvironment analysis using seismic attributes has led to increase the success rate not only in exploration, but also development and production phases in the basin.

CHAPTER 2

GEOLOGY OF THE STUDY AREA

2.1 Introduction

This chapter summarizes the geology of the Tertiary sedimentary rocks of the Thrace Basin aiming to build a base for the study. It has three major parts: global tectonic origin, structural and stratigraphic setting of the basin, respectively. The first part focuses on the global tectonic origin of the basin using mostly the literature survey. The second part describes the diagnostic structural elements using mostly seismic reflection interpretation results of the writer. The third part focuses on stratigraphic history of the basin using the literature survey and field observations of the writer.

Tertiary sedimentary rocks of the Thrace Basin consist of mostly siliciclastic and volcanoclastic rocks with partly carbonates. The sediment thickness reaches up to 9000 m in the central parts, and thins towards the margins of the basin. As the study area is covered by the Pliocene Kırcaşalılı Formation, the Miocene Ergene Formation and the Eocene Soğucak Formation, the Oligocene and Eocene Formations expose to surface in the southern part of the basin as a result of the Miocene uplift and erosion (Figure 2.1). The North Anatolian fault is a 1200 km long major

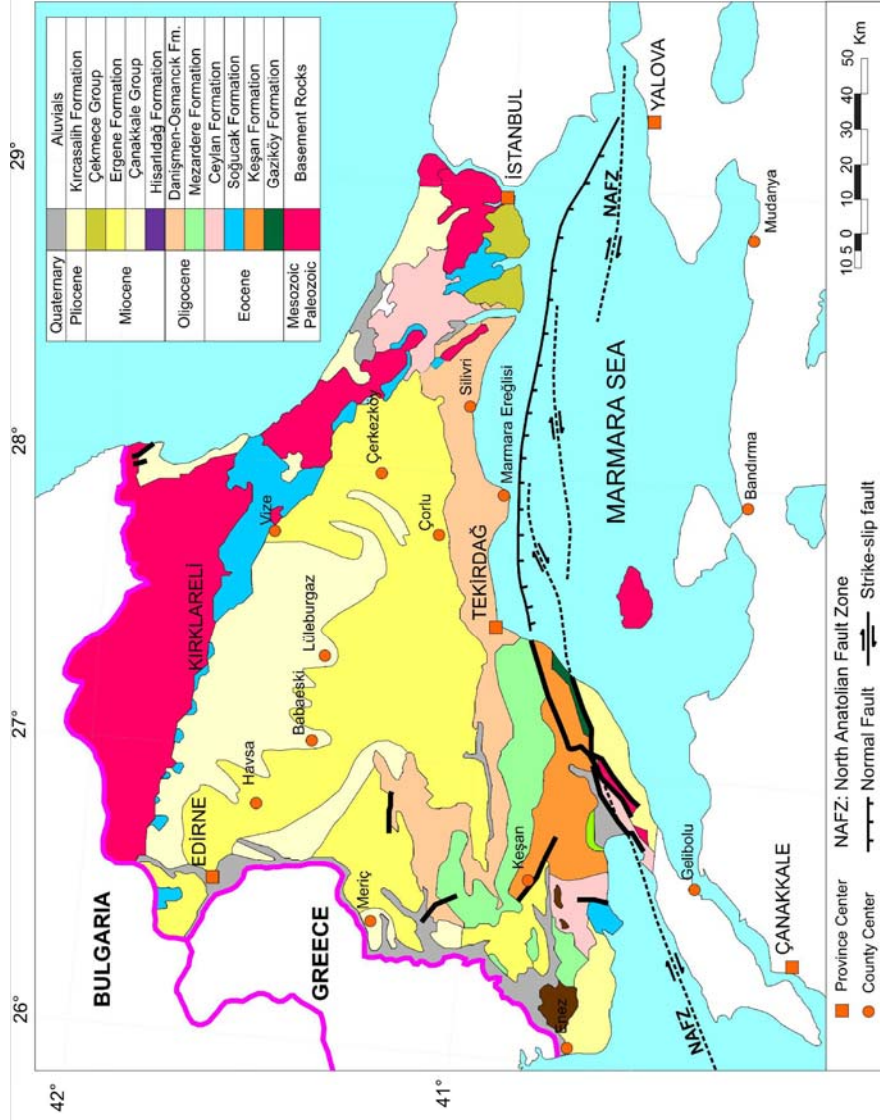


Figure 2.1 The geology map of the Thrace Basin. Most of the area is covered by the Miocene Ergene Formation (yellow color) and the Pliocene Kırcasaliñ Formation (pale yellow color). Southern part of the basin was uplifted and eroded in Late Miocene. This led to expose many formations at the surface. The map was taken from Siyako and Huvaz, 2007.

right-lateral strike-slip fault bounding the Thrace Basin in the south (Perinçek, 1991).

2.2 Origin of the Thrace Basin in Global Tectonic Concept

Thrace Basin can be defined as the depression area between the Istranca Massif in the north, the Rodop Massif in the west and the Sakarya Continent in the south, filled with a volcano-sedimentary succession of Tertiary age. The oldest rocks of the volcano-sedimentary succession of the Thrace Basin were formed in a remnant oceanic basin, left after the total consumption of the NeoTethyan ocean floor, caused by the collision between the Istranca-Rodop Massif in the north and the Sakarya Continent in the south (Yılmaz and Polat, 1998). The colliding continental fragments and the suture were collectively covered by the Lower Eocene Karaağaç Formation (Yılmaz et al., 1997).

The Pontides are an east-west trending orogenic belt, representing an amalgamated tectonic entity in which three tectono-stratigraphically different sectors may be distinguished; the western Pontides, the central Pontides and the eastern Pontides (Yılmaz et al., 1997) (Figure 2.2).

The western Pontides are composed of the following tectonic elements a) the Istranca-Rodop massif, b) the Istanbul-Zonguldak zone, c) the Armutlu-Almacık zone, d) the Sakarya continent (Yılmaz et al., 1997).

The Intra-Pontide Suture in Thrace separates the Istranca-Rodop Massif in the north from the Sakarya Zone in the south (Figure 2.3). It

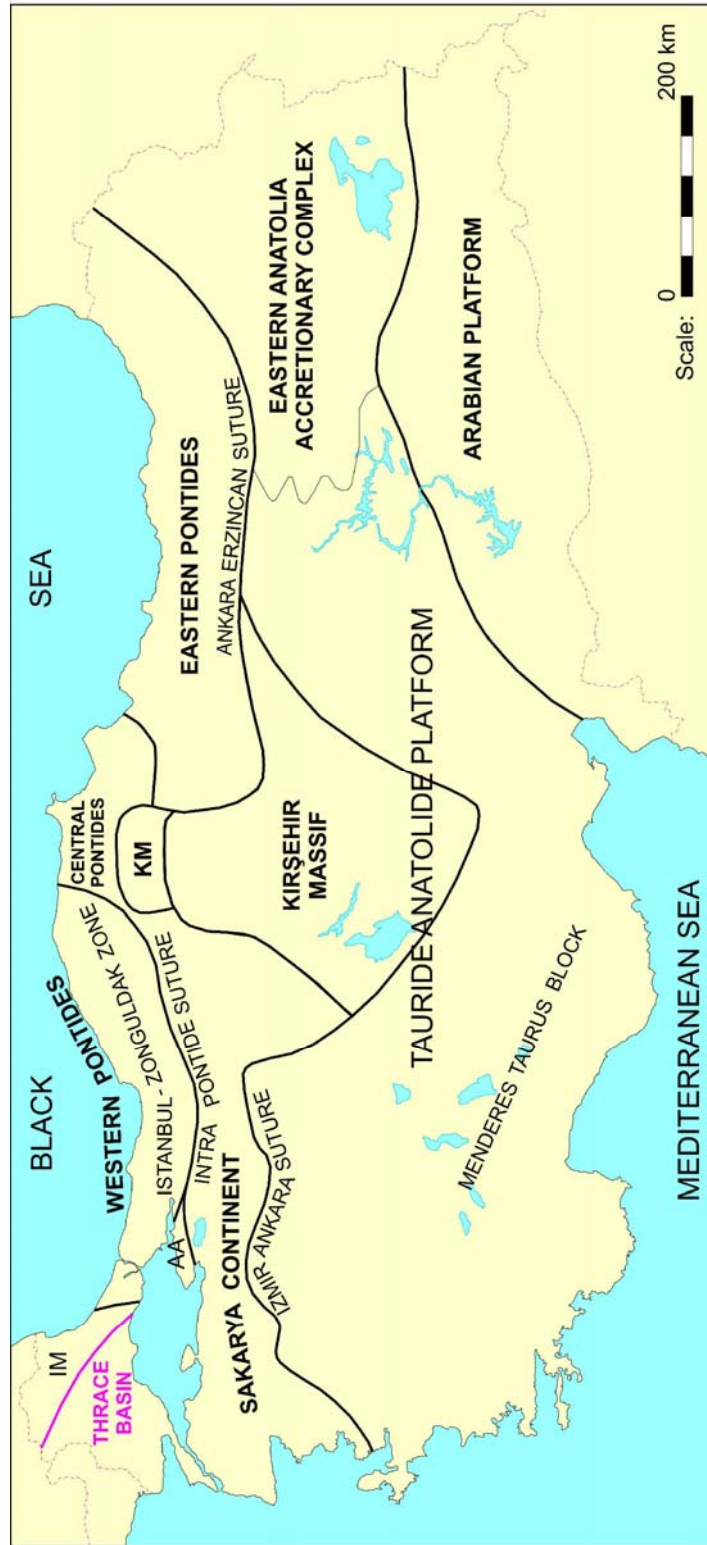


Figure 2.2 The Turkish orogenic collage with major tectonic divisions of the Pontides. The Western Pontides are composed of; a) the Istranca-Rodop Massif (IM), b) the Istanbul-Zonguldak zone, c) the Armutlu-Almacik Zone (AA) and d) the Sakarya Continent. KM: Kargı Massif (redrawn from Yılmaz et al., 1997).

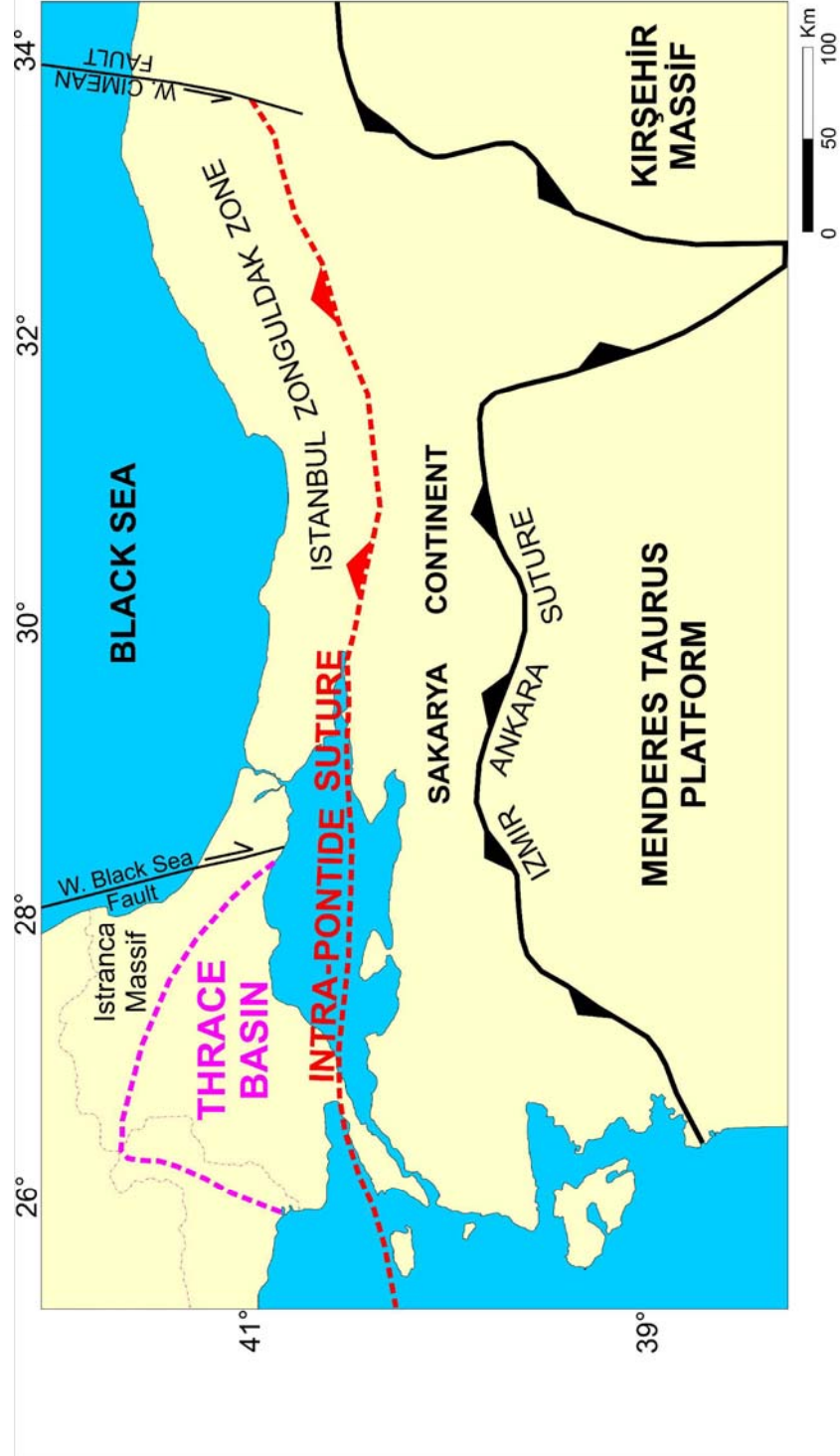


Figure 2.3 The Intra-Pontide Suture (red color dash line) in the Thrace Basin separates the Istranca-Rodop Massif in the north from the Sakarya Continent in the south. It extends under the Marmara Sea between ophiolitic melange in the Geyve-Armutlu area in the east, and Gulf of Saroz and Şarköy in the west according to Şengör and Yılmaz (1981).

extends in an east-west direction under the Marmara Sea between the scattered outcrops of ophiolitic mélangé in the Geyve-Armutlu area in the east, and around the Gulf of Saros and Şarköy in the west (Şengör and Yılmaz, 1981).

Late Cretaceous-Early Eocene Tethyan evolution of western Turkey is characterized by ophiolite obduction, metamorphism, subduction, arc magmatism and continent-continent collision (Okay et al., 2001). The Pontides were exposed as a result of the collision between the Pontides and Sakarya continents at the end of Late Cretaceous (Yılmaz et al., 1997).

Görür and Okay (1996) suggested that this continental collision obliterated the eastern part of the Intra-Pontide Ocean to the south of the Istanbul zone. Its western part remained open and continued to subduct northward throughout the Eocene. The contraction associated with this oceanic subduction could not be accommodated by the relative movement between the Istanbul and Sakarya zones. To accommodate this contraction, the Rodop-Pontide magmatic arc developing on the overriding Istranca zone started to rift and extend, thus forming the Thrace Basin. Figure 2.4 shows a geological cross-section, depicting the major structural elements of the Thrace Basin and the surroundings.

Upper Cretaceous-Paleocene Lört Formation and the observations of Okay and Tansel (1992) at the north of Şarköy revealed that the continental collision between two continents had not occurred by Middle Paleocene and

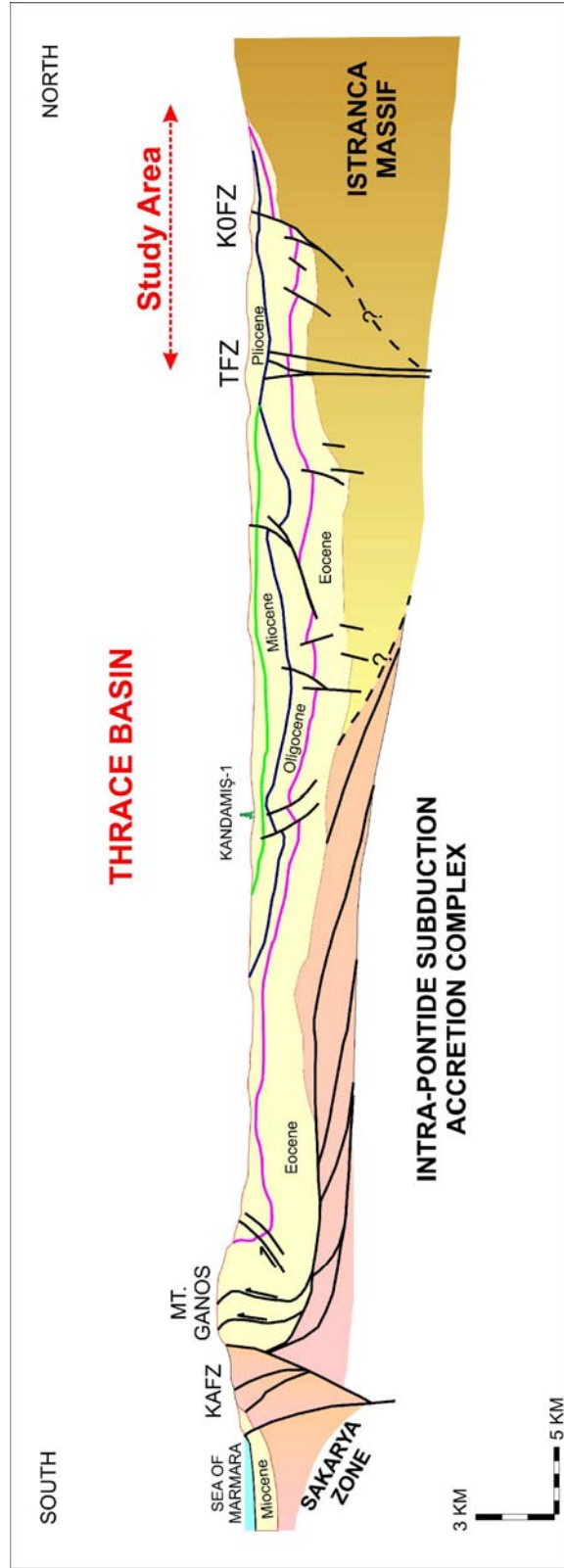


Figure 2.4 The geological cross-section shows the structural relationship between the Thrace Basin and the surroundings (from Görür and Okay, 1996). TFZ: Terzili Fault Zone, KOFZ: Kuzey Osmaniç Fault Zone, KAFZ: Kuzey Anadolu Fault Zone. The study area is situated between the TFZ and the Istranca highland.

the Intra-Pontide Ocean had existed as a deep oceanic basin at least until the Middle Paleocene.

On the other hand, some researchers (Doust and Arıkan, 1974; Perinçek, 1991; Coşkun, 2000) claimed that Thrace has an intermontane origin. In addition to the Thrace, Tuz Gölü, Çankırı-Çorum, Sivas and Erzurum basins were also interpreted as Tertiary intermontane basins between the Pontide and the Tauride mountains by the same researchers.

The major source of uncertainty may be limited field observations and lack of deep seismic reflection and well support. In addition, few researchers tend to apply gravity and magnetic models in their interpretations. Gravity and magnetic models (e.g. Özaydın and Erol, 1981) reveal some characteristics of the basement structure. More complicated gravity and magnetic models may give important contributions to the studies about the origin of the basin.

2.3 Structural Setting

Extensional tectonic regime shaped the development of the Thrace Basin in Late Middle Eocene (Turgut et al., 1991). Major structural elements are the basement-involved normal faults, trending northwest to southeast in the north and southwest to east in the south. The northern trend characterizes the shelf-slope break, the margin fault, named as Kuzey Osmaniye Fault Zone (Turgut et al., 1991). The fault zone involves parallel, sub-parallel, high angle basement-involved normal faults and impacts on

facies distribution (Figure 2.7). However, the southern shelf-slope break is smoother and no major facies break occurs.

The basin has completed its first stage of development by the Oligocene (Turgut et al., 1991). Although many of the basement faults in the central part of the basin became inactive, the margin faults continued their activity. As a result, an imbalance in the rate of sedimentation occurs between the central and the marginal parts of the basin. This also caused the development of the inverted structures (Turgut et al., 1991).

Strike-slip tectonic regime affected the basin in the Middle Miocene (Perinçek, 1991). Major structural elements are right lateral strike-slip faults, trending northwest to southeast. Two sub-parallel strike-slip fault zones cross the entire basin, named as from north to south respectively, Kuzey Osmancık Fault Zone and Terzili Fault Zone (Turgut et al., 1991). The biggest displacement takes place in the Terzili Fault Zone in the central parts of the basin. Intense erosion has taken place in restraining bends. This fault zone shows most of the characteristic features of strike-slip faults on seismic sections; such as releasing bends; restraining bends, positive and negative flower structures.

2.3.1 Seismic Expression of the Strike-Slip Thrace Fault System, Northwest of the Thrace Basin

The Thrace Basin is mostly covered by the Mio-Pliocene deposits in the studied area. Therefore, the subsurface characteristics of the Thrace

Fault System were studied using two-dimensional seismic reflection data, covering the area between the Kuleli-Babaeski paleohigh in the south and the Istranca Highland in the north. Figure 2.5 represents the location of the wells, two-dimensional seismic lines and the cross-sections, which were used in Chapter 2.

The Thrace Fault System is dominated by the strike-slip faults of Pliocene age. The exact age of the fault zone is controversial because the upper part of the seismic sections is under the effect of muting.

Two major fault zones, Terzili and Kuzey Osmançik right lateral strike-slip fault zones are the major structural elements, striking southeast to northwest and west to east, parallel to subparallel, and curvilinear right lateral strike-slip faults, respectively (Figure 2.6).

2.3.1.a Terzili Fault Zone

The largest vertical displacement observed takes place in the central part of the Thrace Basin along the Terzili Fault Zone. The fault zone was identified from south of the Hamitabat Field to the Turkey-Greece border. It crosses the south of the Hamitabat Field, makes a north bend around TZ-2 wells and continues further to westwards until the AK-1 well. The zone between the TZ-2 and AK-1 wells can be defined as a restraining bend where the seismic profiles in structural dip direction exhibit examples of steeply dipping positive flower structures.

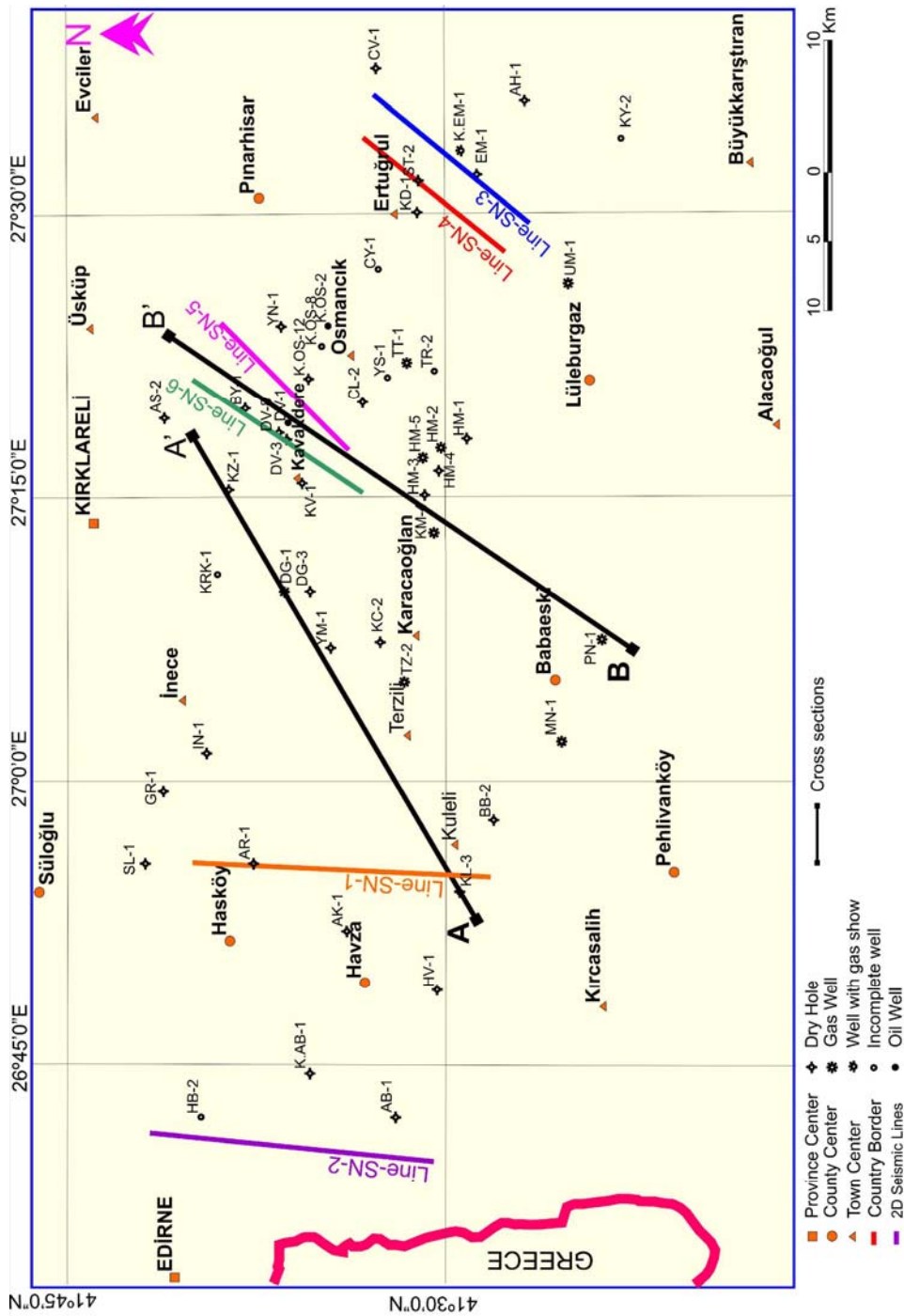


Figure 2.5 The location map of the wells, cross-sections and two-dimensional seismic lines, used in Chapter 2.

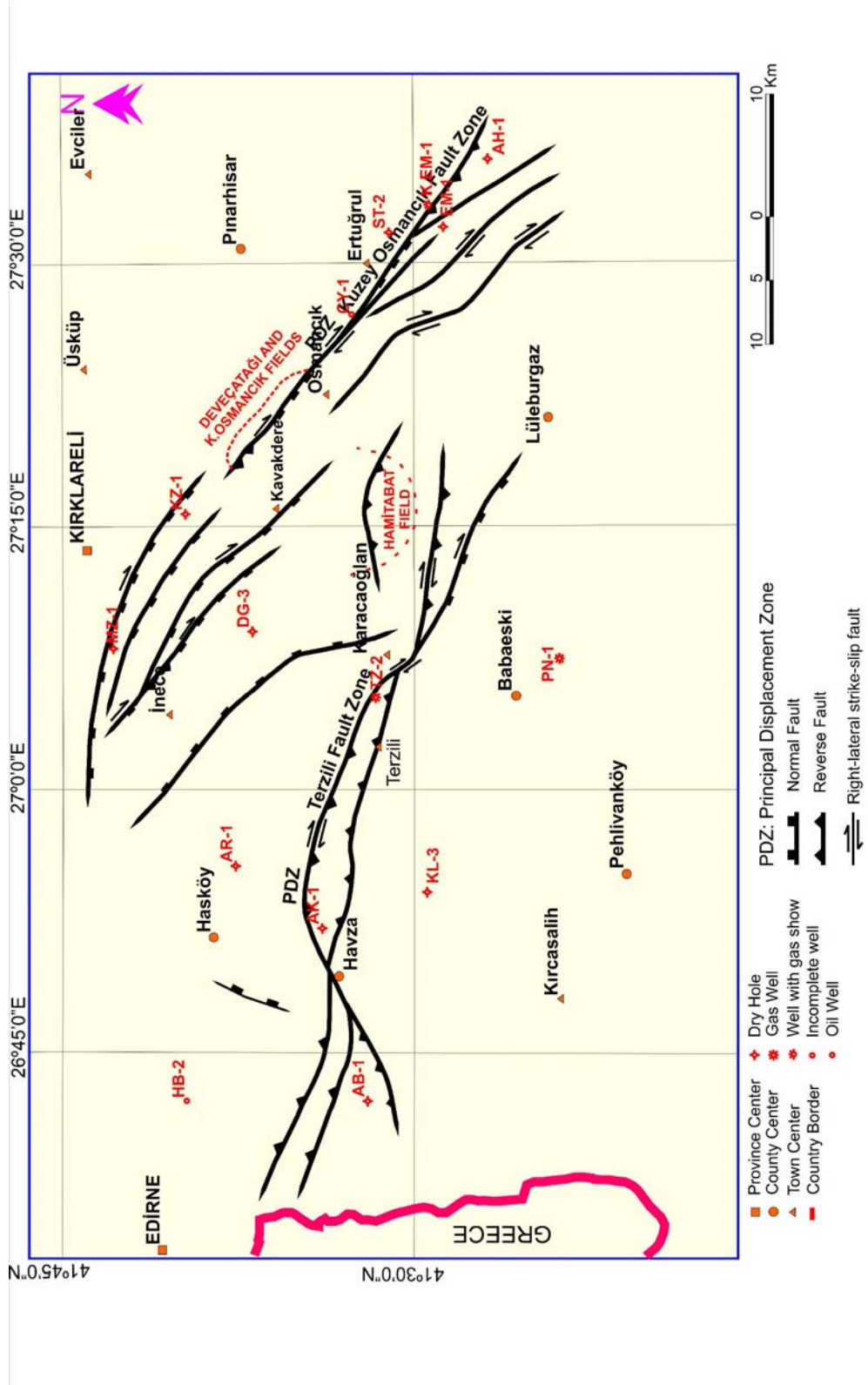


Figure 2.6 The figure shows major structural features of the study area. Terzili and Kuzey Osmancik Fault Zones are major elements of the right lateral strike-slip Thrace Fault System.

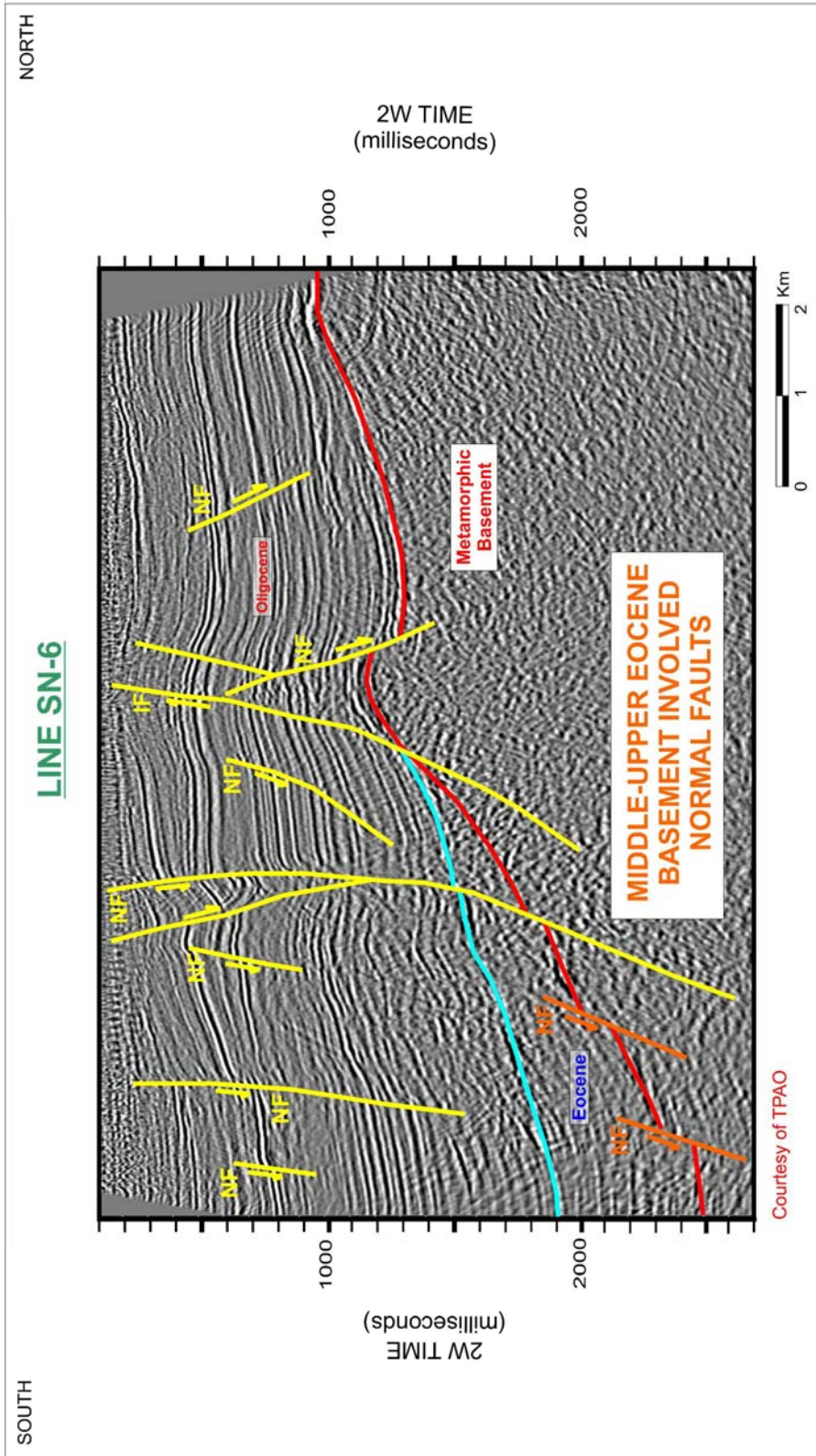


Figure 2.7 A south to north oriented seismic line crossing the northwest of the Thrace Basin. Extensional tectonic regime in Middle Late Eocene was characterized by basement-involved normal faults (orange color). Most of them were reactivated by the Oligocene to Pliocene inversion. Red and blue color horizons represent the basement and Upper Eocene sediments respectively. NF: Normal Fault, IF: Inverted Fault.

Line-SN-1 (orange color) crosses Terzili Fault zone in structural dip direction (south-north) from the Kuleli-Babaeski paleohigh to the AR-1 well (Figure 2.8). This zone is defined as a restraining bend of the Terzili Fault Zone by the interpretation of the seismic sections. The steeply dipping major fault (yellow color) cuts through the metamorphic basement and diverges upward into three branches with reverse components and disappears in the Mio-Pliocene deposits. Another characteristic of strike-slip movement is the juxtaposition of different blocks of the fault zone, as observed in the same section. Thickness changes reach up to 200 m. KL-3 and AR-1 wells located in the opposite blocks of the fault zone confirmed the juxtaposition of the blocks.

In the westward direction, the area from the AK-1 well to the Greece boundary was also defined as a restraining bend of the Terzili Fault Zone. The fault zone makes a south bend, and continues westward to the Greece border. Line-SN-2 (purple color in basemap) crosses the same fault zone from the AB-1 well to the HB-2 well in south to north direction (Figure 2.9). In this zone, the basement-involved major fault diverges upward with reverse components.

2.3.1.b Kuzey Osmancık Fault Zone

The Kuzey Osmancık Fault Zone was identified between the AH-1 well in the east and MZ-1 well in the west along the northern margin of the basin. It crosses the south of the EM-1 well until the CY-1 well and

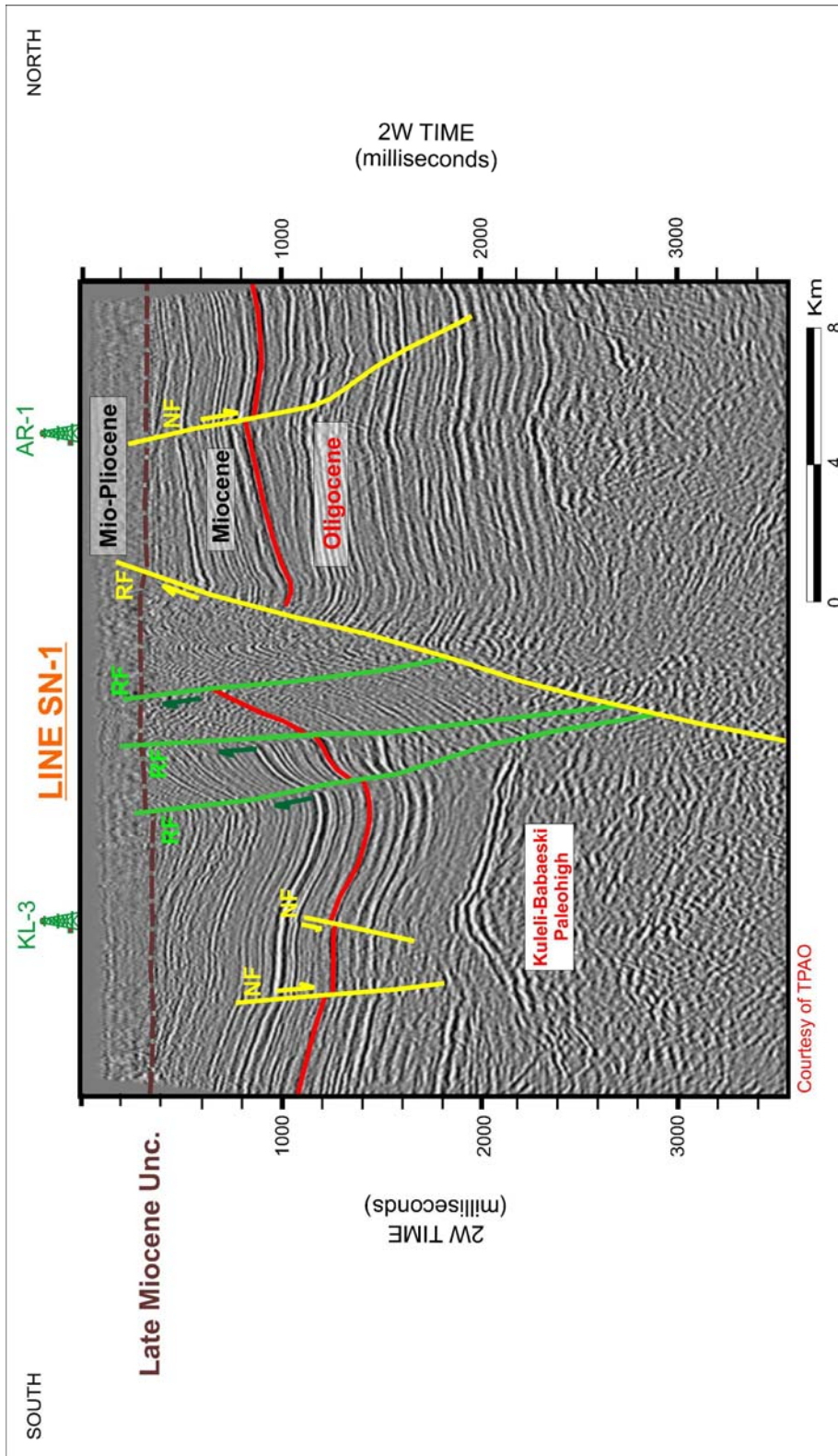


Figure 2.8 A south to north oriented seismic line crossing the Terzili Fault Zone from the Kuleli-Babaeski Paleohigh in the south to the AR-1 well in the north. Steeply dipping major fault in yellow color (principal displacement zone) cuts through the metamorphic basement and diverges upward into three branches with reverse components and disappears in the Mio-Pliocene deposits. This zone can be defined as a positive flower structure. NF: Normal Fault, RF: Reverse Fault.

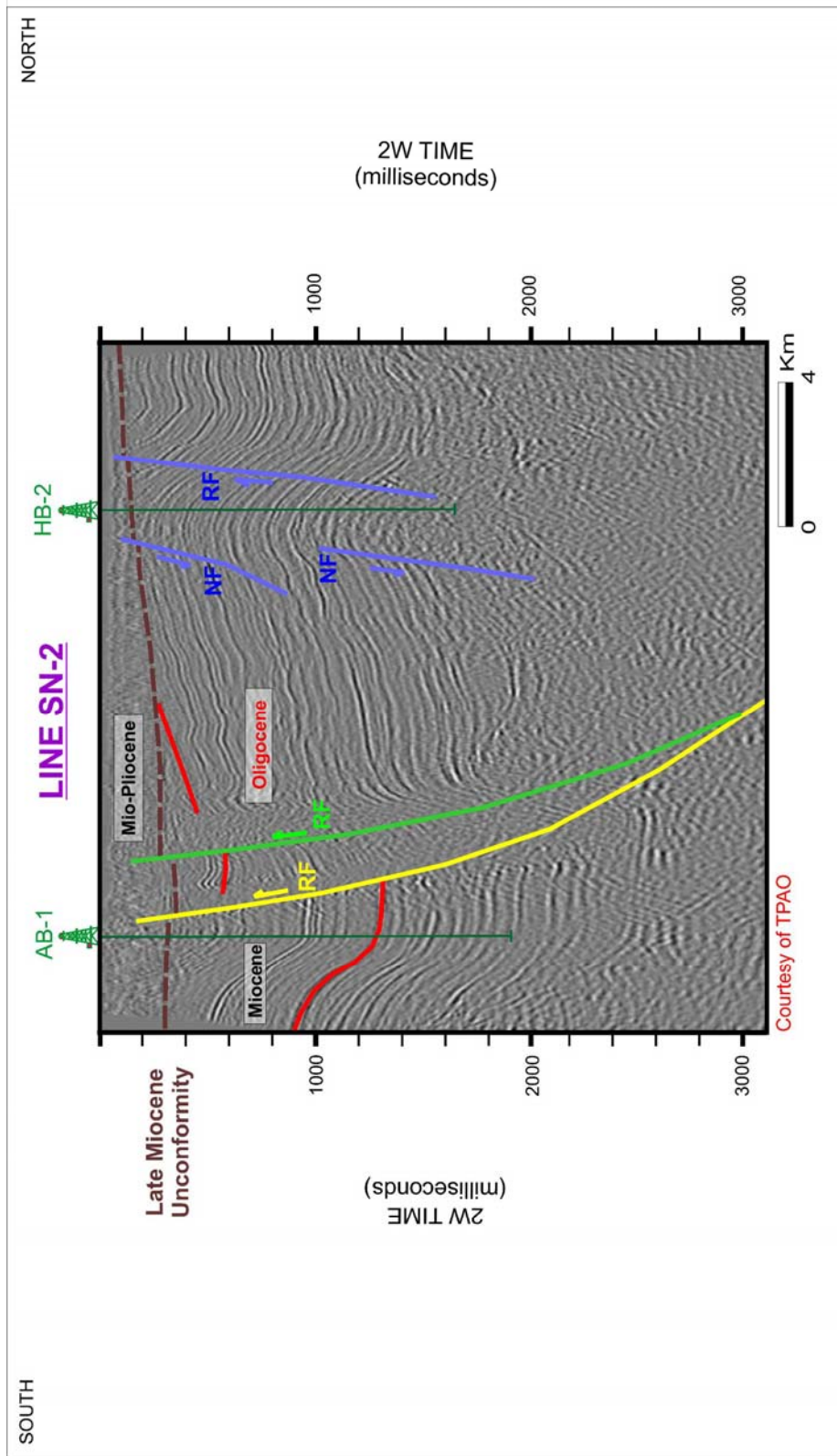


Figure 2.9 A south to north oriented seismic line crossing the AB-1 well in the south to the HB-2 well in the north. In this zone, principal displacement zone of the Terzili Fault diverges upward with the reverse components. NF: Normal Fault, RF: Reverse Fault.

continues to the Deveçatağı and the Kuzey Osmancık Fields as the Late Eocene shelf-slope boundary and then splays into three branches until MZ-1 well.

Although the normal-dip slips on the fault from the seismic profiles were dominant, the transforming of the dip slip from the normal components to the reverse components along the principal displacement zone suggested strike-slip deformation. In order to reveal strike-slip characteristics of the Kuzey Osmancık Fault Zone, four representative seismic lines were selected.

Line-SN-3 (blue color in basemap) crosses around K.EM-1 well in southwest to northwest direction (Figure 2.10). This seismic line demonstrates the major fault with reverse components in the area, which is defined as a restraining bend. In westward direction, the same major fault zone is characterized by normal components around ST-2 well (Line-SN-4 (red color in basemap)-Figure 2.11). Between the Kuzey Osmancık and Deveçatağı fields (Line-SN-5 (magenta color in basemap)), vertical displacement diminishes and the Kuzey Osmancık Fault Zone is characterized by a strike-slip deformation (Figure 2.12).

2.3.2 Results of the Seismic Characterization Study of the Thrace

Fault System

Figure 2.13 and 2.14 show two south to north oriented cross-sections, demonstrating major structural features of the study area. A-A'

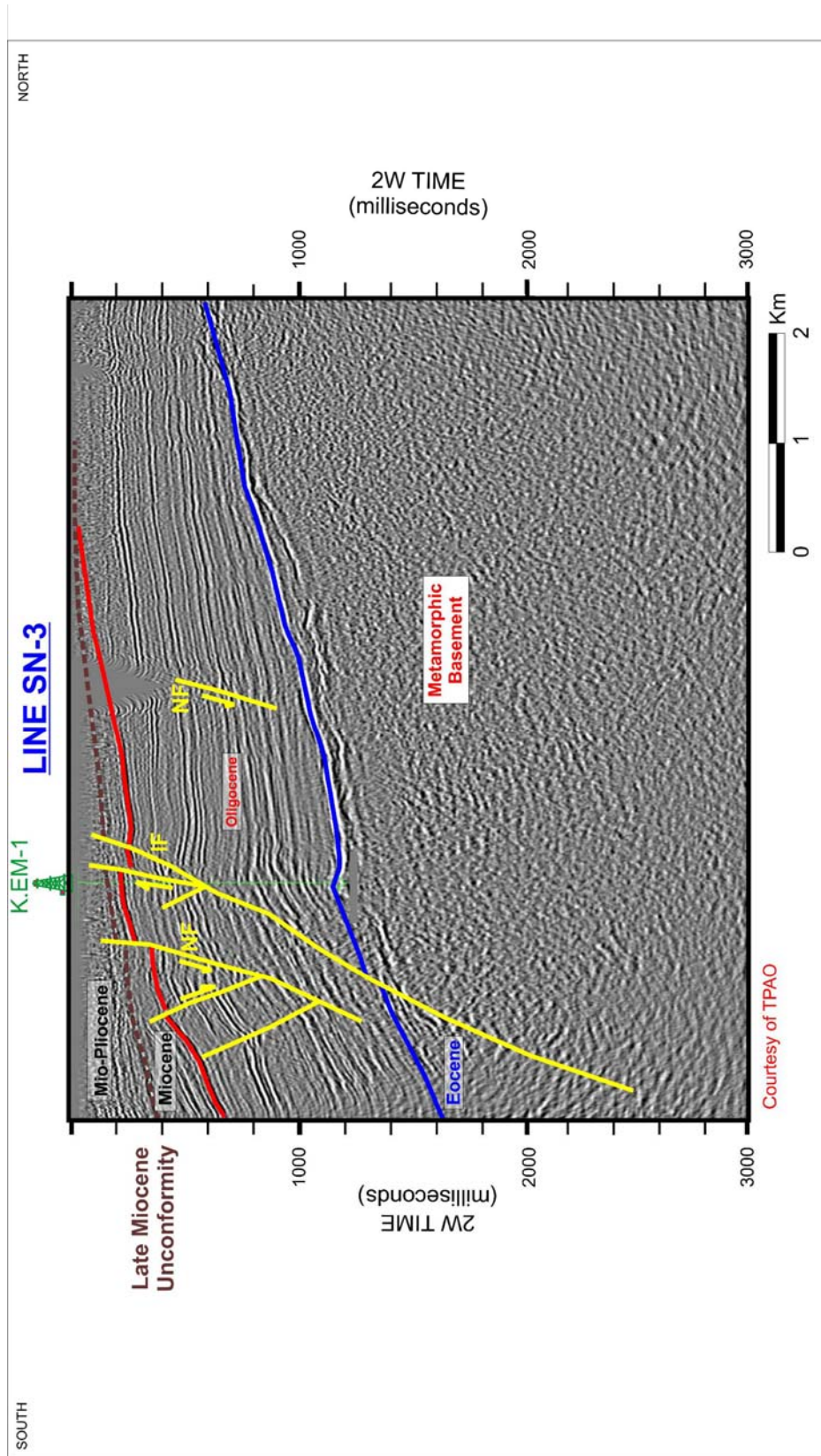


Figure 2.10 A south to north oriented seismic line, crossing the Kuzey Osmancık Fault Zone around the K.EM-1 well. The fault zone is characterized by reverse components. NF: Normal Fault, IF: Inverted Fault.

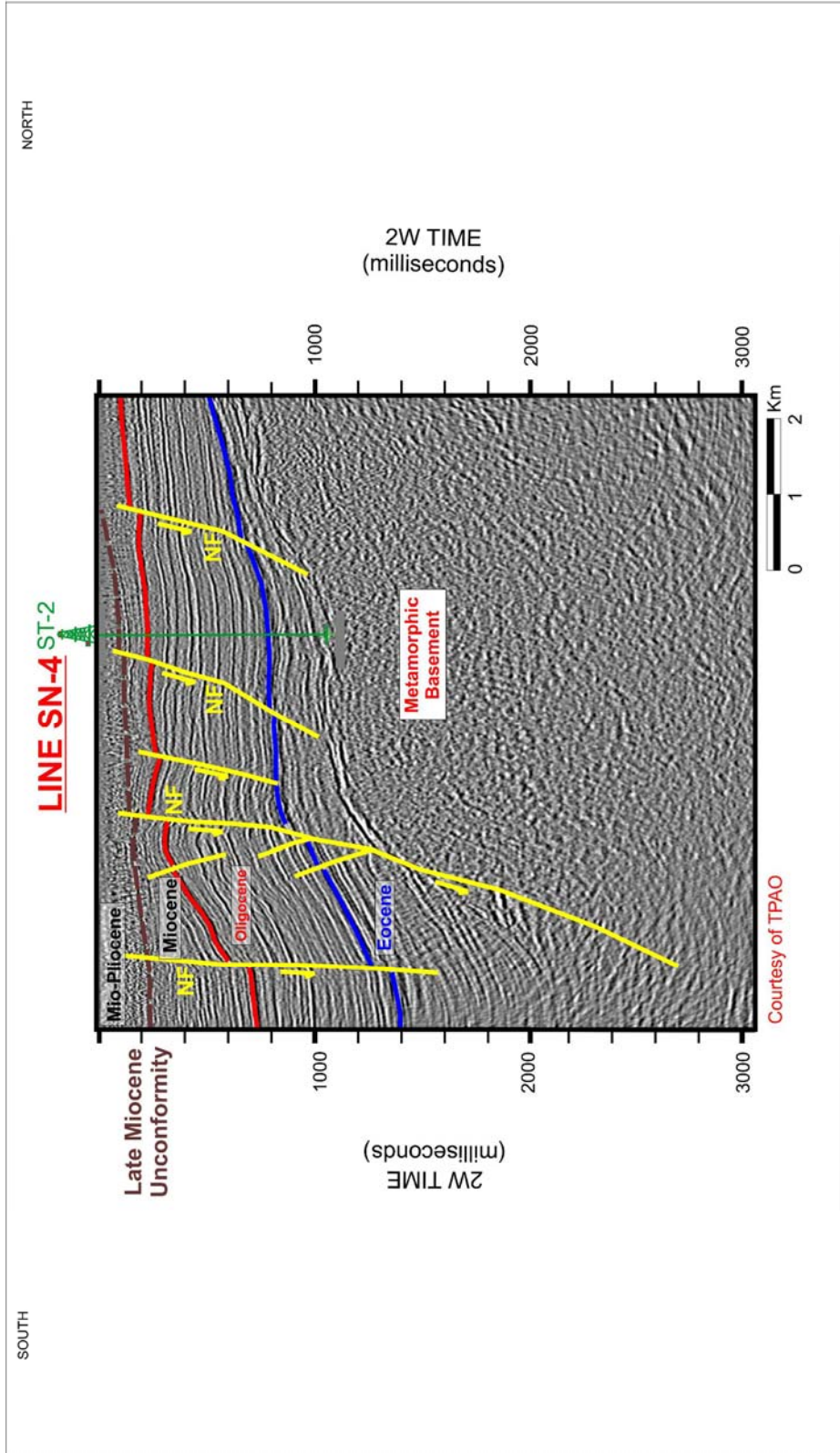


Figure 2.11 A south to north oriented seismic line, crossing the Kuzey Osmancik Fault Zone. In this zone, the major displacement zone is characterized by the normal components. NF: Normal Fault.

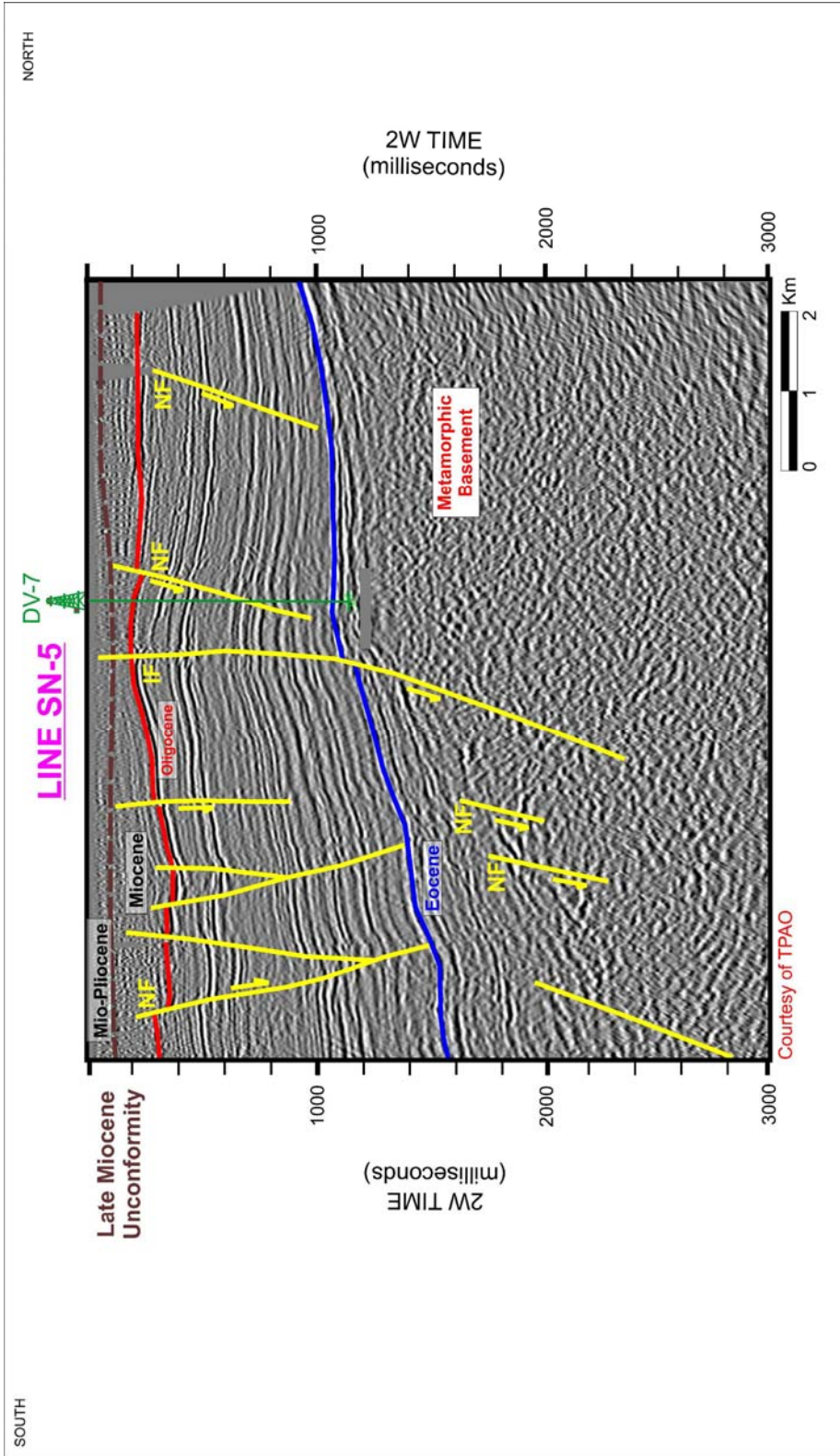


Figure 2.12 A south to north oriented seismic line, crossing the Kuzey Osmancik Fault Zone around the DV-7 well. In this zone, vertical displacement diminishes and the fault zone is characterized by the strike-slip movement. NF: Normal Fault, IF: Inverted Fault.

cross section crosses the study area between the Kuleli-Babaeski paleohigh, the deep central basin and the northern margin of the basin (Figure 2.13). Two major fault zones Terzili and Kuzey Osmancık Fault zones are exhibited on the section. As the Terzili Fault Zone is represented by reverse components, the Kuzey Osmancık Fault Zone is represented by normal components.

B-B' cross-section crosses the study area from the PN-1 well in the central basin to the northern shelf (Figure 2.14). Major structural features in Middle Eocene are the basement-involved normal faults. Most of these normal faults were used as existing weakness zones in strike-slip tectonic regime. The Terzili Fault Zone is represented in this zone with normal components and The Kuzey Osmancık Fault Zone is represented by reverse components.

Collectively, two-dimensional seismic interpretations revealed that the Thrace Fault System of Late Pliocene age; Terzili and Kuzey Osmancık fault zones, was a right lateral strike-slip fault system that concealed by the Upper Pliocene clastics. The age of the fault system was controversial because the upper part of seismic sections (Plio-Quaternary) is under the effect of muting.

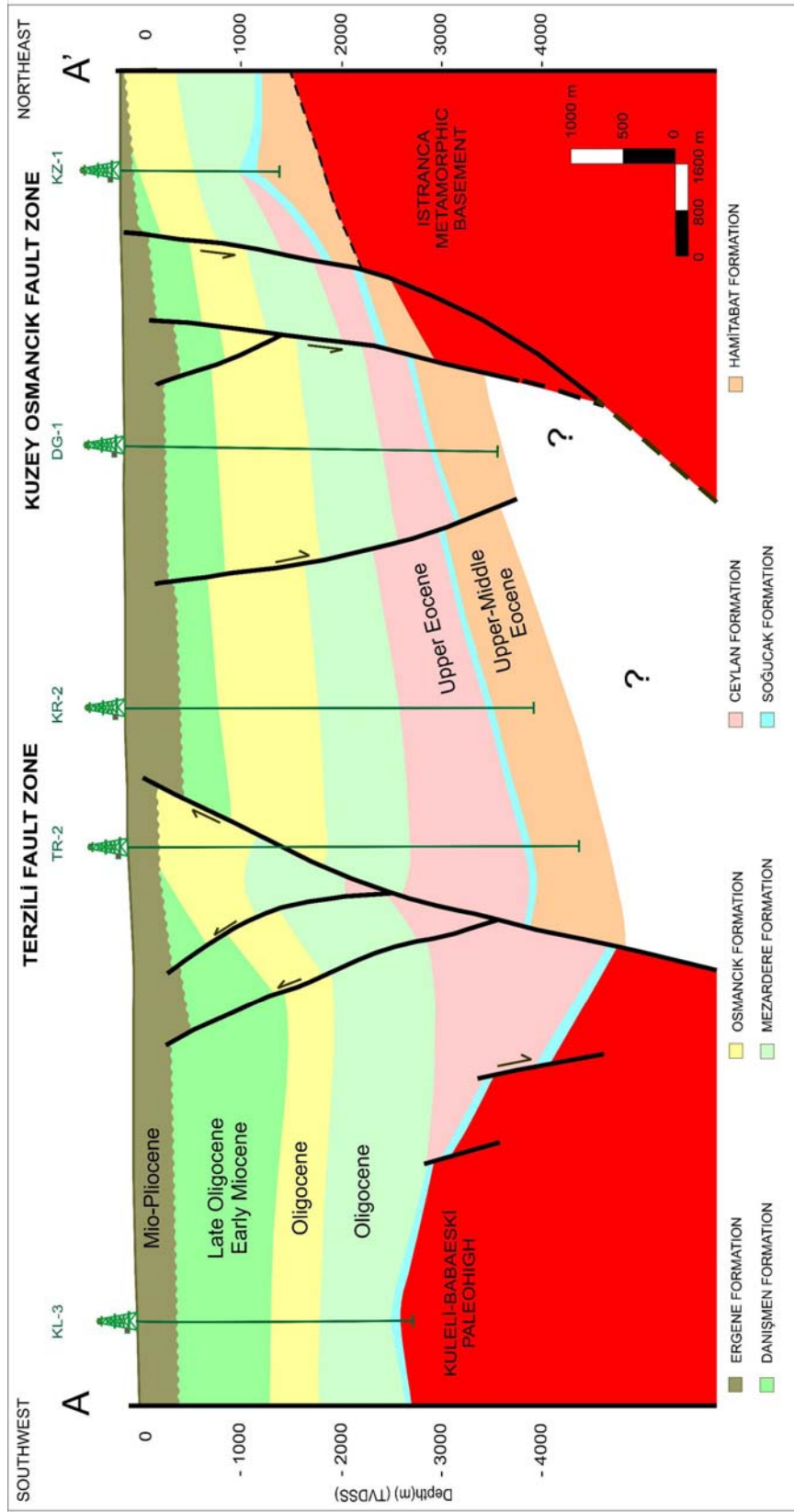


Figure 2.13 A-A' cross-section crosses the Kuleli-Babaeski paleohigh in the south, deep central basin and the northern paleo-shelf of the Thrace Basin. It represents two major fault zones - Terzili and Kuzey Osmancik Fault Zones of the right lateral strike-slip Thrace Fault System. This cross-section has been constructed on the basis of the drilled well and seismic data sets. The location map of the A-A' cross-section is shown in Figure 2.5.

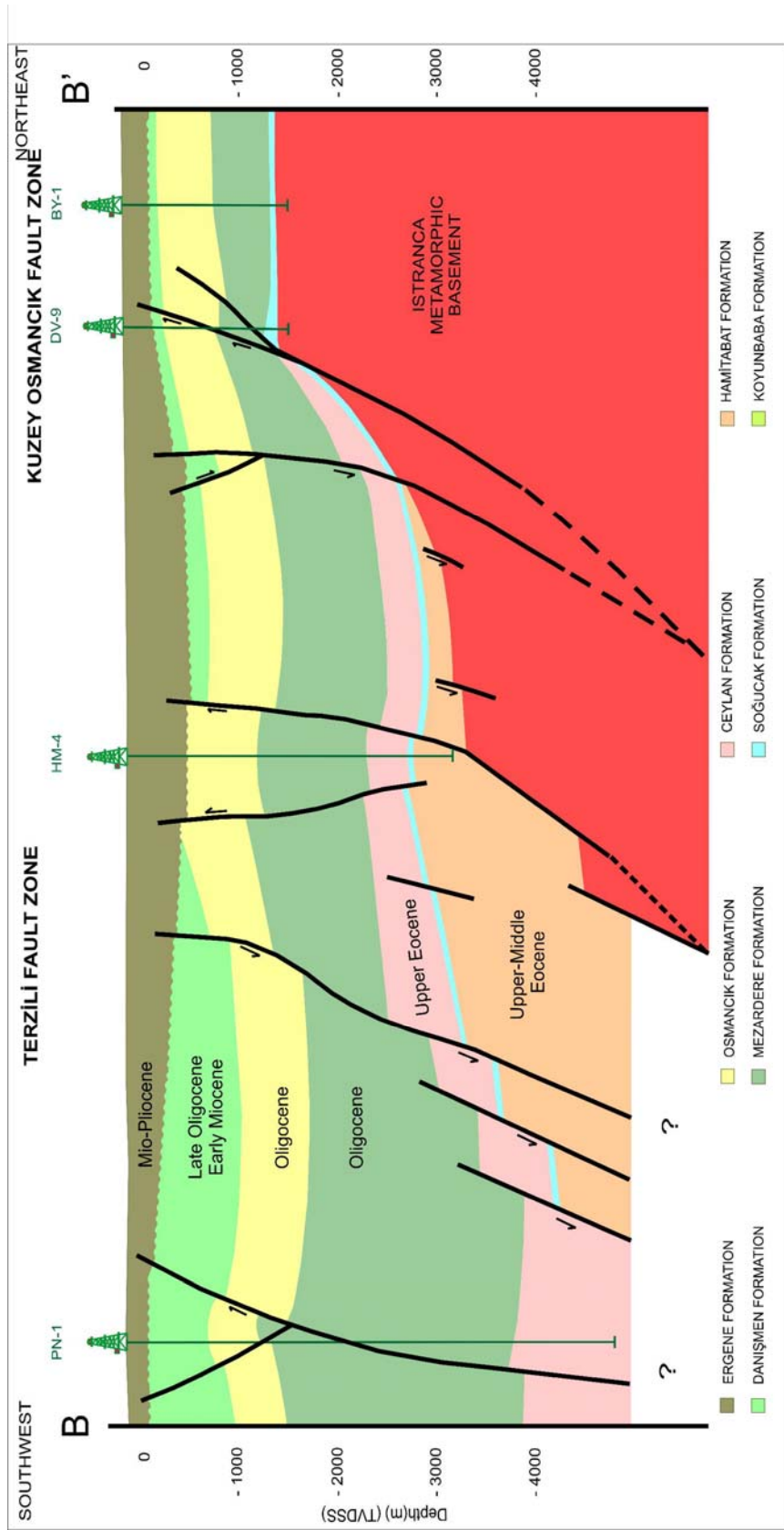


Figure 2.14 B-B' cross-section from the central basin near the PN-1 well in the south to the northern plaeo-shelf. The sediment thickness reaches up to 4500 m and thins towards the northern margin. As the Terzili Fault Zone is represented by normal components, the Kuzey Osmancik Fault Zone is represented by reverse components. This cross-section has been constructed on the basis of drilled well and seismic data sets. The location map of the B-B' cross-section is shown in Figure 2.5.

2.4 Stratigraphic Setting

Extensional fault geometry and the pre-Tertiary topography characterized the rate and facies geometry of the oldest sediments of the basin in the Middle Eocene. Major characteristic features of the basin were;

1. Northern, western and southern highlands,
2. Restricted shelves in the northern and southern margins,
3. Normal faults, trending northwest-southeast in the north and southwest-north in the south,
4. Rapid transition to the deep central basin,
5. Pre-Tertiary paleohighs.

Sedimentation started in late Middle Eocene with a transgression in the southwest northeast direction (Turgut et al., 1983). As reefal to shallow marine sediments were deposited on the shelves and paleohighs, the deep central basin was filled with turbiditic sediments from the highlands. An alternation of shale, claystone, siltstones and fine-grained poorly-sorted sandstones exhibit the signs of having been deposited by turbidity currents (Doust and Arıkan, 1974). Intermediate andesitic volcanism introduced considerable amounts of volcanic ash into the basin (Turgut et al., 1991).

Eocene transgression was followed by a regressive cycle ranging from Lower Oligocene up to early Lower Miocene (Keskin, 1974). This time corresponds to the final stage of subsidence and fast deposition in the basin (Turgut et al., 1983). Dominant facies were fluvial, lagoonal and shallow marine allowing alternation of claystones with thin sandstones and siltstones

streaks (Doust and Arıkan, 1974). Figure 2.15 and Figure 2.16 show the generalized lithostratigraphic section and chronostratigraphic chart of the Tertiary sediments in the Thrace Basin.

Siyako (2006) analyzed the stratigraphic history of the Thrace Basin in seven different time intervals:

1. Paleocene-Lower Eocene: Çeltik Formation.
2. Lower Eocene-Middle Eocene: Karaağaç and Fıçitepe Formations in the Gelibolu Peninsula, Gaziköy and Keşan Formations in south of the Thrace Basin, Hamitabat Formation in the north of the Thrace Basin.
3. Middle Eocene-Lower Miocene: Koyunbaba Formation, Soğucak Formation, Ceylan Formation and Yenimuhacir Group (Mezardere, Osmancık and Danişmen Formations).
4. Upper Oligocene-Middle Miocene: Hisarlıdağ Formation.
5. Miocene: Ergene Formation, Çanakkale and Çekmece Groups.
6. Lowermost Miocene-Pliocene: Trakya Formation.
7. Pleistocene: Kırçasalılı Formation.

This study focused on the Upper Eocene sedimentary units. Therefore, Middle Eocene-Lower Miocene units were described in detail.

SYSTEM	AGE	UNITS	LITHOLOGY	DEPOSITIONAL ENVIRONMENT	
TERTIARY	PLIOCENE	KIRCASALIH FM.		FLUVIAL	
	MIOCENE	ÇANAKKALE GROUP		NEAR SHORE, LAKE FLUVIAL	
				VOLCANICS	
	OLIGOCENE	YENİMUHACIR GROUP	HİSARLIDAĞ FM.		DELTAIC SYSTEM
			DANIŞMEN FM.		
		OSMANCIK FM.		DELTA FRONT	
		MEZARDERE FM. Teslimköy Member		PRODELTA	
	EOCENE	KEŞAN FM.	CEYLAN FM.		PROXIMAL TURBIDITES
			SOĞUCAK FM. KOYUNBAĞA FM.		
		GAZİKÖY FM.	FIÇİTEPE FM.		FLUVIAL
KARAĞAÇ FM.				PROXIMAL-DISTAL TURBIDITES FLUVIAL	
PALEOZOIC MESOZOIC		?	BASEMENT		

Figure 2.15 Generalized lithostratigraphic section of the Tertiary sediments of the Thrace Basin (Siyako, 2006).

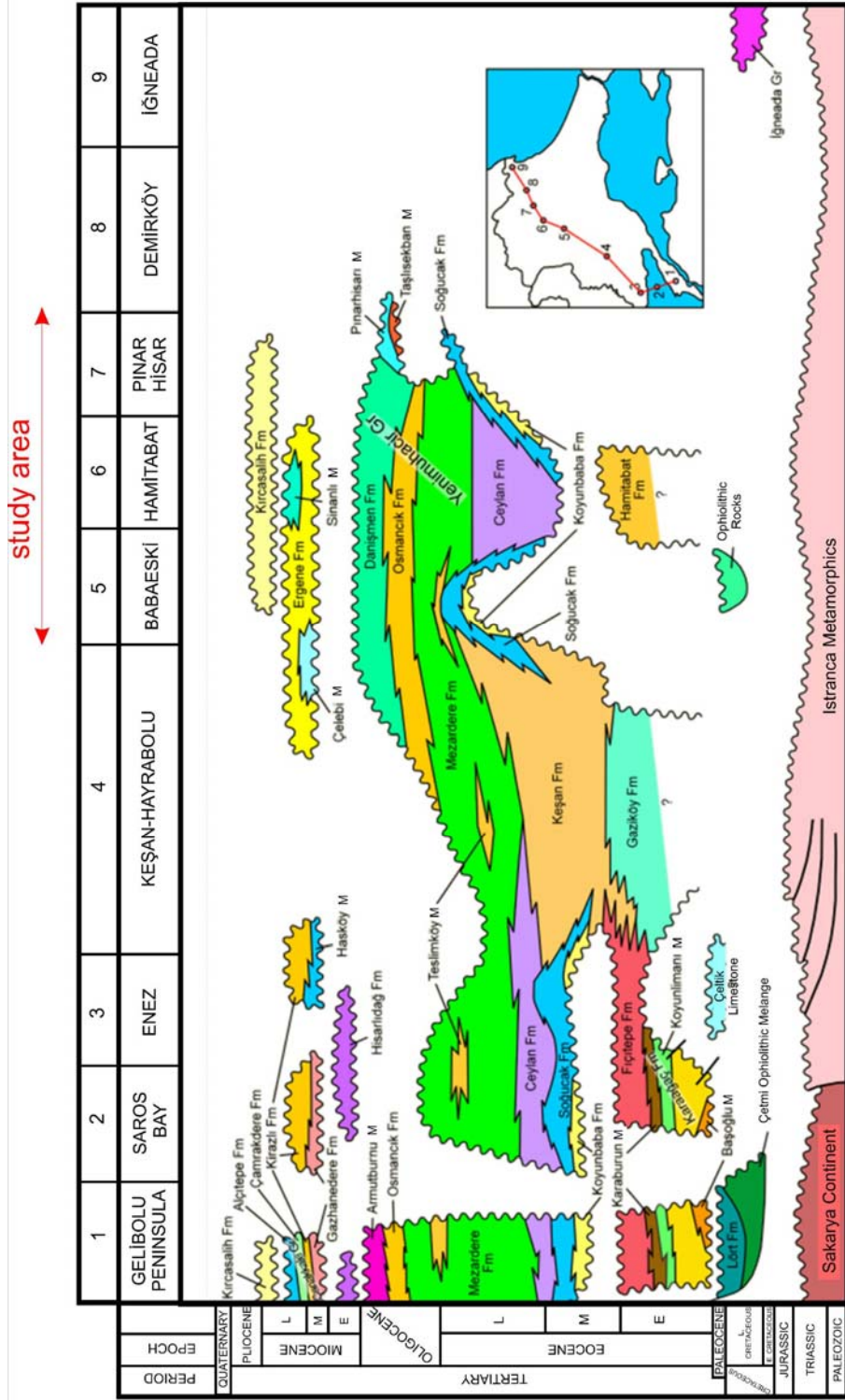


Figure 2. 16 Generalized chronostratigraphic chart of the Thrace Basin from the Gelibolu Peninsula in the south to İğneada in the north. The study area is situated between Babaeski and Demirköy counties (Siyako, 2006).

2.4.1 Lower Eocene-Middle Eocene Interval

Karaağaç Formation

Karaağaç Formation was firstly identified by Sfondrini (1961). The formation was divided into four members (Temel and Çiftçi, 2002; Figure 2.17). From bottom to top; Başıoğlu Member, Saz Member, Koyunlimanı Member and Karaburun Member.

Karaağaç Formation overlies the Lört Formation unconformably and underlies the Fıçitepe Formation with a gradual contact (Figure 2.17). The outcrops are observed only in the Gelibolu Peninsula and Gökçeada in the north Aegean Sea (Figure 2.1).

The formation is mostly composed of interbedded sandstone, shale and pebblestone lithologies. The deposition initiates with transgressive basal conglomerates of the Başıoğlu Member or a neritic limestone layer, which is medium to thickly bedded and has a packstone character (Sümengen and Terlemez, 1991) and grades upward into deep sea turbidites of the Saz Member. Olistostromal pebbles are also observed within sandstone and shale layers. Deep sea turbidites grade upward into prodelta shales and marlstones (Koyunlimanı Member), and pebbly sandstone lithologies of delta front environment at the top. The increase in grain size indicates regressive cycles. Figure 2.18 shows a view from one of the type localities of Karaağaç Formation in Saz Limanı, Gelibolu Peninsula. In this photo, Karaağaç Formation is composed of interbedded sandstone and shale lithologies in a typical turbiditic sequence. The complete Bouma

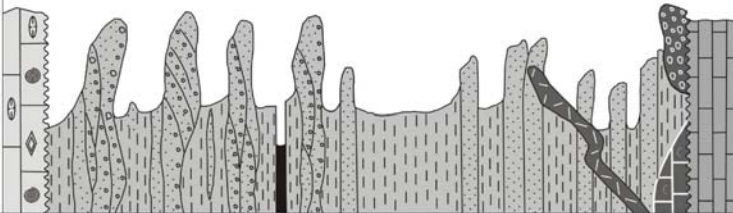
Chrn.	Formations	T (m)	Lithology	Remarks	Environment
LOWER-MIDDLE EOCENE	SOĞUCAK FM.			Wine color, thin to medium bedded, mudstone and siltstone with sandstone intercalations	Reef
	FIÇITEPE FM.	800		Grey-green color, coarse grained, cross bedded, poorly sorted, polygenic pebblestone and sandstone	Fluvial
	KARABURUN Mb.	150		Thin coal layers	Deltafront
	Koyunlimanı Mb.	350		Yellowish beige color, medium to thickly bedded, medium to coarse grained mudstones, alternated with high angle cross bedded sandstones and thin coal layers	Prodelta
	Saz Mb.	540		Grey to dark grey color, thin to medium bedded	Deep Marine
	Başoğlu Mb.	15		Turbidites with coarsening upward Bouma sequence and andesite intrusions	Neritic
	Lört Fm.	150		Grey color, medium bedded, densely fractured, sandy macro fossil fragments, neritic limestones and pebblestones Light grey color, thin to medium bedded, clayly limestones	Pelagic
PALEO CENE					

Figure 2.17 Generalized stratigraphic column of the Early-Middle Eocene units of the Gelibolu Peninsula (from Temel and Çiftçi, 2002).



Figure 2.18 The type locality of the Karaağaç Formation is situated in Saz Limanı, Gelibolu Peninsula. The section is mostly composed of interbedded sandstone and shale lithologies in a typical turbiditic sequence.

(1962) sequence can be observed within this turbiditic sequence (Figure 2.19).

Early Eocene-Early Lutetian age was given to the Karaağaç Formation by Sümengen and Terlemez (1991), Early Eocene age by Önal, (1985) based on benthic foraminifers and nannoplanktons. Toker and Erkan (1985) suggested a Middle Eocene age.

Fıçitepe Formation

Fıçitepe Formation was firstly identified by Sfondrini (1961). It overlies the Karaburun Member of the Karaağaç Formation with a gradual contact and the pre-Tertiary basement rocks unconformably (Figure 2.17) in places where the Karaağaç Formation doesn't exist such as the İbrice Port (southwest of the Thrace Basin), Gelibolu Peninsula and Bozcaada in the north Aegean Sea (Figure 2.1). It underlies the Koyunbaba and Soğucak Formations unconformably.

Fıçitepe Formation is composed of pebblestone, sandstone, mudstone lithologies and thin coal layers (Figure 2.17). Channelized pebbles are mostly derived from limestones, various metamorphic and volcanic rocks. The sandstone is medium to coarse-grained, and exhibit fining upward trend with cross-bedding sedimentary structures. The mudstone is wine-colored and laminated with organic tracks, remnants, fragments of plant roots, desiccation cracks and carbonate concentrations (Sümengen and Terlemez, 1991). These flood plain and fluvial facies should

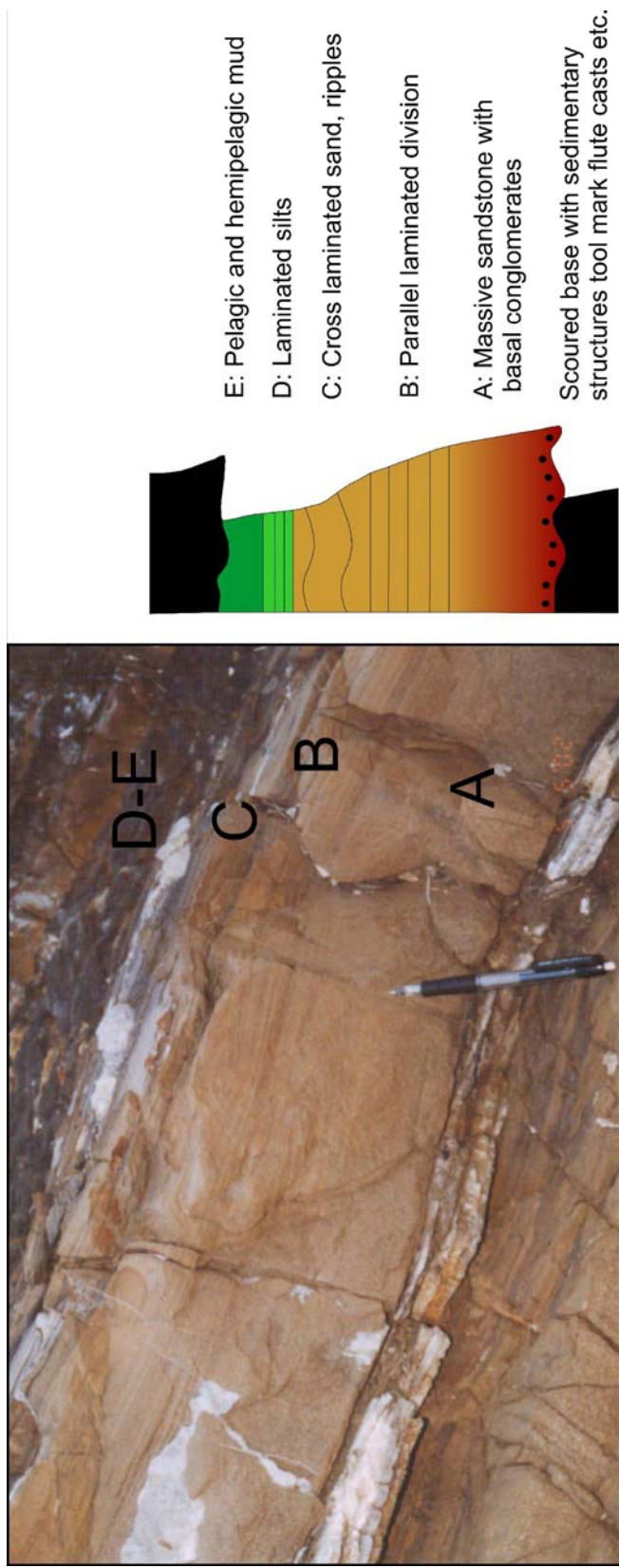


Figure 2.19 A complete Bouma (1962) sequence in a turbiditic section of the Karaağaç Formation in Saz limanı, Gelibolu Peninsula.

have been deposited in a delta top environment of the deltaic system overlying the Karaağaç Formation sedimentation. Figure 2.20 shows a view from the Fıçitepe Formation near Mecidiye village.

Fıçitepe Formation doesn't contain any fossil. An early Miocene age has been assigned to the formation based on its stratigraphic position within known sequences.

Gaziköy Formation

Gaziköy Formation was firstly identified by NV Turkse Shell (1972). Its outcrops extend along southern flanks of Ganosdağ in the northern shoreline of the Marmara Sea (Figure 2.1). Marmara Sea and the intense deformation of the Ganos Fault prevent to observe the base of the Gaziköy Formation. It underlies the Keşan Formation with a gradual contact (Figure 2.21). Gaziköy Formation is composed of interbedded thin sandstone, siltstone and dark gray shale lithologies with tuff intercalations. As dominant lithology is shale, grain size and thickness of sandstone beds increase upward gradually (Yaltrak, 1995). They have sharp base and gradual top with siltstones. The various sandstone bed thicknesses from base to top, missing Ta and Tb divisions in Bouma (1962) sequence, the absence of basal sedimentary structures, the existence of thin laminated sandstone beds, the increase in mud-sand ratio downward, high organic content and non-variable bed thicknesses along high distances indicate that the Gaziköy Formation is deposited in a wide deep marine environment as middle to

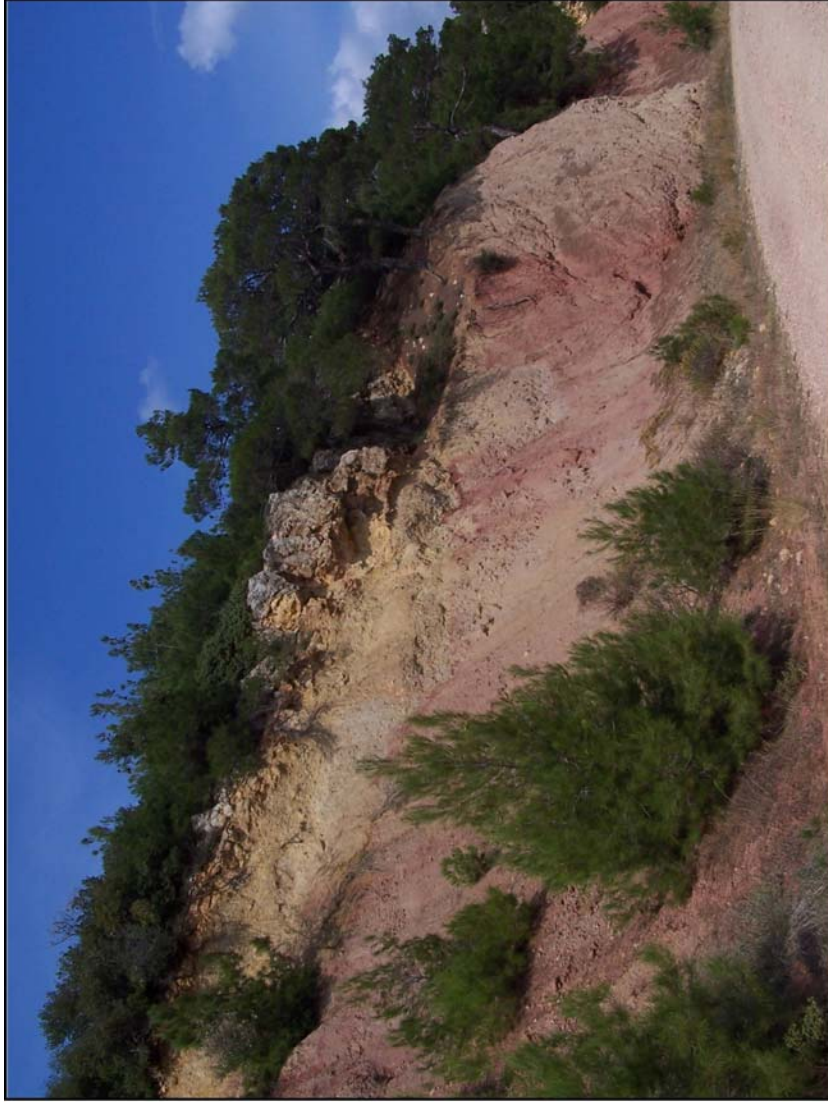


Figure 2.20 Fiçitepe Formation is composed of fluvial channel fill and flood plain deposits with wine color. The photo was taken at the south of Mecidiye village (4495888 N, 462563 E).

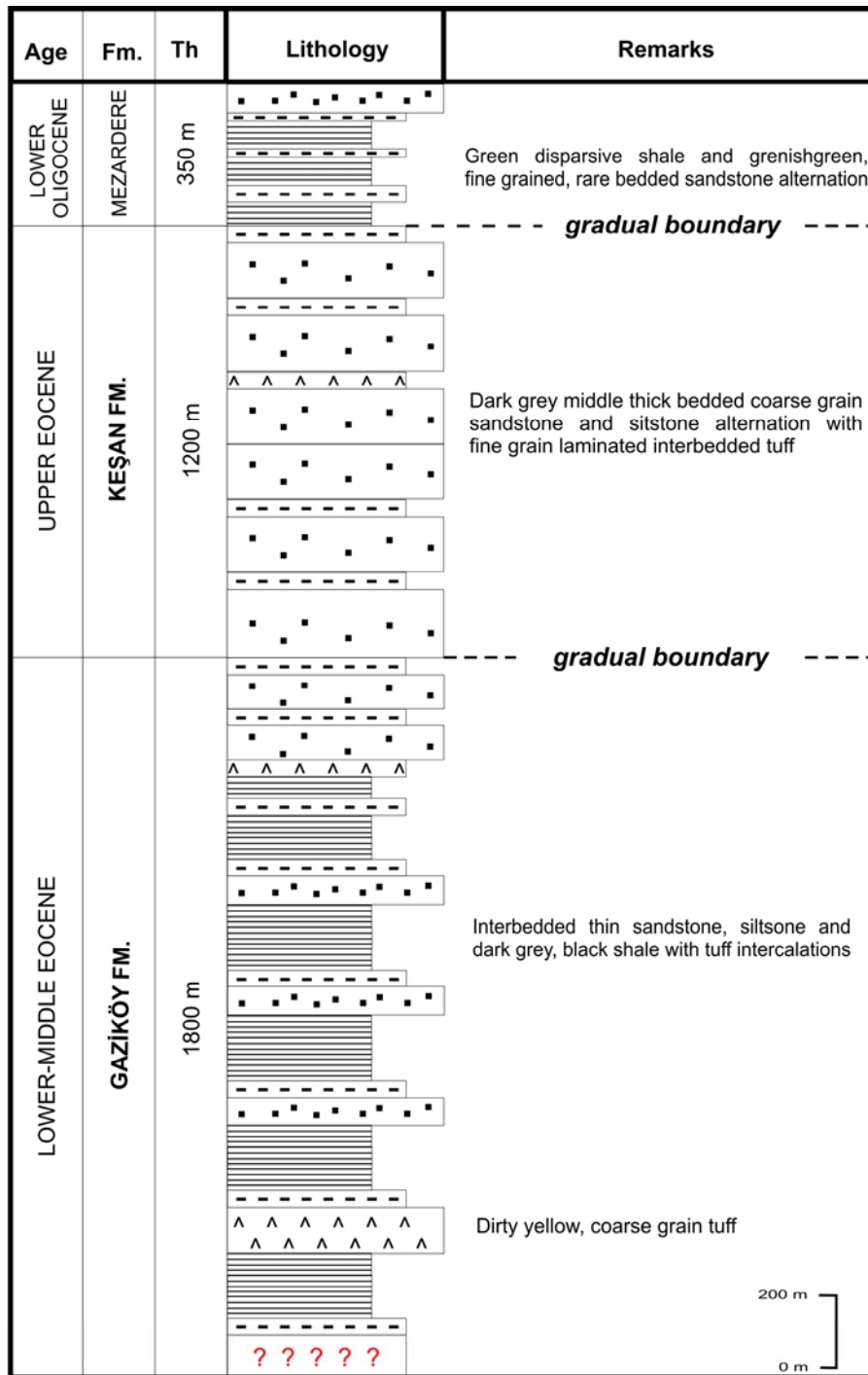


Figure 2.21 Simplified stratigraphic section through the Gaziköy and Keşan Formations along the north of the Ganos Fault (from Yalıtırak, 1995).

distal turbiditic facies (Yaltırak, 1995). Depositional model of the Gaziköy Formation may resemble the outer fan of the sub-marine fan model of Normark (1978) (Figure 2.22).

Based on nannoplanktons, a Middle-Late Eocene age has been assigned to the Gaziköy Formation (Sümengen and Terlemez, 1991).

Keşan Formation

Keşan Formation was identified firstly by Gökçen (1967). Keşan Formation has gradual contacts with the underlying Gaziköy Formation and the overlying Mezardere Formation (Figure 2.21). The outcrops of the Keşan Formation extend from Kumbağ to the Saros Bay in the south of the Ganos Fault (Figure 2.1).

According to Sümengen and Terlemez (1991) lithology description, the formation is composed of thinly bedded, fine-grained sequence of sandstone, siltstone, mudstone lithologies and sequences of medium to coarse-grained, moderately to thickly bedded fining upward channel fill sandstones which show lateral discontinuities. Figure 2.23 shows a view from the Keşan Formation at the northern flank of Işıklar (Ganos) Mountain. The characteristic features of a typical turbiditic sequence (Yaltırak, 1995) were observed. Each sequence initiates with massive to well-bedded pebbly sandstones with a largely eroded base (Figure 2.24). This pebbly bearing level grades upward into medium to coarse-grained, moderately to thickly bedded sandstone. Ta, Tb and Tc-divisions of Bouma (1962) sequence are

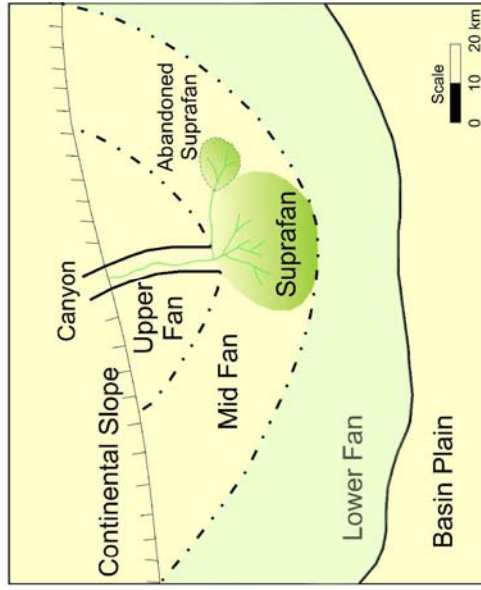


Figure 2.22 A view from the Gaziköy Formation near Uçmakdere along the northern coast of the Marmara Sea. The depositional environment of the Gaziköy Formation resembles the lower sub-marine fan model of Normark (1978).



Figure 2.23 A view from the Keşan Formation at the northern flank of the Işıklar (Ganos) Mountain. The section is composed of moderately to thinly bedded sandstone lithologies alternating with mudstone beds. Along the red arrow sandstone beds exhibit thinning upward trend (4520305 N, 532912 E).



Figure 2.24 Keşan Formation is composed of sandstone beds with erosive base in a turbiditic sequence. The base of massive sandstone beds is characterized by tool marks. The photo was taken from the Işıklar Mountain (4520305 N, 532912 E).

well developed. These sequences are overlain by massive mudstones. The sandstone intervals of varying thicknesses are encompassed by another sandstone dominated sequence, consisting of fine-grained sandstone, siltstone and claystone. The most diagnostic features of sandstone beds within this interval are that they have sharp upper surfaces with current ripples and laterally thin out at a short distance and finally pass into mudstones. Siltstones and claystones are commonly massive and display parallel laminations on millimeter to centimeter scales locally. These characteristic features for the turbiditic section of the Keşan Formation resemble mid-fan of the submarine fan model of Normark (1978). In addition, volcanic matrix of sandstone beds indicates that volcanic activity was active during the deposition (Turgut et al., 1983).

Based on nannoplanktons, the age of the Keşan Formation was given as Late Eocene by Sümengen and Terlemez (1991).

Hamitabat Formation

Hamitabat Formation was firstly identified by Keskin (1974) on the basis of the subsurface data after the discovery of the Hamitabat gas field. Well cuttings, cores, well-logs and seismic data indicate that the Hamitabat Formation overlies the Istranca Metamorphics unconformably (Figure 2.15). The upper boundary of the Hamitabat Formation is discordant with Soğucak and Ceylan Formations.

Hamitabat Formation which is restricted to the deep central basin is mostly composed of alternation of gray color sandstone, siltstone and dark color shale beds in different thicknesses. The depositional environment varies from shallow marine to deep marine (Figure 2.25). Most of the sandstone lithologies are deposited as distal, proximal and inter-channel turbidities in deep marine environment. Figure 2.26 shows a core photo from the Hamitabat Formation in the KY-2 well from the study area. The cored interval is composed of sandstone and thin shale beds, which suggests middle submarine fan model of Normark (1978). On the other hand, extensive burrowing, small scale current ripples and organic production were also observed in other wells, suggesting a shallow marine environment (Turgut et al., 1987).

This study emphasized that the “Hamitabat” turbidite system was deposited in separate depocenters based on their own provenances, sediment delivery pathways, areal extents and the nature of depositional fills. Additionally, due to the great influence of the paleo-submarine morphology along the northern margin in Late Eocene basin fill history, the analyzed wells exhibited varying thicknesses.

The age of the Hamitabat Formation was given as Middle-Late Eocene by Ediger and Batı (1987).

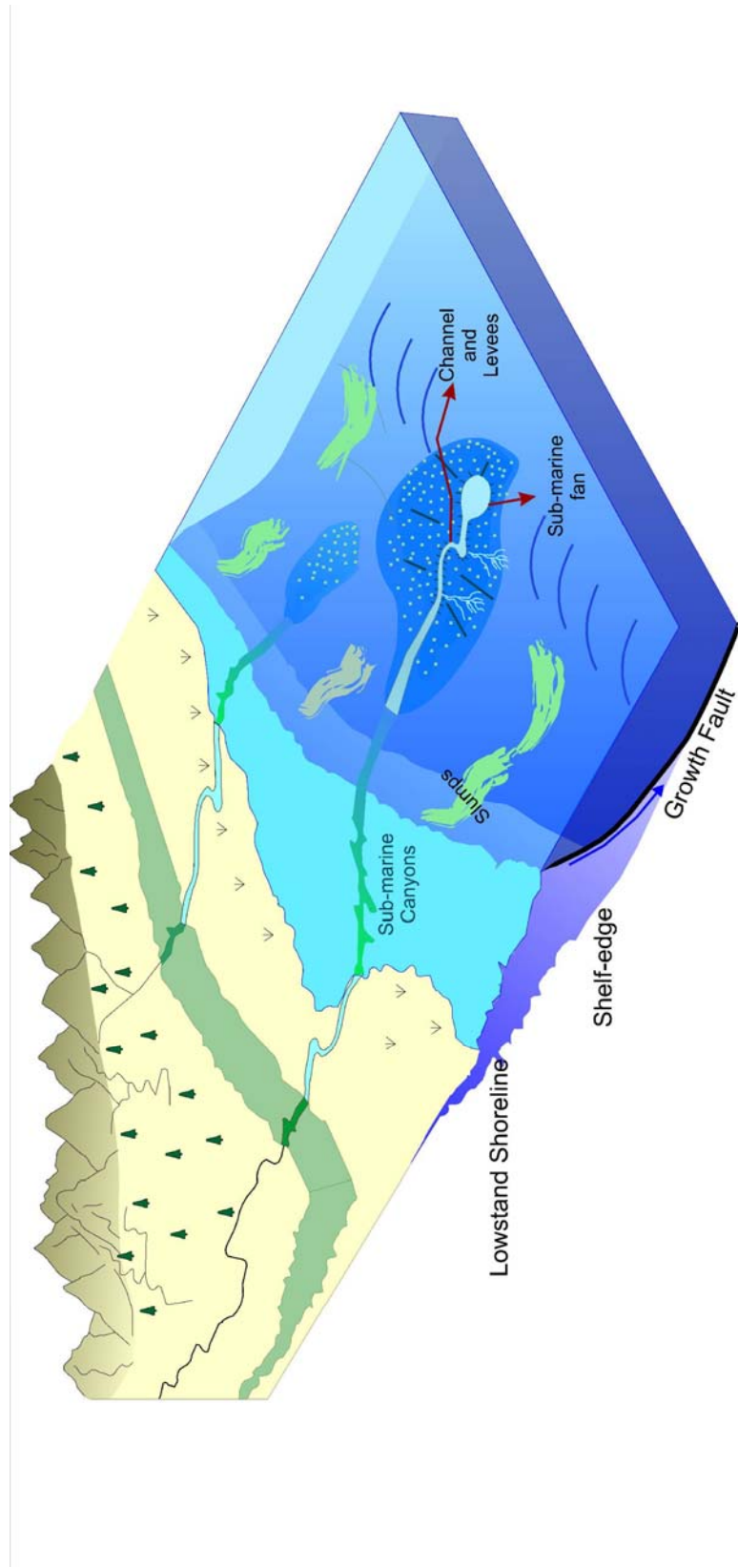


Figure 2.25 The figure depicts the three-dimensional depositional model of the Middle-Late Eocene Hamitabat Formation, which is composed of alternation of gray color sandstone, siltstone and dark color shale beds, deposited in slope setting.

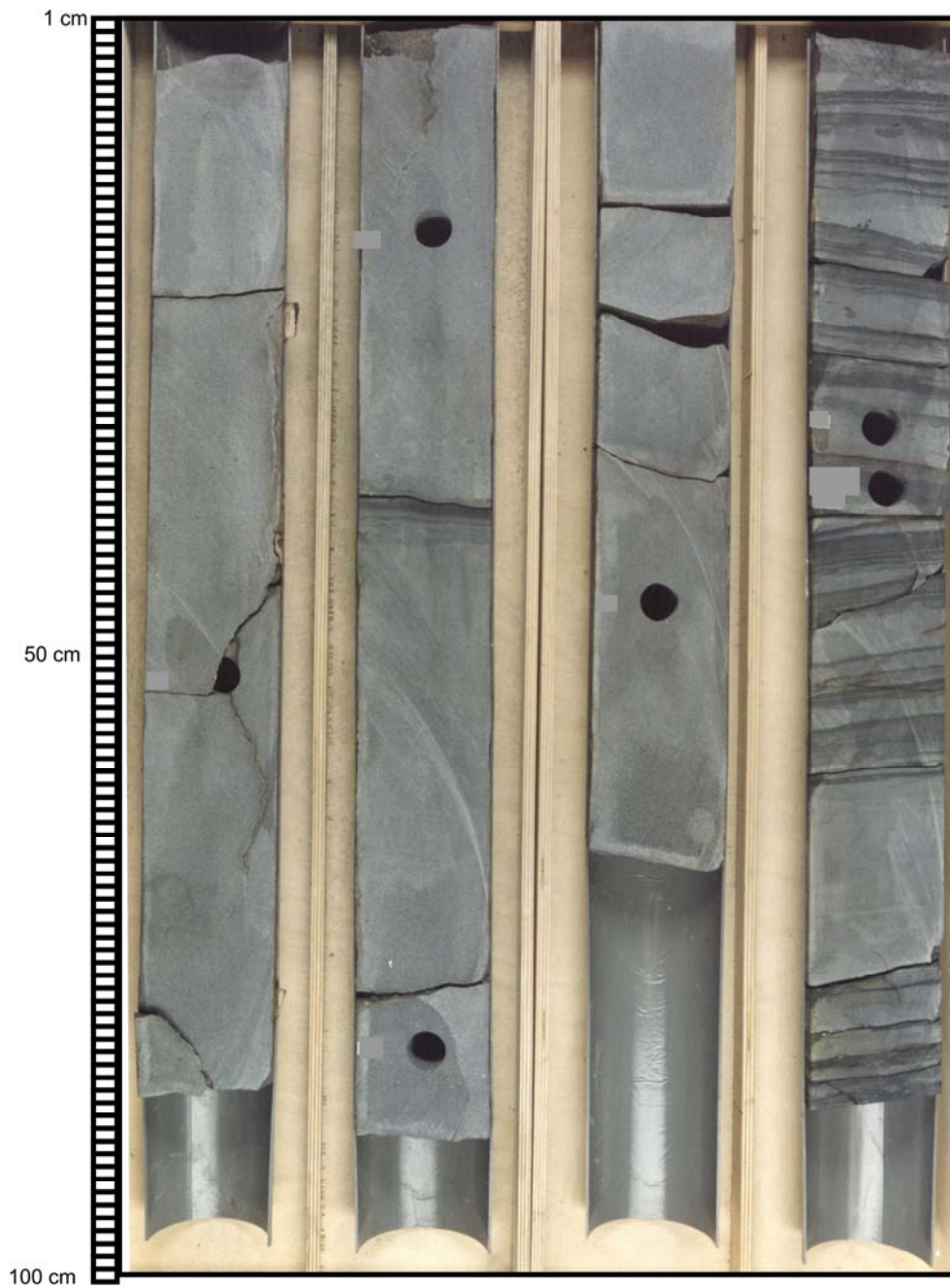


Figure 2.26 The core photograph was selected from the Hamitabat Formation in the KY-2 well. The cored interval is composed of sandstone and thin shale beds, indicating middle sub-marine fan model of Normark (1978).

2.4.2 Middle Eocene-Lower Miocene Interval

Koyunbaba Formation

Koyunbaba Formation was firstly identified by Krausert and Malal, (1957). The outcrops extend along the southern flanks of the Istranca Mountains in the north of the Thrace Basin (Kasar, 1987) (Figure 2.1).

Koyunbaba Formation is underlain unconformably by the metamorphic basement rocks of the Istranca Massif and overlain by the Soğucak Formation with a gradual contact (Figure 2.27). The formation is predominantly composed of pebbles and sandstones, and marl, clay, carbonate and mega blocks of the basement. The deposition starts with basal conglomerates and grades upward into pebbly sandstone, siltstone sandy limestone lithologies. These lithologies are the products of shallow marine environment triggered by the Middle-Late Eocene transgression (Turgut and Eseller, 1999). Koyunbaba Formation is observed along the southern flanks of the Istranca Mountains as well sorted, massive sandstone interval (Figure 2.28). These features were interpreted as beach deposits. Koyunbaba Formation is deposited in various thicknesses related to existing paleotopography. The integration of well-log and seismic data interpretations in this study revealed that the Koyunbaba Formation was observed in very thin thicknesses on paleohighs.

The age of Koyunbaba Formation has been determined as Middle-Late Eocene on the basis of palinological data from drilled wells (Siyako, 2006).

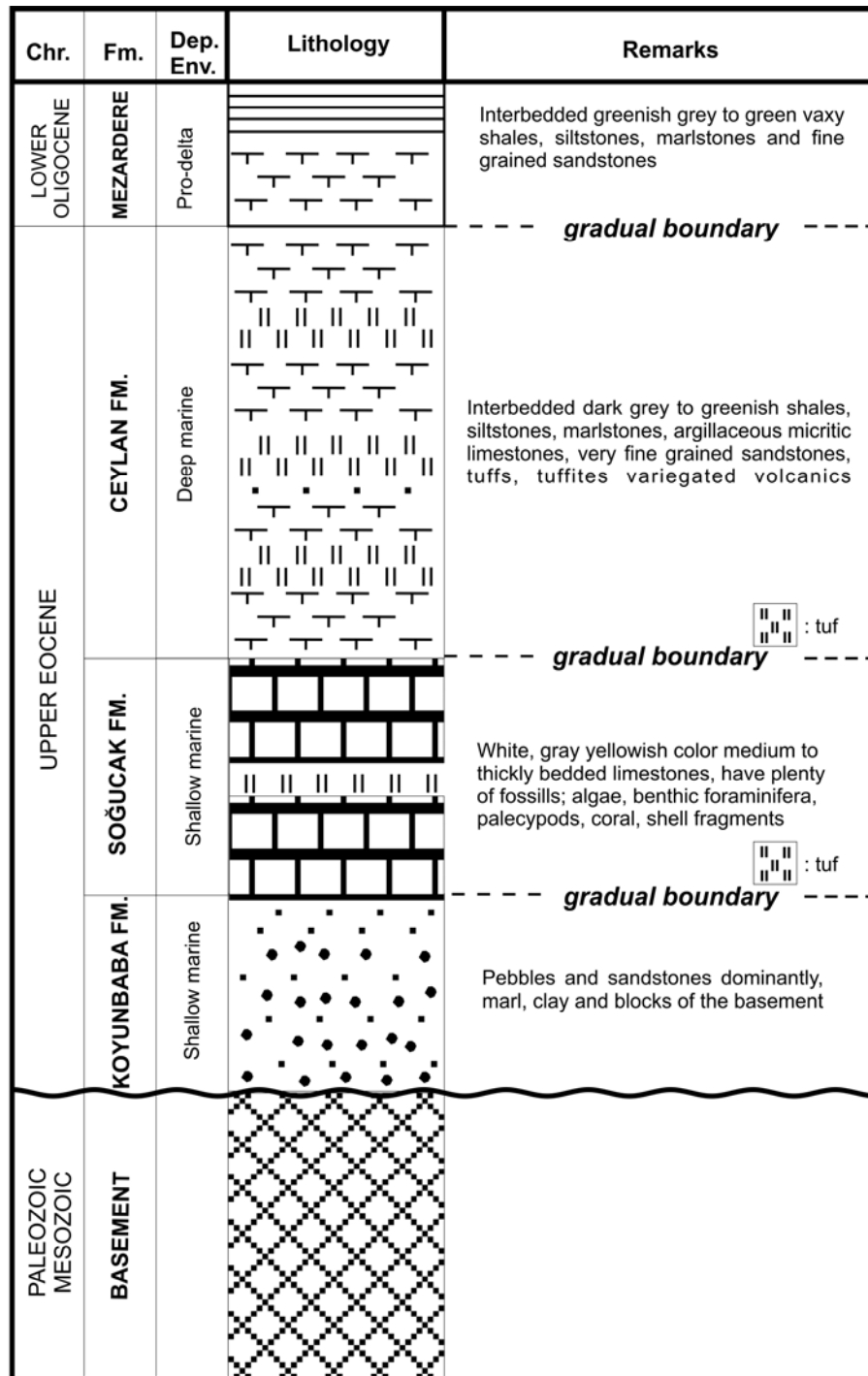


Figure 2.27 A simplified stratigraphic section through the northern shelf of the Upper Eocene sedimentary succession (from Turgut and Eseller ,1999).



Figure 2.28 Koyunbaba Formation is exposed along the southern flanks of the Istranca Mountains. The well sorted, massive sandstone interval was interpreted as beach deposits. The photo was taken near the Hacifakilli village.

Soğucak Formation

Soğucak Formation was firstly identified by Holmes (1961). The formation overlies the Koyunbaba Formation on the northern shelf with a gradual contact (Kasar, 1987) (Figure 2.27) and the Hamitabat Formation in the central parts of the basin unconformably. If Koyunbaba Formation is not present, it overlies the metamorphic rocks of the basement unconformably. In the southern part of the Thrace Basin, it overlies the Fiçitepe Formation unconformably (Figure 2.29). Soğucak Formation shows gradual contacts with the overlying Ceylan (Figure 2.29) and in some places with the Mezardere Formations.

Soğucak Formation is mostly composed of neritic carbonates and reefal bodies and divided into nine microfacies: boundstone, bioclastic packstone, bioclastic wackestone, grainstone, nummulitic packstone-grainstone, lithoclastic-bioclastic packstone of microbreccia conglomerate, peloidal wackestone-packstone, platy algal wackestone and pelagic lime-mudstone (Atalık, 1987; Çubukçu and Erten, 1987). Limestones are in white, gray, yellowish color, mid to thickly bedded, hard with vuggy porosity and have plenty of fossils (Siyako, 2006). According to detailed microfacies analysis on the basis of cores (Atalık, 1987), various depositional environments; open shelf, shelf margin and restricted shelf or lagoon were defined. Open marine environment comprises slope and deep marine deposits, shelf margin is characterized by reefal developments, nummulites banks and the platform sand.

Age	Fm	T (m)	Lithology	Remarks	Environment
OLIGOCENE	Upper	A.Burnu	100	Brownish grey color, polygenic, grain supported, poorly sorted, medium to coarse grained pebblestones	Fluvial
	Middle	Osmançık	800	Grey beige color, thin to medium bedded, thin to medium grained bioturbated, trough cross bedded sandstones with macro shell fragments	Deltafront Deltatop
	Lower		600	Greenish brown color, thinly bedded shales with plant remnants	Prodelta Deltafront
EOCENE	Upper	Ceylan	800	Grey-greenish gray color, medium to thickly bedded, andezitic, lithic-vitric tuffs	Deep Marine Prodelta
	Middle	Soğucak	75	Grey-greenish gray color, thinly bedded, laminated shales	Shallow Marine
	Lower	Fiçitepe		Brownish yellow color, medium to thickly bedded, thin to medium grained, medium sorted sandstones Bouma sequence observed Grey beige color, medium bedded, fractured, reefal limestones with plenty of fossils	

Figure 2.29 Generalized stratigraphic column of the Middle Eocene-Late Oligocene units of the Gelibolu Peninsula (from Temel and Çiftçi, 2002).

Soğucak Formation facies is mostly controlled by the interaction of the relative sea-level change, basin physiography and paleo-topography. As the northern and southern shelves and paleohighs were the suitable places for limestone deposition (Figure 2.30), deep troughs at the center of the basin had become the site of argillaceous biomicrite and detrital micrite deposition for the Soğucak Formation (Turgut et al., 1987). These second type facies are dark gray in color, tight and dense.

As a result of the continued shoreline transgression, the age of the Soğucak Formation ranges between the Late Lutetian and the Early Oligocene (Atalık, 1992). The lower Oligocene age has been assigned by Sirel and Gündüz (1976).

Ceylan Formation

Ceylan Formation was firstly described by Ünal (1967). Its outcrops extend widely south of the Ganos Fault, around Mürefte and Şarköy in the south of the Thrace Basin, north of Mecidiye in southwest Thrace, between Terkos and Çekmece lakes in the east of the Thrace Basin (Keskin, 1974) (Figure 2.1). The Formation overlies gradually the Soğucak Formation, except Bozcaada in the Eagean Sea and Karaburun in the Black Sea coast, where the boundary is unconformable. It is overlain by the Mezardere Formation also with a gradual contact (Figure 2.15 and Figure 2.29).

Ceylan Formation is composed of interbedded dark gray to greenish shales, siltstones, marlstones, argillaceous micritic limestones, very fine

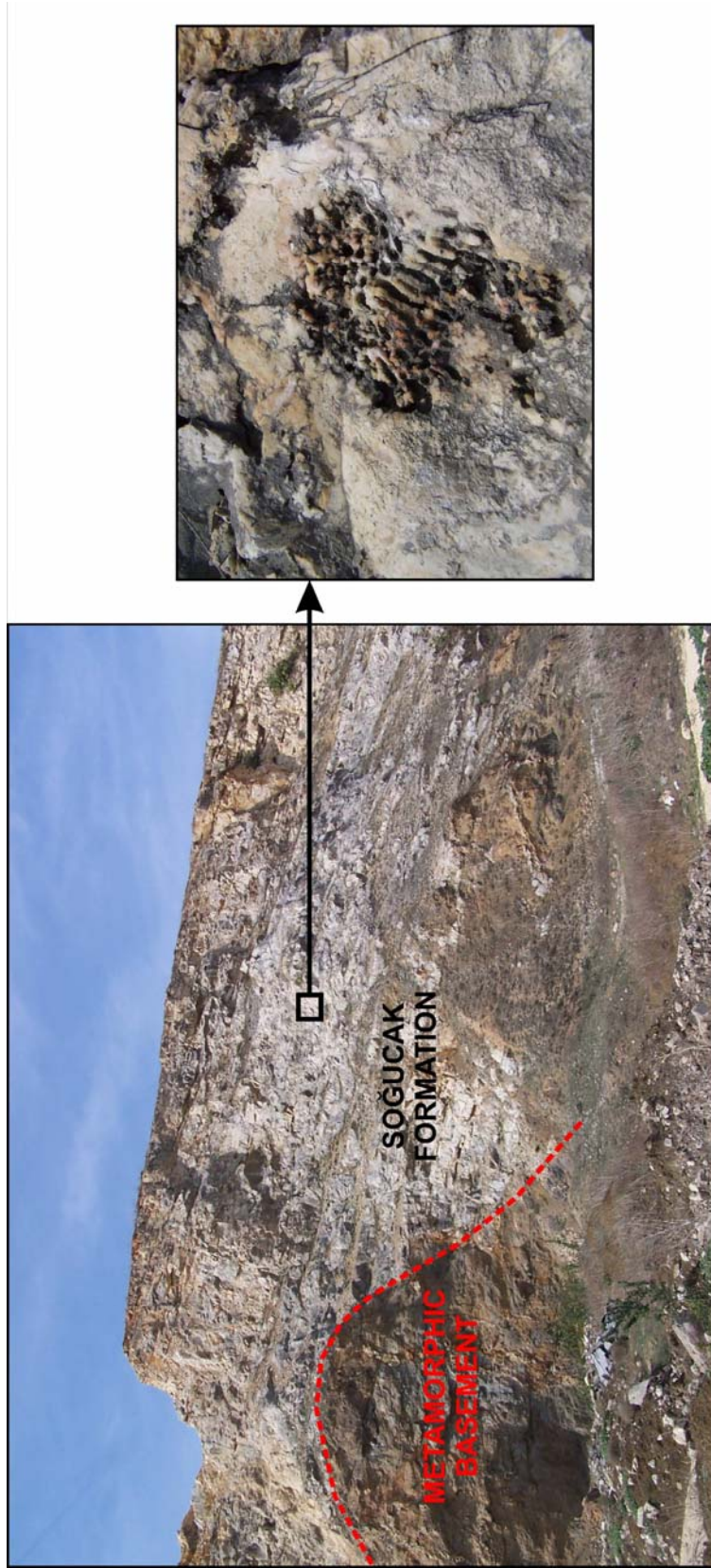


Figure 2.30 Soğucak Formation overlies the metamorphic basement near Çatalca (4553772N, 623529 E). It is mostly composed of neritic carbonates and reef facies, which is rich in corals (on the right).

grained sandstones, tuffs, tuffites and variegated volcanics (Figure 2.31). The complete and missing Bouma sequences and soft sediment deformation (Figure 2.32) are observed within turbiditic facies (Siyako, 2006). As shallow marine facies are deposited in shelves, deep sea turbidites are dominant at the center and slope of the basin. Thick accumulations of sediments in the central basin dominated subsidence with thick tuff flows and active volcanism in extensional tectonic regime (Siyako, 2006). The thickness of some tuff and tuffite layers reaches up to 400 m. Marly intervals have rich planktonic foraminiferal content. Samples which were taken from these intervals exhibit well preserved and abundant planktonic foraminifera. This has used as an evidence of deepening of the basin (Erenler, 1987).

The age of the Ceylan Formation is Late Eocene-Early Oligocene based on the palynology, foraminifers and nannoplanktons studied by Alişan (1985), Gerhard and Alişan (1987), Batı et al. (1993).

Mezardere Formation

The formation was first described by Ünal (1967). The outcrops of Mezardere Formation extend from north of Keşan to Tekirdağ in the south of Thrace Basin (Figure 2.1). It overlies Ceylan and Keşan Formations and underlies the Osmancık Formation with gradual contacts (Figure 2.15 and 2.29).



Figure 2.31 Ceylan Formation is mostly composed of thin bedded, fine-grained sandstone, shale, marl and tuffs, deposited in deep sea environment. The photo was taken near Tayfur village, in the Geilbolu Peninsula at (4470820 N, 456527 E) to the east.



Figure 2.32 Soft sediment deformation is one of the characteristic features in the turbiditic section of the Ceylan Formation, near Tayfur village, in the Gelibolu Peninsula. The photo was taken from (4470820 N, 456527 E) to the east.

Mezardere Formation is composed of interbedded greenish gray to green vaxy shales, siltstones, marlstones and fine-grained sandstones (Turgut et al., 1987) with sporadic tuffite intercalations. Dominant shale lithologies indicate that the Mezardere Formation is deposited in shallow to moderately deep marine environment as a part of prodelta facies of the Yenimuhacir Group (Figure 2.33). Figure 2.34 exhibits a view from the Mezardere Formation, which is mostly made up of vaxy, gray color shale lithologies.

Sandstone dominated interval within shale dominated Mezardere Formation is named as the Teslimköy Member. This sandstone dominated interval was interpreted as offshore bars (Temel and Çiftçi, 2002).

A Late Eocene-Early Oligocene age has been assigned to the Mezardere Formation on the basis of palynologic studies (Alişan and Gerhard, 1987; Ediger and Alişan, 1989; Batı et al., 1993).

Osmancık Formation

The formation was first introduced by Holmes (1961). The outcrops of Osmancık Formation extend from Keşan to Istanbul along the Marmara Sea in the south of Thrace (Figure 2.1). It is underlain by the Mezardere Formation and overlain by the Osmancık Formation with gradual contacts (Figure 2.29).

Osmancık Formation is composed of alternating mudstones and sandstones with subordinate conglomerates, limestones, coal and tuffite

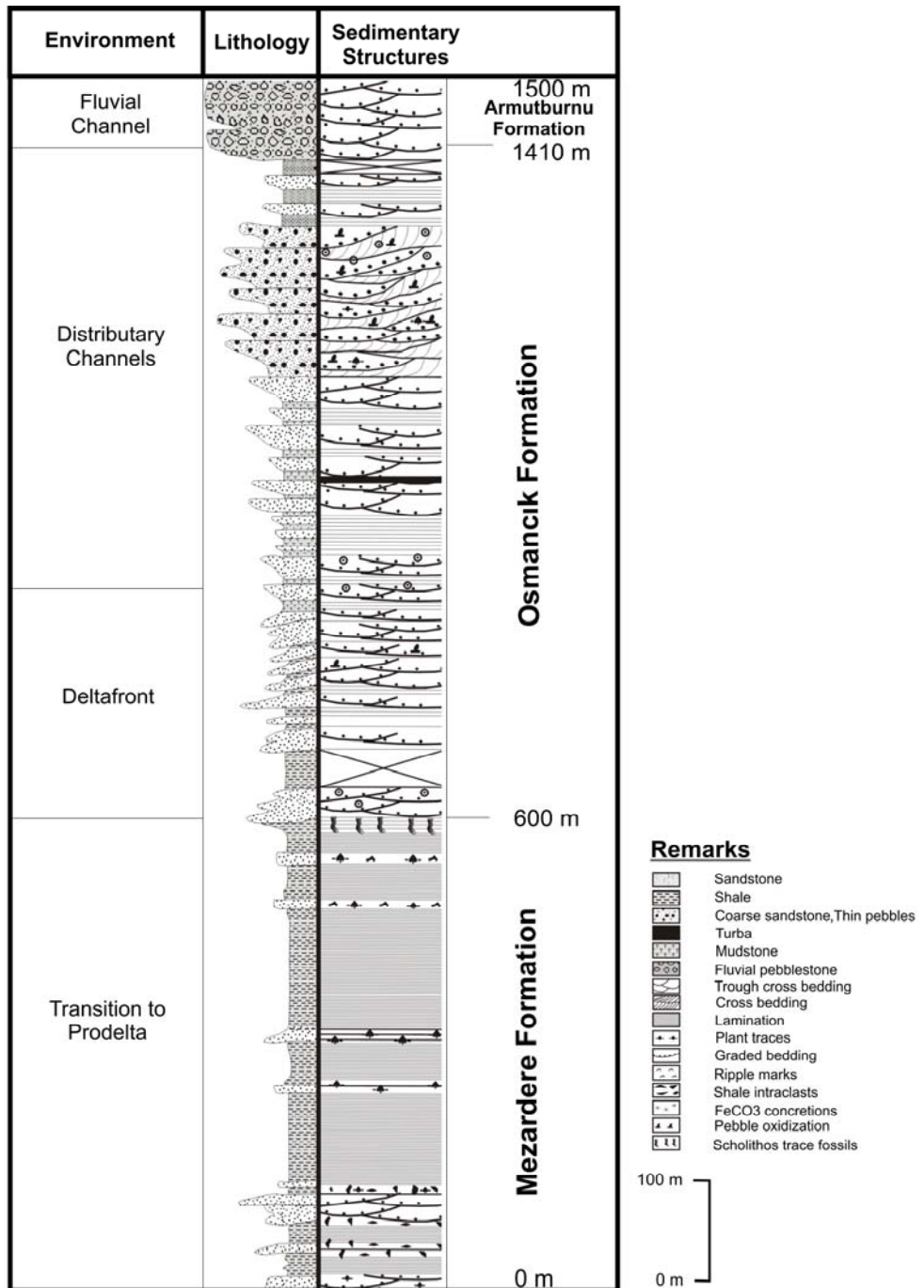


Figure 2.33 Simplified measured stratigraphic section through the Mezardere, Osmancık and Armutburnu formations in Küçükanaftalar village, Gelibolu Peninsula. (from Temel and Çiftçi, 2002).



Figure 2.34 A view from the Mezardere Formation, which is mostly made up of waxy gray color shale lithologies. The photo was taken in a clay quarry near the western exit of Barbaros village (45252'13 N, 536200 E).

beds (Temel and Çiftçi, 2002; Figure 2.33). Mudrocks include light gray mudstones, greenish gray to dark gray mudstones, greenish gray and light to dark gray shales, and light gray siltstones. Sandstones are light gray to gray and very fine to coarse-grained (Atalık, 1992). The most common sedimentary structure is trough and planar type cross stratification. In addition, ripple marks, convolute bedding, flaser bedding, lenticular bedding, ball and pillow structures, load and flute casts are also observed within the Osmancık Formation (Atalık, 1992). Figure 2.35, 2.36, 2.37 show three photos from Osmancık Formation. In these photos, different facies of the Osmancık Formation were displayed.

Well and seismic reflection data suggest that the total thickness of the Osmancık Deltaic System reaches up to 800 to 1000 m. The type section of the Osmancık Formation measured by Atalık (1992) at Yağmurca outcrop is 780 m.

Seismic reflection data is used to subdivide the deltaic system of the Osmancık Formation into parasequences using the geometric relationship between reflection terminations and seismic surfaces (Figure 2.38). Each seismically resolvable parasequence is bounded by flooding surfaces which are demonstrated on seismic sections as high amplitude, continuous and inclined reflections. These reflections were first recognized as two-dimensional geometric indications of deltas by Rich (1951) and named as clinoforms. Paleoenvironmentally, the shallowest portion of clinoforms correspond the boundary between terrestrial and marine environments, and



Figure 2.35 A view from the Osmancik Formation, which is located at two km south of Paşayigit village. Osmancik Formation is composed of sandstone and pebblestone dominated by distributary channel fill deposits. The photo is taken from (4531737N, 469411 E) to the east.



Figure 2.36 A close view of the Osmancik Formation. Distributary channel fill is mostly composed of pebbles.

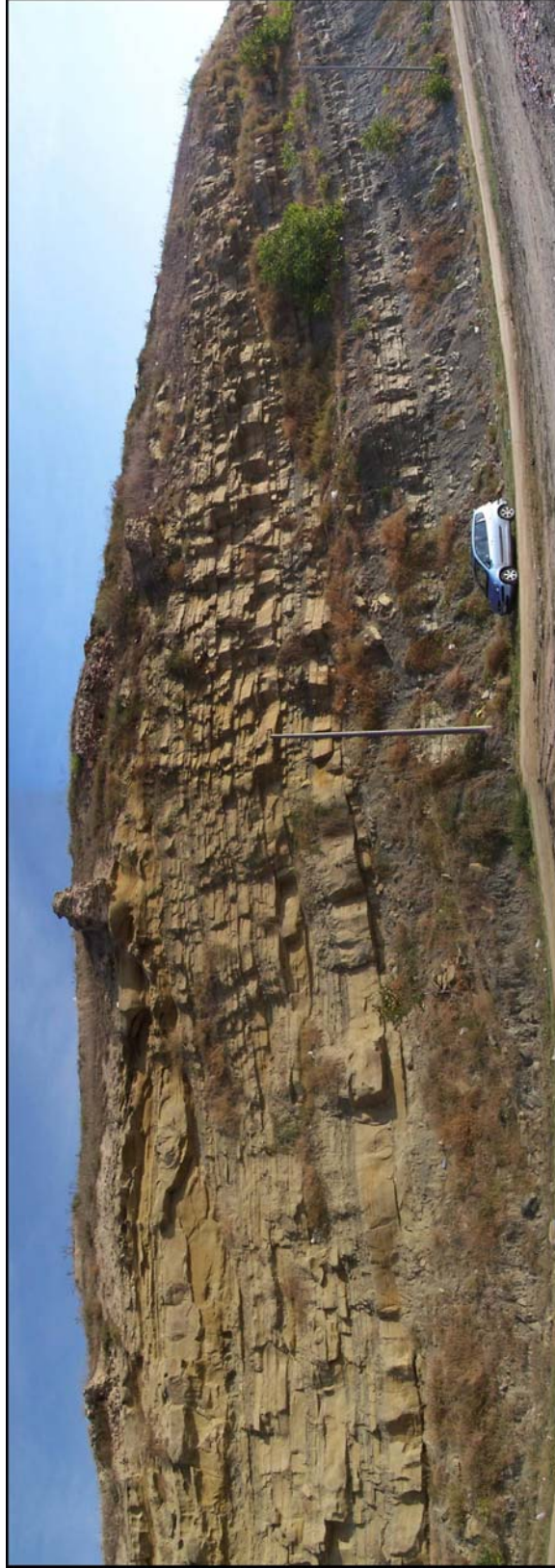


Figure 2.37 A typical fluvio-deltaic coarsening upward trend in the Osmancik Formation can be observed near coast of Marmara Ereğlisi. Grain size and thickness of the beds increase from right to left. The photo was taken from (4535500 N, 580149 E) to the east-northeast.

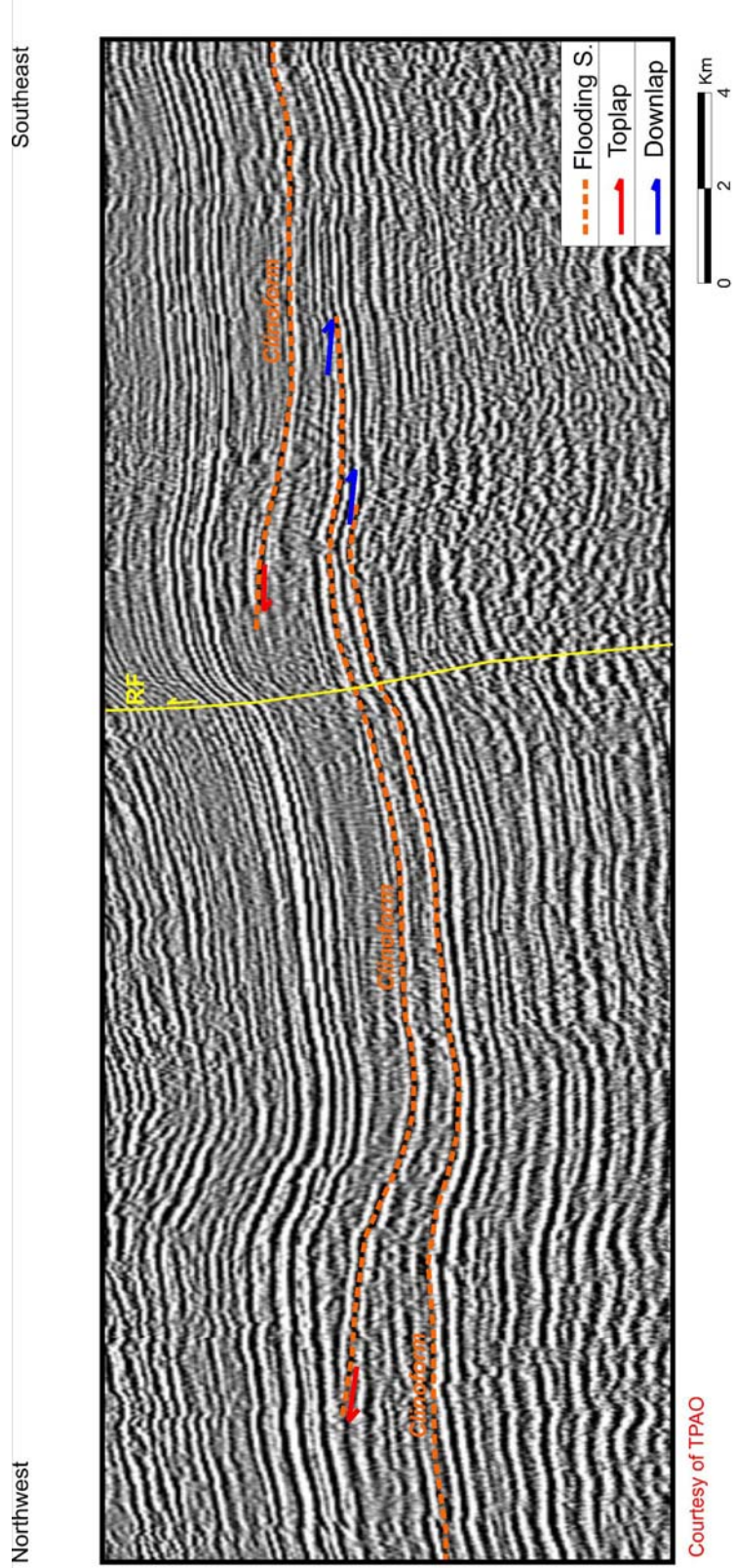


Figure 2.38 Osmancık Formation is composed of progradational deltaic parasequences. On seismic sections, the bounding flooding surfaces of the deltaic lobes are represented by high amplitude, continuous reflections (clinofolds). Poorly continuous, low amplitude seismic packages between flooding surfaces indicate sand dominated intervals. RF: Reverse Fault.

its deepest portion, the boundary between nearshore and offshore environments (Pigott, 1995). Sedimentologically, clinofolds represent a broad transition zone between mechanical and suspension processes, i.e. sand deposited at the distributary mouthbar to the silts and clays of the delta front facies to the muds deposited at the prodelta facies (Pigott, 1995). Sand dominated deltaic lobes are demonstrated by low amplitude, poorly continuous seismic packages.

The age of the Osmançık Formation was dated as Early to Late Oligocene on the basis of stratigraphic relations and palynological data (Lebküchner, 1974; Alişan and Gerhard, 1987; Gerhard and Alişan, 1987; Turgut et al., 1987; Atalık, 1992; Turgut, 1997). The lignite intervals within the delta plain were also dated as Late Oligocene.

Danişmen Formation

Danişmen Formation was firstly identified by Boer (1954). Its outcrops extend from north of Keşan to Istanbul in the south of the Thrace Basin and reaches towards the Istranca Mountains in valleys (Umut et al., 1983) (Figure 2.1). It is underlain by the Osmançık Formation with a gradual contact and overlain by the Ergene Formation with an angular unconformity (Figure 2.15). Figure 2.39 exhibits that Danişmen Formation is overlain by the Miocene Ergene Formation with an angular unconformity.

Danişmen Formation is composed of interbedded shales, marlstones, siltstones, pebblestones and various coaly layers (Figure 2.40). Shales are

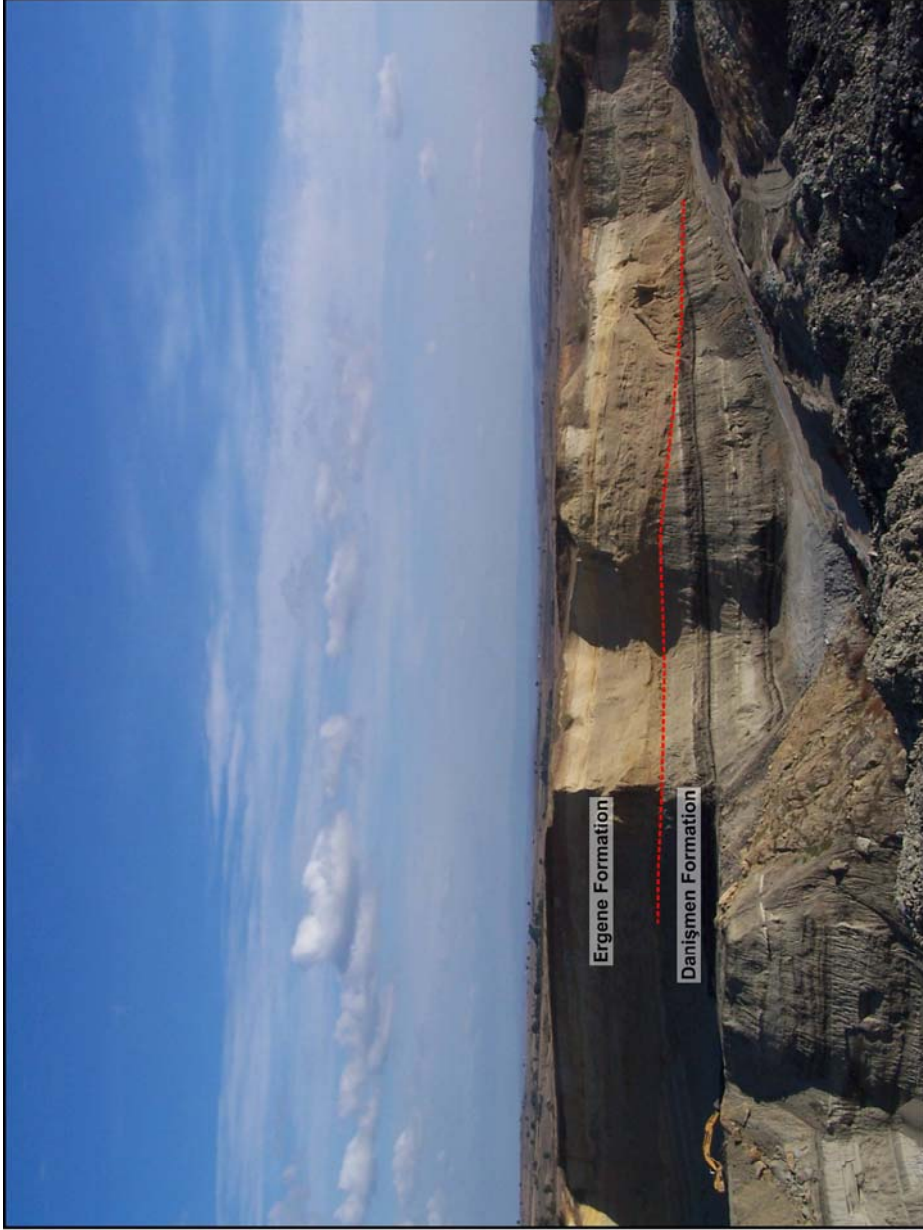


Figure 2.39 Danişmen Formation is overlain by the Miocene Ergene Formation with an angular unconformity (red color). The photo was taken in an open lignite mine near Yörücek village at (4538755 N, 492536 E) to the east-northeast.



Figure 2.40 Danişmen Formation is composed of siltstone, shale and coal layers deposited in delta top environment. The photo was taken in an open lignite mine near Yörücek village.

greenish to gray, varvy, laminated and abundant plant material and fish scales. Silty sandstones are light gray to gray color, very fine-grained, clayly, angular to subangular, poorly sorted and partly carbonate cemented (Turgut et al., 1987). These lithologies are the products of lagoon, swamp, flood plain and fluvial environments.

A Late Oligocene-Early Miocene age has been assigned to the Danişmen Formation by Gerhard and Alişan (1987), Atalık (1992), Batı et al. (1993) based on palynological data.

CHAPTER 3

PRINCIPLES OF RESEARCH METHODS

This chapter reviews the principles of research methods stated in Chapter 1 and their use in sequence stratigraphic framework. It has two major parts. First part focuses on the principles of seismic reflection and well-log methods. Second part focuses on sequence stratigraphic terminology.

3.1 Seismic Reflection Principles

The study section was subdivided into depositional sequences (Mitchum et al., 1977) and related systems tracts (Van Wagoner et al., 1988) based on two-dimensional seismic reflection data set. Seismic reflection is a method of exploration geophysics that uses the principles of seismology to estimate the properties of the subsurface from reflected seismic waves (Sheriff, 2002). When a seismic wave encounters an interface, three phenomena can occur: reflection, refraction and conversion. Reflection is defined as the energy or wave from a source that has been reflected (returned) from an acoustic impedance contrast (reflector) or series of contrasts within the earth (Sheriff, 2002) (Figure 3.1).

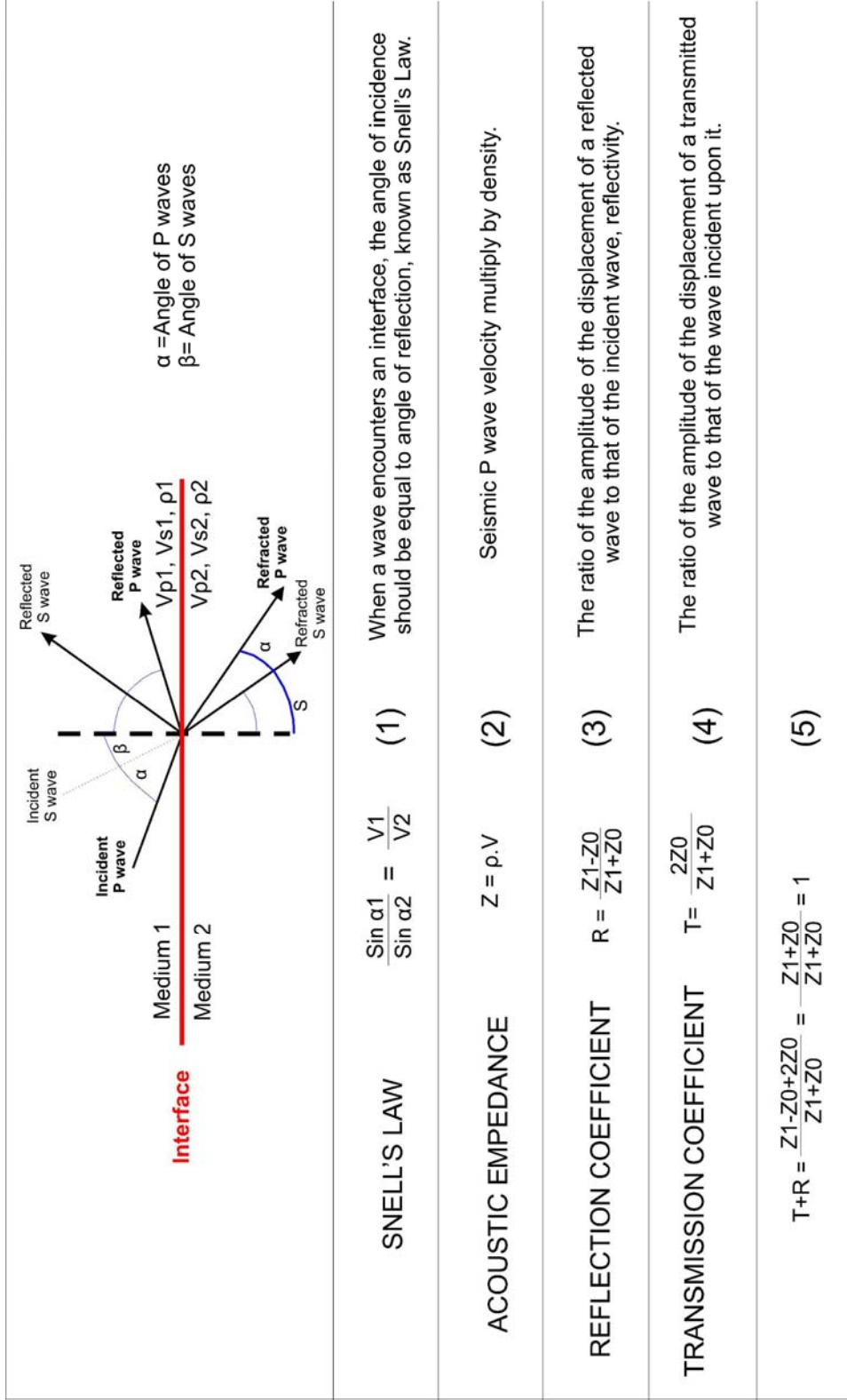


Figure 3.1 The formulas stated above are the key definitions of seismic reflection methods. The definitions were taken from Sheriff, 2002.

When a seismic wave encounters an interface between two materials (lithologies) with different acoustic impedances, some of the energy in the wave will be reflected, while some of the energy will continue (transmitted) through the interface. By observing changes in the strength of reflectors, contrasts in acoustic impedances can be predicted and used to infer changes in the properties of the rocks at the interface, such as density and elastic modulus.

In order to highlight the acoustic impedance properties of the studied interval, sonic and density log responses of the wells were analyzed in the study area (Figure 3.2). The analysis revealed that there were three types of important surfaces, which were detected by strong acoustic impedance contrasts. The interface between sand and shale lithologies exhibits strong acoustic impedance contrast. Especially, the interfaces which correspond to the low velocity flooding surfaces in the Deltaic System of the Osmancik Formation were distinguished by strong acoustic impedance contrast. On seismic sections, they were demonstrated by high amplitude, continuous and inclined reflections, called clinoforms. Second, within the Late Eocene clastic-carbonate mixed system, the surfaces between limestone and marl lithologies were also detected by strong acoustic impedance contrasts. Due to their high velocity content, limestone intervals were easily defined by high amplitude, continuous reflection(s) and distinguished from the overlying and the underlying marl dominated intervals. Third, tuff and marl alternations of

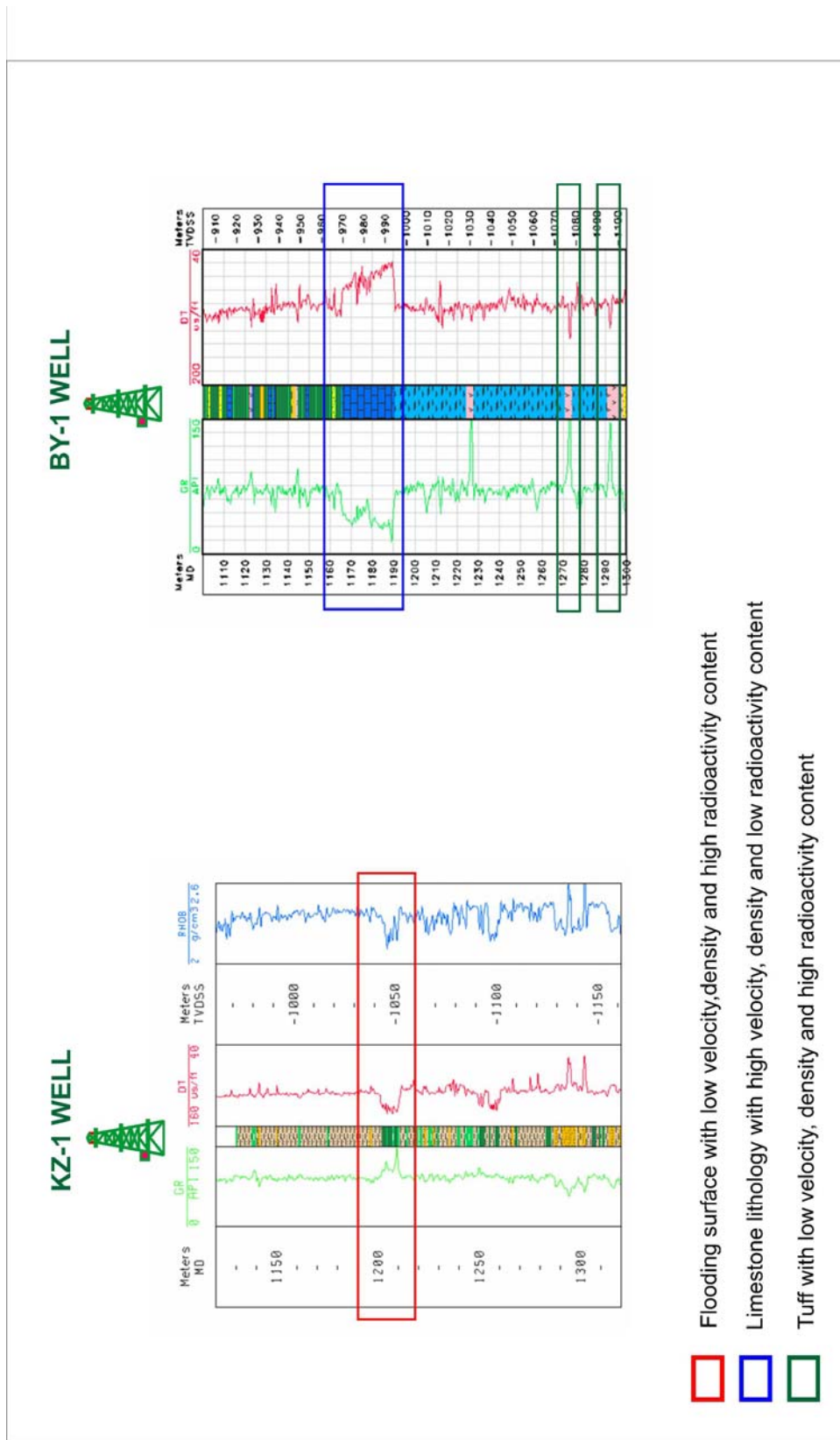


Figure 3.2 The figure shows diagnostic sonic, gamma ray and density log responses of different lithologies from the KZ-1 and BY-1 well. Three important interfaces were detected with strong acoustic impedance contrasts (velocity*density): flooding surfaces, limestone and marl interface, and tuff alternating with the underlying and the overlying lithologies

the Ceylan Formation also exhibited strong acoustic impedance contrast against the overlying and underlying lithologies.

In seismic reflection method, the amplitudes of the movement of the ground with time are measured. Such a measurement is called a seismogram or a seismic trace. The properties of the subsurface (density and seismic velocity) determine the acoustic impedance of a layer. From these impedances, the reflectivity function of the interfaces can be derived (Figure 3.1). This function is convolved with the signal of the seismic wave. The result is a seismic trace, on which also noise is added. There are two important waveforms; minimum phase wavelet and zero phase wavelet (Figure 3.3). The polarity of a seismic data set is called normal when a low impedance medium over a high impedance medium gives a peak at the interface. For example, the interface between the Oligocene low impedance shale and the high impedance sand or the Eocene low impedance marl and a high impedance limestone interval were characterized by a peak during the study. The seismic data used in this study was processed with zero phase wavelet (Figure 3.3).

Seismic display is a graphic hard-copy representation of seismic reflection data (Sheriff, 2002). There are several ways to display seismic traces; wiggle (W), variable area (VA), variable density (VD) and wiggle variable area (WVA) (Figure 3.4). The type of display is preferred depending on the processing sequence and the number of traces. In this study, the

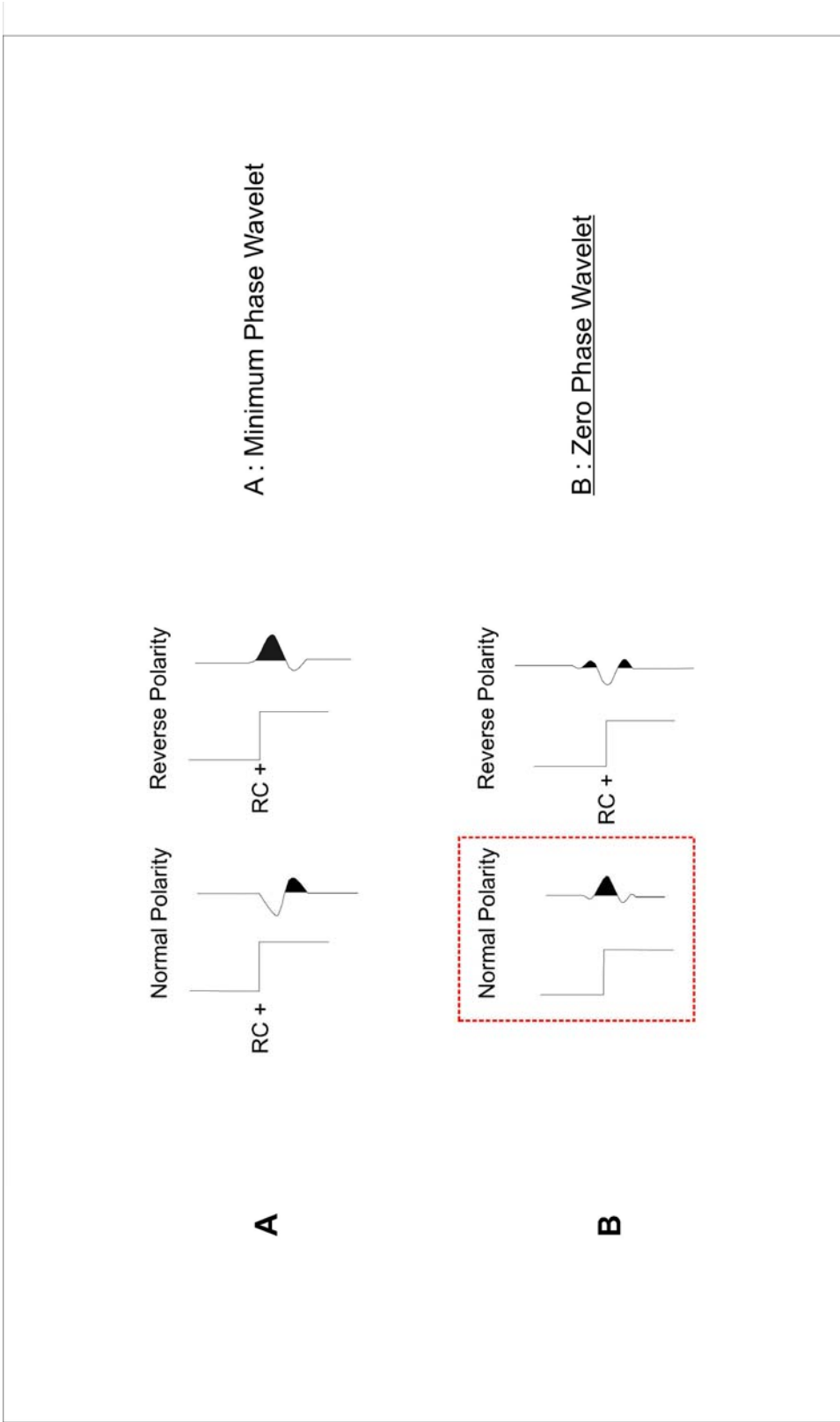


Figure 3.3 A seismic pulse usually consists of only a few cycles. It is time domain reflection shape from a single positive reflector at normal incidence. The figure shows two most important wavelet types used in seismic data processing (Sheriff, 2002). In this study, the seismic data was processed with zero phase wavelet and has a normal polarity, shown in red rectangle.

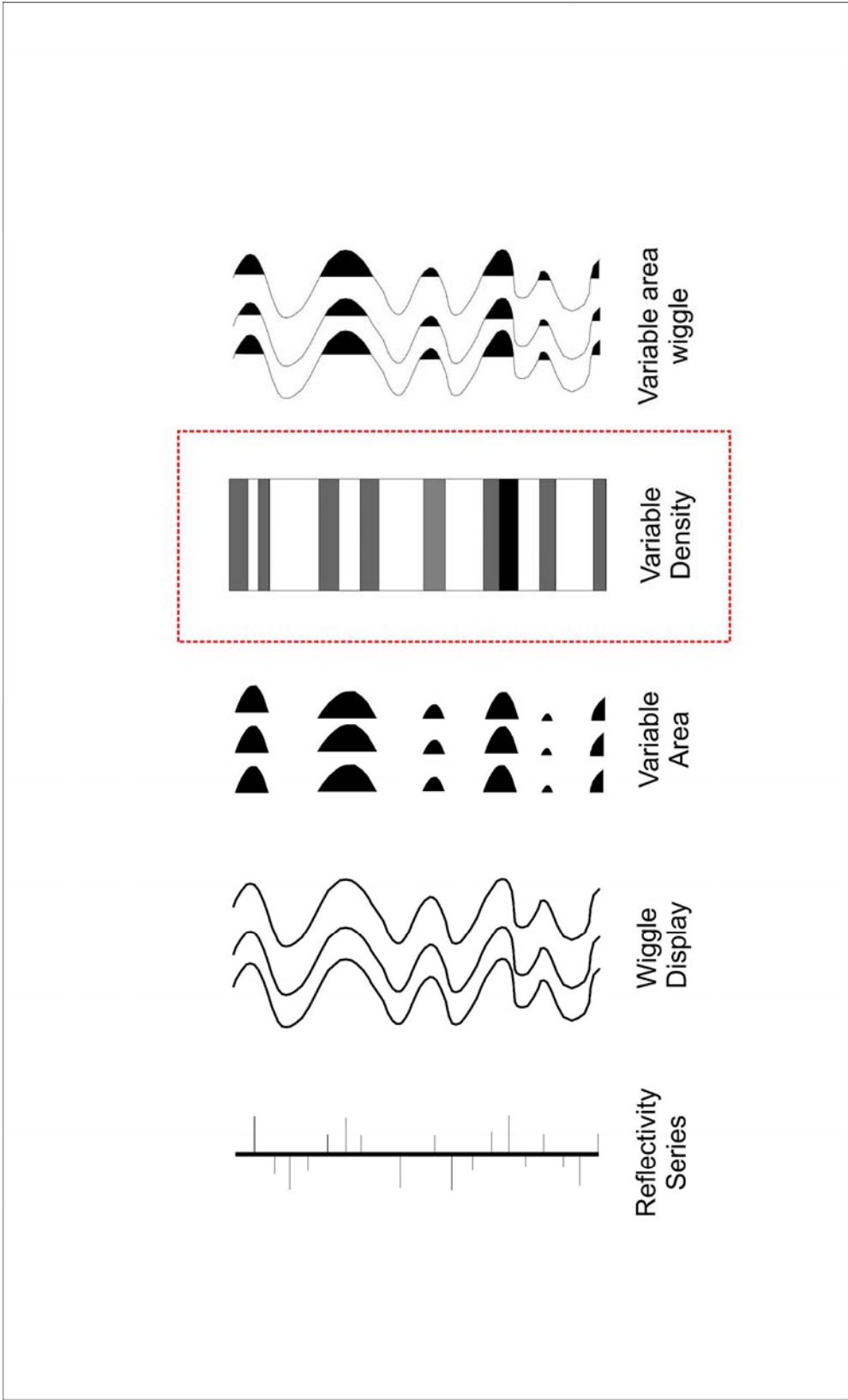


Figure 3.4 Different seismic reflection data display types; wiggle, variable area and variable density. In this study, seismic lines were demonstrated in a variable density display (red rectangle), which was preferred for seismic facies analysis.

seismic lines were demonstrated in a variable density display, which was preferred for seismic facies analysis.

In wiggle display, the amplitude is depicted as a curve for a simple representation. Wiggle-Variable area display is used to trace the seismic horizon line-ups. The right half of the trace is drawn black. Standards by SEG are the positive half of the wave on the right side is colored black, which is called normal polarity. The seismic data used in this study has a normal polarity. Variable area is used when a lot of traces are depicted close to each other, then only the positive half of the traces is plotted. Variable density is used for the interpretation. The amplitudes are often plotted in different greyscales or in colors (variable density). In this way, the differences in amplitudes are more clearly observed.

3.1.1 Resolution

The knowledge of resolution is an important aspect in seismic stratigraphic analysis. It is defined as the ability to separate two features that are close together (Sheriff, 2002). Vertical seismic resolution is a measure of how large an object need to be in order to be seen in seismic. Figure 3.5 compares seismic reflection, well-log and outcrop scale resolution. In seismic reflection method, theoretically (Rayleigh-Kriterium), a layer can be distinguished when it has a thickness of $\frac{1}{4}$ of wavelength (λ). The wavelength is determined by the ratio of the velocity and the frequency of the seismic wave: $\lambda = v / f$. It can be concluded from the formula, the

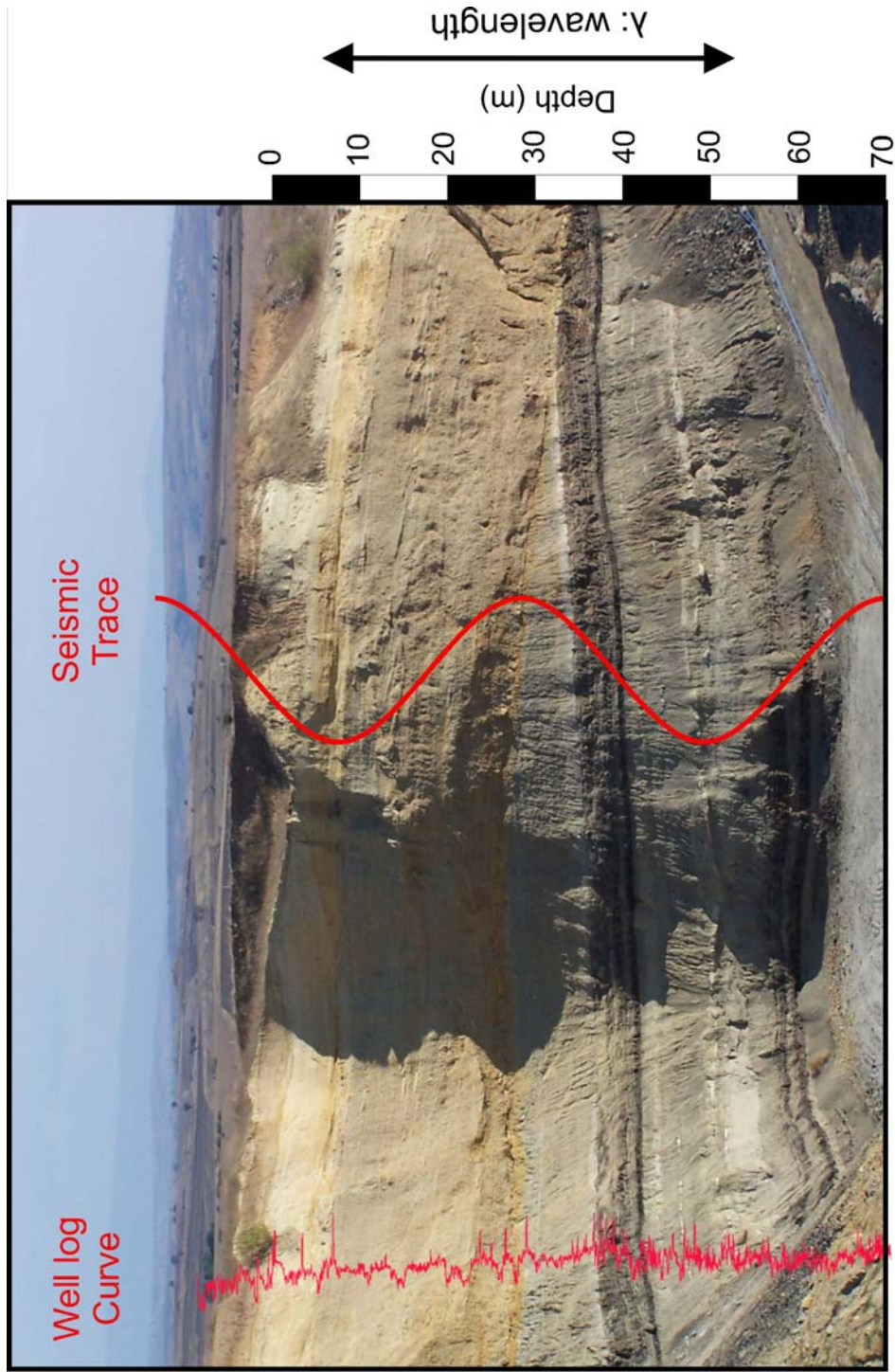


Figure 3.5 The figure compares outcrop, well-log and seismic scale resolution. In seismic reflection method, a layer can be distinguished when it has thickness of 1/4 wavelength theoretically, which is about 10 to 20 m. The photo was taken near Yörücek village in the study area (4538755 N, 492536 E).

higher frequencies increase vertical resolution. Figure 3.6 shows a representative frequency spectrum of seismic reflection data used in this study. The frequency spectrum indicates that maximum frequency is 70 Hz and the average frequency of the seismic data set ranges between 20 and 50 Hz.

It is stated that the vertical resolution is a function of the velocity and the frequency content. For the study interval, the velocity ranges between 2400 and 3400 m/sec. From the above formula, it can be estimated that the beds with 10 to 20 m thicknesses can be distinguished with the seismic reflection method, used in this study.

However, the frequency of the seismic signal will decrease while the velocity and wavelength increase with increasing depth. This means that with increasing depth, the seismic resolution will decrease. Higher frequencies are reflected from relatively shallow reflectors, while the lower frequencies reach deeper. The sediments are becoming more compacted gradually, and therefore the seismic velocity increases with increasing depth. The analysis of sonic log responses from the study area shows the gradual increase in velocity due to post-depositional compaction (Figure 3.7).

3.1.2 Synthetic Seismogram

Synthetic seismogram (or synthetics) is a one-dimensional model of seismic waves traveling through the subsurface. In the study concept, basic

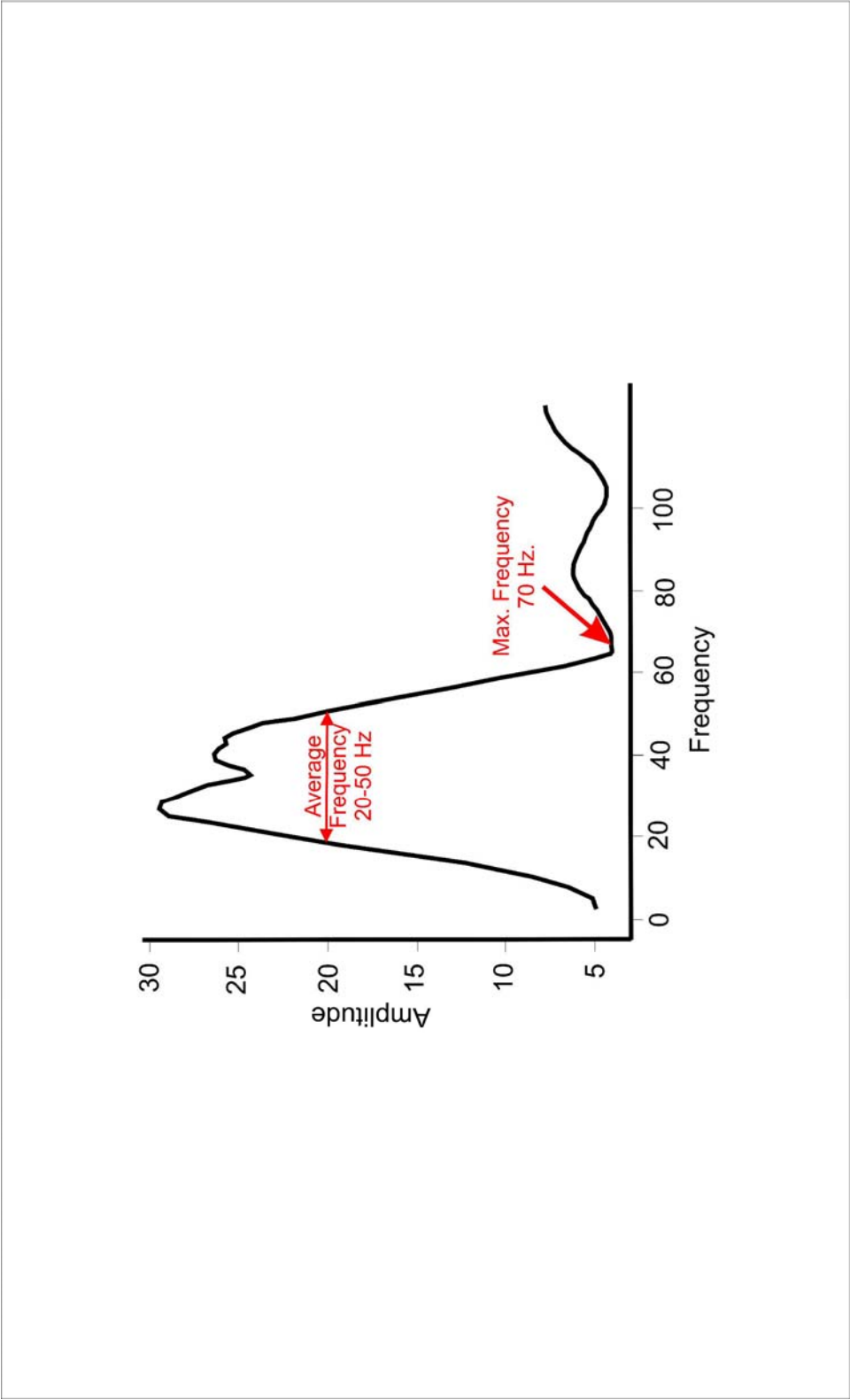


Figure 3.6 The figure shows a representative smoothed frequency spectrum of two-dimensional seismic reflection data, shot in the northwest of the Thrace Basin. Maximum frequency is about 70 Hz and the average frequency ranges between 20 and 50 Hz.

DG-3 WELL

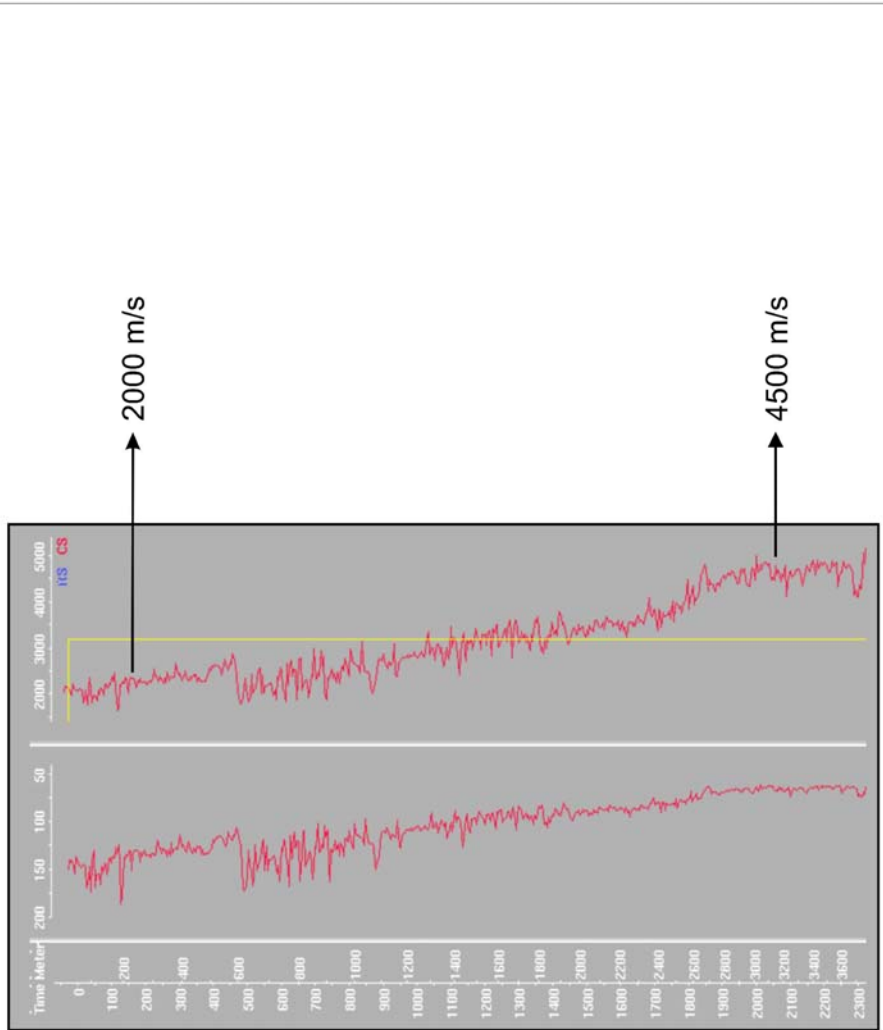


Figure 3.7 The figure shows sonic log data of the DG-3 well. The gradual decrease in slowness or increase in velocity (m/sec) with depth reflects the compaction effect in Tertiary siliciclastic sequence of the Thrace Basin. As near surface velocity is about 2000 m/s, at 3000 m depth the average velocity reaches up to 4500 m/s.

sequence stratigraphic surfaces (sequence boundaries, maximum flooding surfaces, transgressive surfaces) in time domain were converted to geological surfaces in depth domain by synthetic seismograms. In this study, SynTool[®] program of the Openworks[®] applications was run to generate synthetics. First, sonic and density logs were used to compute acoustic impedance (formula-1 in Figure 3.1) and reflectivity (formula-2 in Figure 3.1) at the well location. Once the reflectivity at the well was calculated, the selected wavelet (extracted wavelet) was convolved with the reflection coefficient series to produce synthetic trace. Then, the acoustic log was calibrated with check-shot data. By comparing marker horizons or other correlation points detected on the well-logs with major reflections on the seismic section, the quality of the synthetic trace were improved. Figure 3.8 describes the generation of a synthetic seismogram.

KZ-1 well is one of the wells selected from the study area. This well is located in the south of the Kırklareli city center in the northwest of the Thrace Basin (Figure 1.2) and completed in the Oligocene Osmancık Formation. The well exhibited the high quality of the sonic and density log data sets. After check-shot calibration, high correlation coefficient was estimated between synthetic and real seismic trace (Figure 3.9), and time to depth conversion was successfully accomplished in most of the wells.

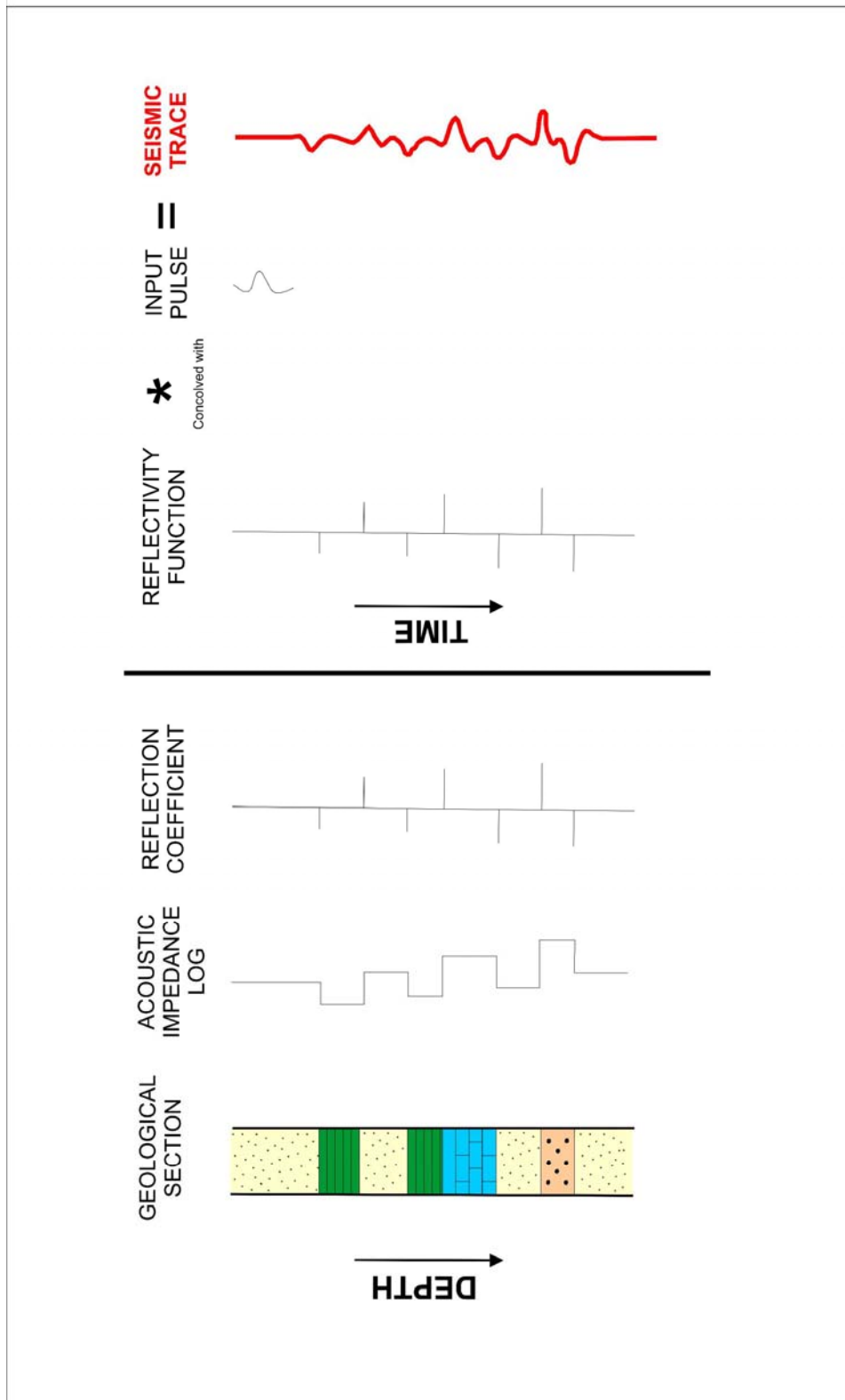


Figure 3.8 Synthetic seismogram is one-dimensional forward modeling from depth section to seismic trace. First, sonic and density logs are used to compute acoustic impedance log and the reflection coefficient. Then, selected wavelet is convolved with reflection coefficient series to produce synthetic trace (red color) (Sheriff, 2002).

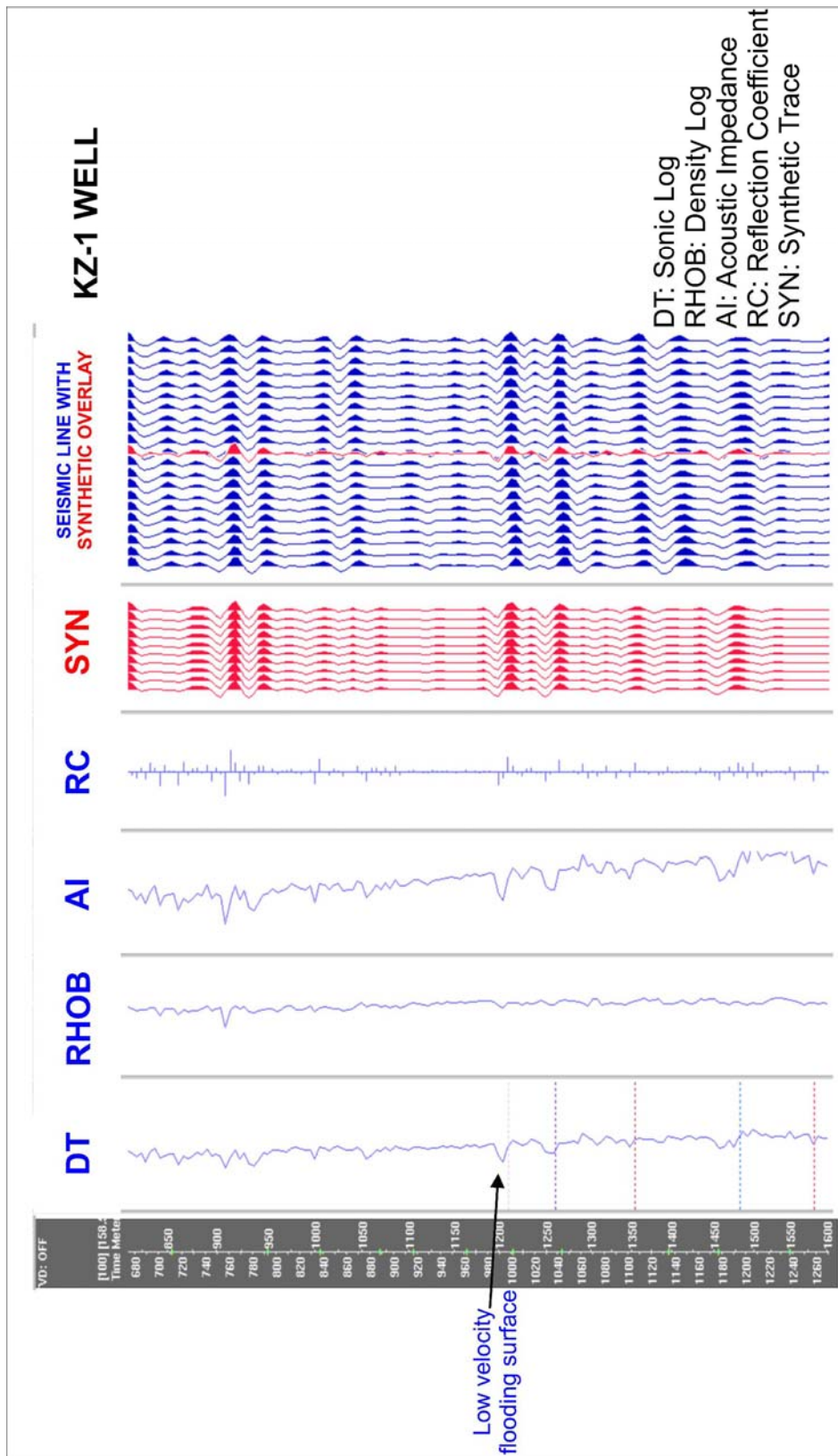


Figure 3.9 Synthetic seismogram was generated using SynTool® application of the Openworks package. The figure shows the synthetic seismogram of the KZ-1 well. Due to high quality sonic and density logs, proper well conditions and check-shot calibration, high correlation coefficient was estimated and time to depth conversion applied successfully.

3.2 Seismic Stratigraphy

Seismic stratigraphy is a method to interpret stratigraphy from seismic data (Mitchum, et al., 1977; Brown and Fisher, 1980; Bertram, 1998). The fundamental principle of seismic stratigraphy is that within the resolution of seismic method, seismic reflections follow gross bedding surfaces and they approximate time lines. This statement does not deny the physical principle of seismic reflection that seismic reflections are generated at abrupt acoustic impedance contrasts (Bertram, 1998). Within seismic resolution limits, correlative impedance contrast come from bedding interfaces and not lateral facies changes. Lateral facies changes are gradual and do not generate reflections (Bertram, 1998).

3.2.1 Reflection Termination Patterns

The studied section was subdivided into depositional sequences (Mitchum, et al., 1977) and related systems tracts (Van Wagoner, 1988) on the basis of geometric relationship between reflection terminations (onlaps, downlaps, truncations, toplaps) and seismic surfaces on 2D seismic sections within seismic resolution limits.

Mitchum et al. (1977) introduced the following reflection termination patterns, which are stated as geometric terms, to apply seismic stratigraphic analysis; onlap, downlap, erosional truncation, toplap. Figure 3.10 shows types of reflection termination patterns observed in two-dimensional seismic reflection lines.

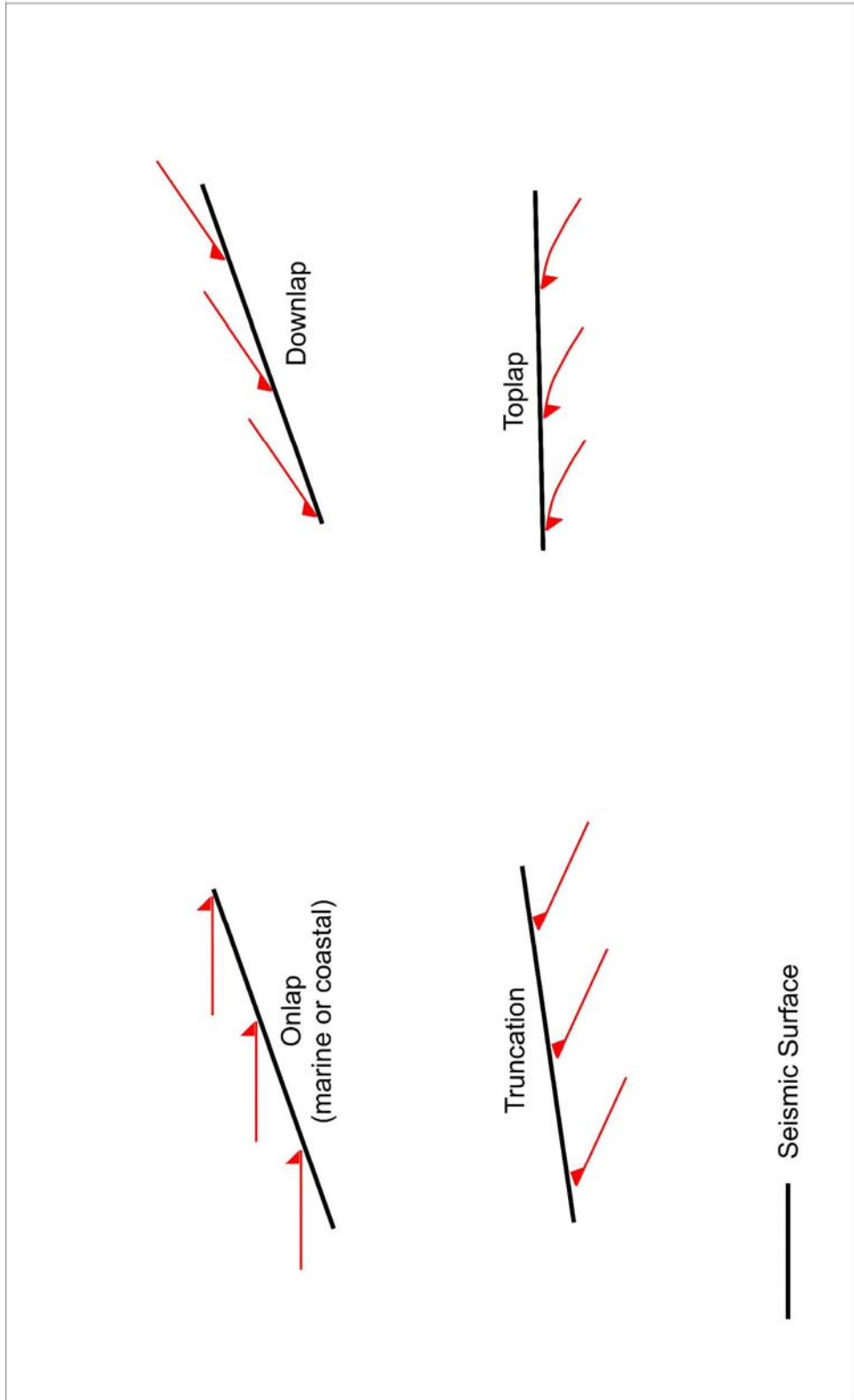


Figure 3.10 Depositional history analysis was carried out on the basis of reflection termination patterns on two-dimensional seismic data. Major seismic reflection termination patterns are shown in red and seismic surfaces in black.

Major reflection patterns stated below were defined on the basis of literature survey, especially, Mitchum et al. (1977) and Bertram (1998).

Lapout is the lateral termination of stratum at its original depositional limit.

Onlap is a baselap in which initially horizontal stratum laps out against an initially inclined surface. It may be marine or coastal origin.

Marine onlap is onlap of marine strata, representing a change from marine deposition to marine non-deposition or condensation, and results from the partial infill of space by marine sediments. Marine onlap reflects a submarine facies change from significant rate of deposition to much lower energy pelagic drape. The seismic surface of marine onlap demonstrates a marine hiatus or condensed interval. The seismic sections from the northern margin of the Thrace Basin exhibited well defined marine onlaps (Figure 3.11A). They were interpreted as the products of Late Eocene deepening in the basin over the pre-Tertiary basement rocks.

Coastal onlap is onlap of non-marine, paralic or marginal marine strata, representing a change from deposition to basin margin (subaerial or shelf) erosion and non-deposition. A landward progression in coastal onlap results from rising relative sea-level, while basinward in coastal onlap results from a fall in relative sea-level.

Downlap is baselap in which an initially inclined stratum terminates downdip against an initially horizontal or inclined surface. Downlap is commonly seen at the base of prograding clinoforms, and usually

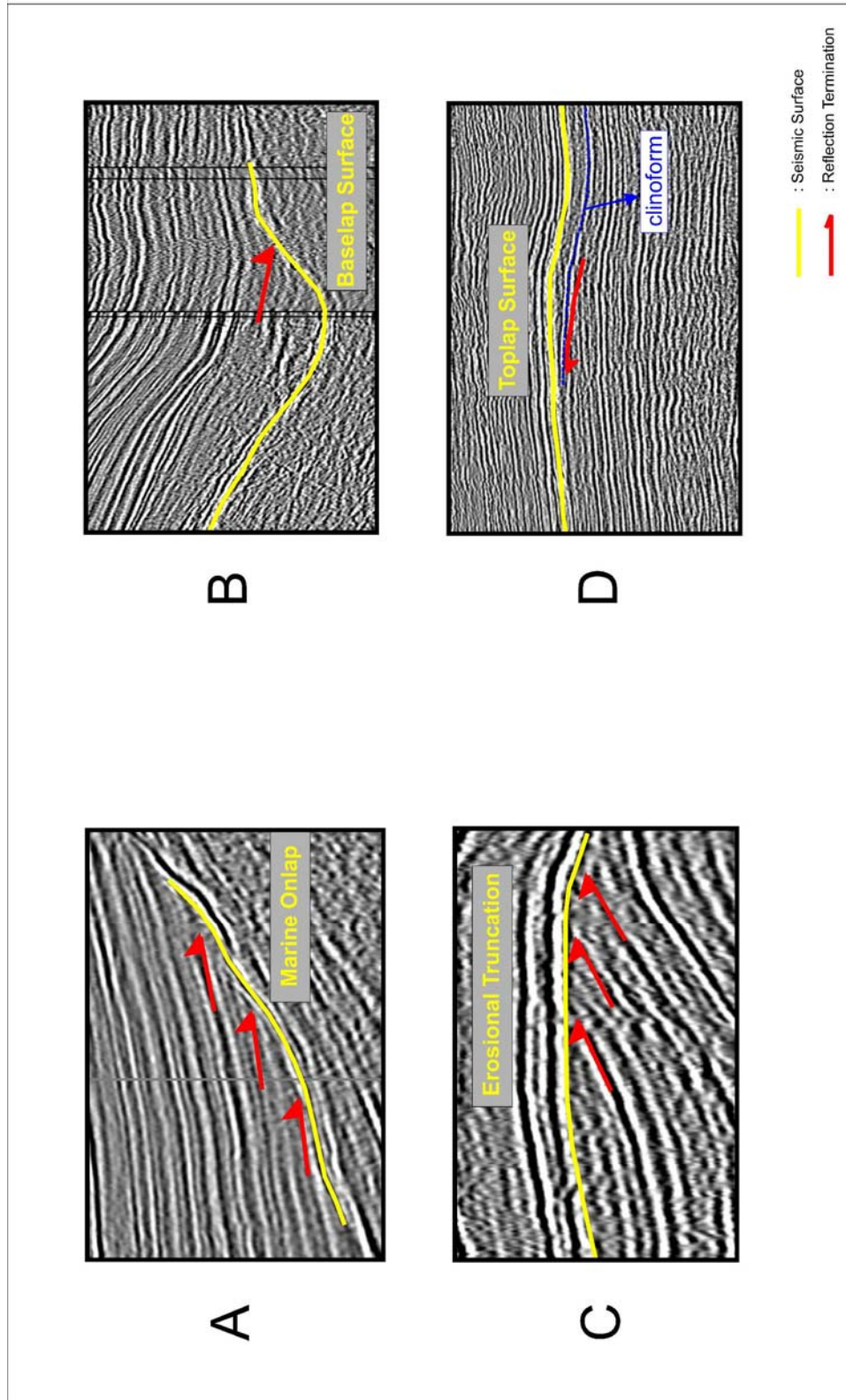


Figure 3.11 Depositional history analysis was carried out on the basis of reflection termination patterns on two-dimensional seismic reflection data. The above seismic lines exhibit diagnostic reflection termination patterns from the study area.

represents the progradation of a basin margin slope system into deep water. Therefore, downlap termination corresponds to a change from slope deposition to marine condensation or non-deposition. Downlap surface represents a marine condensed unit.

Due to structural complexity, onlap and downlap patterns can be misinterpreted. Thus, baselap was preferred as a more convenient term to use for these two terms during the study. The base of slope fan successions of the "Hamitabat" Turbidite System (sequence boundary-1) was defined as a baselap surface against which moderately continuous, prograding clinoforms terminate (Figure 3.11B).

Toplap is lapout at the upper boundary of a depositional sequence, such as clinoforms. In marginal marine strata, it represents a change from slope deposition to non marine or shallow marine bypass or erosion, and the toplap surface is a local unconformity.

Erosional truncation is the lateral termination of a stratum by erosion. It occurs at the upper boundary of a depositional sequence. The erosional surface may be marine surface such as at the base of a canyon, channel or major scour surface, or a non-marine erosion surface developed at a subaerial unconformity. Two types of erosional truncation were observed during the study (Figure 3.11). Seismic line C exhibits an example of subaerial unconformity from the study area. This seismic surface corresponds to the top of the Danişmen Formation, which is identified as an angular unconformity. Second type of erosional surface is characterized by

marine erosion. Seismic line B represents an example of sub-marine erosion, which is defined as base of a sub-marine canyon with well confirmation.

3.2.2 Seismic Facies Analysis

Seismic facies analysis is defined as the interpretation of environmental setting and lithofacies from seismic data (Mitchum et al., 1977). A seismic facies (called seismic package) is a spatially definable three-dimensional unit composed of groups of seismic reflections whose parameters (configuration, amplitude, continuity, frequency and interval velocity) differ from the elements of adjacent facies (Mitchum et al., 1977). The fundamental concept of seismic facies is that a seismic facies is the sonic response to a lithofacies. Reflections within seismic facies, therefore, are inferred to represent stratal surfaces, unconformities and fluid contacts. Lithofacies interpretation of seismic facies involves consideration of internal reflection configurations, boundary relationships, lateral facies relationships and external geometry.

Erosional unconformities, which are diachronous surfaces, generate reflections because they commonly separate strata with different acoustic impedances. In addition, strata below an unconformity are commonly weathered or altered mineralogically, which also creates acoustic impedance contrast (Brown and Fisher, 1980). From the study area, the top of the Danişmen Formation, known as Upper Miocene unconformity, can be

given as an example of a regional erosional unconformity (Figure 3.11C). In most of the wells, the weathered or altered zone was detected by low sonic velocities. Due to the velocity contrast, this surface was easily recognized as a high amplitude, continuous reflection in seismic sections.

Stratal surfaces are conformable surfaces. In geologically, they correspond to depositional surfaces. Reflections will be generated from those surfaces, which coincide with a significant acoustic impedance contrast (Brown and Fisher, 1980). For example, clinoform is a stratal surface. Paleoenvironmentally, the shallowest portion of a clinoform represents the boundary between terrestrial and marine environments, and its deepest portion, the boundary between nearshore and offshore environments (Pigott, 1995). Sedimentologically, a clinoform corresponds to a broad transition zone between mechanical and suspension processes, i.e. sand deposited at the distributary mouth-bar to the silts and clays of the delta front facies to the muds deposited at the prodelta facies (Pigott, 1995). Each seismically resolvable parasequence within the deltaic system of the Osmancık Formation is bounded by flooding surfaces. These surfaces were demonstrated on seismic sections as clinoforms (Figure 3.11D).

Major elements of seismic facies analysis are summarized in Table-3.1.

Table 3.1 Major elements of seismic facies analysis (modified from Brown and Fisher, 1980).

PROPERTIES OF SEISMIC FACIES

INTERNAL REFLECTION CONFIGURATION
Subparallel, parallel, divergent, convergent, hummocky, chaotic, reflection-free, mounded, prograding clinoforms
BOUNDARY RELATIONSHIPS
Terminational Transitional
EXTERNAL GEOMETRY
Sheet, sheet drape, wedge, bank, lens, mound, fill; canyon fill, slope front fill
AMPLITUDE/FREQUENCY
Low, fair, moderate, high, moderate/high
CONTINUITY
Poor, fair, moderate, good, over good
INTERVAL VELOCITY

3.3 Well-logging Principles

Major vertical trends were delineated and interpreted on the basis of mostly gamma-ray logs and sonic logs throughout the study. These trends may indicate lithology and stratal architecture and give distinctive responses for a given depositional environment (Coleman and Prior, 1980; Galloway and Hobday, 1983; Pirson, 1983; Cant, 1984; Rider, 1986).

It is important to stress that the observations which represent the physical properties of rocks should always be checked with any available data for final interpretation. During the study, cutting information, cores if available and seismic reflection data were mostly used for the confirmation of the vertical well log trends. The well data template used during the study is shown in Figure 3.12. The template is composed of five individual tracks. In the first track, the depth is given in measured depth (MD). In the second track, gamma-ray curve is exhibited in API units. The unit scale ranges from 0 to 150. The third track is lithology column, where each lithology is demonstrated by different codes. In the fourth column, sonic log curve is exhibited. The unit scale is expressed in slowness values ($\mu\text{s}/\text{ft}$) and ranges from 40 to 140. In the fifth column, the depth is also given in true vertical depth from the sub-sea (TVDSS).

WELL TEMPLATE



WELL NAME

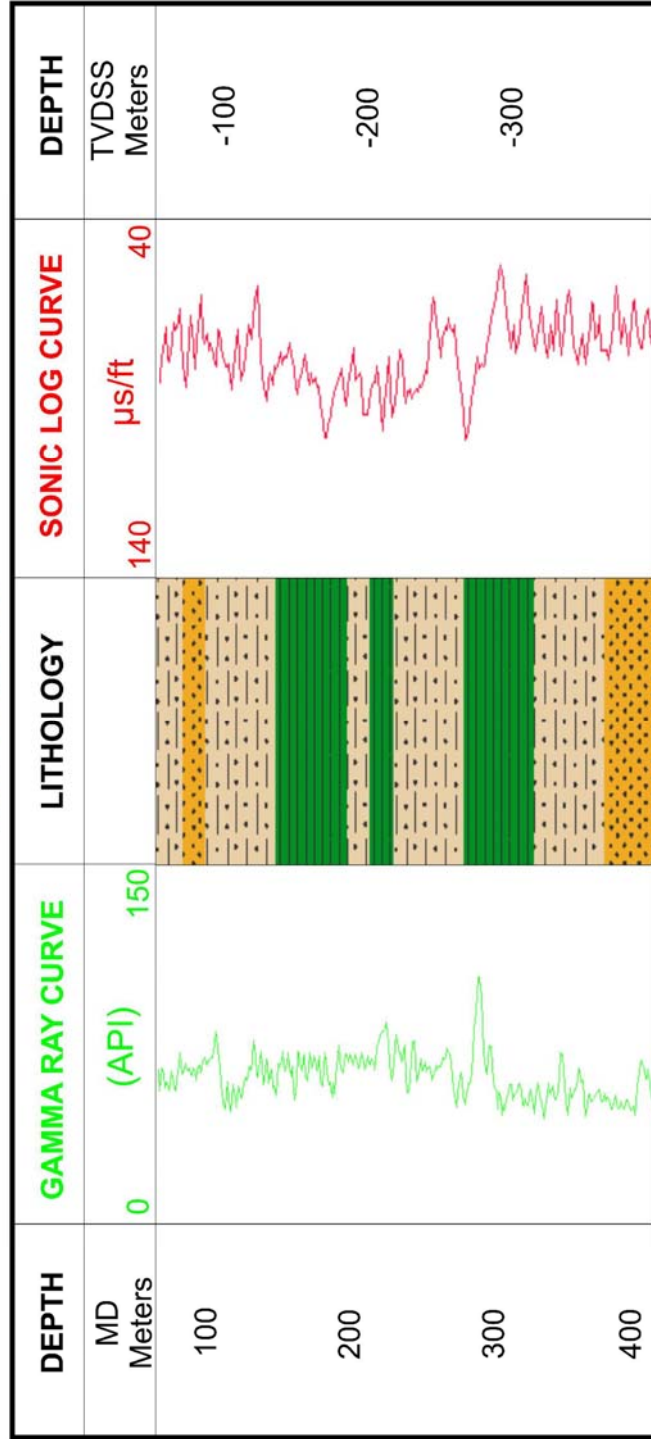


Figure 3.12 The well log data template, used in this study was represented by five different tracks. From left to right; depth (Measured Depth in meters), gamma-ray curve (green), lithology, sonic log curve (red) and depth (true vertical depth from the subsea in meters) are represented respectively.

3.3.1 Gamma-ray Log Principles

Gamma-ray log is one-dimensional record of formations radioactivity. In this study, gamma-ray log responses have been used for the indication of grain size and depositional environment.

Gamma-ray tool measures total natural radioactivity of rocks. Natural radiation of formations are caused by three elemental sources; the radioactive elements of the thorium family, the uranium-radium family and the radioactive isotope of potassium ^{40}K . These three elements emit gamma rays spontaneously.

The unit of radioactivity used for natural gamma-ray logs is API (American Petroleum Institute). This unit is based on an artificially radioactive concrete block at the University of Houston, Texas, USA. This concrete block is defined to have a radioactivity of 200 American Petroleum Institute (API) units. This value was chosen because it was considered to be twice the radioactivity of typical shale. The formation is the primary standard for calibrating gamma-ray logs. However, even when properly calibrated, different gamma-ray tools will not necessarily have identical readings downhole because their detectors can have different spectral sensitivities. They will read the same only if the downhole formation contains the same proportions of thorium, potassium and uranium as the Houston standard (Sheriff, 2002). Therefore, grain size discrimination was carried out by the sand-shale baseline method using gamma-ray logs for each well and calibrated with cuttings.

Most of rocks have some degree of radioactivity. In practice, the radioactivity of a rock is generally accepted as a direct function of clay mineral content.

3.3.2 Sonic Log Principles

Sonic log is a one dimensional record of interval transit time of formations. It measures the formations capacity to transmit sound waves. The basic acquisition principle is that sonic source (transducer) at the downhole emits sound waves that travel through the formations and back to the receiver. The tool is basically designed to record compressional or P waves. Sonic values are expressed in microseconds (μ) per foot (1 microsecond is equal to 1×10^{-6}) and symbolized as Δt or DT. The most common transit time interval of rocks ranges between 40 μ s and 140 μ s. In metric depth scale, the transit time is given in μ s/ft.

The capacity of formations to transmit sound waves is a function of lithology, rock texture and notably porosity. Shales exhibit higher transit time (lower velocity) than sandstones with similar porosity. Thus, the sonic log sometimes is used as a grain size indicator. High concentration of organic matter in coal and black shale lithologies give higher transit time. Moreover, travel time measurements are affected by post-depositional cementation and compaction.

Sonic logs have been utilized not only for time-depth conversion but also grain size indication during the study. Lower interval velocity content of

flooding surfaces against the overlying and underlying lithologies was easily detected in sonic logs. Additionally, limestone lithology within the clastic-carbonate mixed system exhibited abrupt velocity contrast and detected easily.

3.4 Vertical Trend Analysis in Well-logs

The following five distinctive log trends were delineated in gamma-ray logs; cleaning-upward trend, dirtying upward trend, cylindrical trend, bow trend and irregular trend (Figure 3.13).

Cleaning upward trend indicates gradual decrease in gamma ray reading as a result of decrease in clay mineral content in low depositional energy. In shallow marine settings, it generally represents upward transition from shale rich to sandy lithologies. Change from clastic to carbonate deposition or gradual decrease in anoxicity may also be represented as gradual cleaning upward trend. During the study, the transition from shallow marine clastics to limestone lithology was observed as cleaning upward trend.

Dirtying upward trend indicates gradual increase in gamma-ray reading as a result of increase in clay mineral content. Gradual upward transition from sand to shale or upward thinning of sand beds may cause this trend. Meandering or tidal channel deposits, retreat or abandonment of a shoreline, e.g., transgressive shoreline shelf, may be represented as dirtying upward trends. Change from carbonate to clastic deposition or

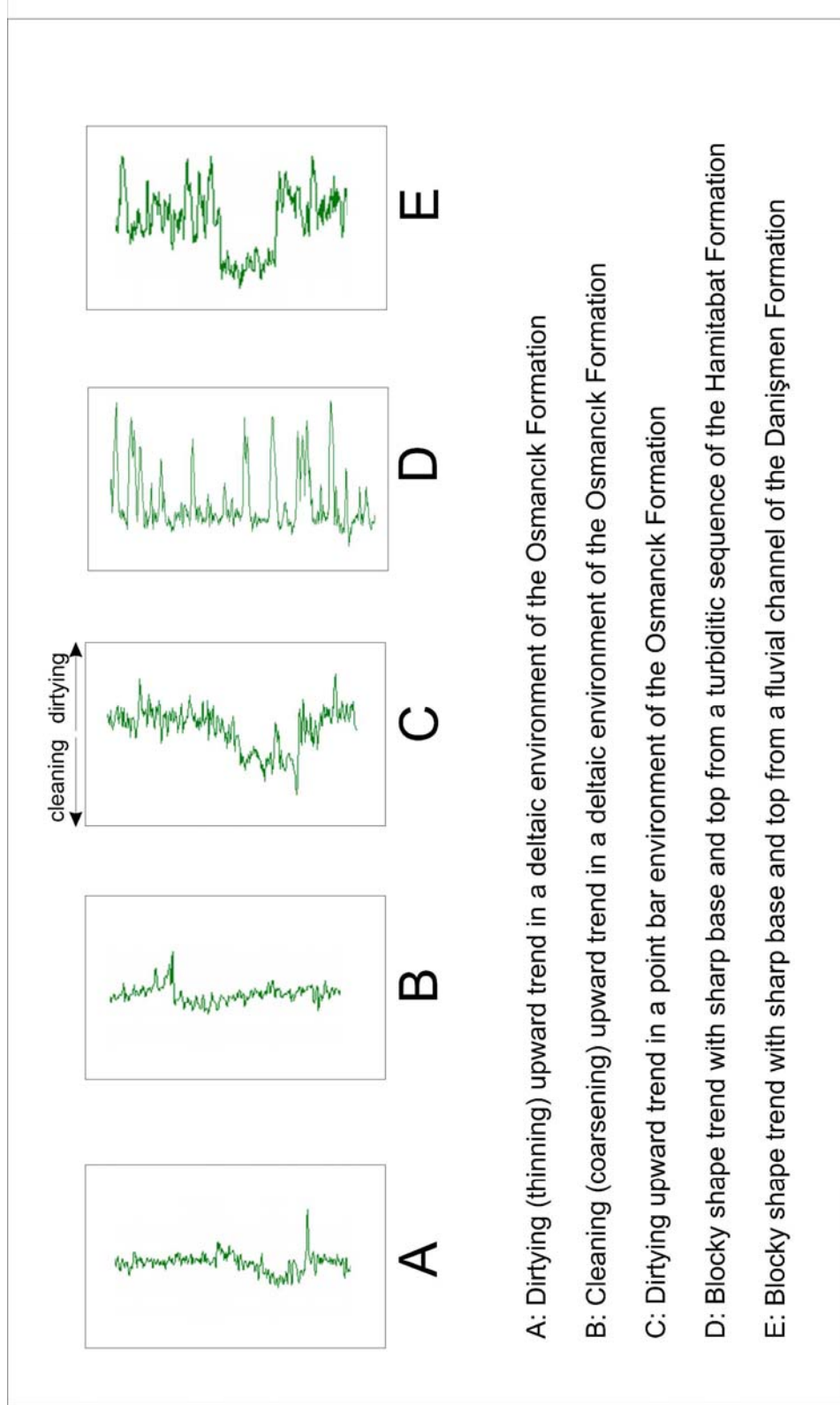


Figure 3.13 The figure shows distinctive vertical log trends observed on gamma-ray curves. These trends may indicate clay content and thus, depositional energy and environment. The data were chosen from various wells in the Thrace Basin.

gradual increase in anoxicity may also exhibit as dirtying-upward transition. In most of the wells, dirtying upward trends were observed where gradual transition from limestone to marl has taken place.

Blocky trend indicates relatively constant gamma-ray reading with sharp boundaries at the base and top. Fluvial channel, turbidite and aeolian sands bounded by shale generally give cylindrical log trends. Within the “Hamitabat” Turbidite System, turbiditic sandstones were detected as cylindrical trends with sharp base and top. Moreover, fluvial channel sands within the deltaic system of the Osmancık Formation represent cylindrical trend (Figure 3.13).

Irregular trend indicates no systematic change on gamma-ray reading. Aggradations of shaley or silty lithology in shelfal and deep marine settings may be exhibited with irregular trends.

3.5 Sequence Stratigraphic Terminology

Posamentier and Allen (1999) defined sequence stratigraphy as the analysis of cyclicity in the sedimentary record as a function of the fundamental parameters which control sedimentation patterns; i.e. sediment supply, tectonic subsidence, sedimentary processes, basin physiography or a way of analyzing how sedimentary basin fill.

Van Wagoner et al. (1988) defined “sequence stratigraphy” as the study of rock relationships within a chronostratigraphic framework of repetitive, genetically related strata bounded by surfaces of erosion or non-

deposition, or their correlative conformities. The basic stratigraphic unit of sequence stratigraphy is the sequence. Figure 3.14 shows well-known “Exxon Slug” which represents major sequence stratigraphic terms and Table 3.2 shows abbreviations of the terms.

A “sequence” is a relatively conformable succession of genetically related strata bounded by unconformities and their correlative conformities (Mitchum et al., 1977). An “unconformity” is a surface separating younger from older strata, along which there is evidence of subaerial erosional truncation or subaerial exposure, with a significant hiatus indicated (Van Wagoner et al., 1988). “conformity” is a bedding surface separating younger from older strata, along which there is no evidence of erosion (either subaerial or submarine) or nondeposition, and along which no significant erosion is indicated (Van Wagoner et al., 1988).

Two types of sequence boundaries are recognized in the rock record; type-1 and type-2 (Van Wagoner et al., 1988). “Type-1 sequence boundary” is characterized by subaerial exposure and concurrent subaerial erosion associated with stream incision, a basinward shift of facies, a downward shift of facies, a downward shift in coastal onlap, and onlap of overlain strata. A type-1 sequence boundary is interpreted when the rate of eustatic fall exceeds the rate of basin subsidence at the depositional shoreline break. A “type two sequence boundary” is marked by subaerial exposure and a downward shift in coastal onlap landward of the depositional shoreline

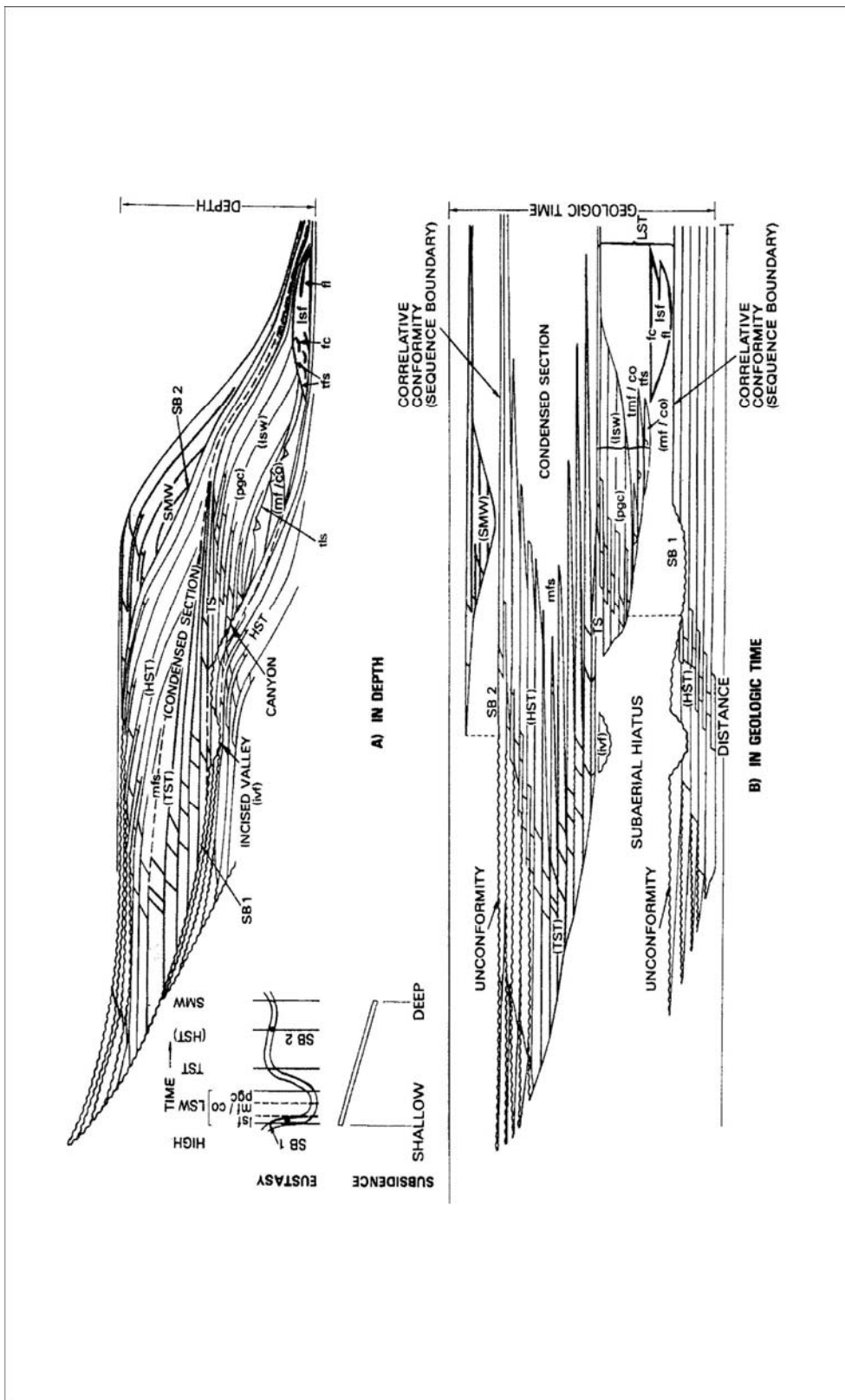


Figure 3.14 The figure shows "Exxon Slug" as a sequence model, which represents major sequence stratigraphic surfaces (from Van Wagoner et al., 1988).

Table-3.2 The table shows the abbreviations used in sequence stratigraphic terminology. Most of them were used in Figure 3.14.

SB	SEQUENCE BOUNDARY	HST	HIGHSTAND SYSTEMS TRACT
SB-1	TYPE 1 SEQUENCE BOUNDARY	TST	TRANSGRESSIVE SYSTEMS TRACT
SB-2	TYPE 2 SEQUENCE BOUNDARY	LST	LOWSTAND SYSTEMS TRACT
SB-3	TYPE 3 SEQUENCE BOUNDARY	FSST	FALLING STAGE SYSTEMS TRACTS
DLS	DOWNLAP SURFACAE	lvf	Incised valley fill
Mfs	Maximum flooding surface	Lsw	Lowstand wedge
Tfs	Top fan surface	Pgc	Prograding complex
Tmf/co	Top mass flow/channel overbank	Lsf	Lowstand fan
TS	First flooding surface above maximum regression	SMW	SHELF-MARGIN WEDGE SYSTEMS TRACT

break. This type of surface lacks both subaerial erosion associated with stream incision and a basinward shift in facies (Van Wagoner et al., 1988).

Type-1 sequence boundary (unconformities with valley incision) can grade into Type-2 sequence boundary (correlative conformities) along depositional strike as well as depositional dip (Posamentier and Allen, 1999) due to the differential subsidence rates in three dimensional extents.

A sequence can be subdivided into three distinct stratigraphic units that are deposited during specific phases of relative sea-level cycle, called systems tracts. A “systems tract” is a linkage of contemporaneous depositional systems, defined by Brown and Fisher (1977). Three types of systems tracts are expressed; lowstand, transgressive and highstand systems tracts (Van Wagoner et al., 1988). They are bounded by basic stratigraphic surfaces of sequence stratigraphy; transgressive surface, maximum flooding surface, sequence boundary. Sediments within a systems tract are not necessarily coeval. It is possible that one type of system tract can form in one area, whereas another type of systems tract can form at the same time in another area because basic surfaces that separate systems tracts do not necessarily have chronostratigraphic significance (Posamentier and Allen, 1999).

“Lowstand systems tract” is defined as a sedimentary succession deposited during periods of falling relative sea-level (early phase), subsequent stillstand, and slow initial rise of relative sea-level (late phase) (Posamentier and Allen, 1999). In practical terms, the lowstand systems

tract includes all the deposits accumulated after the onset relative sea-level fall, as long as shoreline regression continues. Consequently, it includes the entire period of relative sea level-fall, as long as shoreline regression continues (Posamentier and Allen, 1999). Early phase of lowstand systems tract mostly comprises downward-stepping and sea-ward stepping shoreface deltaic and coeval deep water deposits. Late phase of lowstand systems tract contains fluvial fill of incised valleys, prograding shoreline and related deep water deposits if basin physiography permits (Posamentier and Allen, 1999).

“Transgressive systems tract” is defined as the rate of relative sea-level rise increases, the rate at which new accommodation is added eventually exceeds the rate at which sediment is supplied, so that shoreline transgression is initiated and transgressive systems tract is deposited. The transgressive systems tract comprises the deposits accumulated from the onset of coastal transgression until the time of maximum transgression of the coast, just prior to renewed regression (Posamentier and Allen, 1999). The depositional systems during transgressive systems tract time commonly include, from landward to seaward: a thin fluvial depositional system, aggrading coastal plain deposits, wave and current transgressive lag deposits and fine-grained marine mud deposited seaward of the late lowstand deposits (Posamentier and Allen, 1999).

“Highstand systems tract” is developed when relative sea-level rise slows to the rate at which available sediment flux is equal to or greater than

the rate at which accommodation is produced, then transgression ends and either shoreline stillstand occurs or regressions resumes (Posamentier and Allen, 1999). The regressive deposits that form when sediment accumulation rates exceed the rate of relative sea-level rise and increase in accommodation space constitute the highstand systems tract (Posamentier and Allen, 1999). At the onset of highstand systems tract time, much of the shelf and deep basin is dominated by the deposition of the condensed section even though the shoreline is beginning to migrate seaward (Posamentier and Allen, 1999). Major depositional environments of highstand systems tract are incised valley, coastal plain etc.

Depositional sequences of geologic history are induced by four different order eustatic cycles; first, second, third and fourth-order eustatic cycles. A “eustatic cycle” refers to a period of time during which sea-level falls from a highstand position through a lowstand, and returns to a highstand (Mitchum and Van Wagoner et al., 1991). Table 3.3 summarizes basic stratigraphic units which were used in different studies.

First-order eustatic cycles (continental break-up cycles), have time duration greater than fifty million years. They show onlapping against cratons and represented by major tectonically controlled unconformities (Duval et al., 1998).

Second-order eustatic cycles have time duration in the range of 9 to 10 million years. Mitchum and Van Wagoner et al. (1991) expressed the basic stratigraphic unit of the second-order cycle as “composite sequence”.

Table 3.3 Order of cyclicity and basic stratigraphic units of different sequence stratigraphic studies. Cycle here refers time duration between two lowstand position of sea-level.

Vail et al., 1991	Mitchum et al., 1977; Mitchum and Van Wagoner, 1991	Haq et al., 1987	This Study
		Megasequence	
Sequence 3-50 Ma	Composite Sequence 9-10 My	Supersequence	Second-Order Sequence
Sequence 0,5-3 My	Depositional Sequence 1-2 My	Sequence	Third-Order Sequence Depositional Sequence
Parasequence 0,08-0,5 My	Parasequence 0,1-0,2 My	Parasequence	Fourth-Order Sequence
Parasequence 0,03-0,08 My	Parasequence 0,01-0,02 My	Parasequence	Fifth-Order Sequence

It is defined on the basis of long-term displacements of the shoreline and caused by changes in the rate of tectonic subsidence and sea-floor spreading (Vail et al., 1984).

Third-order eustatic cycles have time duration in the range of 0,5 to 3 million years. They are caused by glacial eustasy (Vail et al., (1977), Haq et al., (1987)) stress release at plate margins (Cloetingh, 1992) and tectonically driven variations in sediment supply (Galloway, 1989) as tectonic causes, and geoidal eustasy (Mörner, 1981; Sabadini et al., 1990). The basic stratigraphic unit of third-order cycles is the 'sequence' which is subdivided into systems tracts, as contemporaneous depositional systems (Brown and Fisher, 1977). They are defined on the basis of changes in shelfal accommodation space and bounded by unconformities.

Higher-order eustatic cycles (fourth and fifth-order cycles), pronounced as parasequence cycles, have time duration in the ranges of 0,1 to 0,2 and 0,01 and 0,02 million years respectively. The basic stratigraphic unit of forth and fifth-order cycle is 'parasequence', which is made up of beds and bed sets. Parasequences caused in response to the interaction among the rates of eustasy, subsidence and sediment supply (Van Wagoner et al., 1988).

Parasequence is a relatively conformable succession of genetically related beds or bedsets bounded by marine flooding surfaces or their correlative surfaces. In special positions within the sequence, parasequences may be bounded either above or below by a sequence

boundary (Van Wagoner et al., 1990). Therefore, parasequences have been identified in coastal plain, deltaic, beach, tidal, estuarine and shelf environments (Van Wagoner et al., 1990). It should be avoided to use parasequence term in fluvial environments (Van Wagoner et al., 1990; Posamentier and Allen, 1999).

CHAPTER 4

A SEQUENCE STRATIGRAPHIC APPROACH TO THE DEPOSITIONAL HISTORY ANALYSIS OF THE UPPER EOCENE TURBIDITE SYSTEM

4.1 Introduction

Late Eocene coarse-grained turbidite system and its landward equivalents constitute deposits of the Sequence-1. It is a third-order depositional sequence (Mitchum et al., 1977) and comprises the oldest sediments of the studied interval. In lithostratigraphic nomenclature (Figure 4.1) (Turgut et al., 1987; Siyako, 2006), it composes the upper part of the Hamitabat Formation, which is made up of mostly the alternation of sandstone and shale beds deposited in various environments from deep to shallow marine. Sequence-1 is dated as Late Eocene on the basis of planktonic foraminifers (Erenler, 1987; Ediger et al., 1998). The turbidite system is underlain by two major substrata; pre-Tertiary metamorphic rocks of the Istranca Massif and Lower to Middle Eocene siliciclastic unit.

Metamorphic rocks of the Istranca Massif are composed of pre-Triassic basement rocks and the overlying Triassic-Jurassic age metasedimentary rocks (Pamir and Baykal, 1947; Çağlayan et al., 1988; Üşümezsoy, 1990; Okay and Yurtsever, 2006). They are exposed to surface

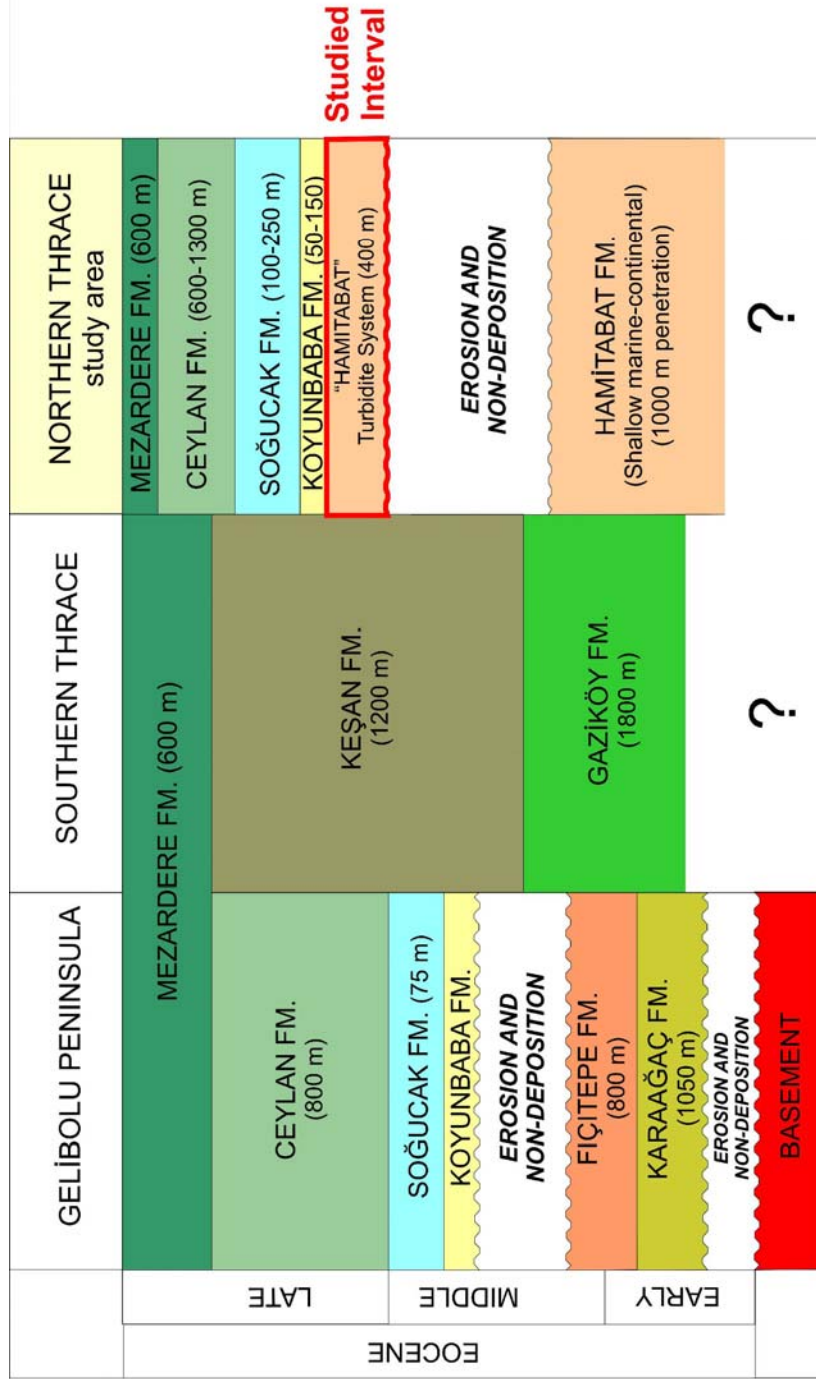


Figure 4.1 Stratigraphic relations of the Eocene formations in the Gelibolu Peninsula, southern Thrace and northern Thrace. This study focuses on northern Thrace. The studied interval (Sequence-1) constitutes Late Eocene "Hamitabat" turbidite system (in red rectangle) in northern part of the Thrace Basin (modified from Siyako, 2006).

from Çatalca near Istanbul to the Bulgaria territory in a 200 km long (east to west) and 25-30 km wide (north to south) zone (Okay and Yurtsever, 2006). Pre-Triassic part was metamorphosed in amphibolite and high-grade green schist facies, and cut by the Paleozoic granitoids. The overlying terrestrial and shallow marine Triassic and Jurassic sedimentary rocks were metamorphosed and deformed in compressional regime in Late Jurassic and Early Cretaceous in green schist facies (Pamir and Baykal, 1947; Çağlayan et al., 1988; Üşümezsoy, 1990; Okay and Yurtsever, 2006). This type of basement rocks was penetrated by most of the wells along the northern margin of the basin.

Second type of substrata is the Lower to Middle Eocene siliciclastic unit. They compose the lower part of the Hamitabat Formation and its depositional environment varies from terrestrial to shallow marine. This sedimentary package was penetrated by the HB-2, KRK-1, AR-1 and DG-3 wells in the study area.

4.2 “Hamitabat” Turbidite System

A turbidite system is defined as a body of genetically related mass-flow and turbidity current facies and facies associations that were deposited in virtual stratigraphic continuity (Mutti and Normark, 1987, 1991). Shanmugam (2000) also states that the classification of sediment gravity flows into Newtonian flows (e.g. turbidity currents) and plastic flows (e.g. debris flows) based on fluid rheology and flow state is a meaningful and

practical approach. The Figure 4.2 depicts the major elements of a turbidite system in a three-dimensional model.

Like many other turbidite systems, facies and geometry of the “Hamitabat” turbidite system were affected by the changing basin floor morphology instead of a uniform basin floor. The terms; ponded turbidites (Van Andel and Komar, 1969; Prather et al., 1998), contained turbidites (Pickering and Hiscott, 1985) and/or confined turbidites (Lomas and Joseph, 2004) have been used to characterize sediment gravity flows and their deposits which fill the floor of an enclosed depression area (mini basin, sub basin, ponded basin) and are unable to surmount the bounding slopes.

“Hamitabat” turbidite system was analyzed in three major depocenters based on their own sediment delivery pathways, areal extent and facies architecture. These depocenters were named as the Western, Northwestern and Northeastern depocenters respectively according to their paleo geographic locations. Western sediment delivery fed by western provenance was controlled by the enclosed submarine morphology. On the other hand, the Northwestern and Northeastern depocenters fed by the northern provenance were deposited in southeast to northwest oriented growth fault controlled depressions.

The characteristics of the “Hamitabat” turbidite system were analyzed in the following workflow: First, the approximate boundaries of the depocenters were defined on the basis of reflection terminations patterns from 2D seismic data. Secondly, depositional fill of each depocenter was

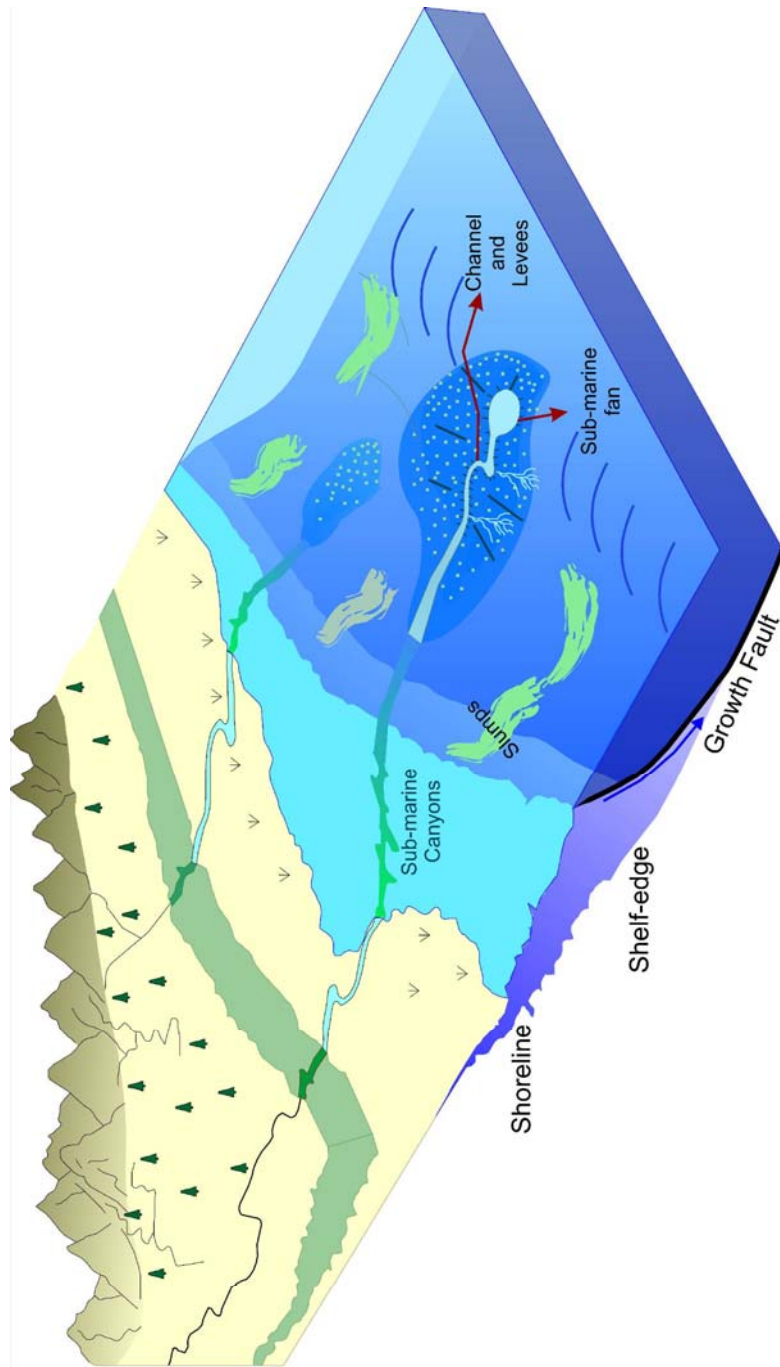


Figure 4.2 The figure depicts major elements of a turbidite system in a three-dimensional depositional model (redrawn from Mutti and Normark, 1991).

analyzed using seismic facies study. Thirdly, vertical trends in gamma-ray and sonic log responses were utilized for depositional history analysis in sequence stratigraphic approach. The location map of the well and 2D seismic data sets, used in Chapter 4 was shown in Figure 4.3.

Line-WE-1 is a regional seismic line (composite line) crossing the study area from the HB-2 well in the west to the KM-1 well in the east (Figure 4.4). The blue color seismic packages represent coarse-grained turbidite filled depocenters overlying the Sequence Boundary-1 (red color dashed line). The varying thicknesses of the seismic packages and bounding topographic highs suggest the confined nature of depocenters and the role of the submarine morphology on depositional fill. The base of the seismic packages characterizes sea-floor morphology, which was defined as the Sequence Boundary-1. This boundary characterizes the base of the study interval and separates Lower-Middle Eocene and Upper Eocene sediments.

4.2.1 Western Depocenter

Western depocenter is restricted to the westernmost part of the study area. K.AB-1 well in the south, AR-1 well in the east and northern shelf-slope bounding fault characterizes the extent of the Western depocenter. Its areal extent was shaped by the enclosed sea-floor morphology. The areal extension of the Western depocenter was defined based on 2D seismic

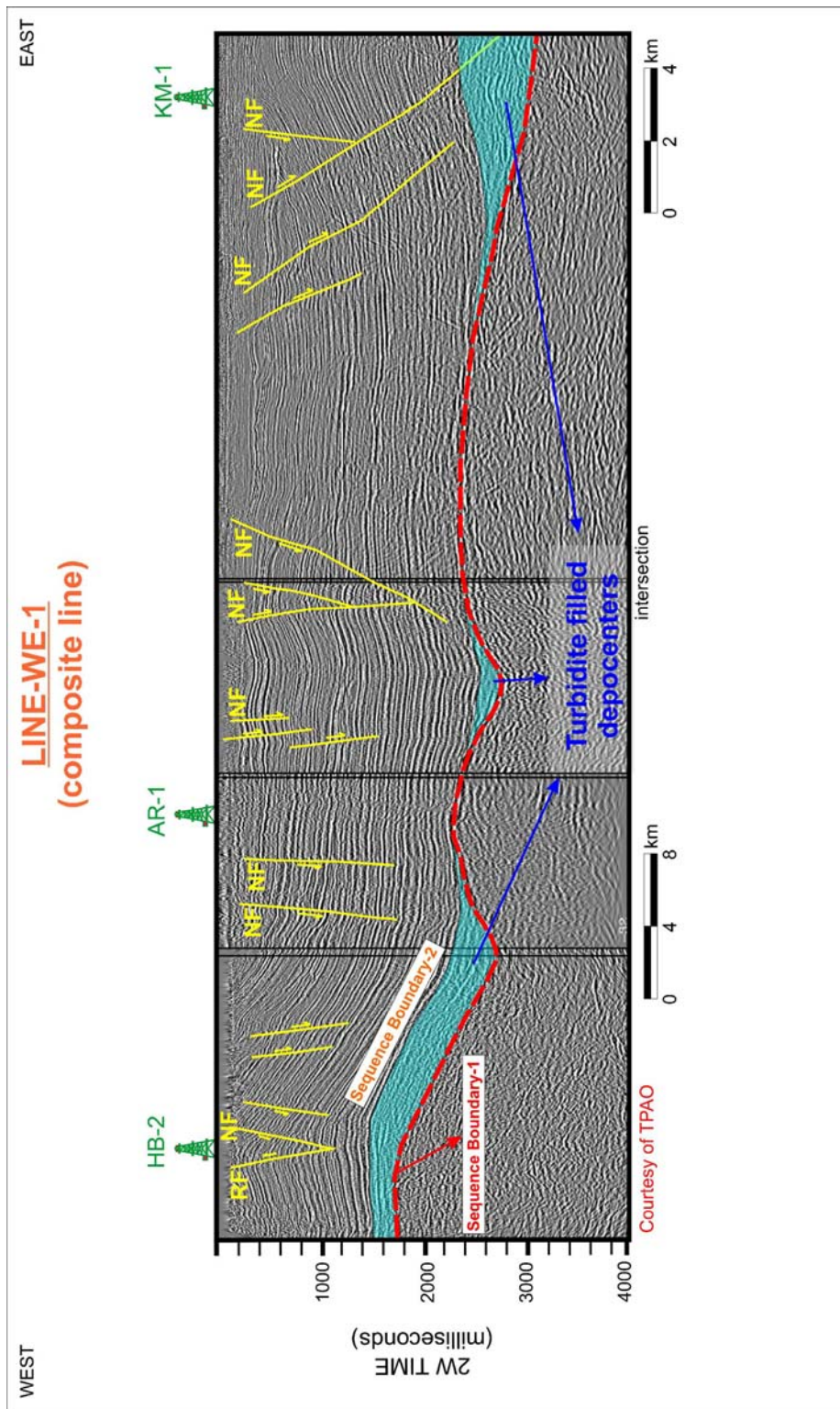


Figure 4.4 A strike oriented regional seismic line, crossing the study area from the HB-2 well in the west to the KM-1 well in the east. The blue color seismic packages represent confined nature of the “Hamitabat” turbidite system. NF: Normal Fault, RF: Reverse Fault.

data set. However, the representative seismic lines only were displayed in the thesis.

Major characteristics of the Western depocenter were defined on the basis of seismic facies analysis. Then, results were confirmed with gamma ray and sonic log responses, and cuttings data from the HB-2 well, which was the only well penetrated the Western depocenter fill.

Line-SN-1 is a south to north oriented seismic line (Figure 4.5). This line crosses the western depocenter in perpendicular to the depositional dip direction. In this line, canyon fill external seismic geometry of the Western depocenter is exhibited. The canyon is composed of chaotic internal seismic reflection configuration. The interpretation of east to west and south to north oriented seismic lines revealed that the sediment flow direction was estimated approximately from northwest to southeast. The canyon fill external seismic geometry was affected by post-depositional tectonic activities. In order to remove this effect, the seismic line was flattened to the upper boundary of the canyon. Figure 4.6 exhibits the paleo-canyon geometry of the western depocenter. The base of the canyon reflects the magnitude of the submarine erosion.

Line-WE-2 is a west to east oriented seismic line (zoom line) extending from the HB-2 to the AR-1 well (Figure 4.7) in parallel to the depositional dip direction. The blue color seismic package represents the Western depocenter. The lower sequence boundary was defined as a baselap surface (red color dashed line), against which moderately

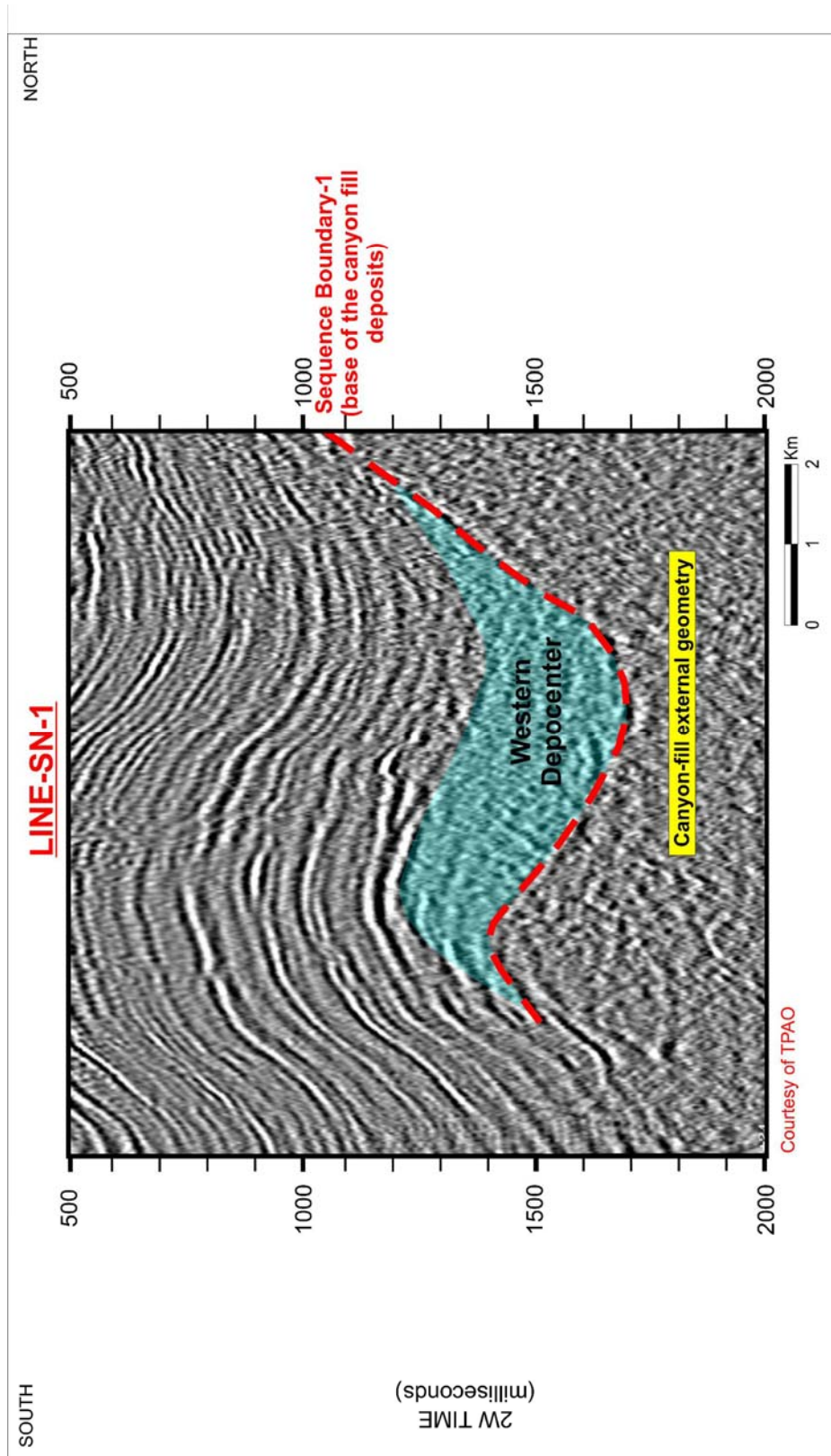


Figure 4.5 A south to north oriented seismic line, crosses the Western depocenter in perpendicular to the depositional dip direction. The blue color seismic package represents canyon fill external geometry and chaotic fill internal reflection configuration. The area was affected by post-Miocene strike-slip tectonic regime.

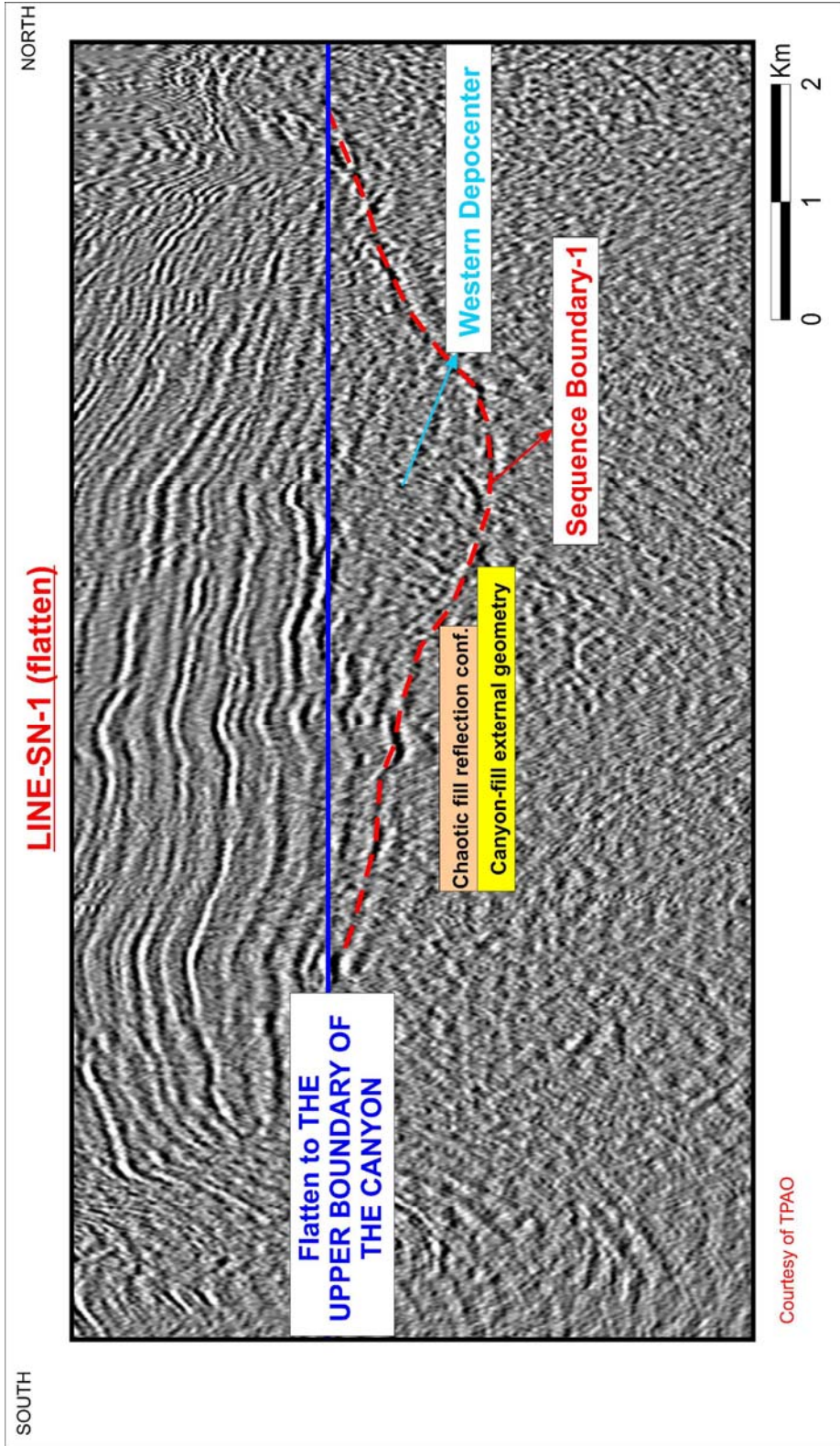


Figure 4.6 In order to remove the post-depositional tectonic effect, the seismic line was flattened to the upper boundary of the canyon fill. Red color dashed-line reflects Late Eocene sea floor morphology and the magnitude of the incision

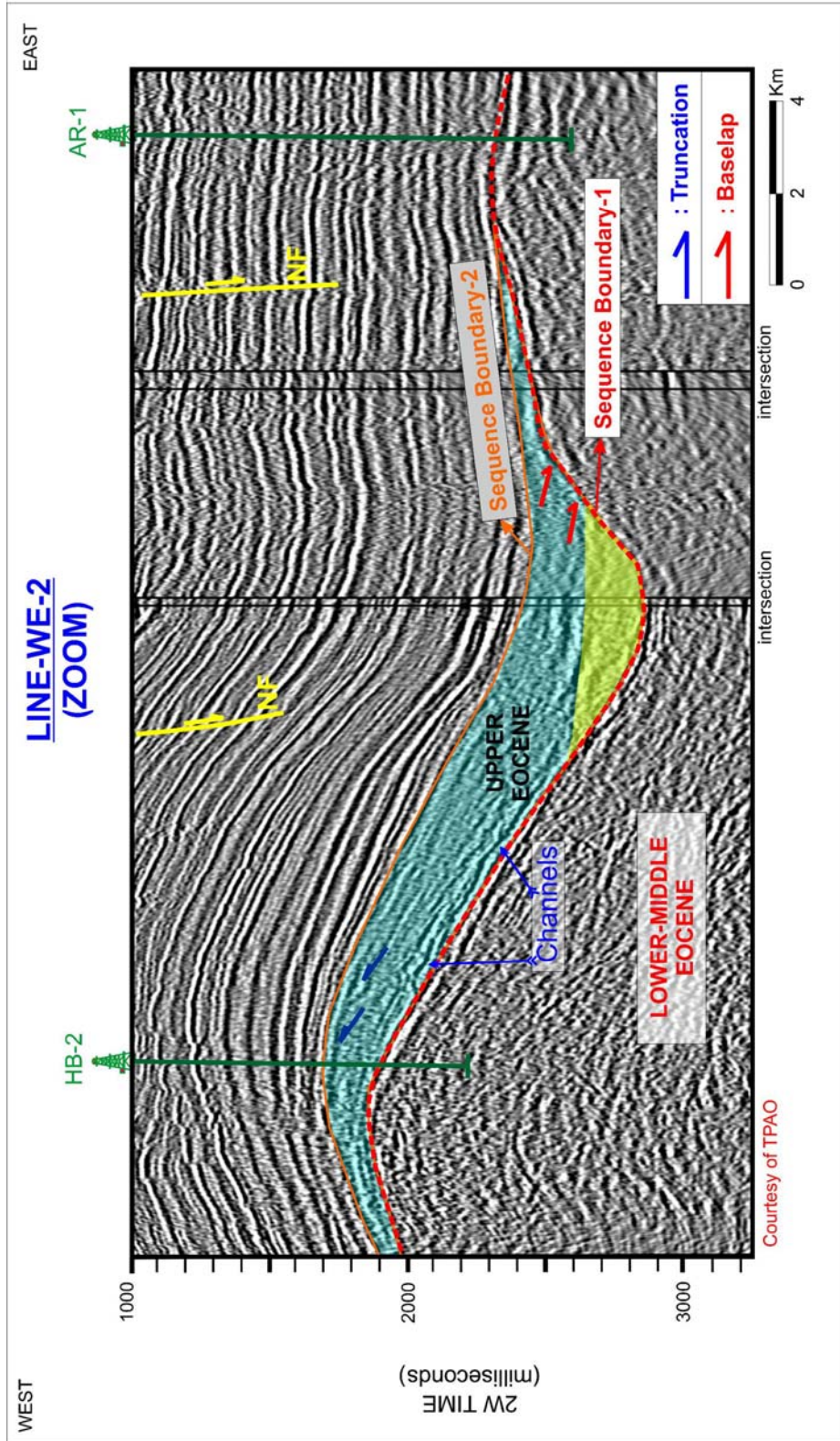


Figure 4.7 A west to east oriented seismic line from the HB-2 to the AR-1 well. The blue color seismic package represents the Western depocenter. The area was affected by the post-Miocene strike-slip tectonic regime. NF: Normal Fault.

continuous, prograding clinoforms terminate (red arrows). The upper sequence boundary (Sequence Boundary-2) was the continuous positive reflection at the top of the moderately continuous reflection package. Against this surface, moderately continuous, prograding clinoforms terminate updip, (dark blue arrows).

On this seismic package, high amplitude reflection between blue and yellow seismic packages characterizes ponding and filling stages. Prather et al. (1998) described the depositional process of the ponded basins in five different stages (Figure 4.8). Ponding is known as sediment gravity flows fill the accommodation space. This stage represents how topographic relief influences the depositional fill. Second, filling is the accommodation stage until the rate of deposition exceeds the rate of formation of accommodation space. Third, sediment fill spills downslope to another depocenter during spill phase. Fourth phase is slope adjustment, during which a localized truncation surface is formed from erosion of the upslope basin as the equilibrium profile adjusts to the downslope basin. In the backfill stage, the filling of the space above the truncation surface occurs as the downslope basin fills. In the drape stage, sediment influx reduces at the end of a depositional cycle due to either rising eustatic sea-level or slope system avulsion. Figure 4.9 demonstrates the evolution of the Western depocenter as response to the changing sea-floor morphology. For this purpose, Line-WE-1 was flattened to represent ponding and filling stages and changing accommodation space. In Figure 9A, the seismic line was flattened to the

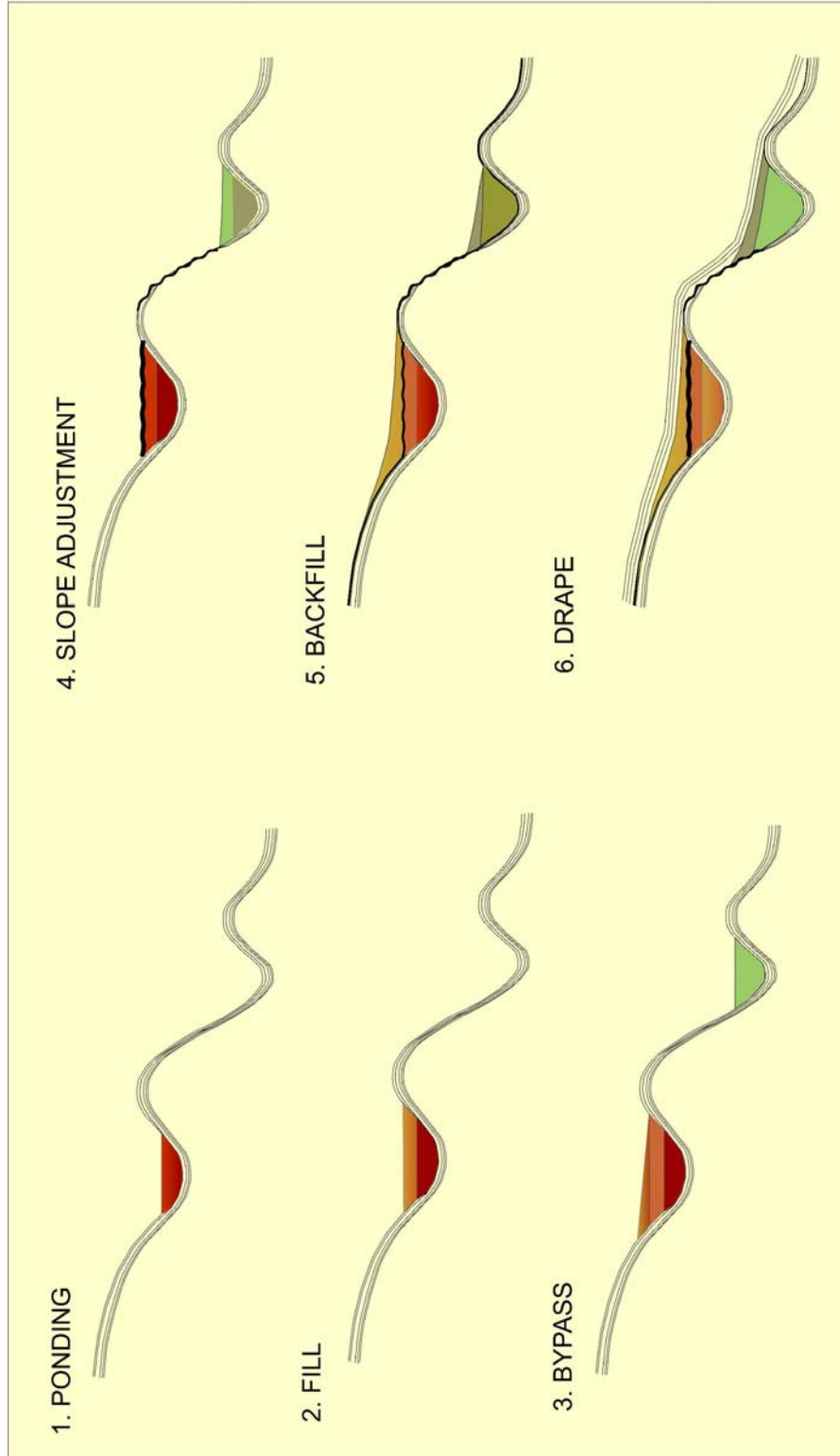
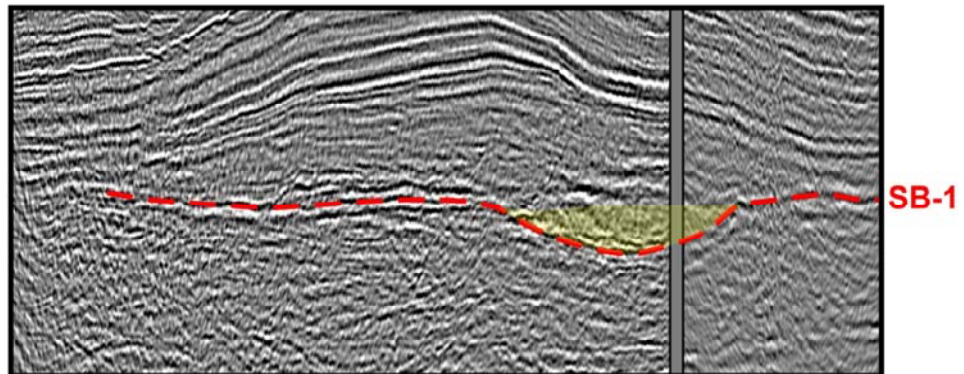


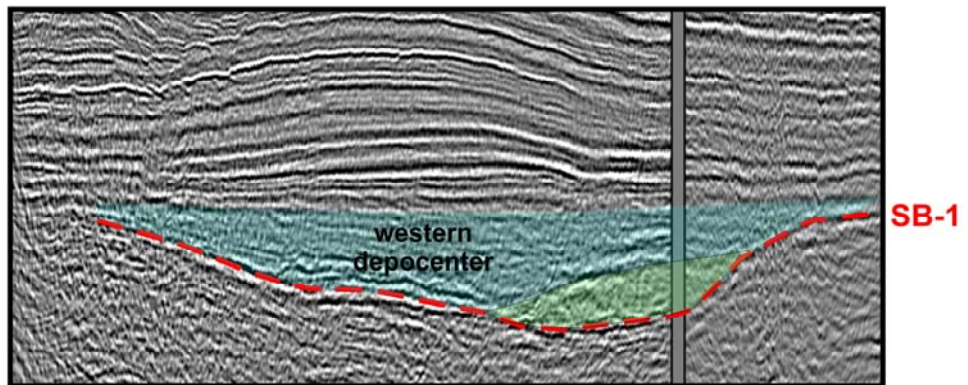
Figure 4.8 The figure shows Prather et al., (1998) model, which described the evolution of salt withdrawal Gulf of Mexico subbasins in six subsequent stages. In my study, seismic data indicated that the Western depocenter has similar evolution, where sea-floor morphology was major controlling factor of the sedimentation.

WEST

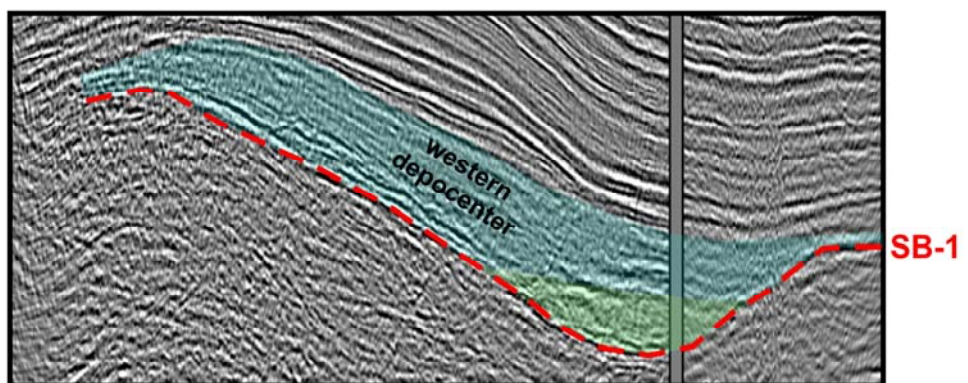
EAST



A) Flatten to ponded phase of the Western depocenter



B) Flatten to filling phase of the Western depocenter



C) Present-day seismic expression of the Western depocenter, which was affected by post-depositional tectonic activities.

Figure 4.9 Three seismic lines demonstrates the evolution of the Western depocenter by changing sea-floor morphology. SB-1: Sequence Boundary-1.

ponding stage. In this phase, sediment gravity flows fill the accommodation space (yellow color package). In Figure 9B, as response to the changing sea-floor morphology, sediment gravity flows fill the increased accommodation space. As a consequence of high subsidence and uplift ratio, sea-floor morphology has changed and formed the increased accommodation space as an enclosed depression area. Both stages are demonstrated by chaotic internal reflection configuration and separated by a high amplitude reflection. The Figure 9C shows the present-day representation of the Western depocenter on the seismic section. Three-dimensional seismic data set will give a better understanding of the evolutionary stages.

HB-2 well penetrates the Western depocenter in a proximal location. The studied interval is composed of slope fan deposits. The upper and lower sequence boundaries were placed to 1695 and 2200 m in the HB-2 well respectively (Figure 4.10). These boundaries also characterize the top and base of the Western depocenter. The studied interval is composed of slope fan deposits, which directly overlie the continental deposits. According to Ediger et al. (1998), the continental zone (deeper than 2200 m) was interpreted as part of a braided river system under the effect of natural oxidization. This interval represents Early-Middle Eocene age sediments of the Thrace Basin and is out of scope for this study.

The lower boundary of the slope fan deposits was placed to the top of red colored sandstone and shale alternations from cuttings confirmation.

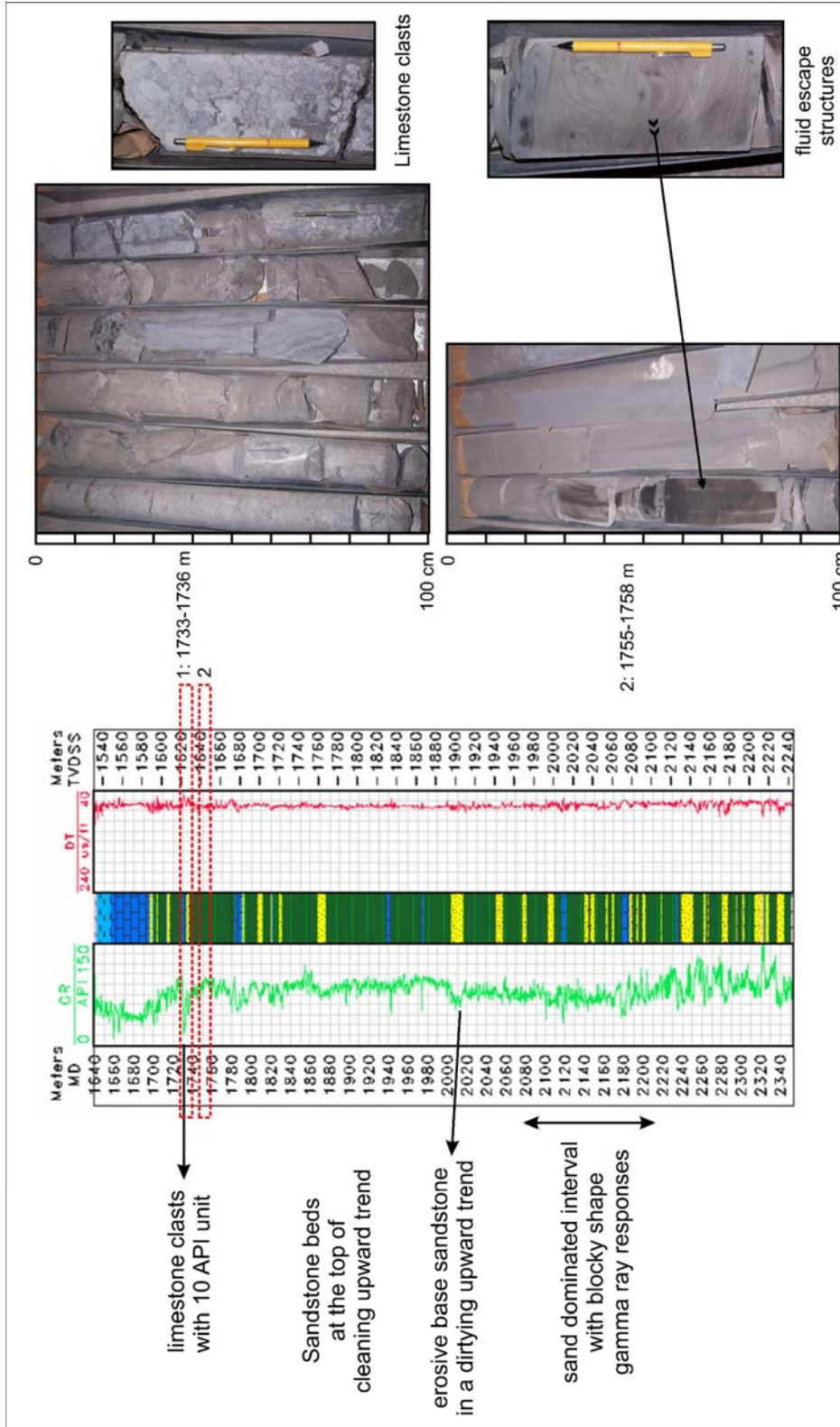


Figure 4.10 Gamma-ray curve (green color on the left) and sonic log curve of the HB-2 well (red color on the right) are exhibited. In the cored interval, limestone clast were observed as debris flow deposits between 1733 and 1736 m. Additionally, fluid escape structures were observed between 1755 and 1758 m.

Between 2100 and 2200 m, a sandstone dominated interval was observed. In this interval, sandstone beds were observed as blocky shape gamma-ray responses with erosive base and top. The overlying unit was shale dominated between 1800 and 2100 m. A diagnostic erosive base sandstone interval and overlying dirtying upward grain size was observed at 2015 m. Dirtying upward trend with sharp base was interpreted as debris flow deposits and overlying muds. Between 1695 and 1900 m, some cleaning upward trends were dominant. Limestone clasts, observed in gamma-ray logs with 10 API units also indicated proximal location of the HB-2 well in the Late Eocene paleo-slope. Debris flow conglomerates, transported limestone clasts and incomplete Bouma (1962) sequences (Çubukçu and Erten, 1987) observed within the cored intervals between 1729-1737 m and 1751-1758 m indicated the proximal location of the HB-2 well.

4.2.2 Northwestern Depocenter

The Northwestern depocenter is restricted to the area between the Kuzey Osmançık Fault zone in the north, YM-1 well in the south and south of the KV-6 well in the west. According to the source type classification of Galloway (1998), the source type can be classified as a point source, which was represented as a canyon fill external seismic geometry on seismic sections. Approximately northwest to southeast sediment delivery pathway was estimated based on seismic data set.

Both west to east oriented (Figure 4.11) and south to north oriented (Figure 4.12) seismic lines were used to represent approximate areal extension of the Northwestern depocenter. On the west to east oriented seismic line (Line-WE-3), which is perpendicular to the depositional dip (Figure 4.11) approximately 6 km wide and 400 m deep canyon fill at around 1500 msec represents the external geometry of the northwestern depocenter (purple color seismic package). The base of the canyon was shown by red color dashed line, which was highly erosive. Canyon fill seismic package is composed of chaotic internal reflection configuration.

Line-SN-2 (Figure 4.12) is an intersecting seismic line in the west-east and south-north directions. The seismic line shows that the Northwestern canyon was developed on the hanging block of a normal fault. The development of the canyon was controlled by a syn-sedimentary normal fault in a high angle slope environment.

KRK-1 and DG wells penetrated the Northwestern depocenter. In comparison to the western and Northeastern depocenter fills, it is mostly composed of coarser sediments. The nature of the dominant facies which was mostly composed of sandstone and conglomerates was shaped by intense influence of the steep slope gradient and syn-sedimentary faulting. To investigate the characteristic features of the Northwestern depocenter, DG-3 and KRK-1 wells, located at the hanging fault block were analyzed.

Slope fan deposits and the underlying and overlying units were recognized in KRK-1 well. Gamma-ray and sonic log responses between

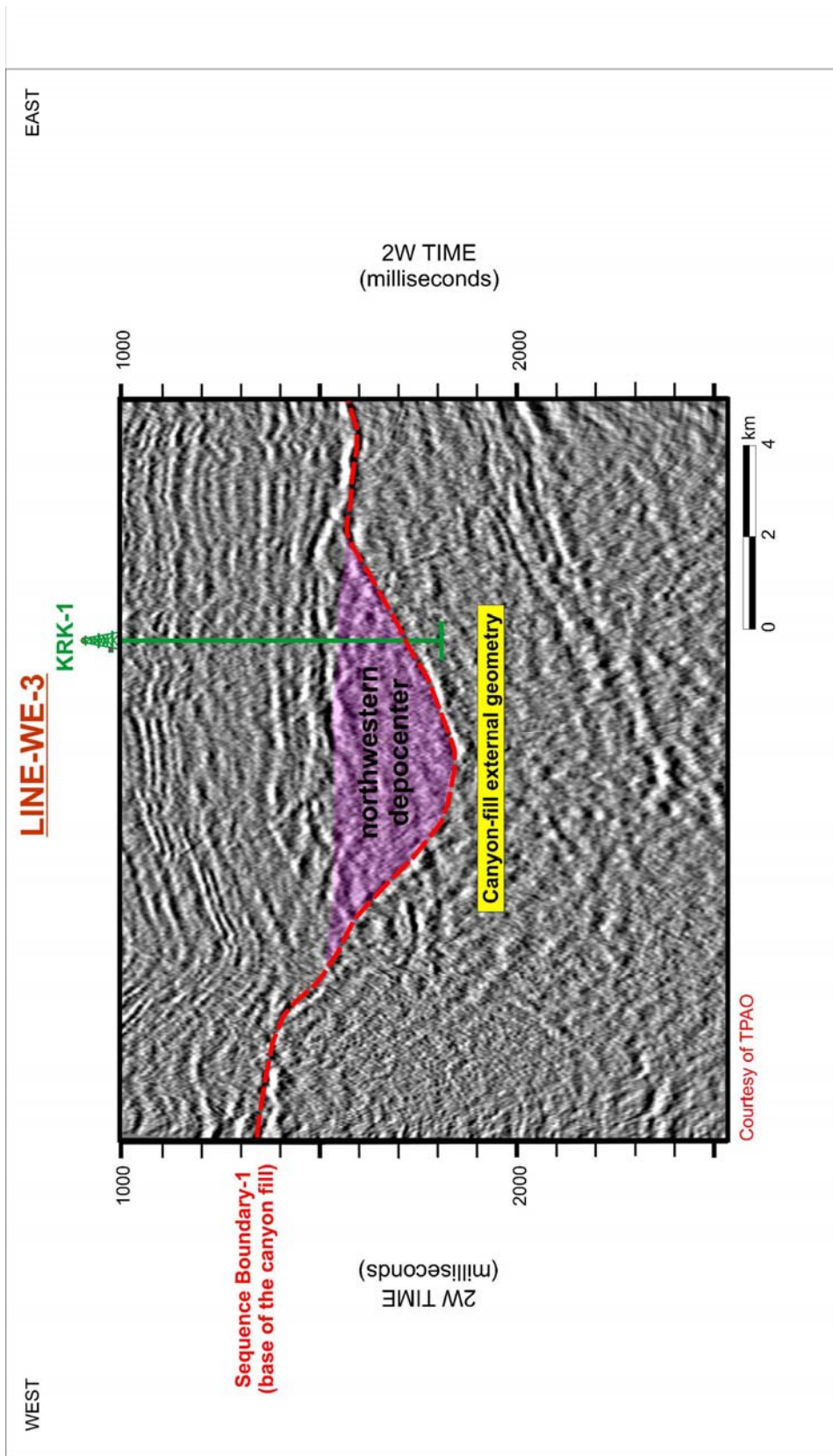


Figure 4.11 The seismic line crosses the north of the study area in parallel to the depositional strike direction. Purple color seismic package at around 1500 msec demonstrates canyon fill external reflection geometry. Canyon fill is composed of chaotic reflection configuration.

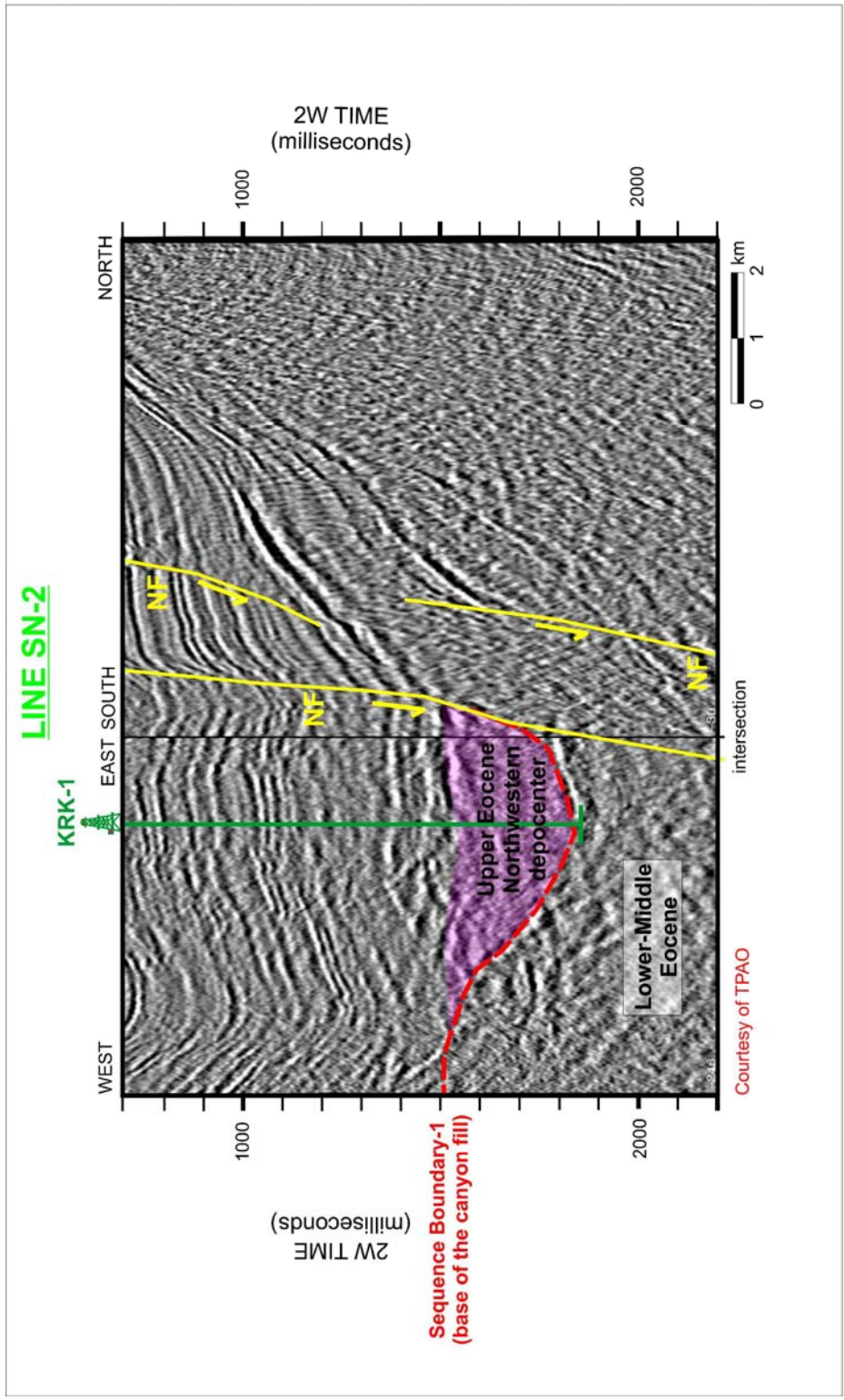


Figure 4.12 A west to east and south to north intersecting seismic lines. Purple color seismic package demonstrates the normal fault controlled canyon development, which constitutes the northwestern depocenter. NF: Normal Fault.

2062 m and 2579 m were analyzed (Figure 4.13a) and confirmed with cuttings. The slope fans directly overlie the continental deposits. The continental deposits were identified as red color, unconsolidated conglomerates with irregular gamma-ray and sonic log responses with thin claystone interval at the top. Between 2140 m - 2490 m, the slope fan succession was represented by conglomerates with blocky shape gamma ray responses. The sharp base of blocky shape gamma-ray responses and size of the conglomerates (at 2141 m with core confirmation: Figure 4.13b) indicated that the Northwestern depocenter was composed of highly erosive base sediments with high energy gravity flows. The thickness of the blocky shape gamma-ray responses ranges between 1 m to 7 m. In this succession, lower sequence boundary was placed at 2520 m at the base of slope fans. The overlying sequence boundary (Sequence Boundary-2) was placed at 2140 m.

The vertical trends in DG-3 well between above and below 3480 m represented different character (Figure 4.14). The coarse grained continental units were dominant below 3480 m with thick blocky shape gamma-ray responses. This unit was overlain by finer grained size sediments with irregular and higher gamma-ray responses. This interval continued with coarse-grained sandstones and conglomerates alternating with shale reflecting blocky shape gamma-ray responses. Van Wagoner et al., (1990) suggested that sharp upper and lower boundaries of individual beds are defined as typical high energy gravity flows in slope setting. The

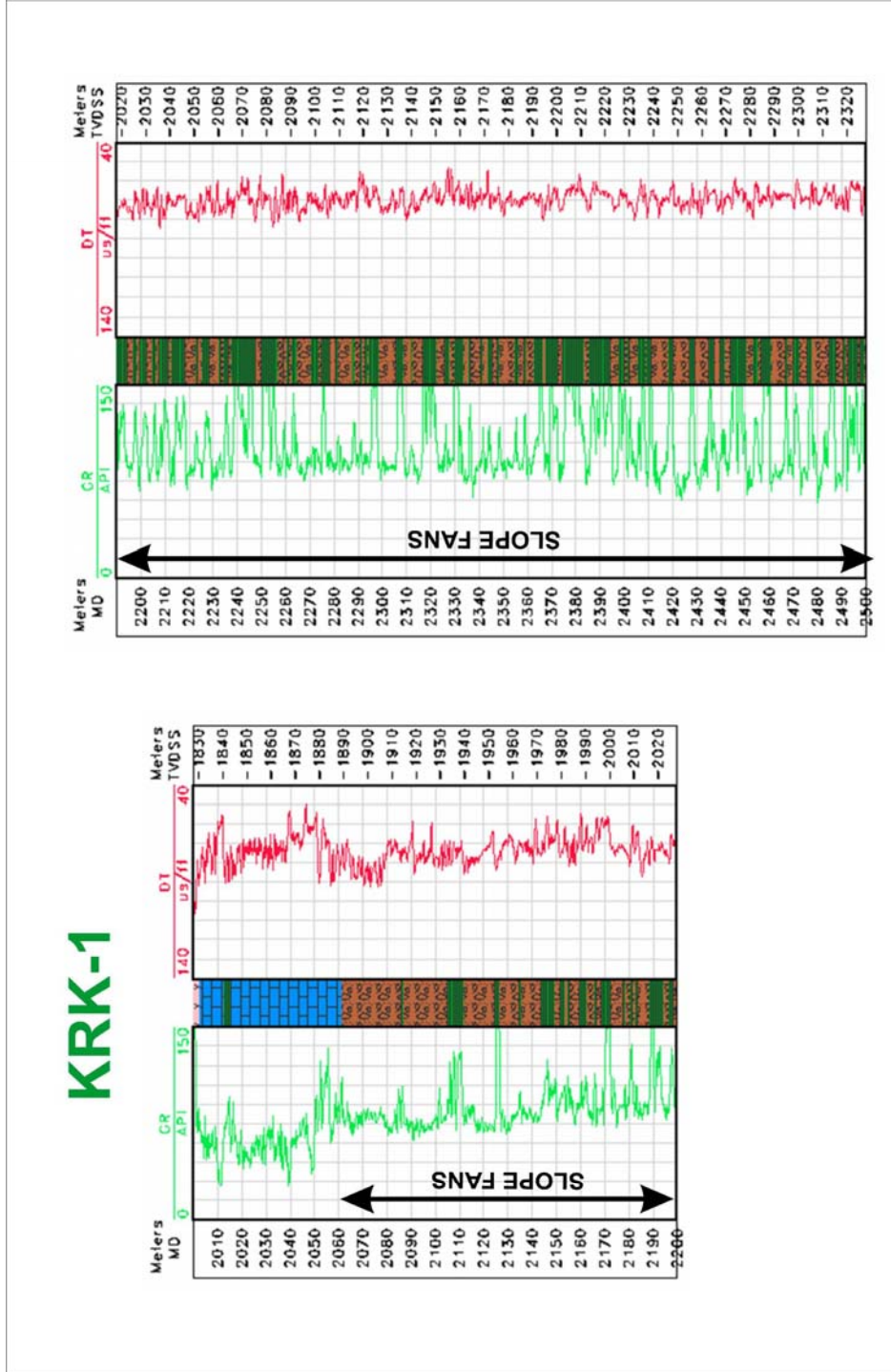


Figure 4.13a KRK-1 well gamma-ray (green on the left) and sonic log (red on the right) responses in the Northwestern depocenter. The fill is mostly composed of erosive base conglomerates TVDSS: true vertical depth from sub-sea, MD: measured depth.

**KRK-1 WELL
CORED INTERVAL (2141-2145 m)**

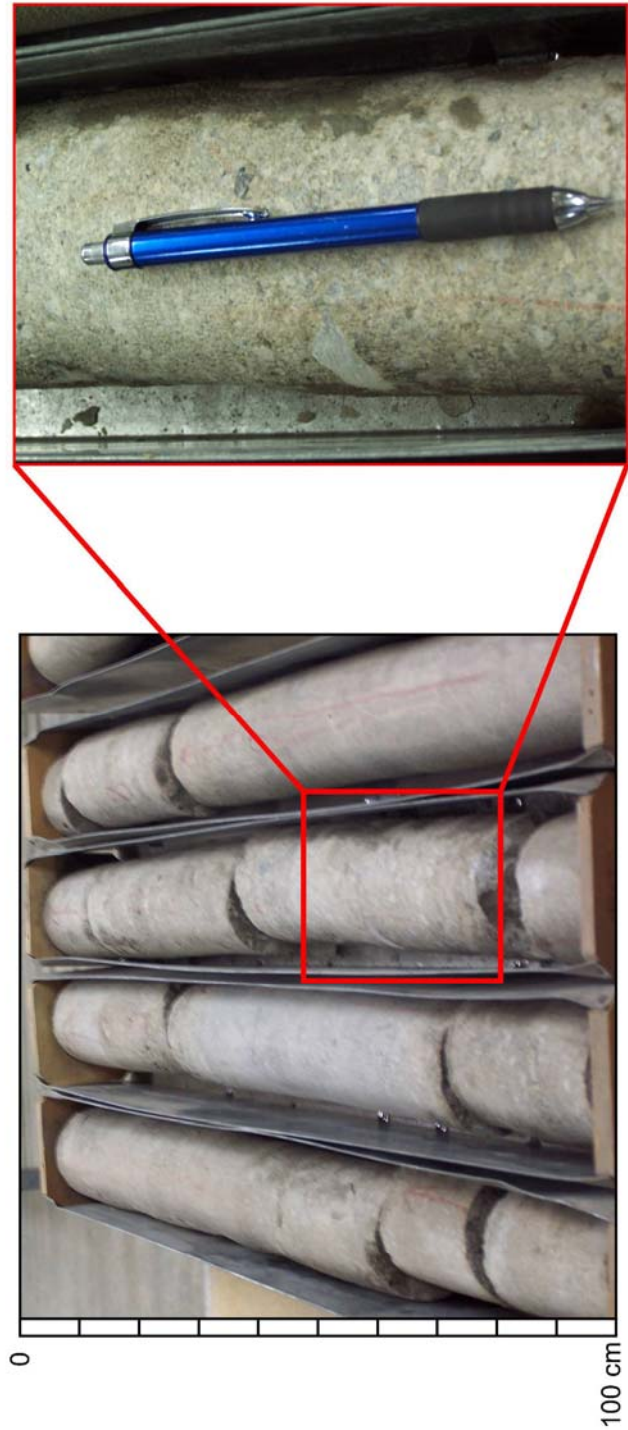


Figure 4.13b Cored interval between 2141-2145 m in the KRK-1 well indicates, the Northwestern depocenter is composed of erosive base conglomerates.

DG-3

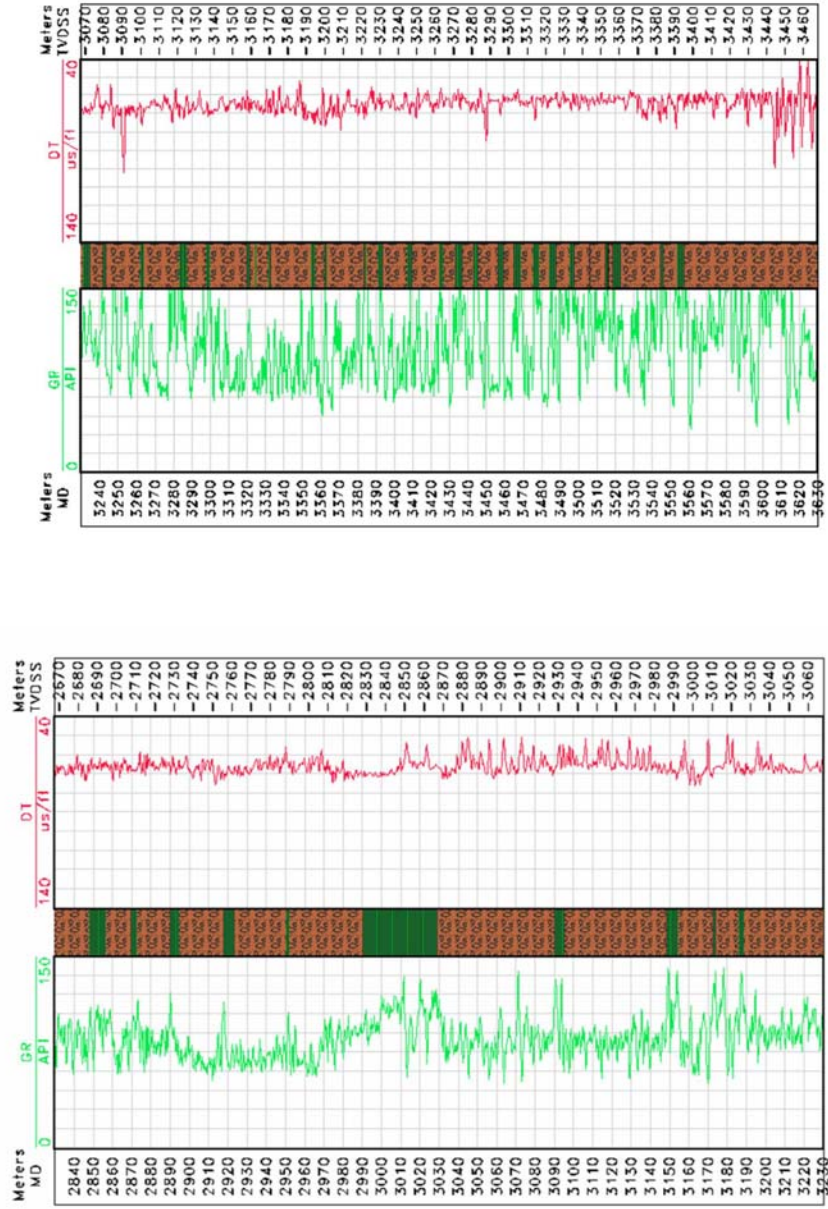


Figure 4.14 Gamma-ray (green on the left) and sonic log (red on the right) responses of the DG-3 well. TVDSS: true vertical depth from sub-sea, MD: measured depth. The Northwestern depocenter is characterized by erosive base and high density gravity flows.

thickness of the individual sandstone and conglomerates ranged from 1 to 7 m.

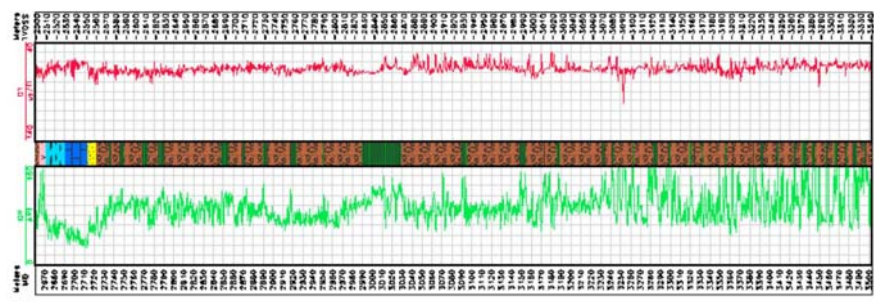
In this succession, the base of the slope fan succession, characterized by blocky shape gamma-ray responses was identified as the Sequence Boundary-1 (SB-1). This boundary is represented on seismic sections as a highly erosive surface. This sequence boundary was also recognized by Gerhard and Alişan (1986) on the basis of palynology analysis in DG-3 well. A major decrease in abundance and diversity of dinoflagellates and an increase in terrestrial palinofoms at around 3450 m indicated a major break in sedimentation, an unconformity surface. Figure 4.15 shows the gamma-ray and sonic log correlations of the KRK-1 and DG-3 wells.

4.2.2 Northeastern Depocenter

Northeastern depocenter is extended in a relatively larger area in the central basin between the CL-2 and the KY-2 well trend in the south and the Kuzey Osmançık Fault Zone in the north with sediment delivery pathways, which were composed of a multiple channel system on the northern shelf.

The sediment delivery pathways of the Northeastern depocenter were analyzed in the first step. Approximately east-west trending seismic lines on the northern margin of the basin exhibit channelized reflections (Figure 4.16). On the left side of the Line-WE-4, at around 500 msec, high amplitude channelized reflections were observed. Their width was as large

KRK-1



DG-3

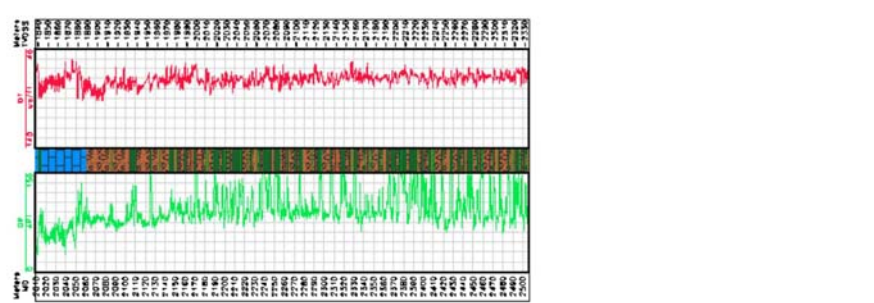


Figure 4.15 Gamma-ray (green on the left) and sonic log (red on the right) responses of KRK-1 and DG-3 wells. TVDSS: true vertical depth from sub-sea, MD: measured depth.

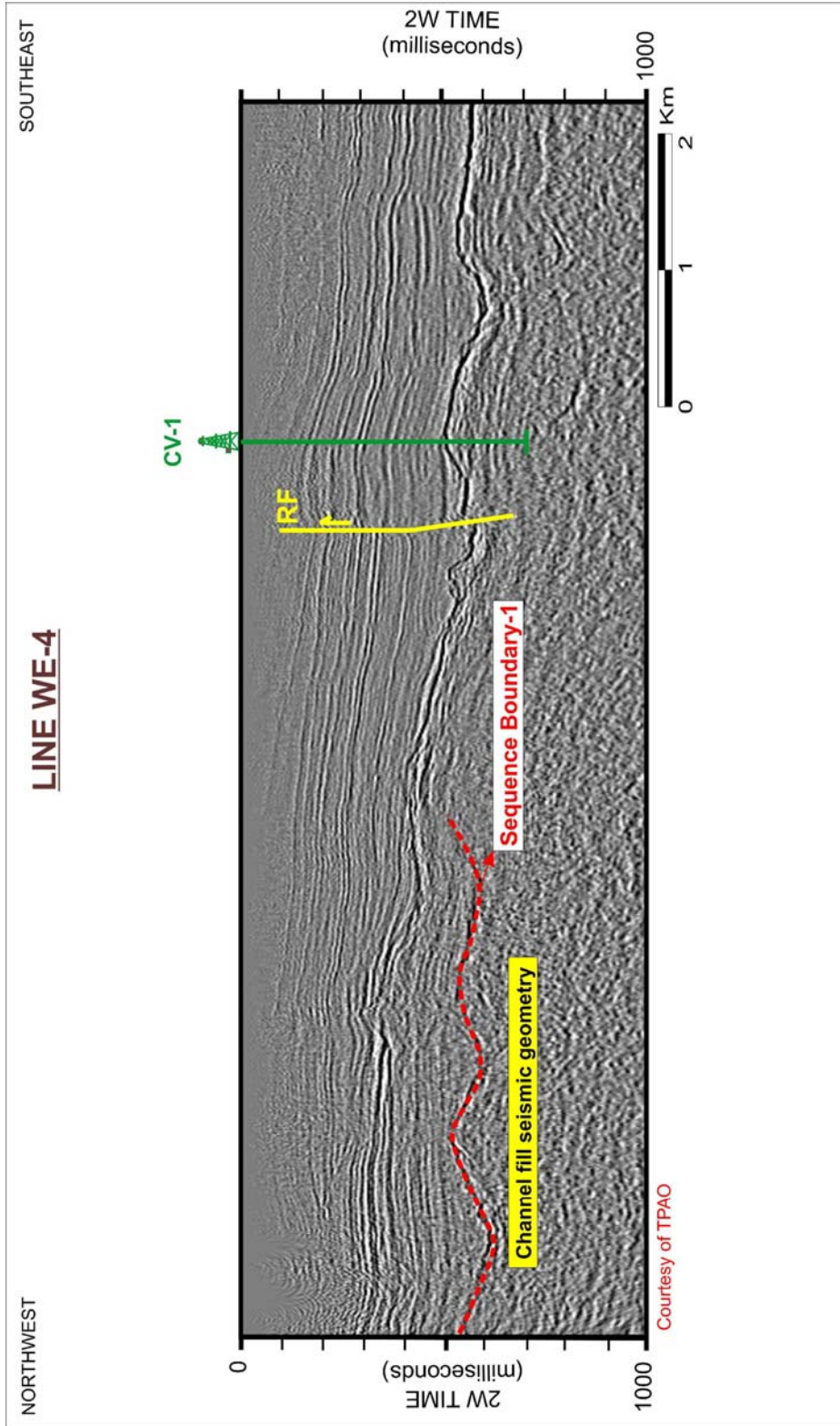


Figure 4.16 Seismic line crosses the northern shelf in the northwest to southeast direction. Channelized reflections shown in red dashed line are interpreted as the base of incised valley deposits. They incised the metamorphic basement and delivered large amount of sediments to the northeastern depocenter. RF: Reverse Fault.

as 1,5 km and thickness reached up to 150 m in depth. The magnitude of incision decreases and the width increases basinward. The fill of these channels were mostly composed of chaotic internal reflection configuration. These channelized reflections were interpreted as lowstand bypass system, which incised the northern shelf and used as sediment delivery pathways basinward (continental equivalents of the Northeastern depocenter). Figure 4.17 sketches isolated incised channel fill deposits. The well data drilled in the northern paleo-shelf confirmed (KV wells) that these channels underlain by the metamorphic rocks of the basement. The fill was mostly composed of poorly sorted, coarse-grained, unconsolidated continental to shallow-marine deposits (Eren, 1987). The width and thickness of the incised valleys revealed that a large volume of the Northeastern depocenter was fed by these channel system as multi-point sources or the line source according to source type classification of Galloway (1998) instead of a large canyon.

These incised valleys are observed within the northern paleo-shelf to the Kuzey Osmançik Fault zone. This fault zone almost characterizes the depositional limit of the Northeastern turbidite filled depocenter. In the paleo-northern shelf, the sequence-1 is represented by mostly isolated channel fill deposits. Gamma-ray and sonic log responses in the Kavakdere-6 well mostly exhibit dirtying upward and irregular gamma-ray and sonic log responses. With the cutting confirmation, the fill is composed of pebblestones alternating with shale in 60 m thick interval (Figure 4.18). The detailed core analysis by Eren (1987) suggested that the size of poorly

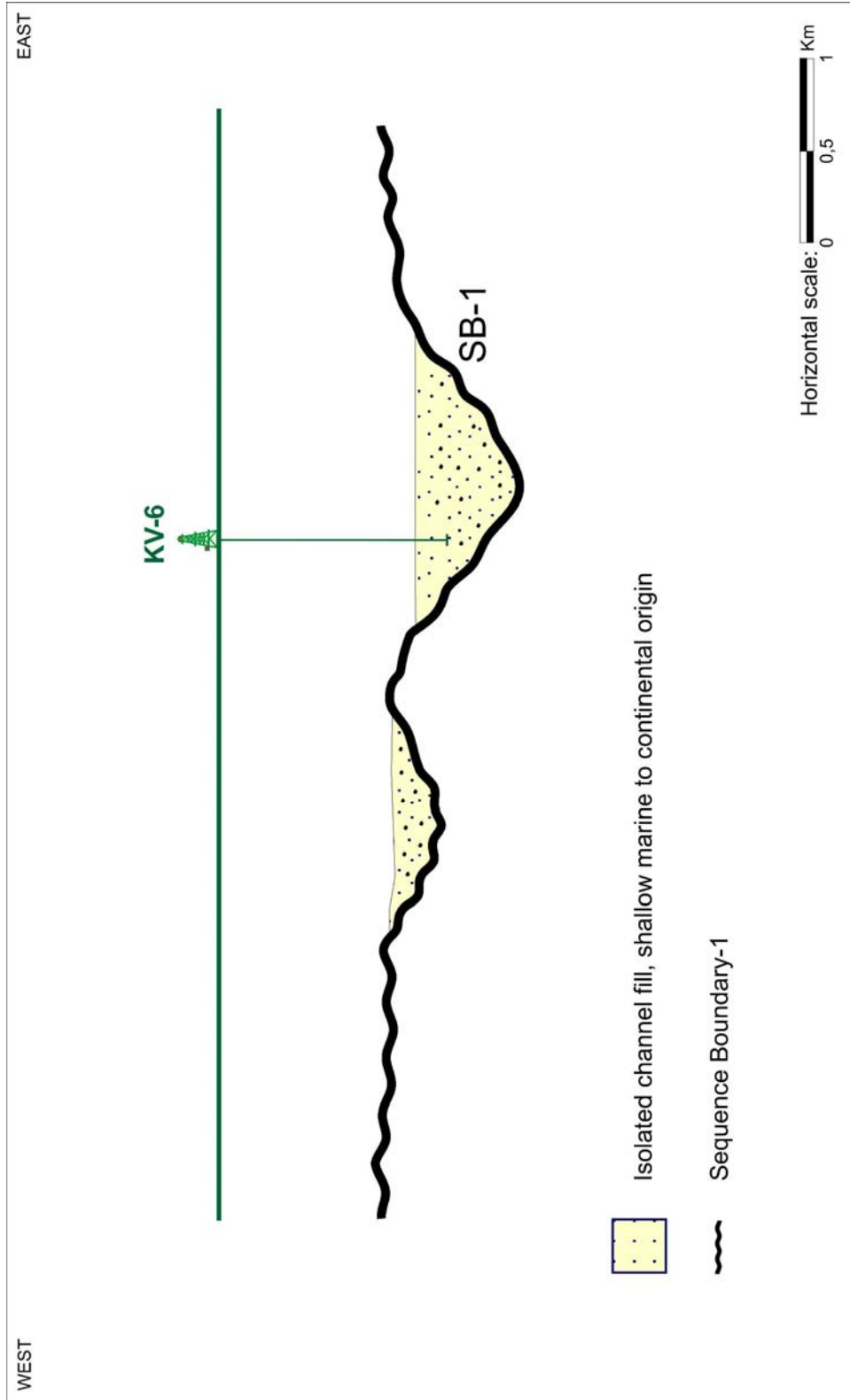


Figure 4.17 The figure sketches isolated incised valley deposits in the northern margin of the basin in the Late Eocene. The well data suggests that these valleys incised the metamorphic basement rocks and are composed of unconsolidated continental to shallow marine deposits.

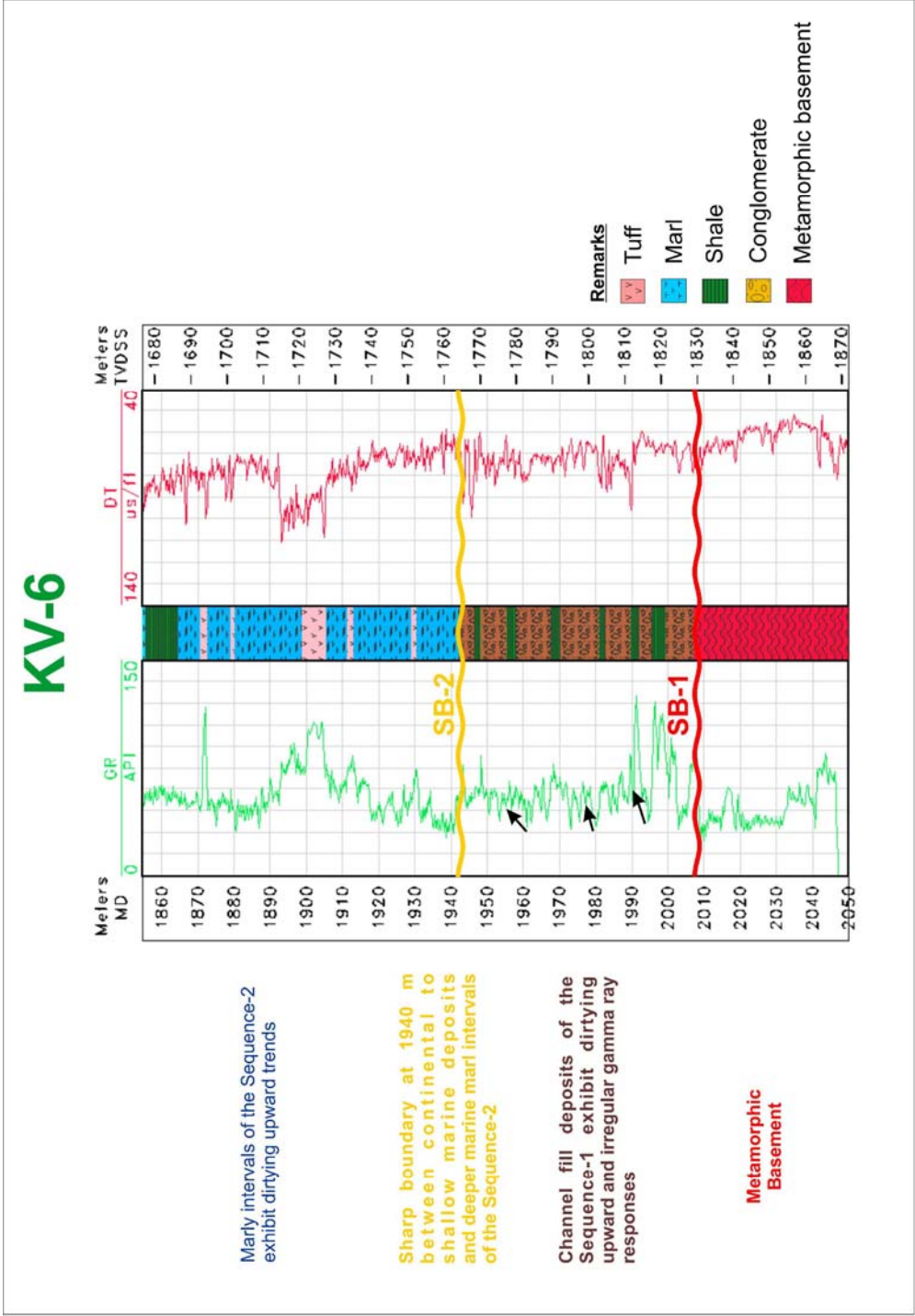


Figure 4.18 KV-6 well gamma ray (green on the left) and sonic log (red on the right) responses. TVDSS: true vertical depth from sub-sea, MD: Measured Depth, SB: Sequence Boundary.

sorted pebbles in this interval reaches up to 5 cm in diameter and the composition of pebbles indicates volcanic and metamorphic origin.

The basinward equivalents of the incised channels were turbiditic fill of the Northeastern depocenter. The fill is demonstrated by the blue color seismic package on north to south trending seismic Line-SN-3 (Figure 4.19). The Northeastern depocenter is thickest in the central part and thins towards the northern margin in a slope front fill external seismic geometry. The seismic package is composed of low amplitude, chaotic internal reflection configuration. Basal onlaps to the metamorphic basement was recognized in this seismic package. The northern edge of the seismic package represents the paleo shelf-slope boundary.

Two wells located along the seismic section were analyzed. AH-1 well was located in the northern paleo-shelf in the north side of the section. Isolated channel fill deposits were not observed in this well. Deposits of the Sequence-2 directly overlie the metamorphic basement. KY-2 well in the south penetrated the Northeastern depocenter. No clear indication of depositional environment was observed on the basis of vertical trends on the logs between 4570 and 4411 m. In this well, shale dominated interval between 4411 and 4475 m; sand dominated interval between 4480 m and 4540 m and another sand dominated interval between 4543 and 4562 m were observed on the basis of gamma-ray and sonic logs and this has been confirmed with cuttings (Figure 4.20). Within this succession, two clean gamma-ray readings were detected with 15 to 20 API units at 4475 and

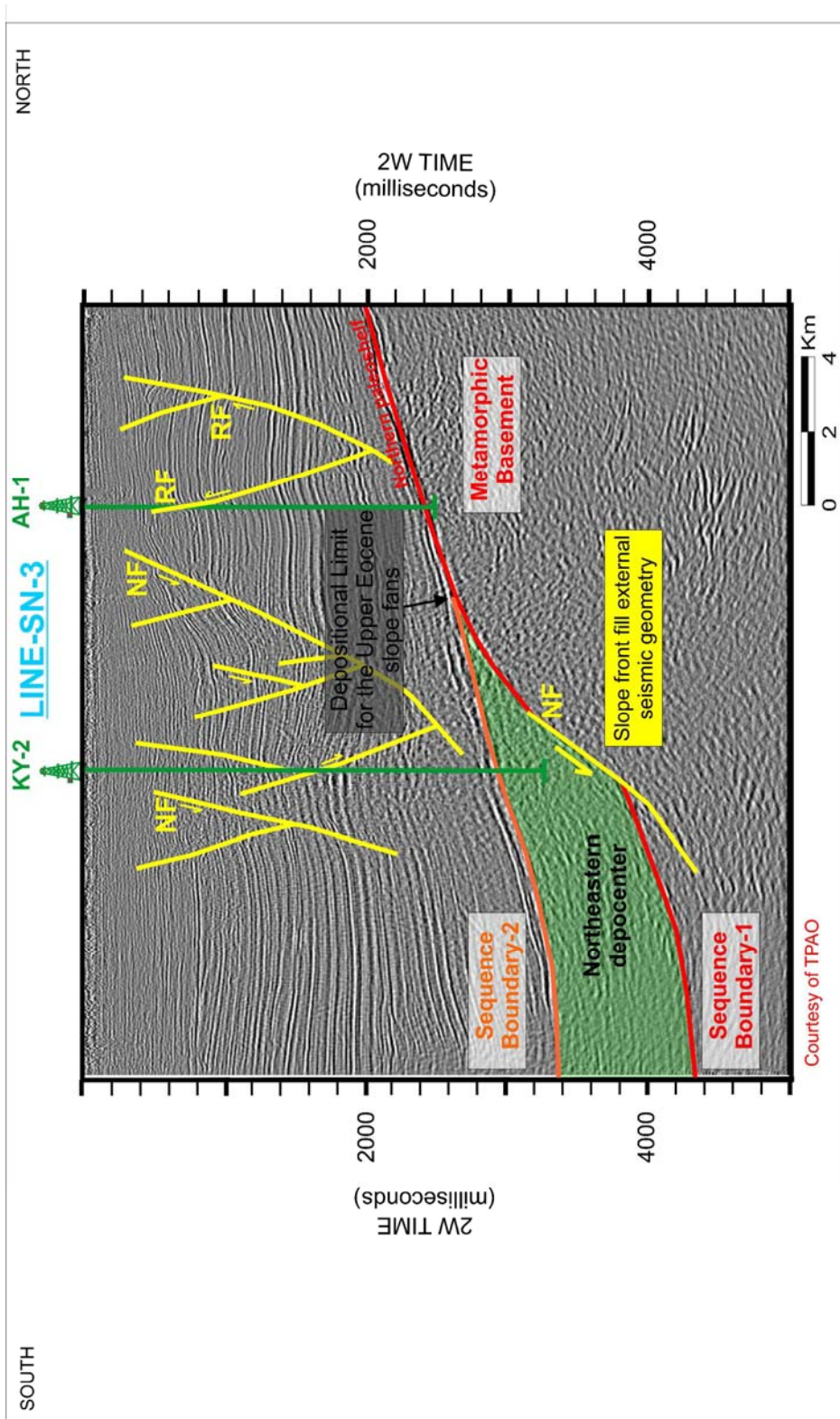


Figure 4.19 South to north oriented seismic line exhibits the northeastern depocenter of the "Hamitabat" Turbidite System. It is observed as a slope front fill external seismic geometry and chaotic internal reflection configuration. NF: Normal Fault, RF: Reverse Fault.

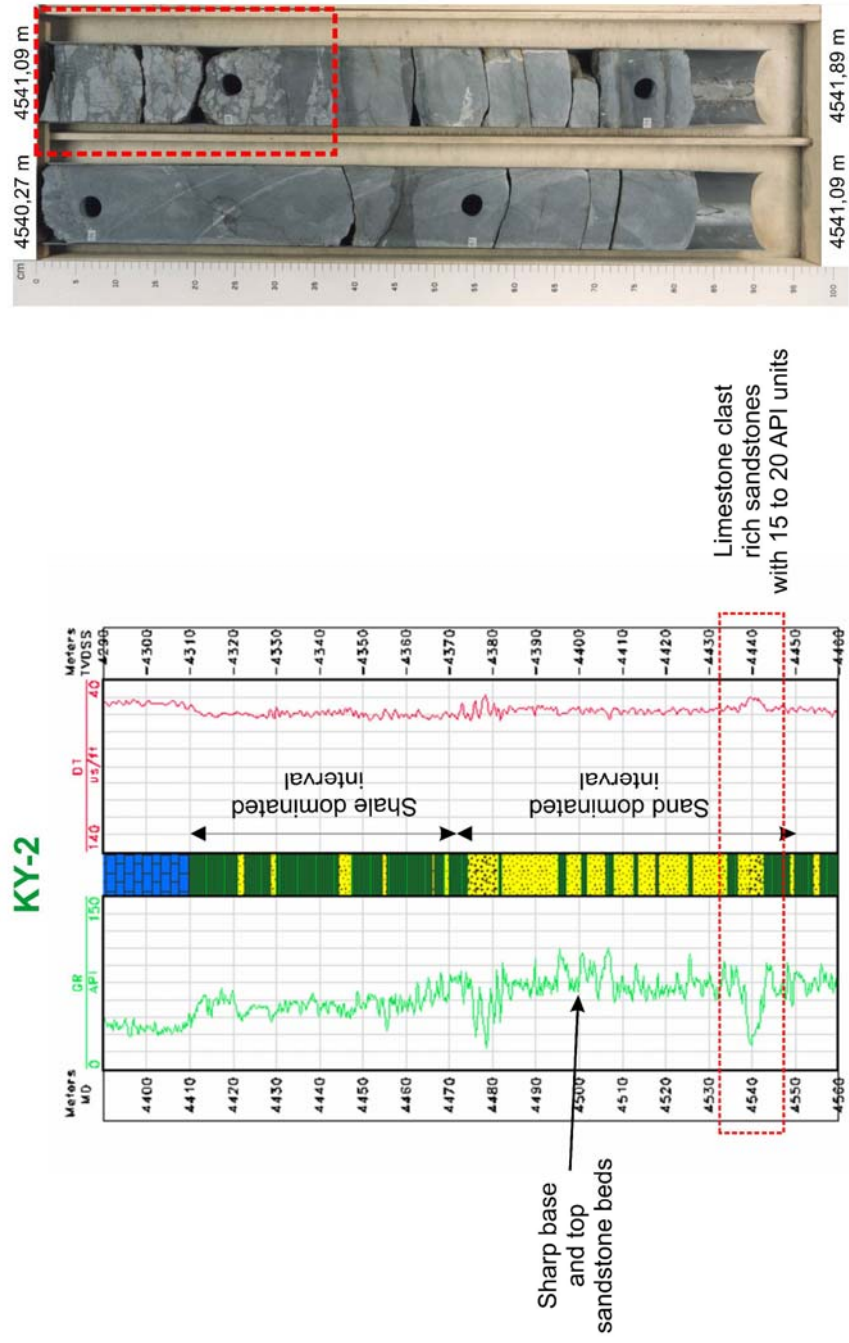


Figure 4.20 KY-2 well gamma ray (green on the left) and sonic log (red on the right) responses are shown. TVDSS: true vertical depth from sub-sea, MD: Measured Depth. Red color rectangles indicate limestone clast rich sandstones, and their gamma ray response with 15 to 20 API units on the left. Grain size ranges from sand to cobble. Limestone clasts are formed by bioclasts (benthic foraminifera, corals) and lithoclasts (nummulitic wackestone-grainstone).

4540 m respectively. Very low gamma-ray readings correspond to carbonate clasts rich sandstone intervals. They were interpreted as proximal debris flow deposits. Similar observations were also made in CL-2 well (Figure 4.21). Within the sandstone dominated interval between 4480 and 4540 m, base of sandstone beds were generally defined as sharp bases, indicating erosional base turbidite deposits.

CL-2 well is also located in the Northeastern depocenter. In this well, (Figure 4.21), deposits of the Sequence-1 overlie the metamorphic basement rocks. The siliciclastic sequence starts with red colored unconsolidated metamorphic origin conglomerates with irregular gamma-ray and sonic log responses. The top of the unconsolidated unit was set as the Sequence Boundary-1 at 2930 m. The next interval continues by a sand prone interval. In this interval, up to 5 to 6 m thick sandstone beds alternating with shales dominantly exhibit blocky shape (sharp base and top) and minor dirtying upward gamma-ray responses. This blocky shape interval is overlain by 60 m thick interval with cleaning upward trends between 2710 and 2770. Between 2585 and 2705 m, shale dominated interval was observed. Another interval dominated with blocky shape gamma-ray and sonic log responses was recognized between 2424 m and 2585 m. Two clean gamma-ray readings were detected with 15 to 20 API units at 2595 and 2670 m, respectively. Their confirmation with core data indicated that very low gamma-ray readings corresponded to carbonate clasts rich zones within sandstone dominated intervals. Above this interval,

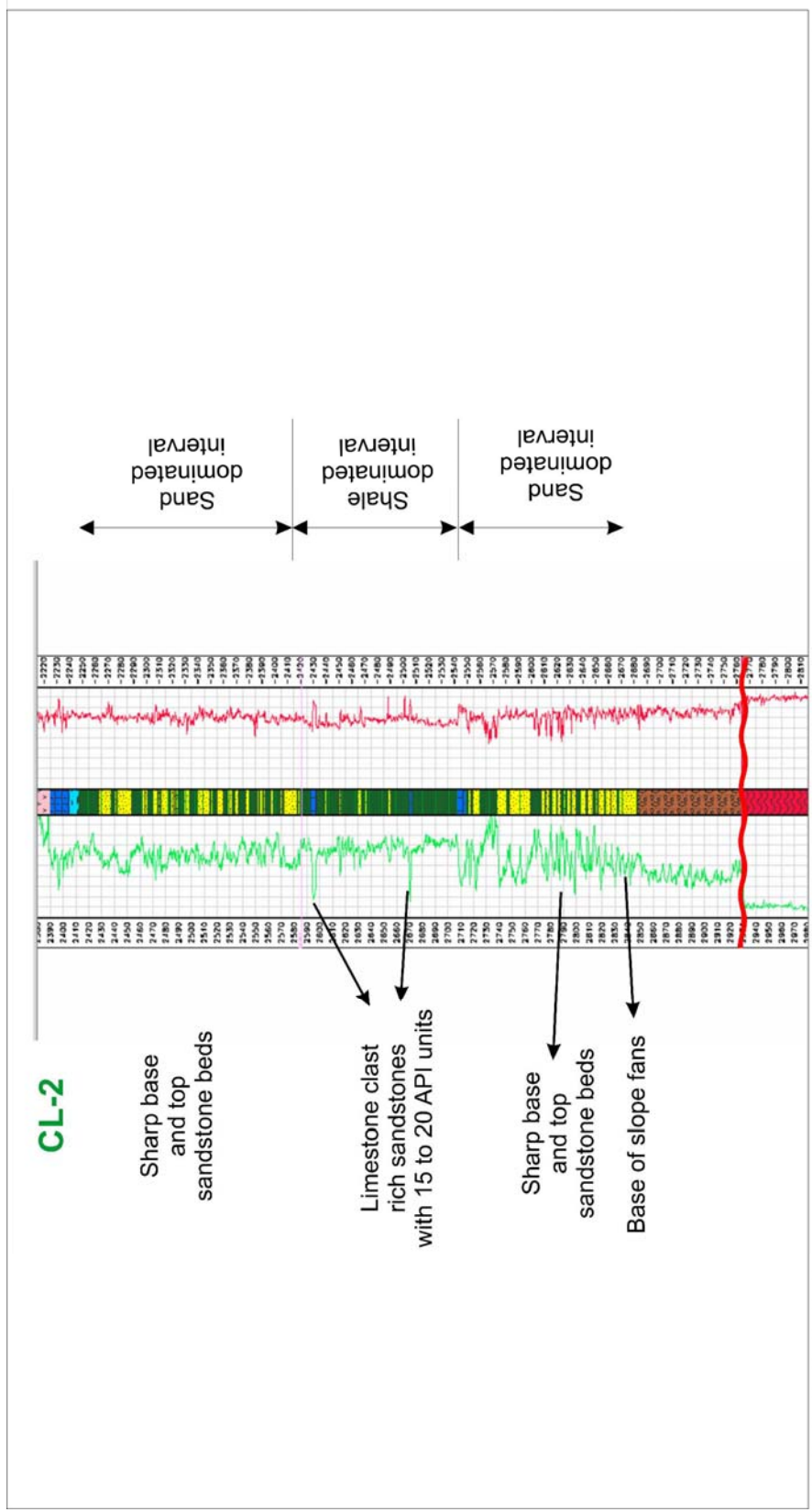


Figure 4.21 CL-2 well gamma ray (green on the left) and sonic log (red on the right) responses are shown. TVDSS: true vertical depth from sub-sea, MD: Measured Depth. The interval exhibits sand dominated, shale dominated and shale dominated intervals respectively. Blocky shape gamma ray responses within the sand dominated interval represent sharp base and top sandstone beds, which were interpreted as turbiditic sandstone intervals. Moreover, limestone clast rich sandstones with 15 to 20 API units gamma ray log responses were observed.

marls alternating with tuffs were recognized and confirmed with cuttings. The top of the marly interval was defined as a Sequence Boundary-1.

Line-WE-5 (Figure 4.22) is oriented in the northwest to southeast direction. On this seismic line, the Northeastern depocenter is represented by chaotic internal reflection configuration. The northwestern part of the orange horizon represents the continental to shallow marine deposits and the southeastern part represents the slope fan successions. Along the seismic line, three wells are located from northwest to southeast; KV-6 well, CL-2 well and TT-1 well respectively (Figure 4.23)

4.3 Results of the Analysis:

Comparison of the Characteristic Features of Three Major Depocenters in the “Hamitabat” Turbidite System

Sequence-1 is a third-order sequence, dated as Late Eocene. As the sequence-1 consists mainly of channel fill deposits along the northern margin of the basin, thick succession of mass flow and turbidity currents are the major elements in slope setting. Dominant lithology of slope setting was mostly shaped by the slope gradient, tectonic activity and enclosed sea-floor morphology.

The paleo-physiographic setting was characterized by a discrete shelf-slope break, oriented in southeast to northwest direction in the northern margin of the basin. The base of the Sequence-1, (corresponding to the sequence boundary-1) was defined on the northern paleo-shelf with

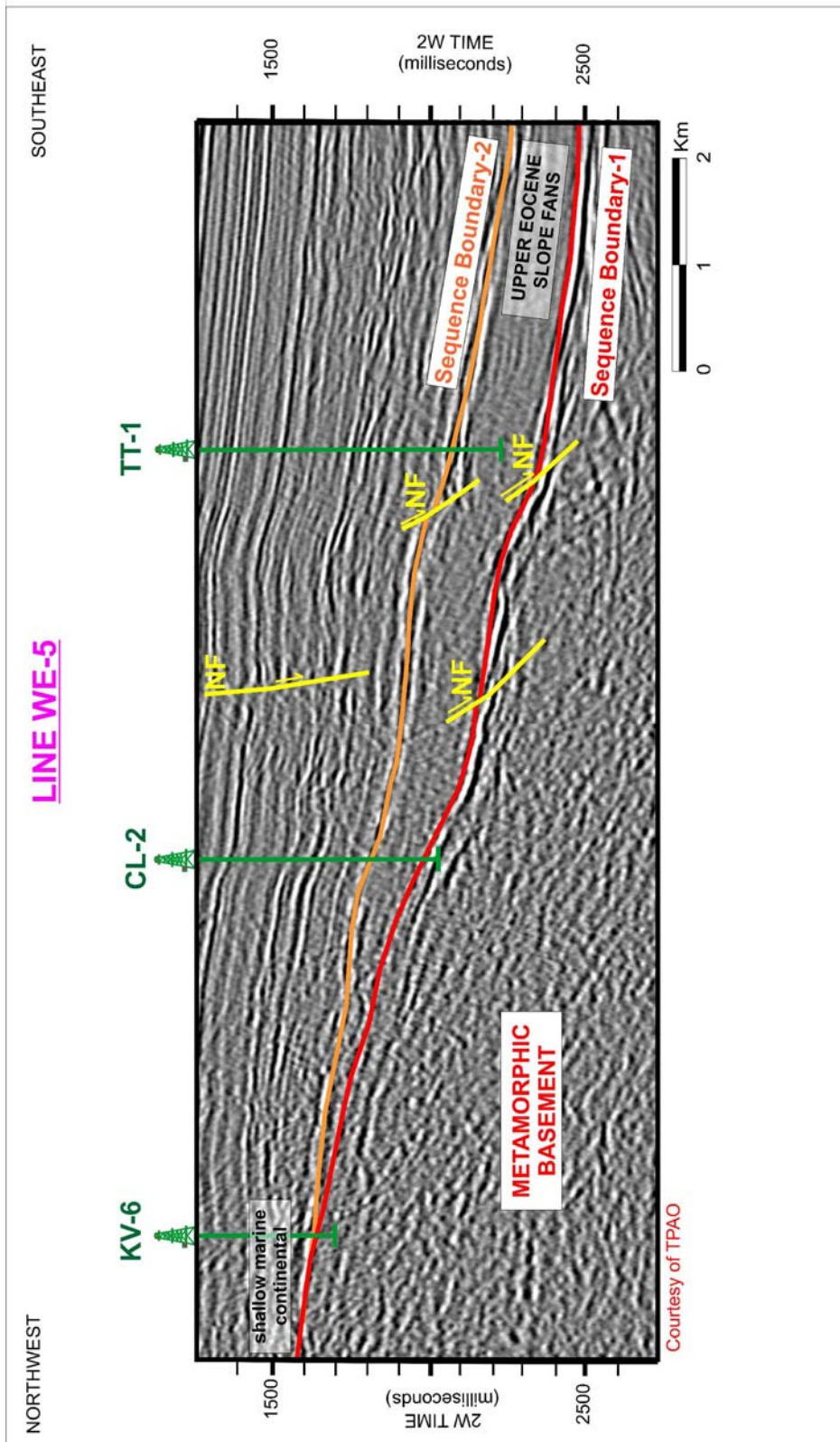


Figure 4.22 LINE-WE-5 is oriented in the northwest to southeast direction. The northeastern depocenter is represented by chaotic internal reflection configuration. NF:Normal Fault.

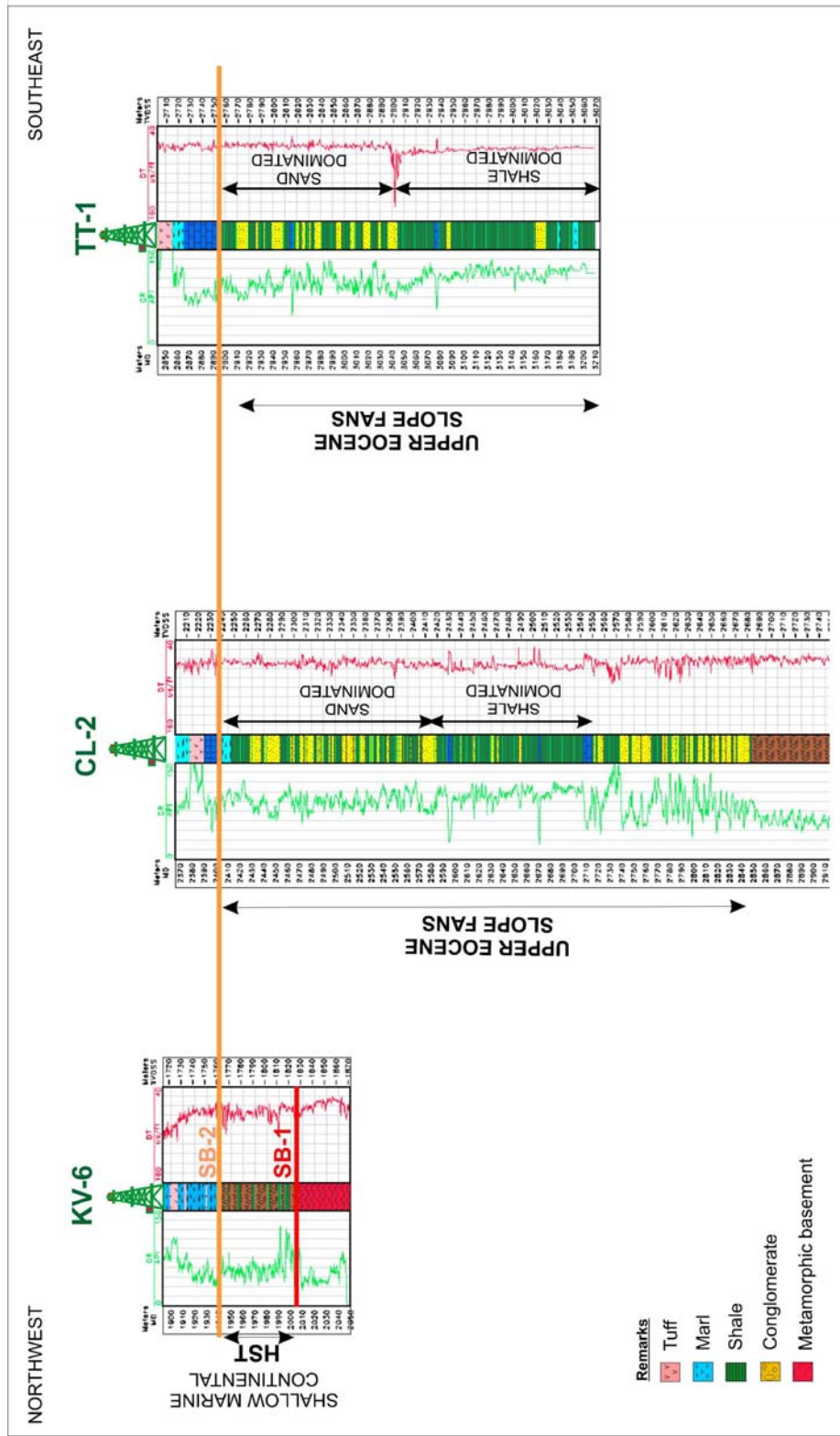


Figure 4.23 The well-log correlation of the KV-6, CL-2 and TT-1 wells within the Northeastern depocenter. SB: Sequence Boundary, HST: Highstand Systems Tract

the base of channel fill deposits and channel geometry on seismic sections. The channels observed in the northern shelf, interpreted as lowstand bypass systems, incised the metamorphic basement and delivered large amount of deposits basinward.

In slope setting, the base of slope fans was set as a sequence boundary. This sequence boundary on seismic sections was recognized as a baselap surface, against which progradational reflections terminate. The baselap surface characterizes the changing sea-floor topography, which was affected by differing subsidence and uplift ratio. This sequence boundary was also recognized by Gerhard and Alişan (1986) on the basis of a major decrease in abundance and diversity of dinoflagellates and increase in terrestrial palinofoms. This change may indicate a major break in sedimentation, an unconformity surface.

“Hamitabat” turbidite system was analyzed in three major depocenters in slope setting on the basis of their own sediment delivery type, dominant facies, areal extent and different seismic and well-log responses. They were named as the Western, Northwestern and Northeastern depocenters according to their geographic locations (Figure 4.24). Table 4.1 summarizes the characteristic features of three major depocenters of the “Hamitabat” turbidite system.

The paleo-physiographic setting in the Late Eocene was characterized with a discrete shelf-slope break, oriented in approximately southeast to northwest direction in the northern margin of the basin. The

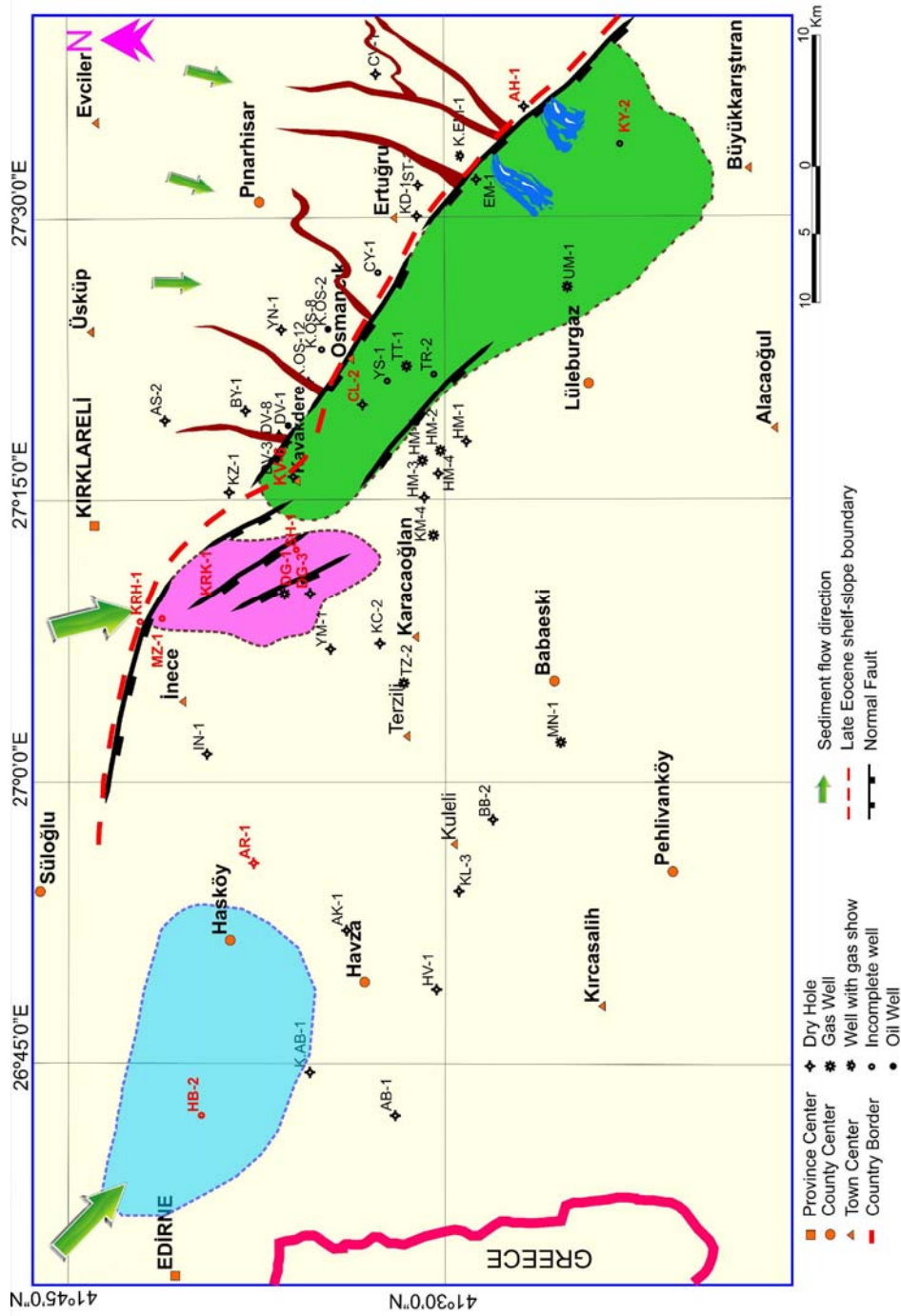


Figure 4.24 "Hamitabat" turbidite system was analyzed in three depocenters and named as Western, Northwestern and Northeastern depocenters respectively based on their geographic location. Blue, purple and green colors exhibit approximate areal extension of the Western, Northwestern and Northeastern depocenters, respectively.

Table 4.1 The characteristic features of three major depocenters of the "Hamitabat" turbidite system.

	WESTERN DEPOCENTER	NORTHWESTERN DEPOCENTER	NORTHEASTERN DEPOCENTER
Basin physiography	Enclosed depressions	High slope gradient narrow shelf, enclosed depressions	Low slope gradient wide shelf, relatively uniform basin floor
Dominant Lithology	Alternation of fine to medium-grained sandstone with shale	Alternation of coarse-grained sandstone, conglomerate with shale	Alternation of fine to medium-grained sandstone with shale
Source Type	Point source	Point source	Multi point (line) source
Source Direction	W-NW	NW-N	N
Thickness (m)	500 m well penetration in the HB-2, close thickness calculation from seismic	~ 500 m well penetration in KRK-1 well	~ 450 m well penetration in CL-2 well
Areal Extent (km²)	~ 300 km ² 3D seismic required for better estimation	In smaller size better seismic coverage required for better estimation	In a larger area between Kavakdere and the KY-2 well
Well Penetration	HB-2	KRK-1, DG-1-2-3, SH-1, MZ-1	CL-2, KY-2, TR-2
Seismic Facies	Chaotic internal reflection conf. Canyon fill external geometry (confined)	Chaotic internal reflection conf. Canyon fill external geometry	Chaotic internal reflection conf. Slope front fill external geometry

southeast northwest trending shelf-slope break makes a north bending nearby Kavakdere and continues to westward in parallel to east-west direction (Figure 4.24). A diagnostic change between two locations could be realized in the shelf and slope positions. Between the KY-2 well and KV-6, the basin physiography was characterized by a relatively larger shelf with gentle slope gradient. Between the KV-6 well and the IN-1 well, the basin physiography was characterized by a steep slope gradient and a narrow shelf. This diagnostic change affected the erosional and depositional features of the "Hamitabat" depocenters. The basin physiography in the northwest of the study area with a narrow shelf and a steep slope gradient dominated the development of a large canyon. On the other hand, relatively wider shelf and a gentle slope gradient dominated line type source for turbidite fan system in the northeast of the study area. Line type source was characterized by a multi-channel system in the wide northern shelf on the basis of seismic reflection data. Two different physiographic settings were depicted in Figure 4.25. Depositional dip and strike oriented seismic lines showed that the Western depocenter was fed by the northwest direction and extended under the effect of the changing submarine topography. As a consequence of high subsidence and uplift ratio, sea-floor morphology has changed. A northwest to southeast trending topographic high between the AR-1 well and the KC-2 well bounded the sediments in the Western enclosed depression in the western part of the study area. The Northwestern depocenter was directly fed by the northern provenance as

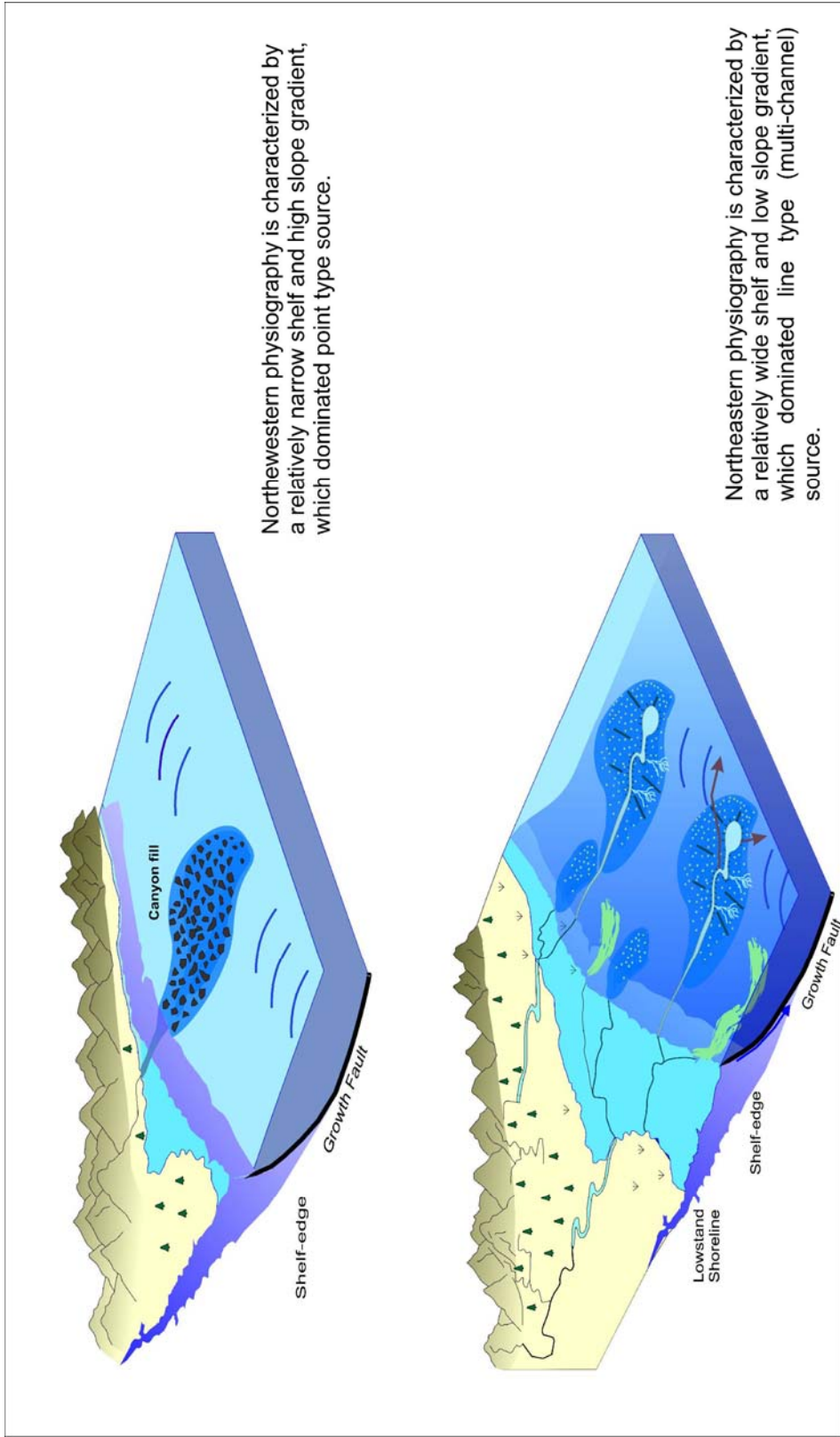


Figure 4.25 The Northwestern and Northeastern depocenters represent different nature of depositional fill, which was mostly shaped by the Late Eocene basin physiography in the northwestern part of the Thrace Basin..

isolated canyon fill deposits with highly erosive character. On the other hand, channel system observed on seismic sections suggested that the Northeastern depocenter sediment delivery pathways were from northwest to southeast and characterized by multi-channel system. Additionally, the northeastern depocenter were extended in a larger area in the northeast part of the study area. Both the areal extent and the facies of the Northwestern and Northeastern depocenters were strongly affected by the growth fault geometry.

This study suggested that steep angle slope gradient and related syn-sedimentary tectonic activity are the major sources of high energy gravity flow deposits (slumps-slides) in isolated canyons in the Northwestern depocenter (Figure 4.26). Seismic data showed that the canyon was formed in the hanging fault block of the southeast to northwest trending normal fault. This indicates that the accommodation space was mostly controlled by the sea-floor subsidence. The erosive base of the beds is conglomeratic reflecting mass movement of sediments. Relatively gentle slope gradient played an important role to the deposition of fine to medium-grained turbidites and minor slide and slump deposits. In Ediger and Batı (1987), 400 m/1 million year deposition rate was roughly estimated on the basis of seasonal deposits (lamina) from cores in HM-25 well. Probably, faster deposition rate would be expected for the Northwestern depocenter.

Mitchum et al. (1993) generated a model representing the different character of depositional fill in different fault blocks, which was controlled by

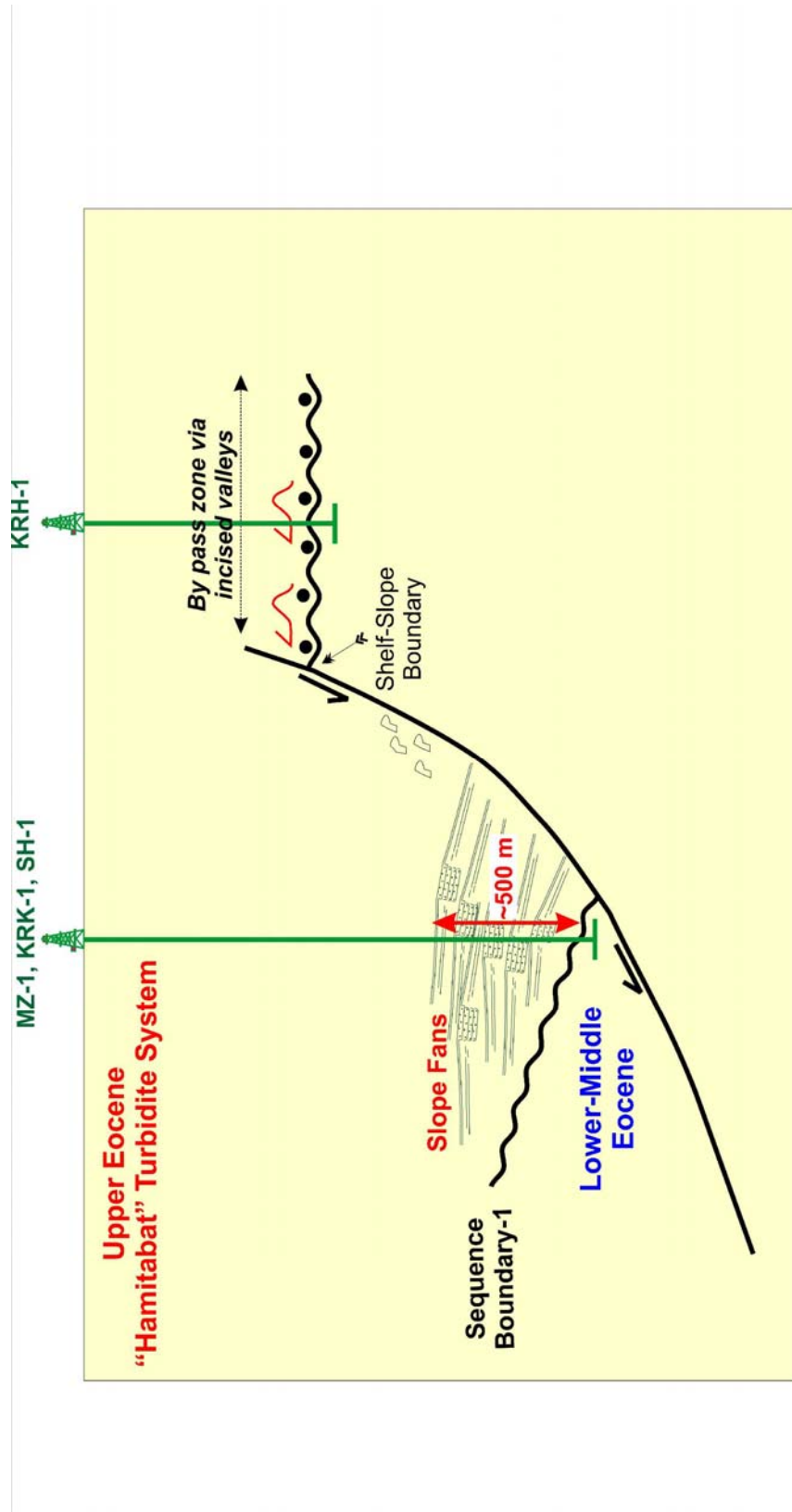


Figure 4.26 This study suggested that syn-sedimentary tectonic activity are the major source of high energy gravity flow deposits.

expansion faulting in sequence stratigraphic framework (Figure 4.27) in Gulf of Mexico. Gulf of Mexico is composed of typical diapir controlled many subbasins, bounded by a large contemporaneous expansion faults. Based on integrated well log, seismic and high resolution biostratigraphic analysis, Mitchum et al. (1993) generated an idealized depositional model, revealing the great influence of growth faulting. In their model, as basin floor fan and slope fan (the products of LST) comprise the downthrown side of the fault, the lowstand prograding complex, overlying TST and HST observed in both sides of the fault.

The comparison of the characteristics of each depocenter suggested that facies character of the northwestern depocenter was highly affected by the steep slope gradient. Due to the continuous tectonic activity during deposition, both sides of the fault blocks were never balanced and the hanging fault block is composed of thick succession of slope fan deposits (Figure 4.26). The fill is mostly conglomeratic with erosive bases. On the other hand, the existence of the incised channel system in the northeastern shelf and the progradational character, observed in the Western depocenter indicated that the third-order lowstand position of the sea-level may only promote the submarine canyon development and may be stated as a secondary factor.

Reading and Richards (1994) classified the depositional systems of the deepwater basin margins into twelve types regarding to their grain size (from mud to gravel dominated) and feeder systems (point source to

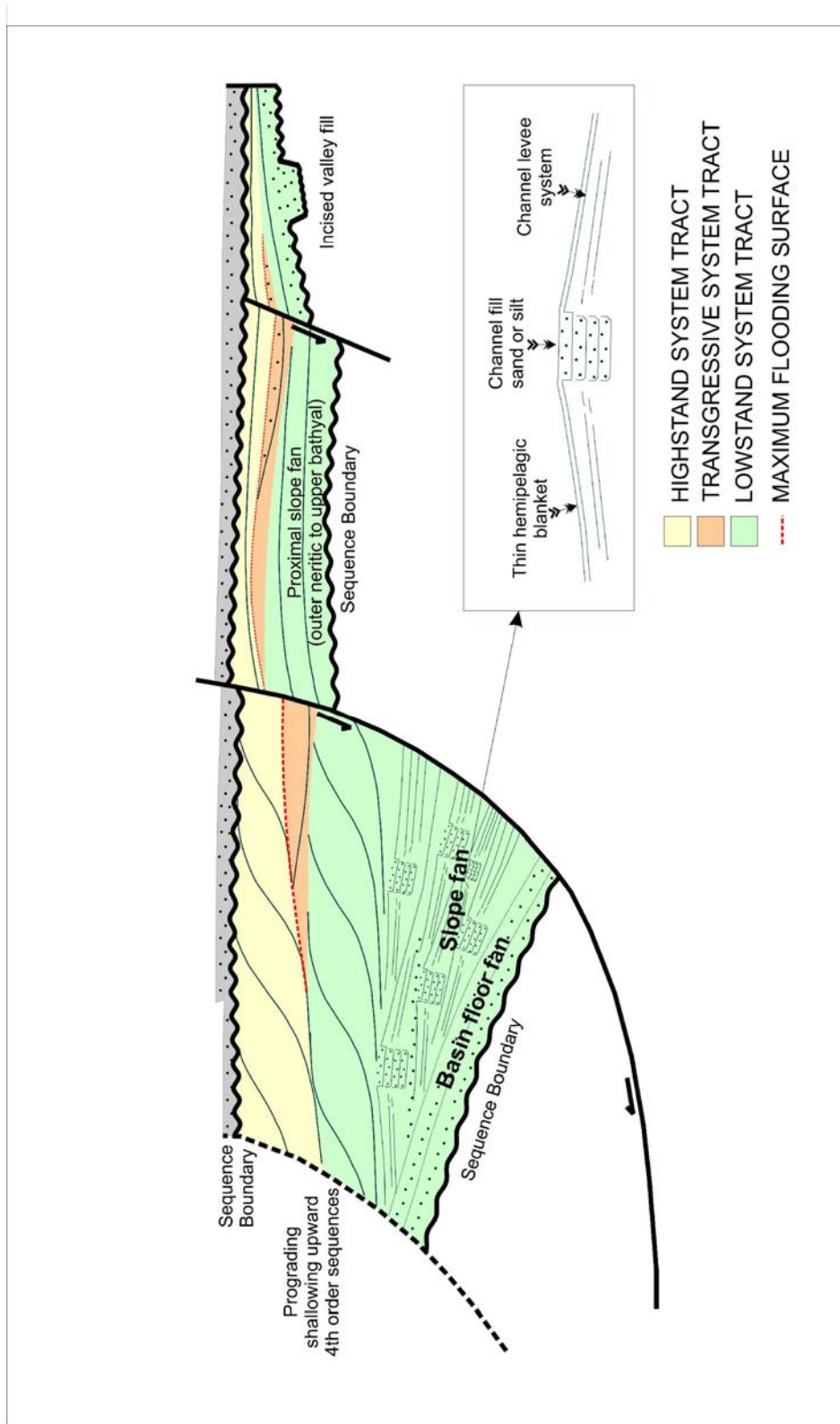


Figure 4.27 Idealized sequence stratigraphic model of expanded Late Cenozoic sub-basin, redrawn from Mitchum et al., 1993.

multiple sources). The results of my study contribute to their study that even in a single basin varying basin morphology can shape the grain size distribution and the feeder system. In the northeast of the study area, the existence of shelf with gentle slope dominated the multi-channel source system. Whereas, the steep slope and the narrow shelf dominated the point source canyon formation with coarser fill.

Gervais et al. (2004) also made similar observations along the Corsica margin in the western Mediterranean Sea. They emphasized the Oligo-Miocene tectonic evolution and paleo-basin morphology of the Corsica margin in the western Mediterranean Sea. They observed different feeder systems in the eastern and the western margins. They indicated that the western Corsica margin was characterized by numerous deep canyons, which were developed in a steep slope without a continental shelf. On the other hand, eastern margin was characterized by moderately developed continental shelf with shallower canyons and channels on a gentle slope.

Bruhn and Walker (1995) examined the importance of global and regional variables as a controlling factor in canyon development and turbidite deposition.

During the Late Cretaceous, the Campos Basin was situated in a passive margin with a narrow and steep shelf. There was an important uplift in the adjacent hinterland and movement along the basin margin faults. This time corresponds to the second-order eustatic sea-level rise by Haq et al.

(1987). During this time, the effect of fluctuations of relative sea-level were minor and source remained relatively close to the shelf-slope break.

They claimed that in the Campos Basin tectonic control played an important role on sediment supply and local sea-level fluctuations instead of eustasy in the Late Cretaceous. Canyon formation and turbidite deposition were dominated by listric normal faults. Despite the long term sea-level rise (Haq et al., 1987), coarse turbidites were deposited in canyons along the Brazilian continental margin.

Clift (1996) observed that erosion and mass-wasting along the Southeast Greenland during the Oligocene were related to the rapid subsidence of the oceanic crust of the Irminger Basin, resulting in the steepening of the continental slope. He suggested that this event can not be explained by eustatic fall. Instead, it should be driven by the tectonic subsidence.

The results of the analysis in this study emphasized that instead of eustasy, regional tectonic activity (high subsidence rate) dominated the slope instability and the deposition of thick succession of coarse-grained systems with erosive bases. Tectonic activity plays a major role in the spatial development of many destructional slope systems e.g. Millington and Clark (1995), Trincardi et al. (1995), Clift (1996) in Galloway (1998).

CHAPTER 5

A SEQUENCE STRATIGRAPHIC APPROACH TO THE DEPOSITIONAL HISTORY ANALYSIS OF THE UPPER EOCENE CLASTIC-CARBONATE MIXED SYSTEM

5.1 Introduction

Sequence-2, Sequence-3 and Sequence-4 constitute the mixed carbonate-clastic system. Shallow marine siliciclastics of the Koyunbaba Formation, shallow marine carbonates of the Soğucak Formation and coeval basinward pelagic limestones, and marl-tuff alternations of the Ceylan Formation are major lithologies of this system (Figure 5.1). On the basis of foraminiferal analysis, the depositional age of the studied interval has been dated as Late Eocene (Erenler, 1987).

Basin physiography in Late Eocene is shaped by a discrete shelf-slope break. As shelf setting is characterized by shallow marine carbonates and marl dominated intervals, basinal setting is composed of pelagic limestone, marl and tuff alternations. Therefore, the wells were analyzed in two different physiographic setting: shelf and basinal. Three-dimensional depiction of the Late Eocene depositional model in the northwest of the Thrace Basin is shown in Figure 5.2.

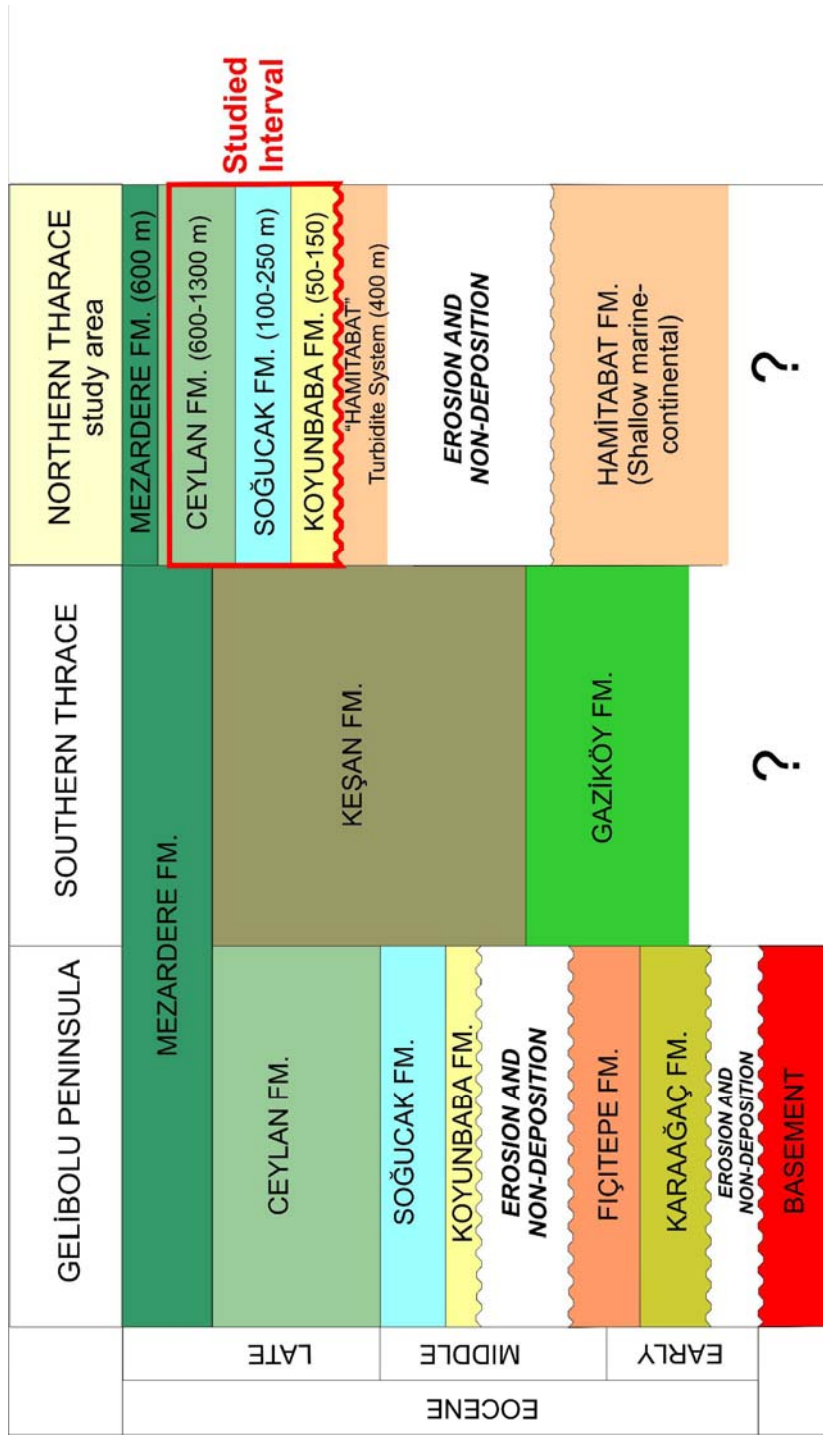


Figure 5.1 Stratigraphic relations of the Eocene formations in the Gelibolu Peninsula, southern Thrace and northern Thrace. This study focuses on northern Thrace. The studied interval (Sequence 2, 3 and 4) constitute the Late Eocene Koyunbaba, Soğucak and Ceylan Formations (in red rectangle) in the northern part of the Thrace Basin (modified from Siyako, 2006).

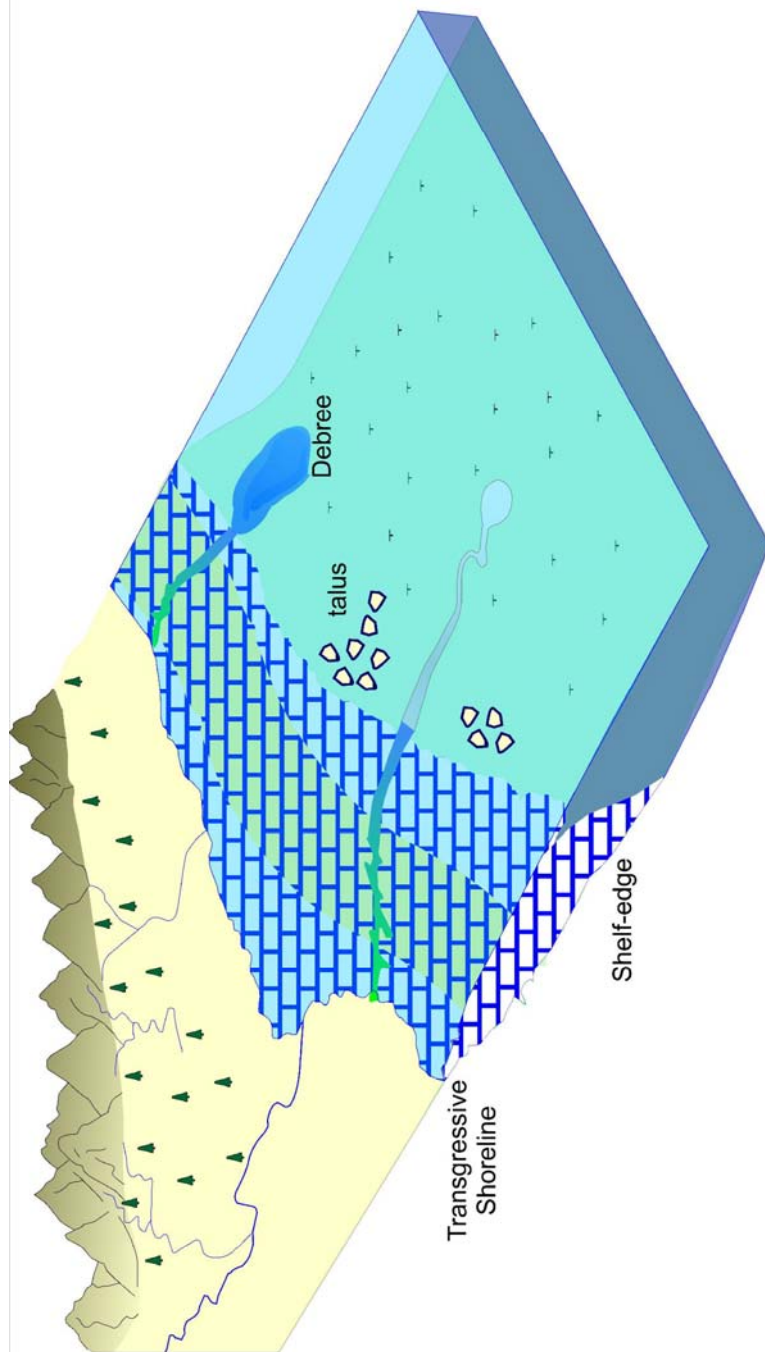


Figure 5.2 A three dimensional depiction of Late Eocene depositional model in the northwest of the Thrace Basin. Basin physiography in Late Eocene is shaped by a discrete shelf-slope break. As shelf setting composed of initial clastics and shallow marine carbonates, basinal setting is composed of pelagic limestone, marl and tuff alternations.

For the depositional history analysis in sequence stratigraphic approach; first, limestone and marl dominated intervals were investigated in detail in the northern paleo-shelf where diagnostic vertical trends were observed. Major reason was that the growth profile of carbonates and related marl deposition are very sensitive to sea-level fluctuations in shelf settings (Kendall and Schlager, 1981). Radioactivity content of two lithologies exhibited abrupt contrast so that vertical trend analysis on the basis of gamma-ray logs was carried out with ease. Second, reflection termination patterns on seismic sections were analyzed to define sequence boundaries and stacking patterns, and integrated with log analysis. The surface between limestone and marl lithologies was recognized by strong acoustic impedance contrast (velocity multiply by density ($\rho \cdot V$)) (see Chapter 3). Due to their high velocity content, limestone intervals were easily defined by high amplitude, continuous reflection(s) and distinguished from the overlying and underlying marl dominated intervals. Third, depositional dip (south-north) and depositional trend (west-east) oriented seismic sections were utilized for basinward correlations. The location map of seismic and well data sets, used in Chapter 5 is shown in Figure 5.3.

5.2 Carbonate and Marl Dominated Deposition as Response to Relative Sea Level Changes

Relative sea-level change is one of the major factors, controlling the growth profile of carbonates (Kendall and Schlager, 1981; Neumann and

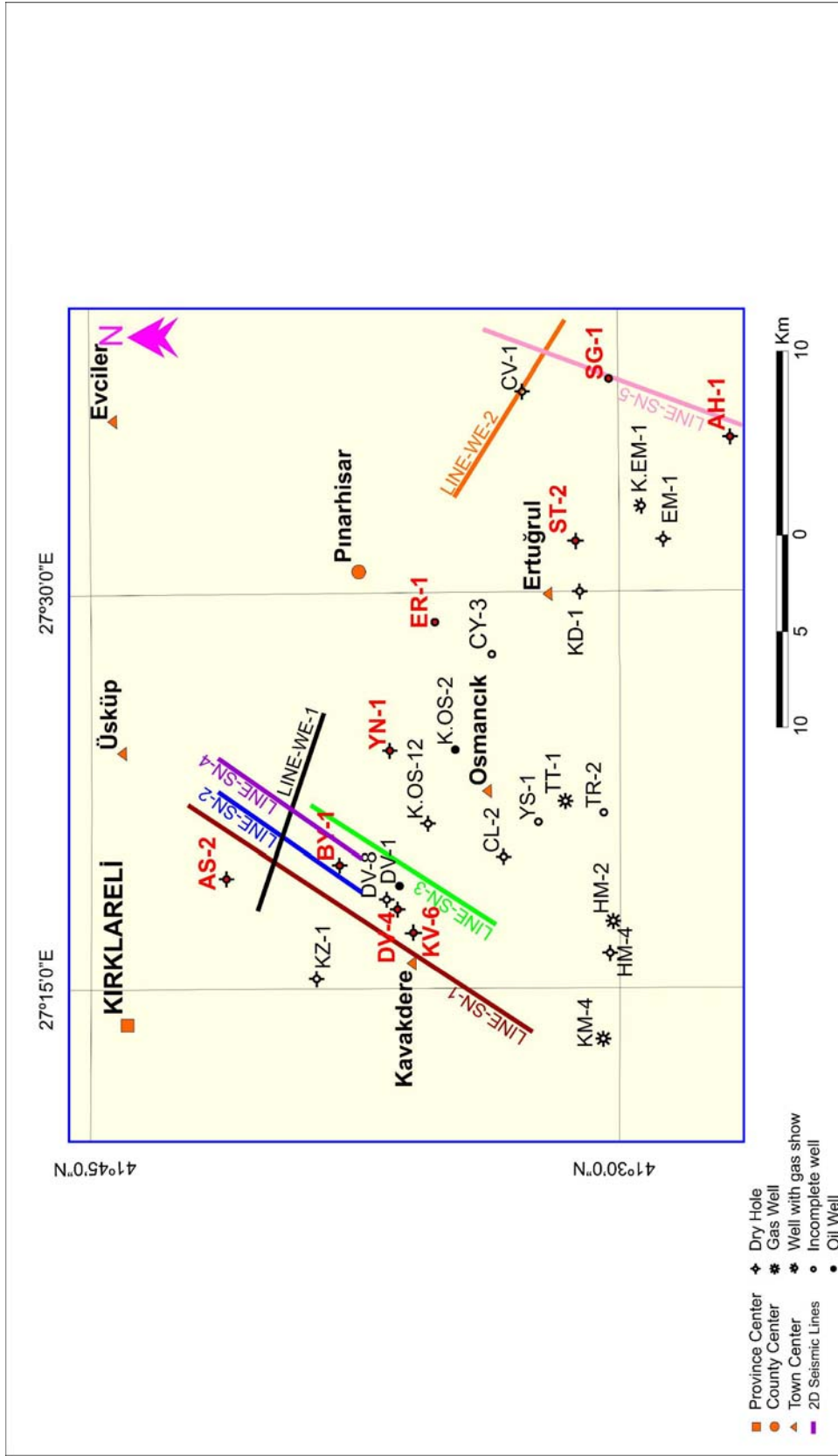


Figure 5.3 Location map of two-dimensional seismic reflection and well data sets. Studied wells are shown in red colors.

McIntyre, 1985; Handford and Loucks, 1993; Soreghan and Dickinson, 1994; Pittet et al., 2000) and marl deposition (Pittet et al., 2000). Characteristic responses of carbonates as response to the specific phases of relative sea-level are summarized by Pittet et al. (2000) in the following phases (Figure 5.4):

Phase-1 is a start-up phase, during which rapid rise of relative sea-level initiates carbonates production but below its full growth potential (Kendall and Schlager, 1981)

Phase-2 comprises catch-up and keep-up phases. During catch-up phase carbonate production increases so that sediment accumulation catches-up with sea-level (Kendall and Schlager, 1981). During keep-up phase, carbonate production matches the rate of rise and the platform remains at or very close to sea-level (Kendall and Schlager, 1981)

Phase-3 is called give-up phase by Neumann and McIntyre (1985) or drop-down phase by Pittet et al. (2000). Rapid sea-level rise may outpace carbonate production, and the carbonate producing environments are drowned or shifted towards shallower areas. Commonly, this phase corresponds to condensed sediments with slowing rate of carbonate production (Pittet et al., 2000).

Phase-4 also corresponds to catch-up and keep-up phases of Kendall and Schlager (1981). During slowing sea-level rise in the highstand, carbonate production again becomes intense on the platform where more aggradational and progradational stacking patterns are observed.

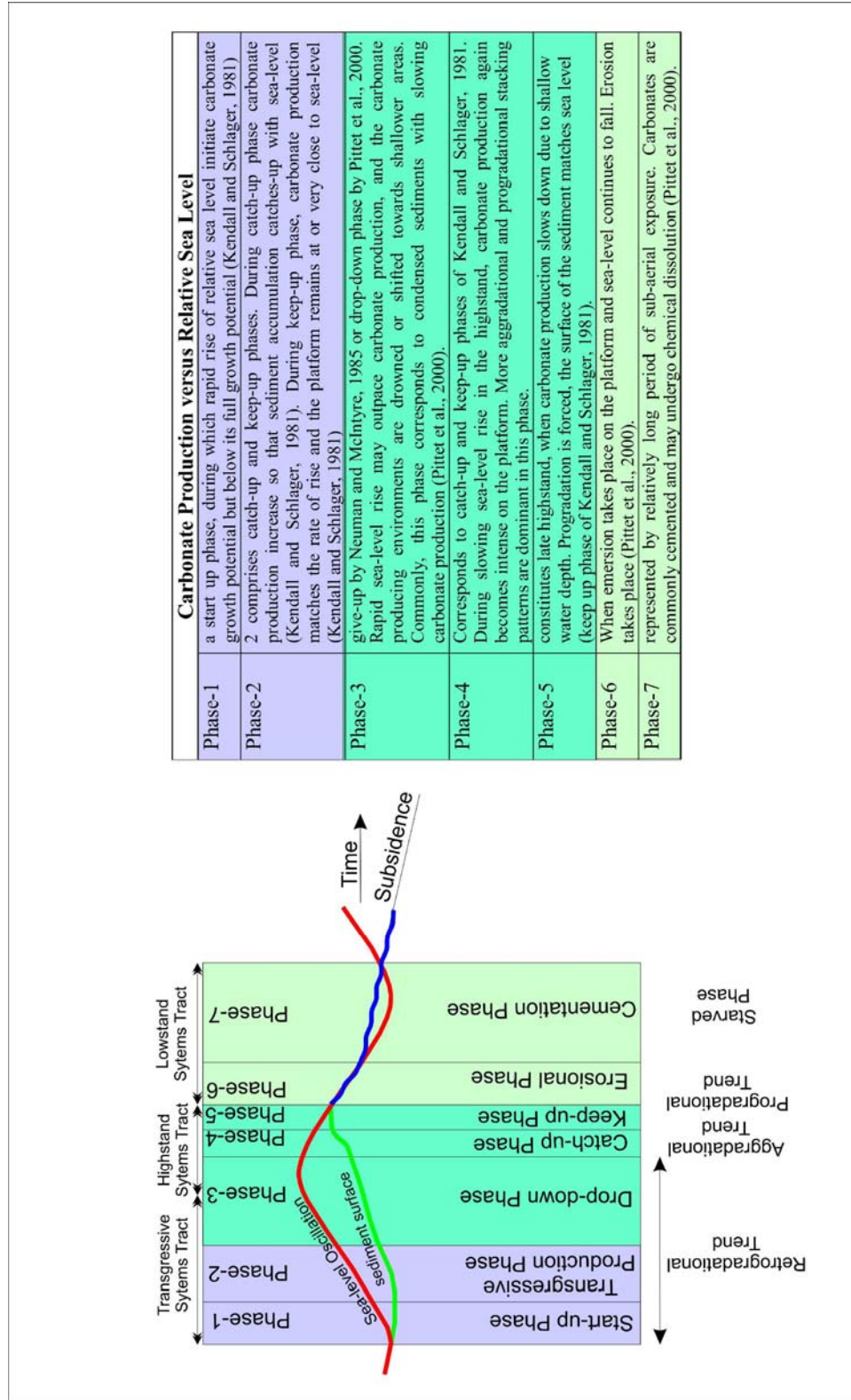


Figure 5.4 Characteristic responses of carbonates as response to specific phases of relative sea-level (by Pittet et al., 2000).

Phase 5 constitutes late highstand, when carbonate production slows down due to shallow water depth. Progradation is forced and the surface of the sediment matches sea-level (keep-up phase of Kendall and Schlager, (1981)).

Phase 6 when emersion takes place on the platform and sea-level continues to fall. As a result, erosion may take place (Pittet et al., 2000).

Phase 7 is represented by relatively long period of subaerial exposure. Carbonates are commonly cemented and may undergo chemical dissolution (Pittet et al., 2000).

There are two major scenarios related to relative sea-level fluctuations during which marl accumulation may take place. In the relative sea-level fall scenario, there are two phases. During the drop-down phase, carbonate production slows down on the platform, condensation occurs in the deep shelf and marl deposited (Pittet et al., 2000). During the cementation phase, shallow platform is exposed and cemented, carbonate production takes place only at the basin margin and marl is deposited in deep shelf environment (Pittet et al., 2000). In both phases, carbonate production slows down at the shallow platform and condensation takes place in deeper environments, causing marl dominant intervals in deep shelf setting.

The second possible scenario for marl deposition is the rapid relative sea-level rise. During this phase, partial or total drowning of the platform takes place. Facies exhibits retrogradational stacking pattern; shallow water

carbonates overlain by deeper water sediments, mainly marls (Kendall and Schlager, 1981; Pittet et al., 2000).

5.3 Late Eocene Basin Physiography in the Northwestern Thrace

Line-SN-1 (Figure 5.5a) is a regional seismic line in the south to north direction. Left side of the seismic line (towards the south) shows basinward and right side of the seismic line (towards the north) landward direction of the basin. Major structural features observed were shaped by the post-Miocene strike-slip tectonic regime. In order to remove the post-depositional tectonic effects, the seismic line was flattened to Late Eocene (Figure 5.5b). At the top of the reflection-free zone, high amplitude, continuous reflection (red color) depicts the basin physiography in Late Eocene.

At the bottom part of the line (Figure 5.5a), reflection-free zone represents Paleozoic age metamorphic rocks of the Istranca Massif. Late Eocene clastic-carbonate mixed system was formed by the shoreline transgression. The diagnostic shelf-slope break in the middle part of the section separates deep marine-slope deposits to the south and carbonate shelf setting to the north. The wells located in this zone tested shelf margin carbonates. Throughout the study area, the shelf-slope boundary is followed by the Kuzey Osmancık Fault Zone, a normal fault and reactivated by the post-Miocene strike-slip tectonic regime.

Towards the north (landward direction), the shelf is represented by shallow marine shelf carbonates and deep shelf marly intervals (Figure

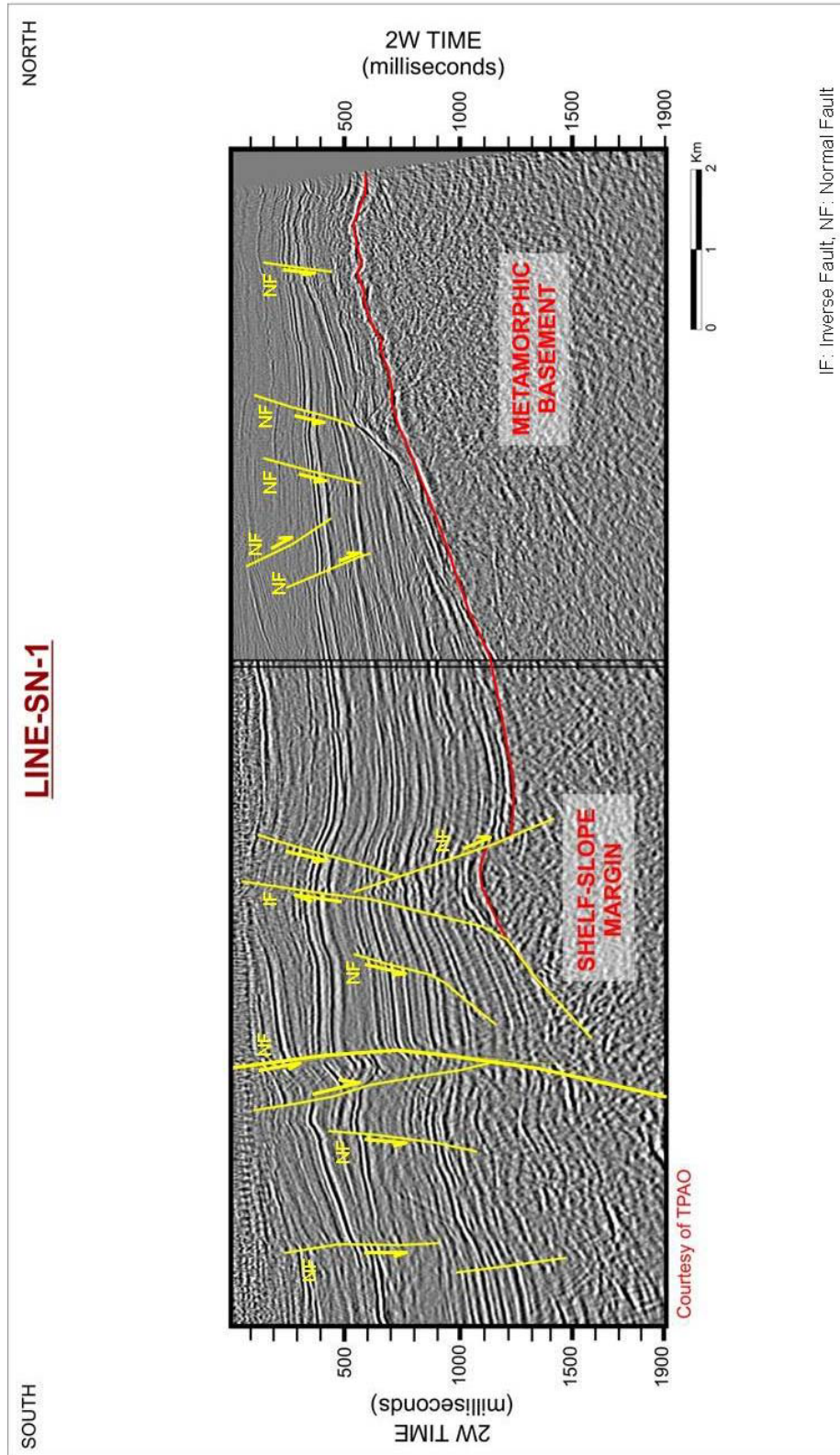


Figure 5.5 Line-SN-1 is a regional seismic line oriented in south to north direction. This line represents major physiographic features of the northwestern part of the Thrace Basin. Towards the south, basinward and towards the north landward direction is indicated respectively. Major structural features were shaped by post-Miocene strike-slip tectonic regime. Red color horizon represents the boundary between the Tertiary sediments and metamorphic rocks.

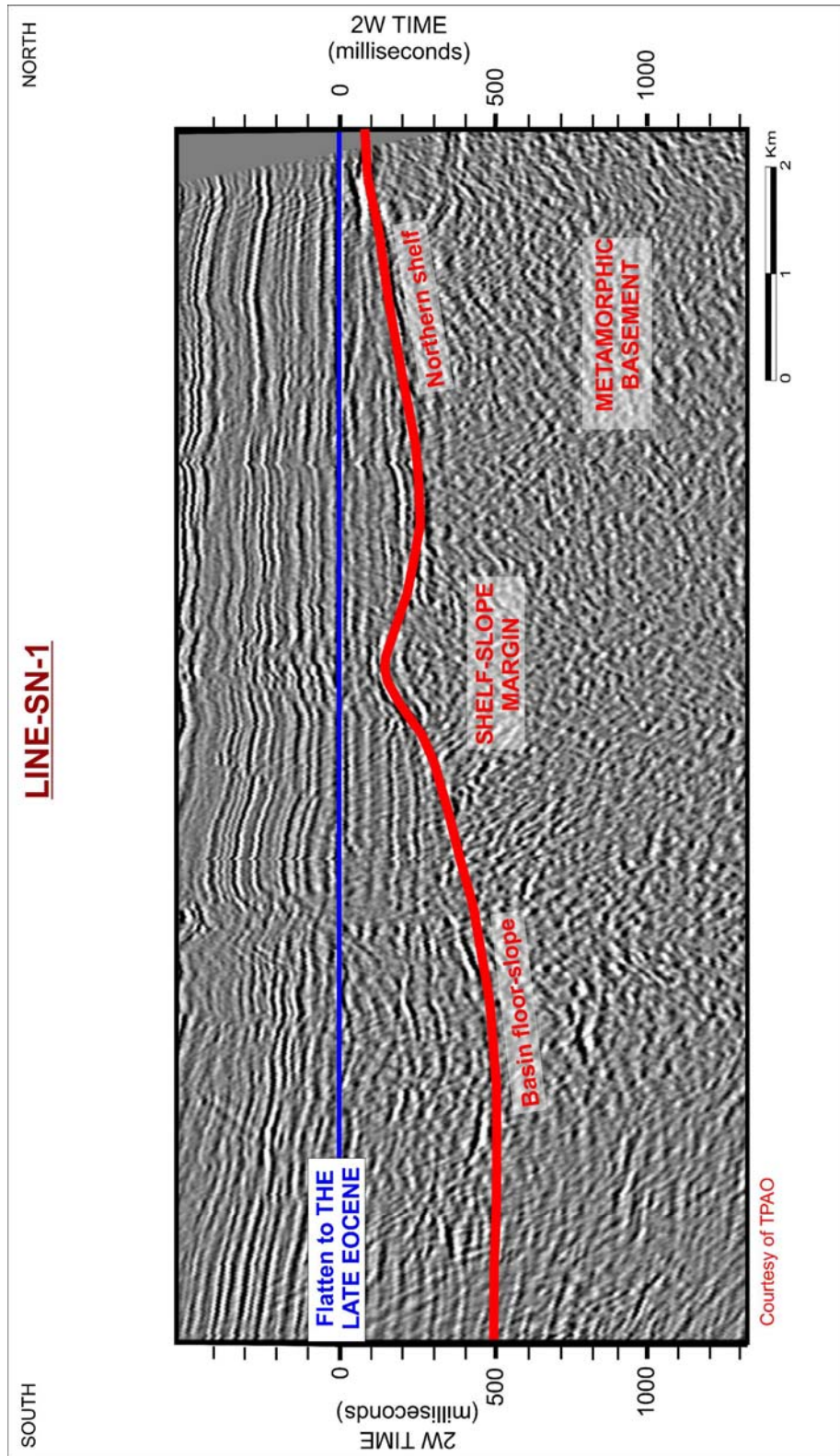


Figure 5.5b Line-SN-1 is a regional seismic line, oriented in south to north direction. Towards the south, basinward and towards the north landward direction is indicated respectively. Red color horizon represents the approximate basin physiography in Late Eocene.

5.5a). The limestone interval was distinguished by a high amplitude, continuous reflection, which is the next positive peak overlying the basement rocks. On the other hand, the overlying marl interval was observed as low amplitude, moderately continuous reflections. BY-1 well located within this zone penetrated the platform carbonates overlying the basement rocks. Within this zone, vertical thickness of limestones varies from 30 to 50 m. The seismic line shows that the thickness increases towards the north. AS-2 well data confirmed that within this zone, the thickness reaches up to 200 m. This was probably caused by increased carbonate production as a result of gradual relative sea-level rise towards the north. The top of the limestone interval was observed as an onlap surface. Onlapping reflections represent deeper marine deposits, mostly marl and tuffs, and termination of the carbonate production. The well data confirmed that along this surface shallow marine carbonates were overlain by deeper marine deposits. Due to their high velocity content, limestone intervals were easily recognized by high amplitude, continuous reflection(s) and distinguished from the overlying marl dominated interval.

Line-SN-1 (Figure 5.6) is a zoom seismic line, which focused on the shelf margin and slope. Shelf margin carbonates (blue color) were observed in a mounded seismic geometry, underlain by the metamorphic rocks of the Istranca Massif in the middle part of the section at around 1150 msec. Towards the south, slope deposits are observed in a wedge shaped seismic package (green color). There are two production fields; the Deveçatağı Field

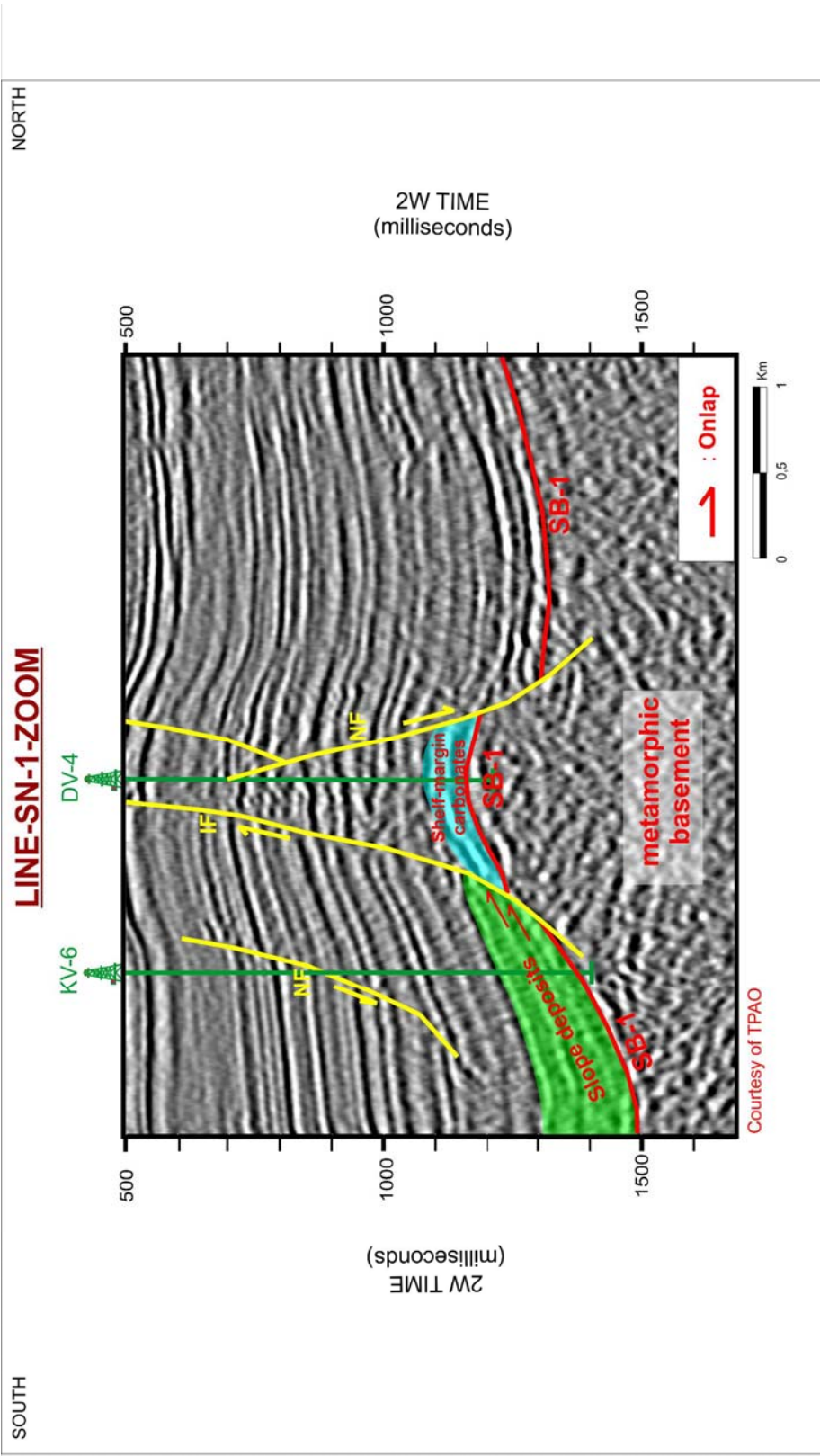


Figure 5.6 A South to north oriented (zoom) seismic line, representing the shelf-slope boundary in Late Eocene. Red color arrows indicate slope deposits onlap onto the shelf-edge. The well data confirms that this zone is the sediment bypass zone in the slope. Wedge shape seismic package (green color) is composed of marl and tuff alternations, and blue color seismic package is composed of shelf-margin carbonates. SB-1: Sequence Boundary-1, NF: Normal Fault, IF: Inverted Fault.

is located in the Late Eocene shelf margin and the Kavakdere Field is located in Late Eocene paleo-slope.

Towards the south (basinward direction), slope deposits are represented by a wedge shaped seismic package (green color) (Figure 5.6). High amplitude, parallel, inclined reflections with good continuity onlap onto the shelf-edge. The well data reflected in the KV-6 well (Figure 4.18) that this zone is a bypass zone. The sedimentary package is composed of marl and tuff alternations and overlies the continental to shallow marine channel fill deposits of the Sequence-1 unconformably (Figure 5.13).

5.4 Sequence Stratigraphic Analysis

Sequence-2, Sequence-3 and Sequence-4 constitute Late Eocene clastic-carbonate mixed system in the northern shelf setting. They mostly exhibit retrogradational stacking patterns. Due to their genetic similarities, they were analyzed together.

In the current literature (Kendall and Schlager, 1981, Handford and Loucks, 1993), bounding surfaces of carbonate and clastic-carbonate mixed sequences are identified on the basis of two major surfaces; either base of lowstand deposits or base of transgressive deposits.

The base of lowstand deposits is characterized by subaerial unconformities and related karstification. When relative sea-level falls below the shelf margin, the once flooded platform is subaerially exposed and unable to produce carbonate sediments. Instead, only productive part of the

platform is the slope (seaward of the slope) (Handford and Loucks, 1993). In Pittet et al. (2000) model, this stage corresponds to the Phase-6.

In this study, bounding surfaces of sequences were defined as the base of transgressive deposits. The base of transgressive deposits is very diagnostic for carbonate deposition (Kendall and Schlager, 1981; Handford and Loucks, 1993). Under most conditions, carbonate accumulation starts with initial transgression of the shoreline. This stage may correspond to start-up (Phase-1), catch-up or keep-up (Phase-2). Vail et al. (1977), (1984) also proposed that the flooding surface between a highstand systems tract and overlying transgressive systems tract, without evidence of sea-level fall or lowstand deposits has particular usefulness in carbonates (Caron et al., 2004).

To detect and correlate transgressive surfaces by seismic and well-log data is an appropriate method. The sequence starts with start-up or catch-up phases of carbonates. Start-up phase sometimes comprises high energy shallow marine siliciclastic deposits.

Sequence-2 started with initial transgression in Late Eocene. Shallow marine clastics were the first products of transgression of high energy shoreface and ravinement surface. During this phase, carbonate production started depending on the topography throughout the basin. This process corresponds to the Phase-1. Shallow marine clastics exhibited gradual upward transition to limestones. DV-4 well shows a very good example of this relation. Moreover, this gradual relation was observed in the field near

Tekedere village (Figure 5.7). However, in topographic highs, limestones directly overlie metamorphic basement unconformably, seen as in the BY-1 well and near Çatalca in the field (Figure 5.8) where Eocene limestones overlie the metamorphic rocks of the Istranca Massif.

Continued relative sea-level rise increased the carbonate production (Phase-2). According to specific location in given depositional environment such as restricted shelf, shelf margin and open shelf, carbonate production may reach to catch-up and/or keep-up phases. These phases mostly exhibited aggradational to progradational stacking patterns within the shelf environment. The slowing rate of relative sea-level rise in the highstand position of the sea level (Phase-4 and 5) may also lead aggradational to progradational stacking patterns. In the drop-down phase, carbonate production slowed down and marls were deposited in the deep shelf and slope. In the KV-6 well, Sequence-2 is composed of a marl dominated interval, which was interpreted as the products of Phase 6 and 7. Figure 5.9 shows two-dimensional depiction of the evolution of carbonate platform as response to relative sea-level change. The figure depicts the carbonate production on the shelf margin and marl deposition on the deep shelf as response to long-term relative sea-level rise. A) Carbonate production started with rapid rise of sea-level and reaches to its full potential in transgressive production phase (catch up and keep up phase of Kendall and Schlager (1981)). This process constituted transgressive and/or highstand position of sea-level. B) As response to the rapid relative sea-level rise



Figure 5.7 The photo represents gradual transition from Late Eocene shallow marine clastics to limestone lithology, The photo was taken approximately 1,5 km southeast of Hacifakılı village.



Figure 5.8 Late Eocene limestones of Soğucak Formation overlies metamorphic basement unconformably near Çatalca. Similar observations were made in BY-1 well (4553772 N, 623529 E).

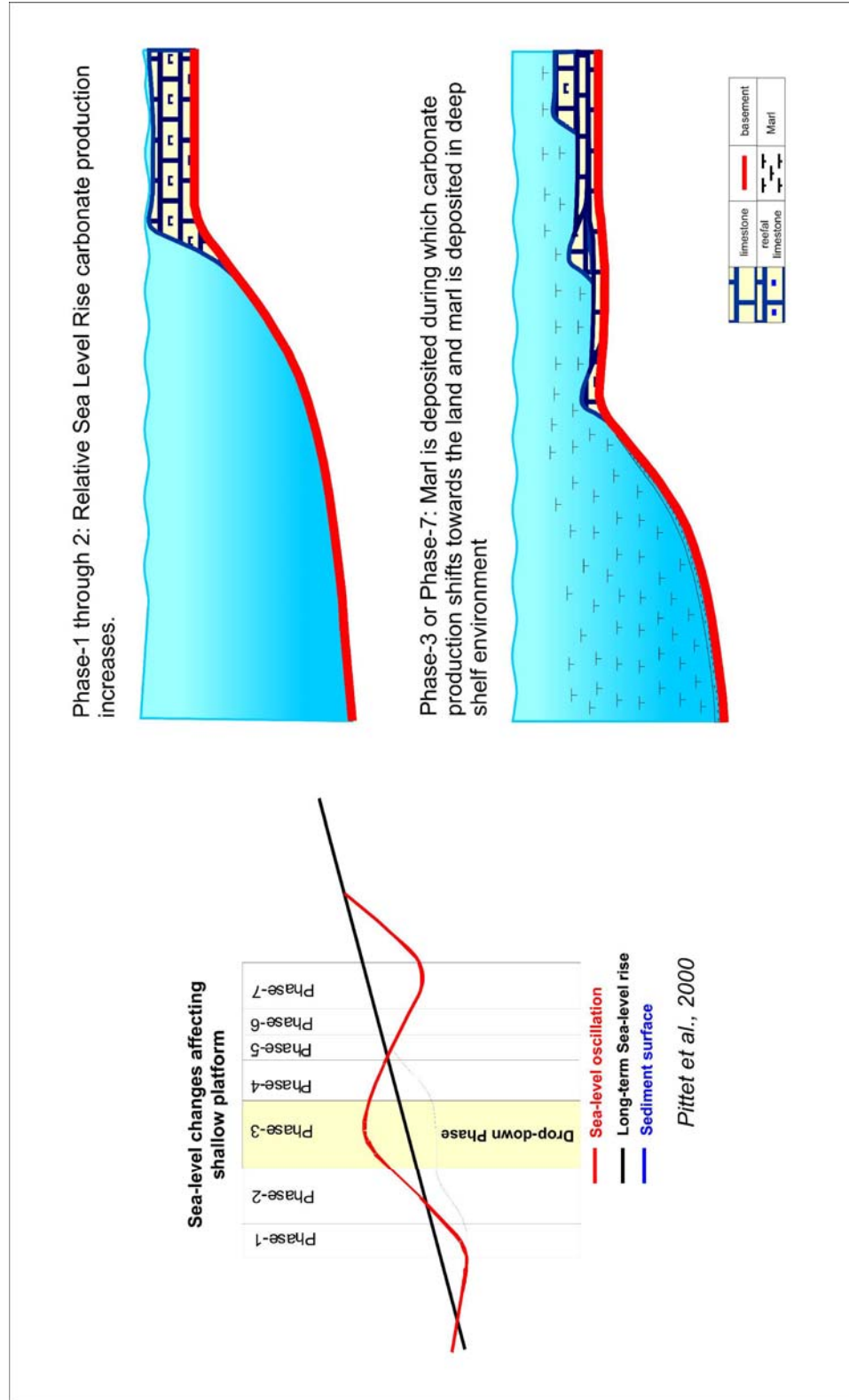


Figure 5.9 Characteristic responses of carbonates and marl deposition as response to long-term relative sea-level rise.

carbonate production slowed down and the shelf was overlain by deeper marine facies, and marl was deposited.

According to detailed microfacies analysis on the basis of cores (Atalık, 1987), three depositional environments; open shelf, shelf margin and restricted shelf or lagoon environments were identified in the studied area. Open marine environment comprises slope and deep marine deposits, shelf margin comprises reefal developments, nummulitic banks and platform sand. In this study, KV-6 well is located along the slope, DV wells are located along the shelf margin. BY-1 and YN-1 wells are located within the area between shelf-slope boundary and lagoon.

The analyzed intervals are mostly composed of limestone and marl dominated intervals (Figure 5.10). Gamma-ray and sonic log analysis with the cutting confirmation suggested that the vertical section in the BY-1 well between 1460 and 1120 m started with a shallow marine carbonate interval overlying the metamorphic basement in Paleozoic age. This type of relation was also observed in the field near Çatalca (Figure 5.8).

The carbonate interval is represented by retrogradational to progradational stacking patterns between 1460 and 1420 m. This interval cut by a major marl interval with a sharp contact (Figure 5.10). This sharp contact between limestone and marl dominated intervals was defined as the Sequence Boundary 3 (Transgressive Surface). The overlying marl interval exhibited retrogradational stacking pattern between 1420 and 1350 m. The interval between 1350 and 1190 m also exhibited retrogradational stacking

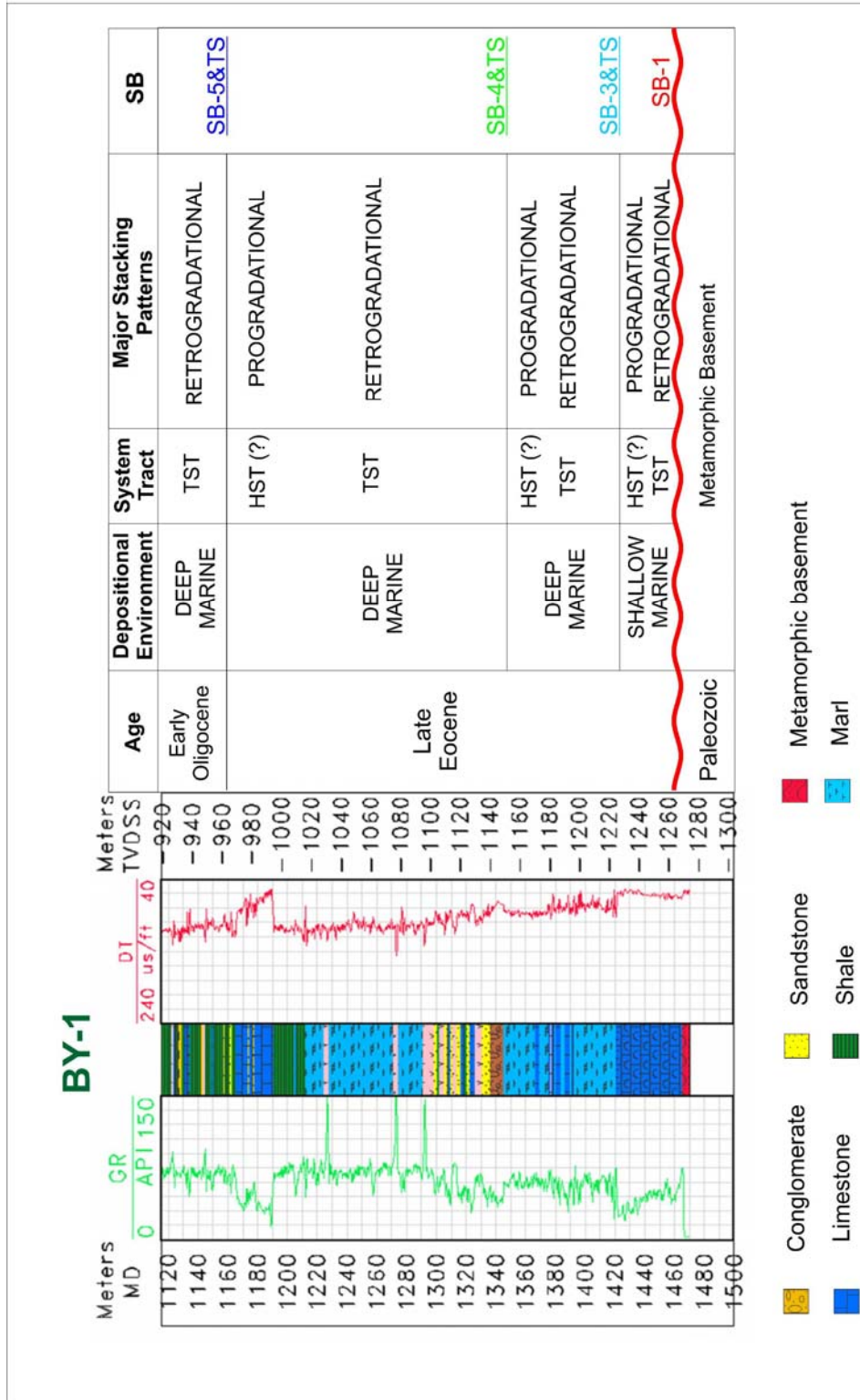


Figure 5.10 BY-1 well gamma ray (green on the left) and sonic log (red on the right) responses are shown. TVDSS: true vertical depth from the sub-sea, MD: Measured Depth, SB: Sequence Boundary, TST: Transgressive Systems Tract HST: Highstand Systems Tract, TS: Transgressive Surface.

patterns. At the base of retrogradational stacking patterns, the sharp contact at 1350 m corresponded to the Sequence Boundary-4. The cuttings confirmed that a marly interval was overlain by coarser sediments along this boundary. This sharp surface might be interpreted as a sharp base of a debris flow. Basinwide correlations indicated that this surface corresponds to relative sea-level rise, instead of relative fall of the sea-level. Samples taken from these intervals have hundreds of well preserved globigerines, reflected deepening of the basin (Erenler, 1987).

Due to the location of the well in deep-shelf environment, the Sequence-3 and Sequence-4 were represented by mostly marl dominated intervals. In this environment, the minor effect of sea-level fluctuations on facies distribution was observed. Therefore, Sequence Boundary-4 was placed between two marl dominated intervals. However, a twenty-five meter thick carbonate layer between 1190 and 1165 m was observed at the top of the marl dominated interval of the Sequence-4. As response to the increased carbonate production in the highstand position of the sea-level, limestone lithology was deposited in deep shelf environment. Therefore, the Sequence Boundary-5 was placed to the top of the carbonate layer. This carbonate layer was correlated to the other wells.

After analyzing vertical trends in individual wells, west to east oriented correlations were utilized (Figure 5.11). First correlation was applied to YN-1, ST-2, ER-1 and SG-1 wells. The wells were chosen from the area between the Late Eocene shelf margin and the lagoon so that

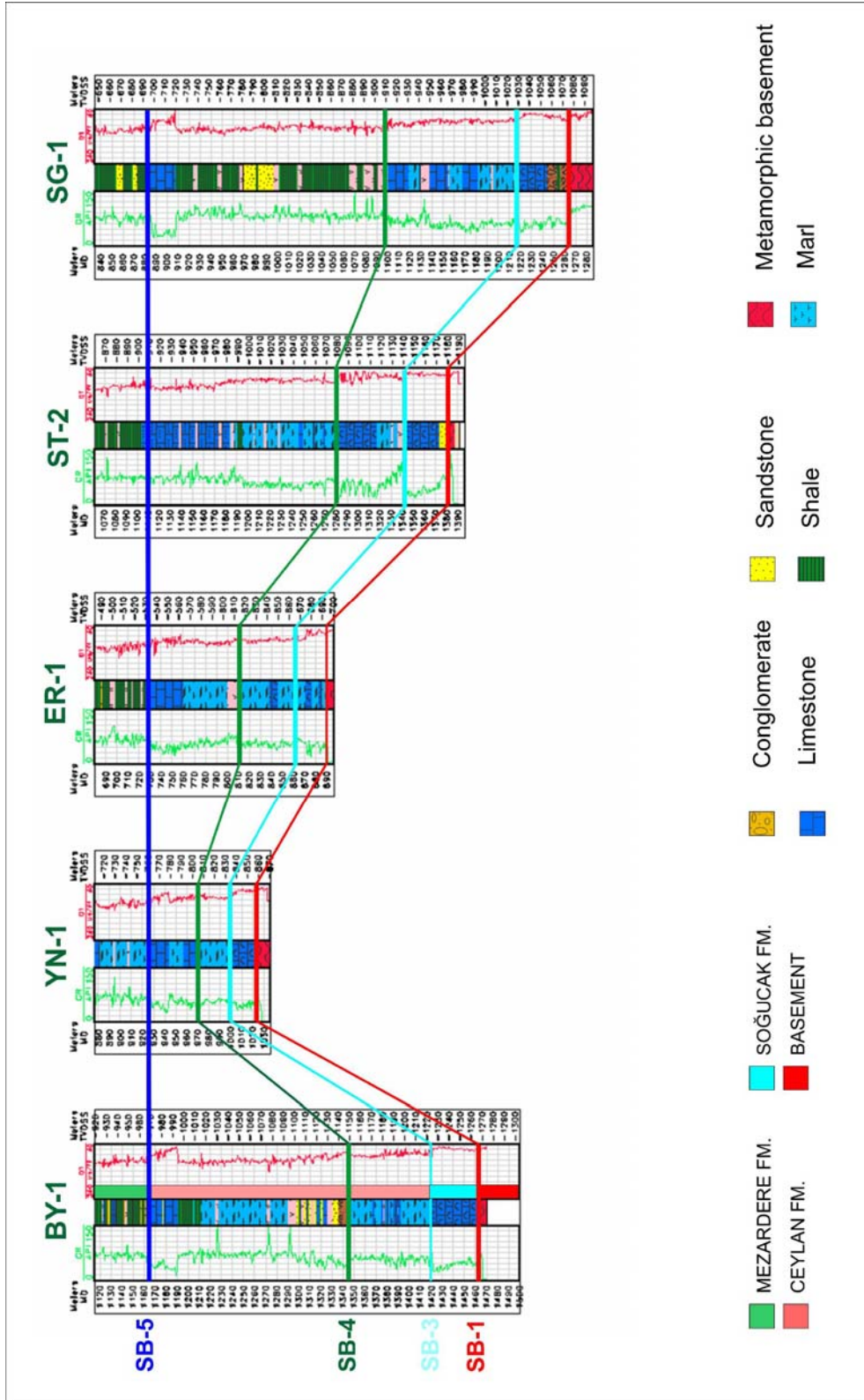


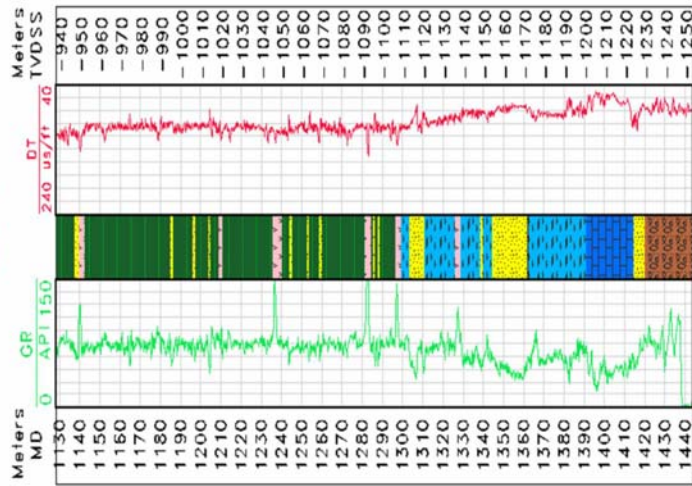
Figure 5.11 West to east oriented gamma-ray (green color on the right) and sonic log (red color in the right) correlation of the wells located along the shelf. Datum is set to SB-5. SB: Sequence Boundary.

similar responses of well-logs could be observed. On the other hand, the existing basin topography has an important effect on facies distribution. Variable thicknesses of sequences were used as a reflection of the basin topography and relative locations of the wells along the shelf.

YN-1 well is another well located along the northern paleoshelf. The vertical section (Figure 5.11) overlying the Paleozoic basement rocks started with a shallow marine carbonate interval with a progradational to retrogradational stacking pattern between 1025 and 1000 m. The carbonate layer was cut by a marl interval with a sharp contact. This interval exhibited retrogradational stacking pattern. The interval between 970 and 1000 m, 970 and 840 m and 840 and 780 m respectively was composed of also limestone and marl alternations with retrogradational stacking patterns.

DV-4 is one of the wells located along the paleo-shelf margin in more basinward direction as compared to BY-1 and YN-1 wells. The section (Figure 5.12) starts with clastics, mostly shallow marine origin conglomerate and sandstones between 1444 and 1417 m. Between 1417 and 1392 m shallow marine limestones were distinguished by very low gamma-ray and high velocity (low slowness) values. Instead of a sharp contact between sandstone and limestone intervals, gradual cleaning upward trend was highly diagnostic overall. This type of relation was observed in the field near Hacifakılı village (Figure 5.7). The upper boundary of the limestone interval was defined as the Sequence Boundary-3. This interval was overlain by a 32 m thick marl interval between 1392 and 1360 m. Between 1360 and

DV-4



Age	Depositional Environment	System Tract	Stacking Pattern	SB
Early Oligocene	DEEP MARINE	TST	RETROGRADATIONAL	SB-5&TS
			PROGRADATIONAL	
Late Eocene	DEEP MARINE	TST	RETROGRADATIONAL	SB-4&TS
			PROGRADATIONAL	
		HST (?)	RETROGRADATIONAL	SB-3&TS
			PROGRADATIONAL	

- Conglomerate
- Limestone
- Sandstone
- Shale
- Metamorphic basement
- Marl

Figure 5.12 Major elements of the Late Eocene sequence stratigraphic framework on the basis of GR and DT correlations from DV-4 well. MD: Measured Depth, TVDSS: True Vertical Depth from the sub-sea, SB: Sequence Boundary, TS: Transgressive Surface, HST: Highstand Systems Tract, TST: Transgressive Systems Tract.

1310 m, another marl interval with retrogradational stacking was observed. The sharp contact at base of retrogradational stacking patterns was defined as the Sequence Boundary-4. The overlying interval exhibited shale and marl alternations with minor siltstone beds. This interval did not indicate any major stacking pattern. Due to basinward location of the DV-4 well, relative sea level fluctuations were not effective in facies character. Therefore, the Sequence Boundary-5 was placed at 1180 m from correlations of BY-1 and YN-1 well. Especially, 1 m thick three tuff intervals at 1236 m, 1281 m and 1296 m at DV-4 well were used as key beds for well to well correlation.

KV-6 well is located in the southward direction of the basin margin (slope-deep marine environment: bypass zone). The vertical section (Figure 5.13) starts with a 35 m thick major marl interval between 1940 and 1905 m. This interval overlies the lowstand deposits of the Sequence-1 with a sharp contact at 1940 m (Sequence Boundary-2) and represents retrogradational stacking pattern. The lower part of the Sequence-3 starts with another marl interval between 1890 and 1850 m with retrogradational stacking pattern. The upper boundary corresponds to 10 m thick tuff layer at 1850 m. Within the Sequence-3 and Sequence-4, a diagnostic vertical trend could not be observed in the wells located in slope and deep marine environments, where relative sea-level fluctuations had minor effects on facies distribution. Therefore, basinward correlations of sequence boundaries were performed on the basis of seismic interpretation technique and major tuff correlations (Figure 5.14a and b).

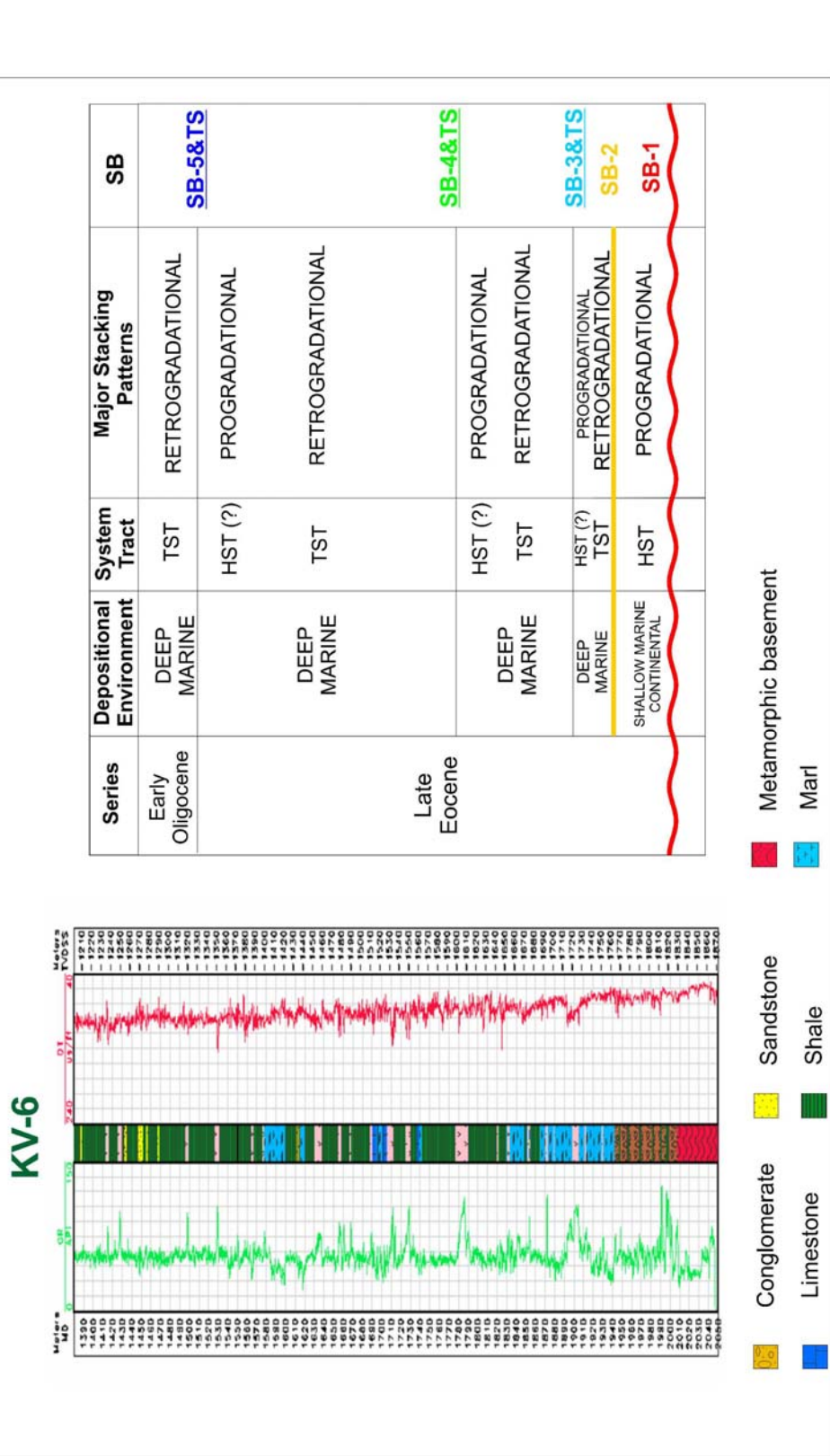
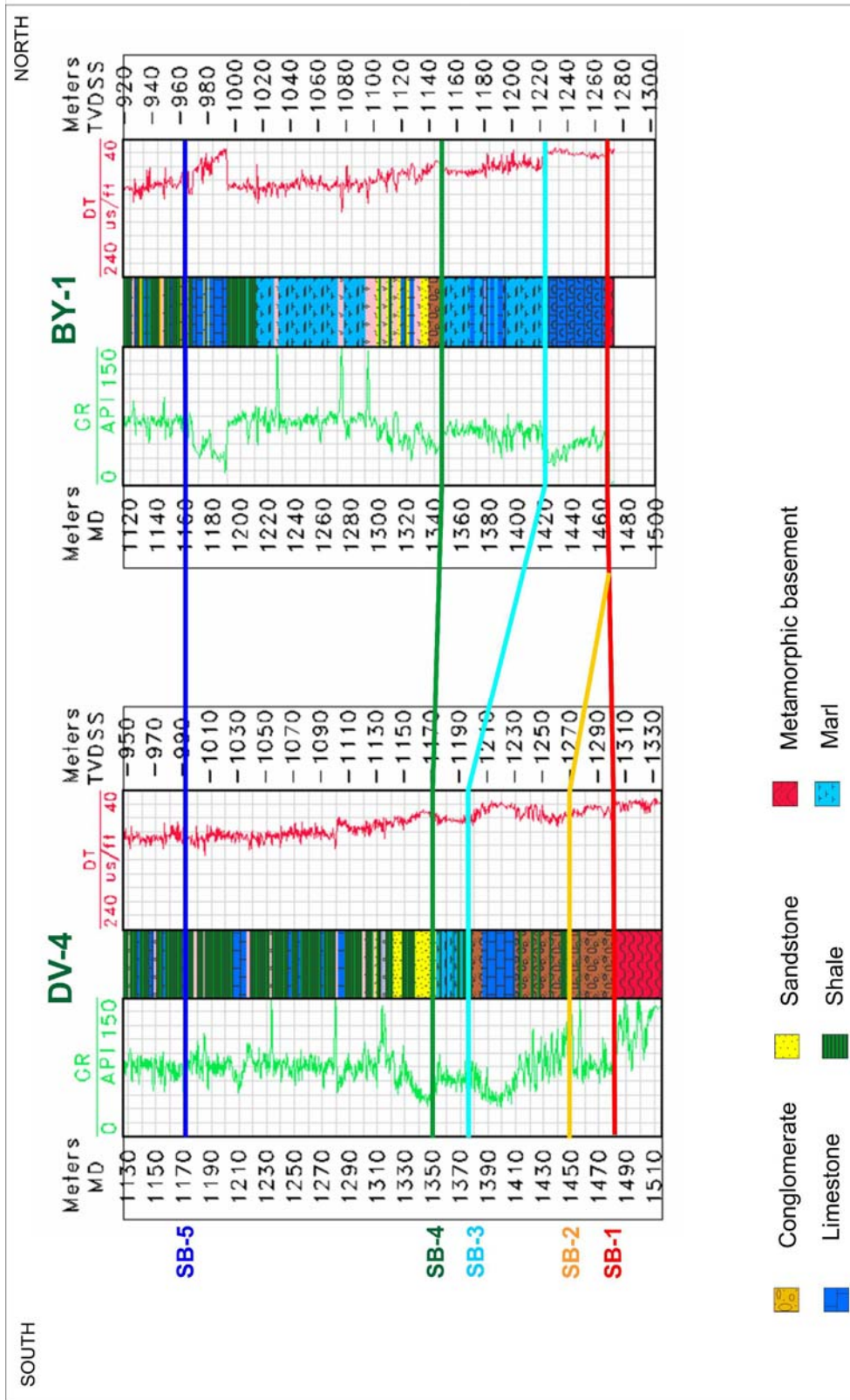


Figure 5.13 KV-6 well gamma-ray (green on the left) and sonic log (red on the right) responses. TVDSS: true vertical depth from the subsea, MD: measured depth, SB: Sequence Boundary, TS: Transgressive Surface, TST: Transgressive Systems Tract, HST: Highstand Systems Tract.



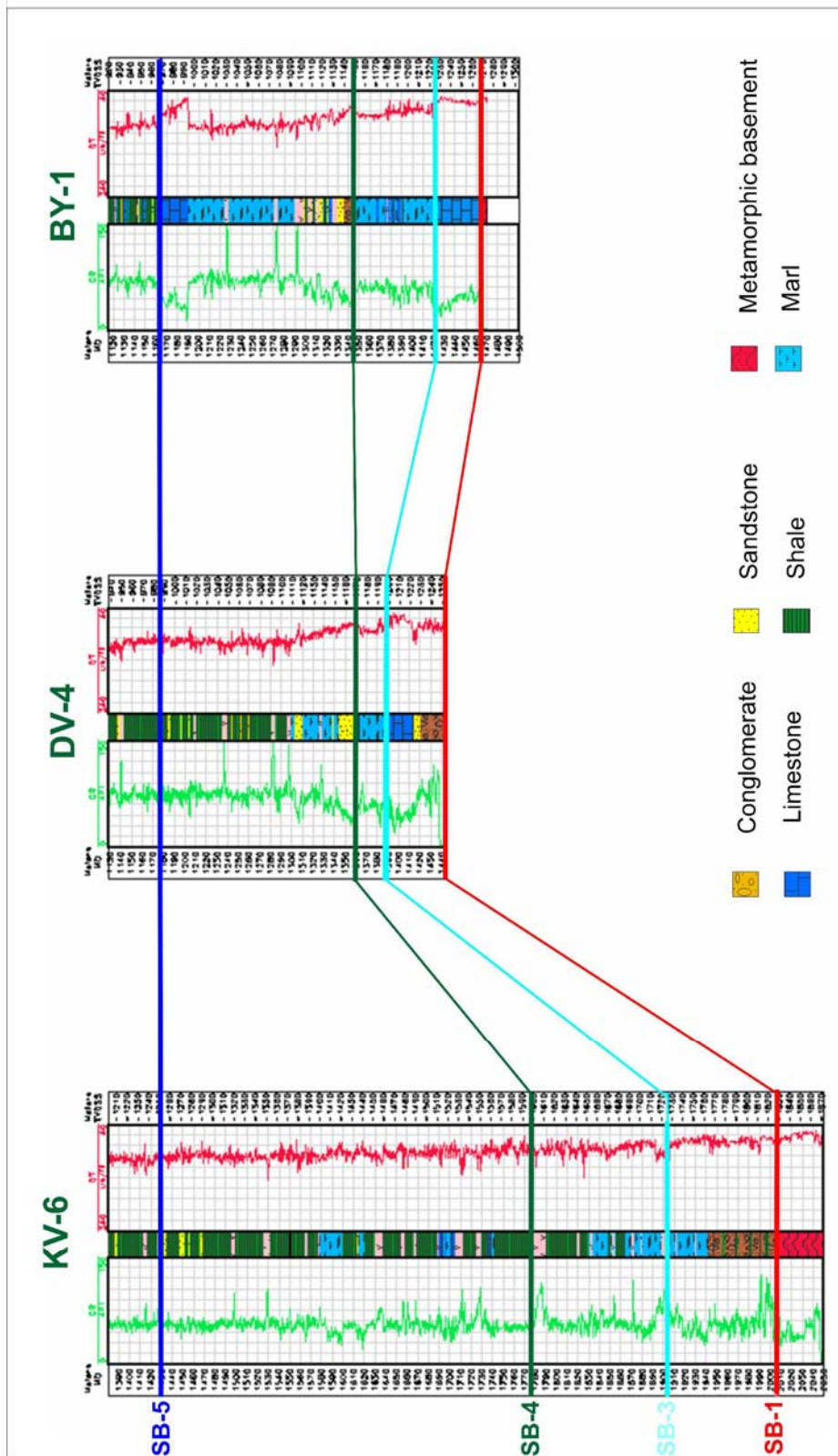


Figure 5.14.b Gamma-ray and sonic log correlations of KV-6, DV-4 and BY-1 wells. DV-1 well is located at the shelf margin, KV-6 and BY-1 wells are located basinward and landward directions respectively. Figure 3.5 shows the well locations along the seismic section. Datum is set as SB-5. TVDSS: True vertical depth from sub-sea, MD: Measured Depth, SB: Sequence Boundary.

Sequence-3 was characterized by the partial drowning of the carbonate platform and backstepping of shallow marine facies. Shallow marine carbonates are overlain by a marl dominated interval in the shelf setting. The base of the marl interval was set as a lower sequence boundary (transgressive surface). This boundary was induced by rapid relative sea-level rise, shoreline transgression, partial drowning of the carbonate platform and the backstepping of facies. Most of the wells in the study area are located in the deep shelf setting. Therefore, Sequence-3 is composed of a marl dominated interval with mostly retrogradational stacking pattern in the wells. This interval is demonstrated by a wedge shaped seismic package (green color) on seismic sections (Figure 5.15) where high amplitude continuous reflections onlap onto the sequence boundary. In landward direction, mounded seismic geometry was interpreted as reefal build-up as a shallow marine carbonate unit. As partial drowning takes place in most of the platform by the gradual sea-level rise, carbonate production backsteps as reefal build-ups related to topographic conditions along the shelf. Line-SN-2 (Figure 5.15) is a south-north oriented (in dip direction) seismic line. At the bottom part of the seismic section, reflection free zone indicates metamorphic basement rocks of the Istranca Massif. The overlying Sequence-2, Sequence-3 and Sequence-4 constitute the Late Eocene clastic-carbonate mixed system in shelf environment. They are mostly characterized by backstepping of facies belts, which is induced by continued relative sea-level rise.

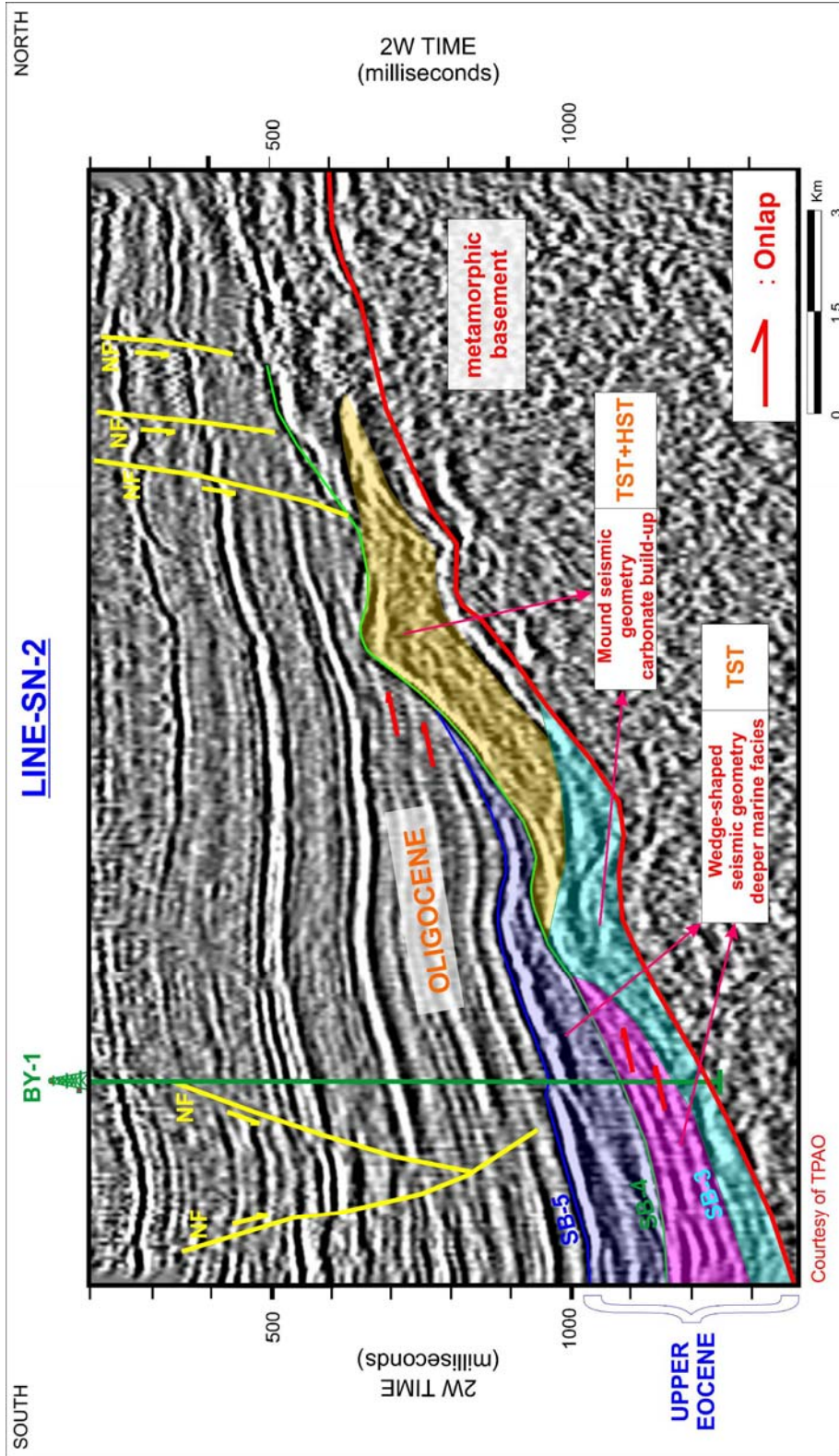


Figure 5.15 Line-SN-2 is a south to north oriented seismic line, which represents partial drowning of the carbonate platform and landward shift of carbonate production in Late Eocene. SB: Sequence Boundary, NF: Normal Fault, TST: Transgressive Systems Tract, HST: Highstand Systems Tracts.

In the southern end of the section, high amplitude reflection with good continuity overlying the metamorphic basement defines the limestone interval between 1300 and 1400 msec. Towards the north, the mound like seismic geometry (blue color) was interpreted as reefal build-up. The overlying wedge shaped seismic package (purple color) is composed of high amplitude, continuous reflection terminations against (onlaps) the edges of the reefal build-up. The well data confirmed that the wedge shaped seismic package is composed of deeper shelf sediments, mostly marls. In the next relative sea-level rise, reefal build-up is drowned and shallow marine limestone production environment shifts towards the landward. The overlying deeper sediments were observed as a chaotic internal reflection configuration (dark blue). The backstepped reefal build-up is shown by yellow color seismic package.

Most of the studied wells are located along the Late Eocene shelf, where the Sequence-3 is mostly composed of marl dominated intervals e.g. BY-1, YN-1, DV-4 wells. These marly intervals suggest a deepening in the basin and termination of the carbonate production. Marly intervals have rich planktonic foraminiferal content. Indications of submarine erosion were observed in the log responses of the wells, these intervals were formed during relative sea-level rise. Samples taken from these intervals have hundreds of well preserved globigerines, reflecting deepening of the basin (Erenler, 1987).

On the other hand, seismic data shows that the carbonate production still continues towards the land as reefal build-ups especially in the northwestern part of the basin. This event is interpreted as partial drowning. Late Eocene carbonate platform drowning was taking place gradually in time. Dominguez and Mullins (1988) observed in the Cat Island Platform in Bahamas Banks that different portions of platforms responded independently to relative sea-level rise by the Holocene flooding (Figure 5.16).

Sequence-4 is also characterized by rapid relative sea-level rise. Marl interval of the Sequence-3 is overlain by another marl interval in deep shelf setting. This interval is composed of mostly retrogradational stacking patterns in the studied wells (BY-1, DV-4). Seismic data shows that marl dominated interval is represented by a wedge shaped seismic package (dark blue color).

Shallow marine carbonates of the Sequence-3 are overlain by this seismic package and the carbonate production backsteps towards the land as seen in the Sequence-3. The top of the carbonate platform is observed as an onlap surface (Sequence Boundary-5). The onlapping reflections represent deep marine facies.

Seismic Line-SN-5 crosses the eastern part of the study area (Figure 5.17). Two marl dominated intervals are demonstrated by a wedge shaped seismic package and separated with limestone intervals. As limestone intervals are distinguished by high amplitude, continuous reflections, low

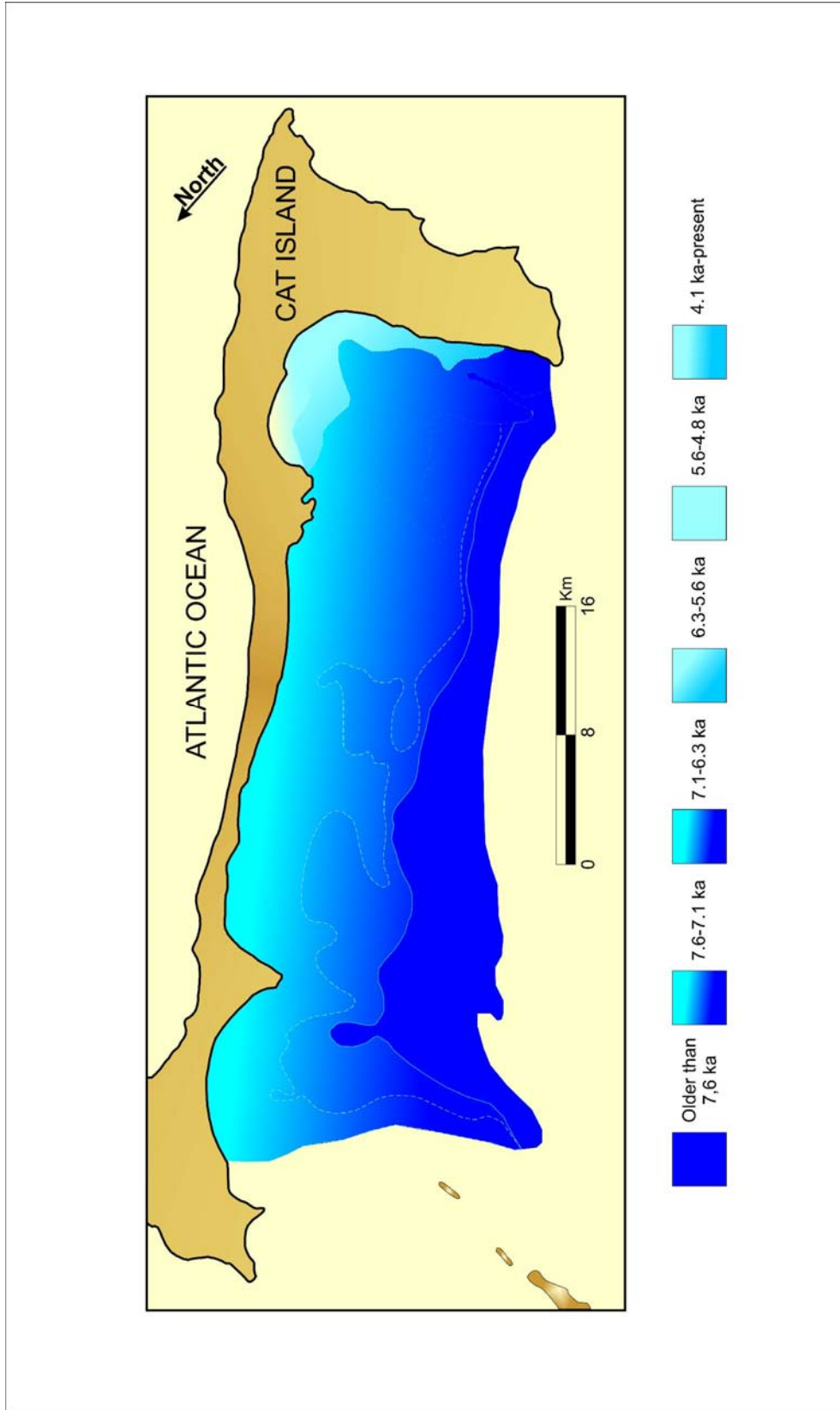


Figure 5.16 Holocene sea-level history on a structure contour along the Cat Island shelf, Bahamas (Dominguez et al., 1988).

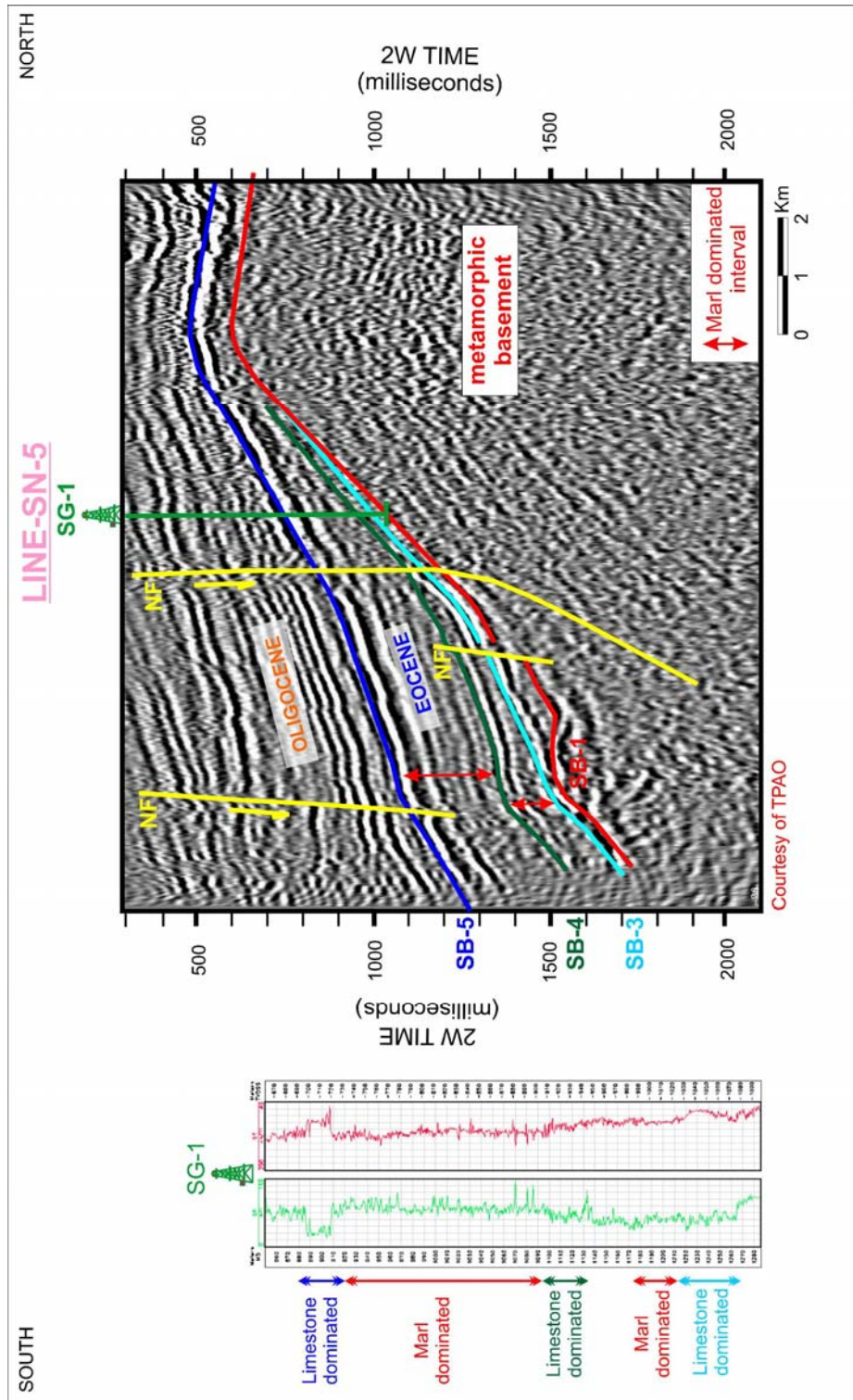


Figure 5.17 Line-SN-5 is a south-north oriented seismic line in the eastern part of the study area. The studied section is composed of marl and limestone dominated intervals. As a result of high acoustic impedance contrast between marl and limestone lithologies, limestone intervals are observed as high amplitude, continuous reflections. SB: Sequence Boundary, NF: Normal Fault.

amplitude, moderately continuous seismic packages correspond to marl dominated intervals. Each marl dominated interval was interpreted as a deepening phase in the basin, partial termination of carbonate production (transgressive surface) and facies shift towards the land. SG-1 well data confirmed that the wedge shaped seismic package was marl dominated and separated with limestone intervals.

The termination of the Upper Eocene clastic-carbonate mixed system is represented in seismic Line-SN-4 (Figure 5.18). This boundary was recognized as high amplitude, continuous reflection. Towards the south, well data confirmed that this reflection corresponds to a twenty m thick limestone interval with comparatively higher velocity content from the overlying and underlying sediments. Towards the north, thicker platform carbonates are expected as seen on the seismic package. The overlying onlaps onto this reflection represent the deeper marine facies with relatively low calcite content. Low calcite content indicates another source direction for overlying sediments. According to Batı et al. (1993), (2002), this boundary may be used as a tentative Eocene-Oligocene contact.

Line-WE-1 (Figure 5.19) is a west to east oriented (parallel to the depositional trend) seismic line, crossing the Late Eocene carbonate shelf. At the bottom part of the section, reflection-free zone shows the carbonate platform. The detection of the lower boundary of the platform (the boundary between carbonates and the metamorphic rocks) is almost impossible. The relatively higher velocity content of the carbonates and cemented platform

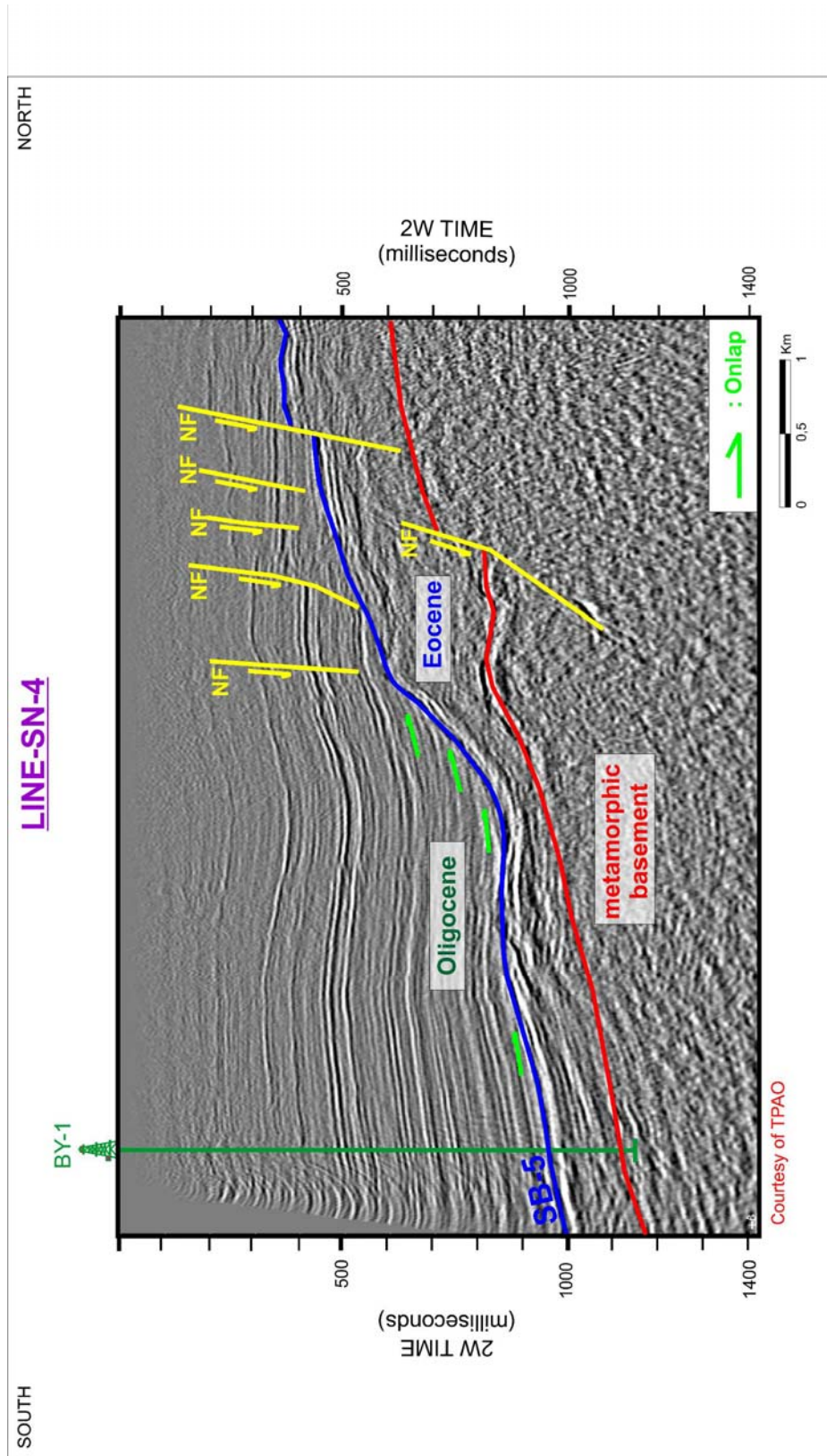


Figure 5.18 The seismic line emphasizes the termination of the Late Eocene carbonate-clastic mixed system, which is shown by blue color horizon. The overlying onlaps (green color arrows) represent deeper marine facies. SB: Sequence Boundary, NF: Normal Fault.

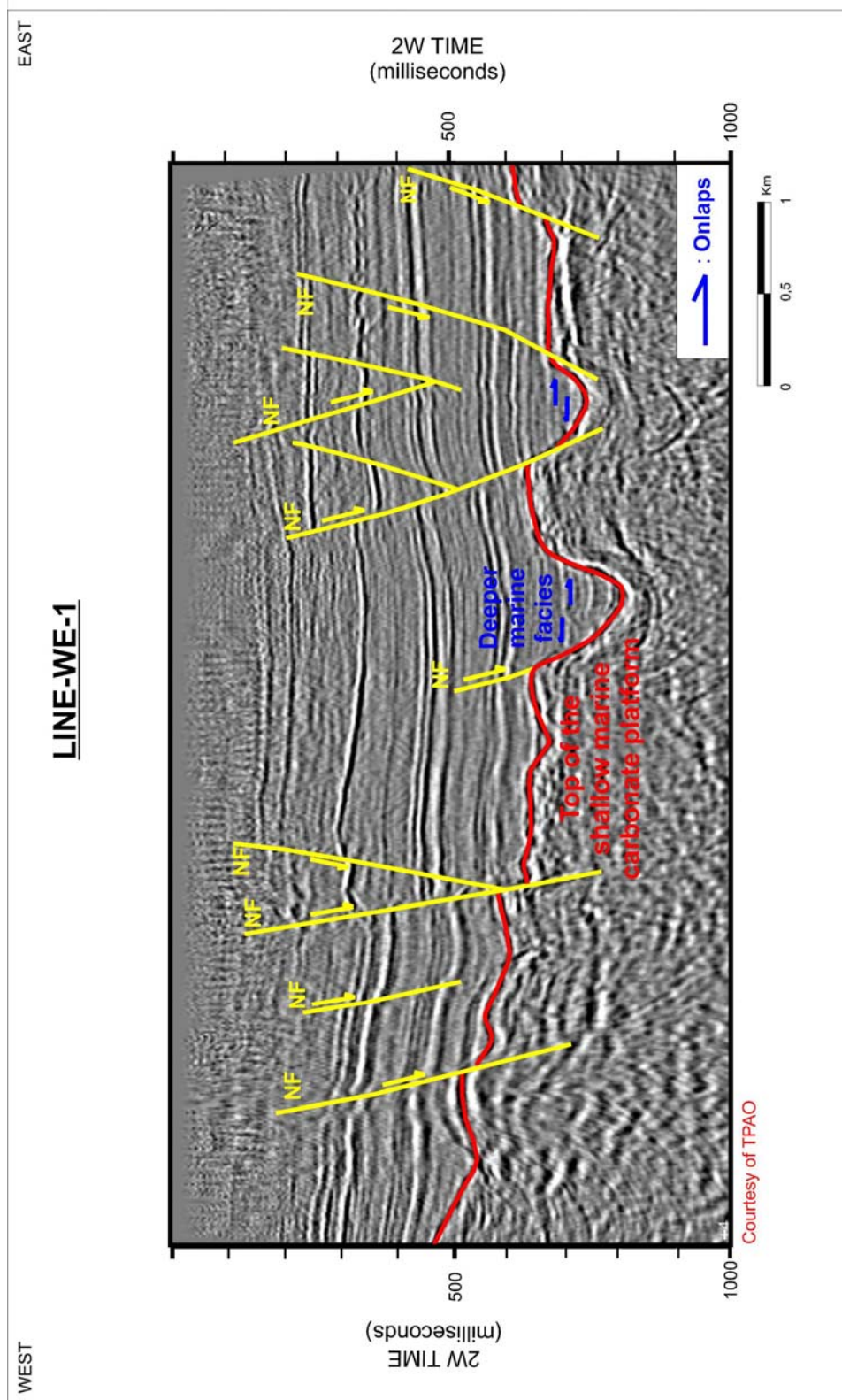


Figure 5.19 West to east oriented seismic line. The red color horizon represents top of the carbonate platform. Two channelized features are composed of parallel onlapping reflections. The fill is mostly marl dominated. They are interpreted as bypass submarine canyons, delivering the sediments to the deeper basin. NF: Normal Fault.

top prevent the seismic signals to penetrate deeper intervals. Therefore, the upper boundary of the platform looks as a seismic basement.

The upper boundary of the platform, the positive peak is characterized by two major channelized features. Their width reaches up to 0,5 km and depth up to 200 m. In basinward direction, parallel seismic sections indicate that their width increases and incision decreases its magnitude. These channelized features are composed of parallel onlapping reflections. The fill is mostly marl dominated. They are interpreted as bypass submarine canyons which delivered the sediments to the deeper basin (Figure 5.20).

5.4 Results of the Analysis

Basin physiography in Late Eocene, shaped by a discrete shelf-slope break, played a dominant role in facies distribution. As the shelf setting in the north is characterized by shallow marine carbonates and marl dominated intervals, basinal setting in the south is composed of pelagic limestone, marl and tuff alternations. Figure 5.21 exhibits a schematic cross-section in south to north direction, depicting major physiographic features of the basin in Late Eocene. The analysis of limestone and marl dominated intervals in the shelf setting suggested that the growth profile of carbonates and related marl deposition was very sensitive to relative sea-level fluctuations in the paleo-shelf setting in Late Eocene.

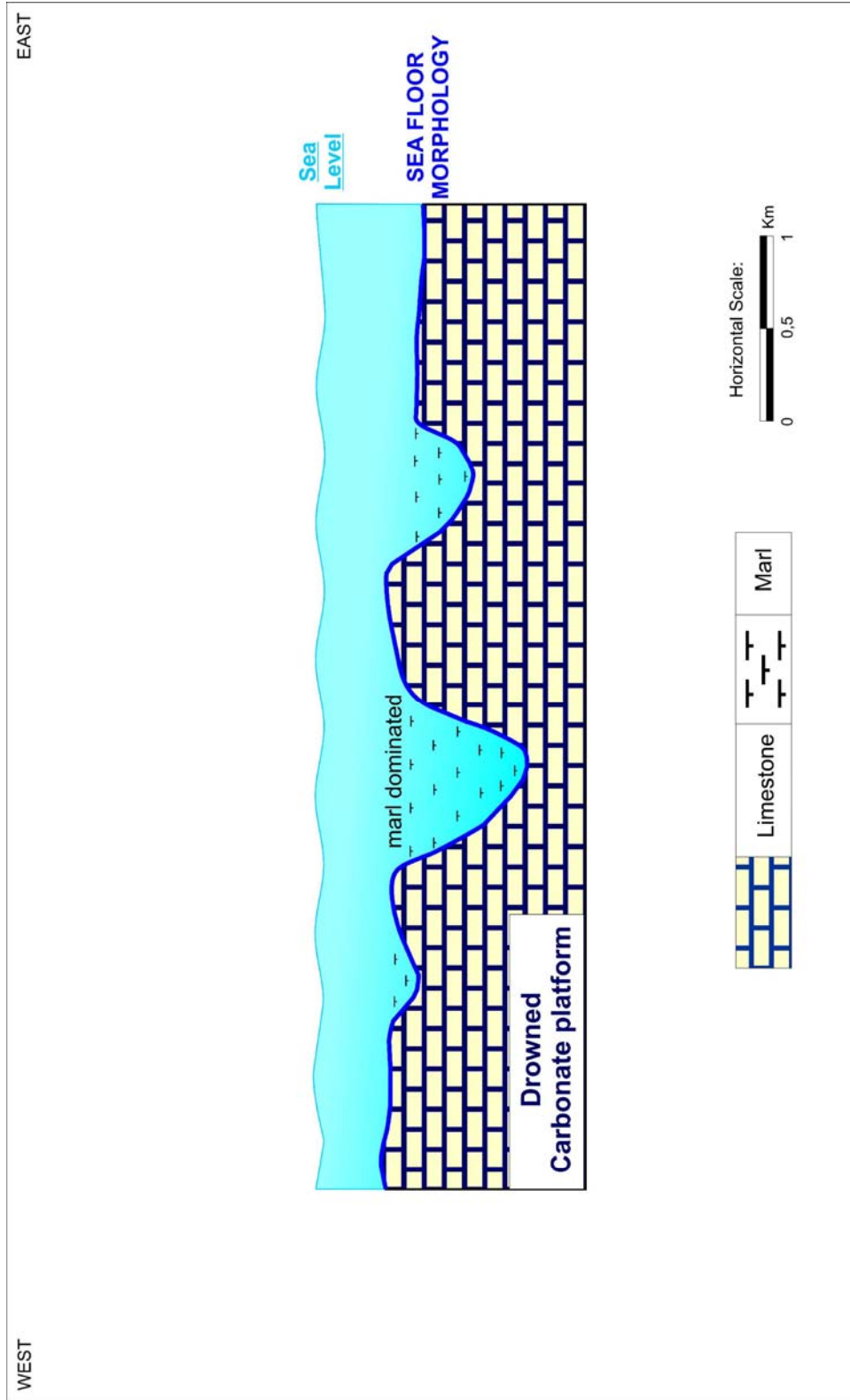


Figure 5.20 A schematic west to east oriented cross section. Late Eocene submarine morphology is shaped by channelized features. They are interpreted as bypassed submarine canyons, delivered most of the detritic material basinward.

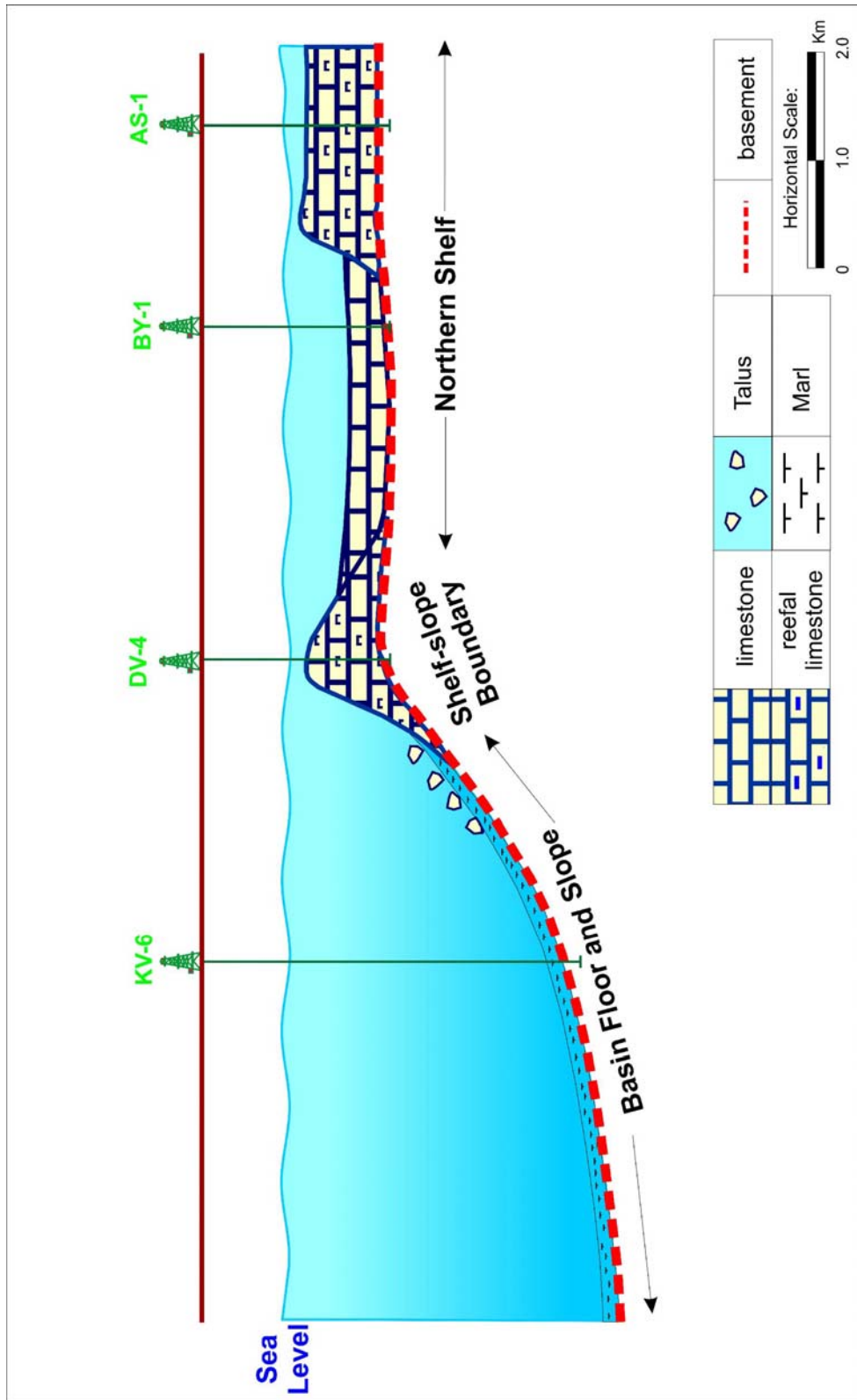


Figure 5.21 The figure shows a schematic cross-section in south to north direction, depicting major physiographic features of the basin in Late Eocene.

Additionally, topographic conditions (topographic highs and lows) in shelf setting were other important factors in carbonate development, backstepping of the facies and drowning. The clastic-carbonate mixed system overlies the shelf topography, which was formerly shaped by the incised channel systems, and tectonically subsided and uplifted areas. In initial transgression of the shoreline, carbonate production started in topographically low conditions.

Late Eocene clastic-carbonate mixed system were subdivided into third higher-order (may be forth, fifth or even higher-order) sequences on the basis of seismic reflection and well data sets. These sequences are triggered by rapid relative sea-level rise. However, the absence of high-resolution biostratigraphic data did not allow calibrating the chronostratigraphic position of the cycles.

In literature, Kendall and Schlager (1981), Neumann and McIntyre (1985), Kerans and Tinker (1997) and Pittet et al. (2000), it is well documented that carbonate platform development and related drowning response higher-orders of magnitude than second or third-order cycles.

Sequence-2 starts with initial transgression in Late Eocene. Shallow marine clastics are the first products of the transgression of high energy shoreface and ravinement surface. During this phase, carbonate production starts depending on topographic features throughout the basin. Shallow marine clastics grade upward into limestones. In topographic highs limestones directly overlies the metamorphic basement unconformably. In

highstand position of the sea-level, the carbonate production increases and a large platform has been developed in the Late Eocene.

Sequence-3 was characterized by partial drowning of the carbonate platform and backstepping of the shallow marine facies. Shallow marine carbonates are overlain by a marl dominated interval in the shelf setting. The base of marl interval is defined as the lower sequence boundary (transgressive surface), which is induced by a rapid relative sea-level rise, shoreline transgression, partial drowning of the carbonate platform and the backstepping of facies. Seismic data represents landward shift of the carbonate build-ups.

Sequence-4 is also characterized by rapid relative sea-level rise. Marl interval of Sequence-3 is overlain by another marl dominated interval in deep shelf setting. This interval exhibits mostly retrogradational stacking pattern in the studied wells in deep shelf environment. At the top of the sequence, highstand systems tract of Sequence-4 is represented by a limestone lithology in deep shelf environment. Additionally, shallower platform carbonates are observed towards the north on the basis of seismic reflection data.

The evolution of the Late Eocene carbonate platform and partial drowning by gradual relative sea-level rise were depicted in a two-dimensional cross section in south to north direction (Figure 5.22). In this figure, three higher-orders of sequences are depicted. The base of marl intervals were defined as the lower sequence boundary for each sequence,

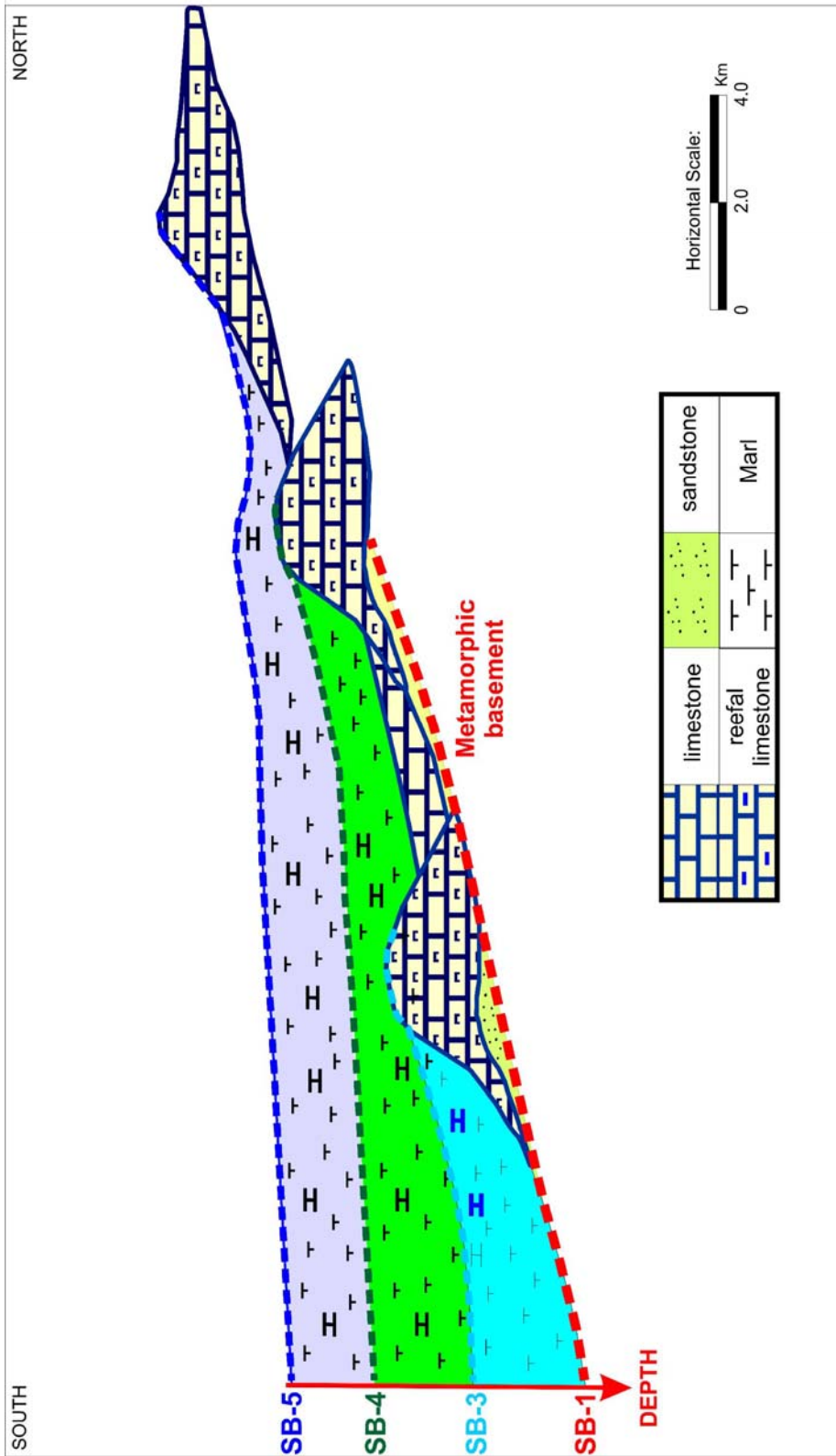


Figure 5.22 The figure sketches the evolution of the partial drowning of the carbonate platform and landward shift of the carbonate production in Late Eocene. SB: Sequence Boundary.

which is induced by relative sea-level rise. The sequences mostly exhibit retrogradational to aggradational stacking patterns. Retrogradational stacking patterns are composed of marl dominated intervals and observed as wedge shaped seismic geometry on seismic sections. Towards the land, mound-like seismic geometry observed on seismic sections is interpreted as carbonate build-ups and may represent aggradational to progradational (?) phases. As response to the continued relative sea-level rise, carbonate production shifts towards the land in the Late Eocene. Due to the location of the exploration wells in deep-shelf environment, the Sequence-3 and Sequence-4 are mostly composed of marl dominated intervals in the wells. In this environment, the minor effect of sea-level fluctuations on facies distribution is observed. However, at the top of the sequence, highstand systems tract of Sequence-4 is represented by a limestone lithology in deep shelf environment. Additionally, seismic data suggested that mound like seismic geometry shifts towards the land, which may be represented by aggradational to progradational (?) stacking patterns.

CHAPTER 6

REGIONAL AND GLOBAL VARIABLES IN THE UPPER EOCENE SEDIMENTARY RECORD OF THE THRACE BASIN

6.1 Introduction

Depositional sequences (Mitchum et al., 1977) are formed in response to the interaction of eustatic change, tectonic activities (subsidence or uplift) sediment supply, accommodation space and paleogeography (Posamentier and Allen, 1999). The interaction of these variables on the sedimentary record is observed as the relative sea-level change, which controls facies distribution and stratal architecture (Table 6.1).

The relative sea-level rise is triggered in the following ways (Posamentier and Allen, 1999);

1. Eustatic sea-level rises and the depth of the initial surface of deposition remains constant.
2. Eustatic sea-level remains constant and the basin subsides
3. The initial surface of deposition subsides and eustatic sea-level rises.
4. The initial surface of deposition subsides faster than eustatic sea-level falls.

Table 6.1 Important regional and global variables on the architecture of sedimentary basin fill (from Posamentier and Allen, 1999).

Stratigraphic Architecture						
Relative Sea-Level		Sediment supply			Physiography	
Eustasy	Total subsidence/ uplift	Substrate provenance and lithology	Vegetation	Fluvial discharge	Tectonics	Sedimentary processes
Climate	Crustal cooling Sediment compaction Tectonics Loading		Climate	Stream piracy Paleo geography		Paleo geography Environmental energy

5. The rate of eustatic sea-level rise is faster than the rate of uplift of the initial depositional surface.

On the other hand, relative sea-level falls occur when eustatic falls are at a greater rate than subsidence or when uplift exceeds the rate of eustatic rise (Posamentier and Allen, 1999).

In certain basins, some variables are more important than others; such as tectonism and sediment supply might be governing factors instead of eustasy. In this chapter, three major factors; regional tectonics, basin physiography, eustasy and their interaction in the sedimentary record were analyzed in detail.

6.2 Regional Tectonics

In regional tectonic concept, Early Eocene, Middle to Late Eocene, and Latest Eocene to Oligocene are characterized by different tectonic regimes. According to Yılmaz et al. (1997), Early Eocene is characterized by compressional tectonic regime caused by south to north compression between two continents (Yılmaz et al., 1997). Late Cretaceous-Early Eocene Tethyan evolution of western Turkey is characterized by ophiolite obduction, metamorphism, subduction, arc magmatism and continent-continent collision (Okay et al., 2001). Görür and Okay (1996) suggested that the continental collision between the Sakarya continent and the Istranca-Rodop Massif obliterated the eastern part of the Intra-Pontide Ocean to the south of the Istanbul zone. Its western part remained open and

continued to subduct northward throughout the Eocene. The contraction associated with this oceanic subduction could not be accommodated by the relative movement between the Istanbul and Sakarya zones. To accommodate this contraction, The Rodop-Pontide magmatic arc developing on the overriding Istranca zone started to rift and extent, thus forming the Thrace Basin (Figure 6.1).

My observations, mostly from 2D seismic reflection and well data sets from the northern margin of the Thrace Basin suggested that the Thrace was affected by a rifting phase in Middle-Late Eocene. Thickness change was observed between different fault blocks. Line-SN-5 is a south to north oriented seismic line (Figure 6.2). The seismic line demonstrates major structural elements of the Early-Middle Eocene tectonic regime. Structural elements of this regime were observed as parallel to sub-parallel, syn-sedimentary normal faults (orange color).

The outcrop-based studies from the Gelibolu Peninsula (Siyako, 2006; Sümengen and Terlemez, 1991; Temel and Çiftçi, 2002; Yaltırak, 1995) suggested that the Lower-Middle Eocene sediments start with deep water clastics and grade upward into deltaic facies of the Karağağaç Formation, and fluvial deposits of the Fıçitepe Formation. The studies from the southern Thrace (Yaltırak, 1995) suggest that Early-Middle Eocene and Late Eocene transition are represented by the Gaziköy and Keşan Formations with a transitional contact. Gaziköy and Keşan Formations were deposited in distal and proximal turbiditic facies, respectively (Yaltırak,

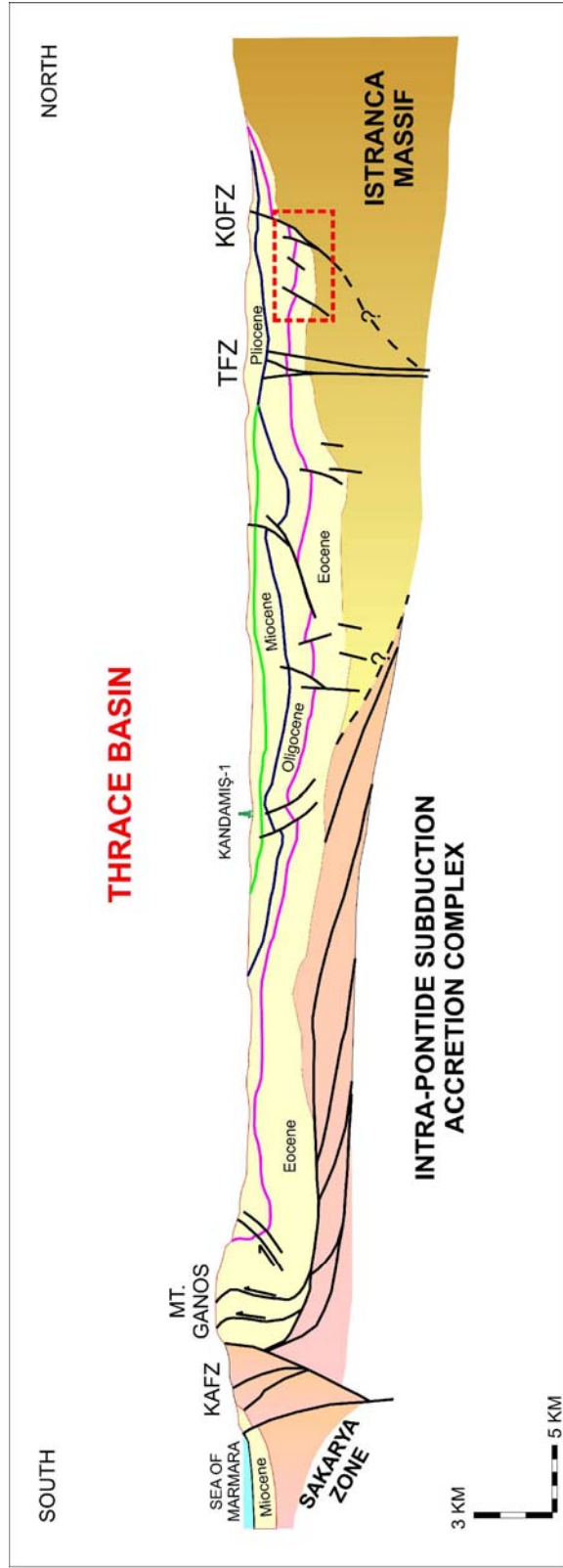


Figure 6.1 The geological cross-section shows the structural relationship between the Thrace Basin and the surroundings (from Görür and Okay, 1996). TFZ: Terzili Fault Zone, KOFZ: Kuzey Osmancık Fault Zone, KAFZ: Kuzey Anadolu Fault Zone. The red rectangle represents the location of the seismic line, displayed in Figure 6.2.

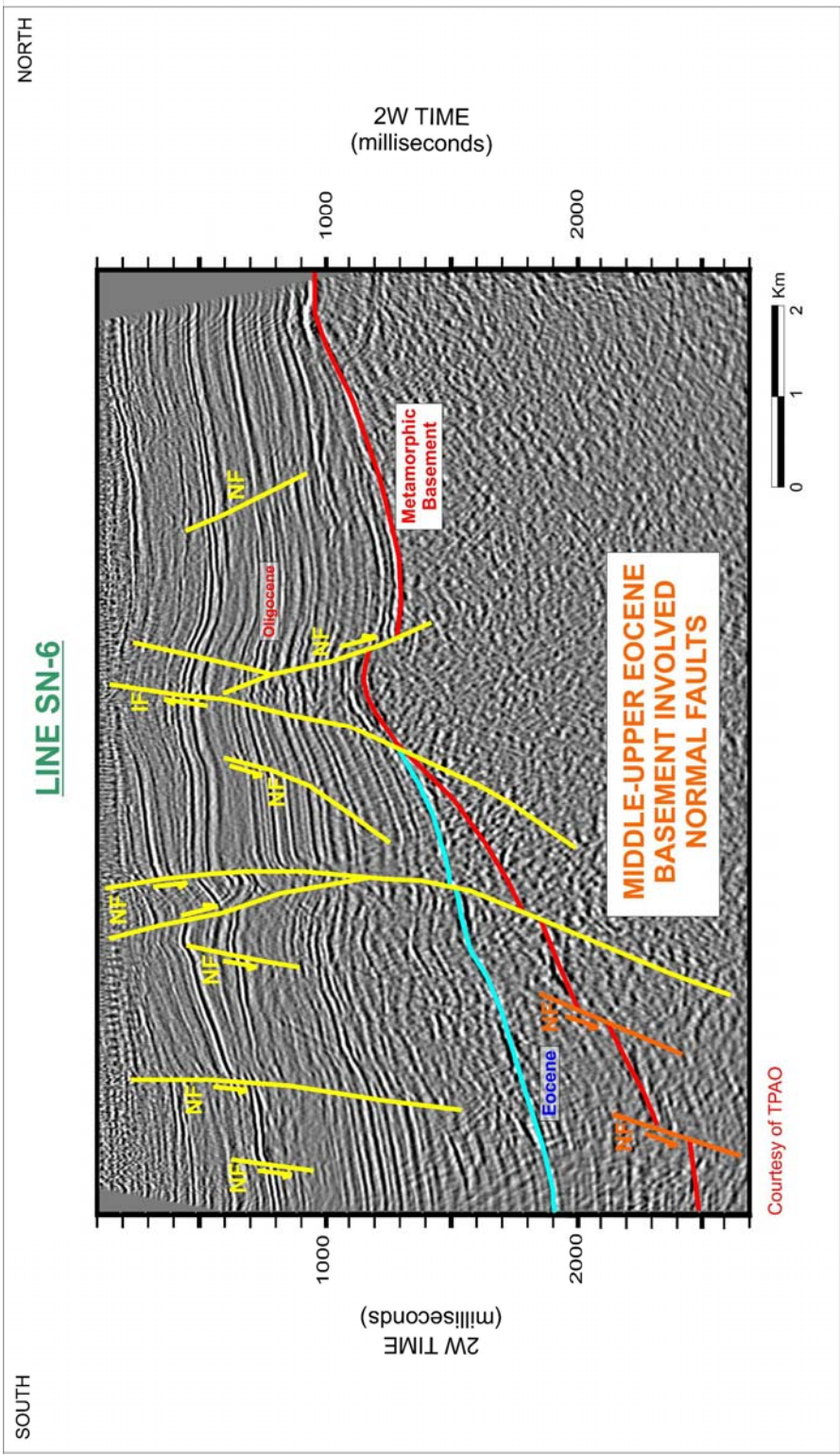


Figure 6.2 A south to north oriented seismic line crossing the northwest of the Thrace Basin. Extensional tectonic regime in Middle Late Eocene was characterized by basement-involved normal faults (orange color). Most of them were reactivated by the Oligocene to Pliocene inversion. Red and blue color horizons represent the basement and Upper Eocene sediments respectively. NF: Normal Fault, IF: Inverted Fault.

1995). In the study area, the age equivalent of these formations is shallow marine and continental deposits of the Hamitabat Formation. A few wells penetrated the Middle Eocene deposits in the studied area. As a consequence of different paleotopographic conditions between Gelibolu Peninsula, the southern Thrace and the northwest of the Thrace Basin and approximately south to north oriented invasion of the Early to Middle Eocene sea, this time is characterized by different depositional environments.

Early part of the Late Eocene in the northwestern part of the Thrace is represented by slope fan successions dominantly in the rifting phase. Most of the age studies point that rich planktonic foraminiferal fossil content of the slope deposits characterizes Late Eocene age (Erenler, 1987; Kasar and Okay, 1992; Batı et al., 1993; Turgut, 1997; Ediger et al., 1998).

This study emphasized that in the early part of the Late Eocene (corresponding to the Sequence-1) tectonic activity was one of the major factors in facies distribution. Hanging fault blocks of the normal faults in the rifting stage dominated the formation of west to east and northwest to southeast oriented submarine canyons and the deposition of thick turbidite successions in extensional tectonic regime (Figure 6.3). The areal extent of the fill was mostly bounded by changing submarine morphology instead of a uniform extent as a result of differing subsidence and uplift ratio.

The comparable studies were published in the literature, where the importance of the tectonic control in facies distribution has stated from

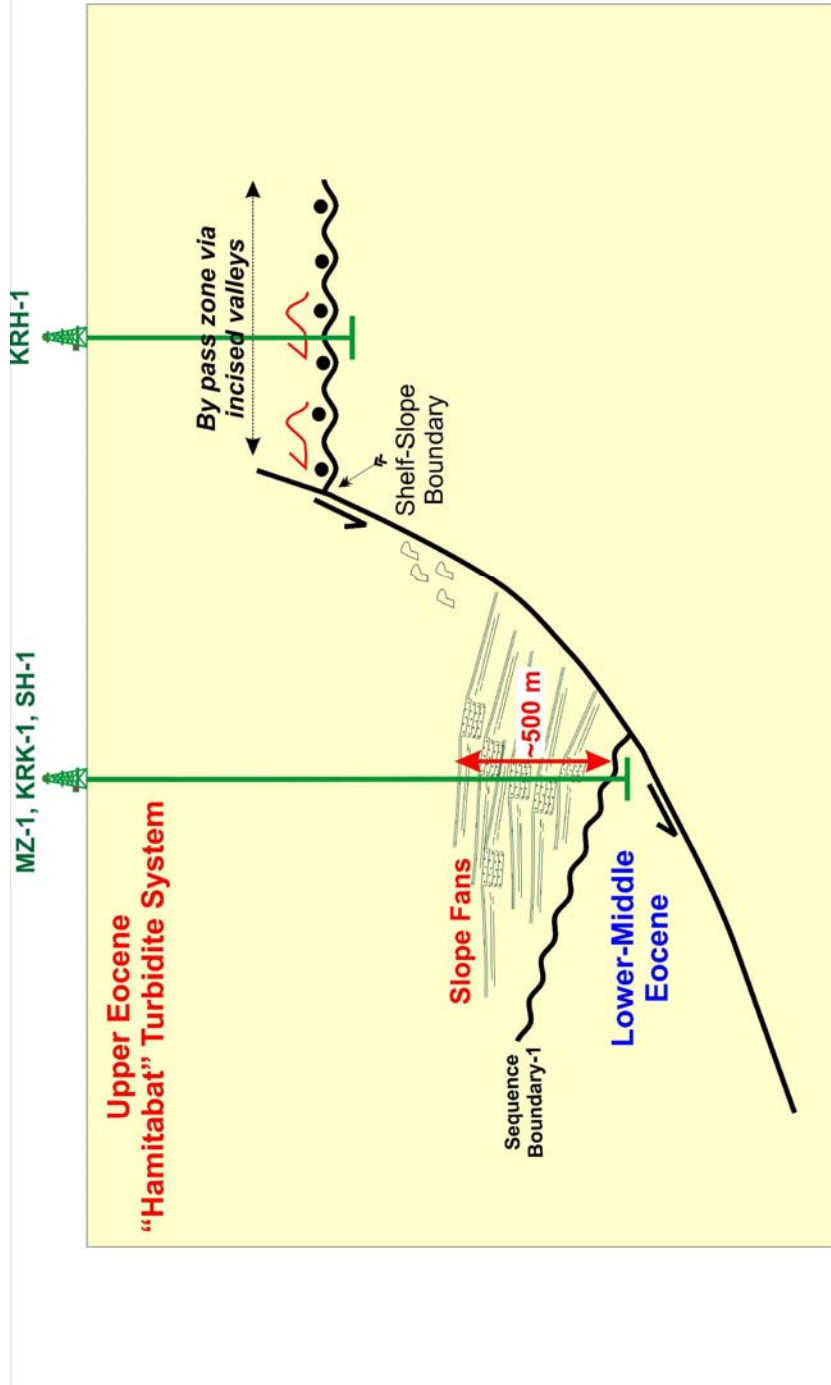


Figure 6.3 This study suggested that syn-sedimentary tectonic activities were the major source of high-energy gravity flow deposits instead of eustasy in Late Eocene in the northwest of the Thrace Basin.

various basins in the world (Bruhn and Walker, 1995; Millington and Clark, 1995; Trincardi et al., 1995; Clift, 1996 in Galloway, 1998).

During the Late Cretaceous, the Campos Basin was situated in a passive margin with a narrow and steep shelf. There was an important uplift in the adjacent hinterland and movement along the basin margin faults. This time corresponds to the second-order eustatic sea-level rise by Haq et al. (1987). During this time, the effect of fluctuations of relative sea-level were minor and source remained relatively close to the shelf-slope break. Bruhn and Walker (1995) claimed that during the Late Cretaceous in the Campos Basin, the contribution of fluctuations of the relative sea-level were minor. Instead, local tectonic control played an important role on facies distribution. Canyon formation and turbidite deposition were dominated by listric normal faults.

Similar observations were also made in Zink and Norris (2004) study. They emphasized that the facies diversity in the basin and submarine canyon formation were linked to the basin tectonism and source area elevation as a major parameter. They recorded an intense proximal sediment input in the rifting phase. On the contrary, during the transition to a more strike-slip dominated regime, they observed abundance of mud dominated distal sedimentary facies due to diminished topographic gradient of the source areas. In the following compressional tectonic regime, proximal deposits were again active.

In my study, the importance of tectonic control was highlighted and stated as a major parameter of submarine canyon formation in Late Eocene. Seismic data exhibited that canyons were developed in the hanging fault block of the normal faults (Figure 6.3) in rifting phase. The core data from the various wells in the basin confirmed that the depocenters were filled with proximal sediments.

In the following time interval of the Late Eocene (corresponding to the deposition of Sequence-2), a more stable tectonic regime was dominant and tectonically induced subsidence rate diminished. Most of the basement involved normal faults have lost their activities. During this time, the shoreline transgression was characterized by the clastic-carbonate mixed system. Shallow marine clastics were the first products of this transgression of high energy shoreface and ravinement surface. During this phase, the carbonate production started depending on the configuration of the topography throughout the basin. Shallow marine clastics graded upward into limestones. During the highstand position of the sea-level, the carbonate production increased and a large platform was developed in Late Eocene. Gradual shoreline transgression also caused the partial drowning of the carbonate platform and the backstepping of facies.

The most outcrop-based studies from the Gelibolu Peninsula and southern Thrace (Sümengen and Terlemez, 1991; Temel and Çiftçi, 2002; Siyako, 2006) stated that Late Eocene time is characterized by a regional

basin deepening. Shallow marine carbonates were overlain by deeper marine deposits of the Ceylan Formation in the Late Eocene.

Shallow marine carbonates in the Gelibolu Peninsula were dated as Middle Eocene. On the other hand, in the northern margin of the Thrace Basin shallow marine carbonates were dated as Upper Eocene. This suggested that shoreline transgression started in Middle Eocene in Gelibolu Peninsula and continued northward gradually in Late Eocene. Siyako and Huvaz (2007) also stated that Middle Eocene transgression was initiated in the southern Thrace and progressively affected the northern Thrace in Late Eocene.

Under the transpressional tectonic regime in latest Eocene and Oligocene, the eastern and central Pontides as well as the Sakarya continent were gradually elevated above the sea (Yılmaz et al., 1997). As a consequence of the regional uplift, Upper Eocene marine sediments were replaced by evaporites and then continental red beds, during the Oligocene in several basins (Yılmaz et al., 1997). A right lateral strike-slip fault system has begun to develop in the Oligocene (Yılmaz et al., 1997).

This time interval was recognized as the transition from deeper to shallower depositional environments throughout the Thrace Basin. A major deltaic system, called the Yenimuhacir Deltaic System, was dominant, which was defined as an elongate to lobate shaped fluvial dominated deltaic system (Atalık, 1992; Turgut, 1997). The dominant lithologies were very fine to medium-grained sandstones, interbedded with greenish grey shales and

siltstones (Atalık, 1992; Turgut, 1997; Siyako, 2006). An Early to Late Oligocene age has been assigned on the basis of stratigraphic relations and palynological data (Gerhard and Alişan, 1986; Turgut, 1987; Atalık, 1992; 1997; Batı et al., 2002; Siyako, 2006). The lignite intervals within the delta plain were also dated as Late Oligocene (Batı et al., 1993).

6.3 Basin Physiography

The paleo-physiographic setting in Late Eocene was characterized by a discrete shelf-slope break, oriented in approximately southeast to northwest direction in the northern margin of the basin.

The facies of the Late Eocene “Hamitabat” turbidite system was shaped by paleo-basin physiography. The southeast northwest trending shelf-slope break in the northern margin of the Thrace Basin makes a north bending nearby Kavakdere and continues to westward (Figure 6.4). Between KY-2 well and KV-6 well, the physiography was exhibited by a relatively larger shelf and a gentle slope gradient. On the other hand, between Kavakdere and IN-1 well, the basin physiography was exhibited by a narrow shelf and a steep slope gradient. This diagnostic change affected the erosional and depositional features of the “Hamitabat” depocenters. The basin physiography with a narrow shelf and a high angle slope gradient dominated the canyon formation in the northwest of the study area. On the other hand, relatively wider shelf and gentle angle slope gradient dominated the multi-channel system. These channels fed fine to medium-grained

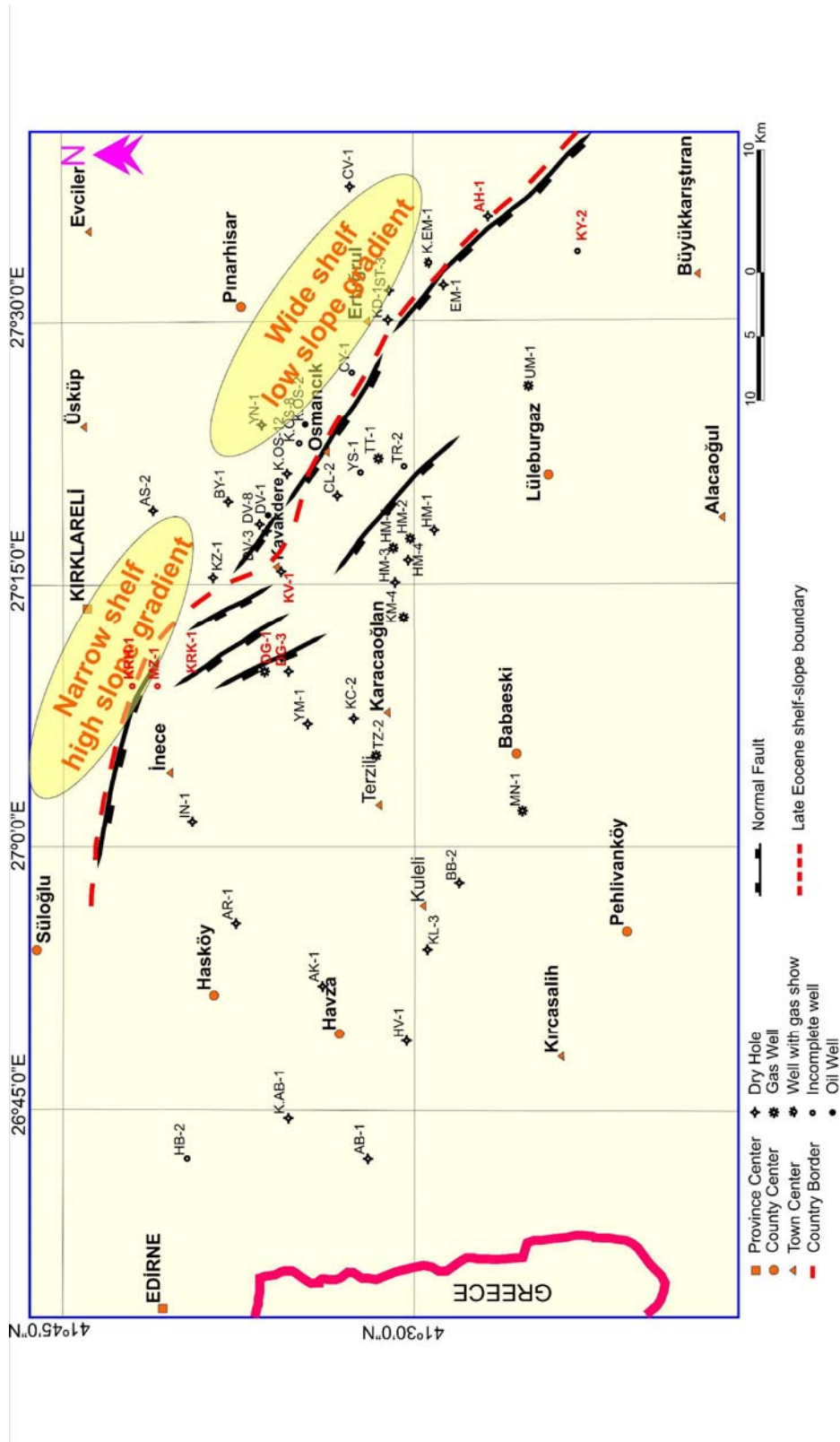


Figure 6.4 "Hamitabat" turbidite system depocenters were shaped by the basin physiography. The southeast northwest trending shelf-slope break (red color dashed line) makes a north bending nearby Kavakdere and continues westward in parallel to east west direction. Between KY-2 well and KV-1, the physiography was characterized by a relatively larger shelf and low slope gradient.

sandstone rich turbidites, slide and slump deposits in the northeast of the study area. This difference was depicted in Figure 6.5.

Reading and Richards (1994) classified the depositional systems of the deepwater basin margins into twelve types regarding to their grain size (from mud to gravel dominated) and feeder systems (point source to multiple sources). The results of my study contribute to their study that even in a single basin varying basin morphology can shape the grain size distribution and the feeder system. In the northeast of the study area, the existence of shelf with gentle slope dominated the multi-channel source system. Whereas, the steep slope and the narrow shelf dominated the point source canyon formation with coarser fill. The wells penetrated the submarine canyons reflected that the fill was composed of erosive base conglomeratic intervals. Reading and Richards (1994) stated that coarse grained slope fans have small sizes and tend to be developed in tectonically active basins; e.g. rift or strike-slip basins on the hanging wall of the faults. According to their grain size based classification, gravel-rich systems are developed in basins with high angle slope gradients and narrow shelf preferentially.

Thick accumulations of slope deposits fill the depressions and modify the paleo-physiography of the basin floor. The areal extent of the fill was mostly bounded by changing paleo sea-floor morphology instead of a uniform extent. Due to approximate north to south and northwest to southeast directed sediment loading, sea-floor tilted southward. Sediments

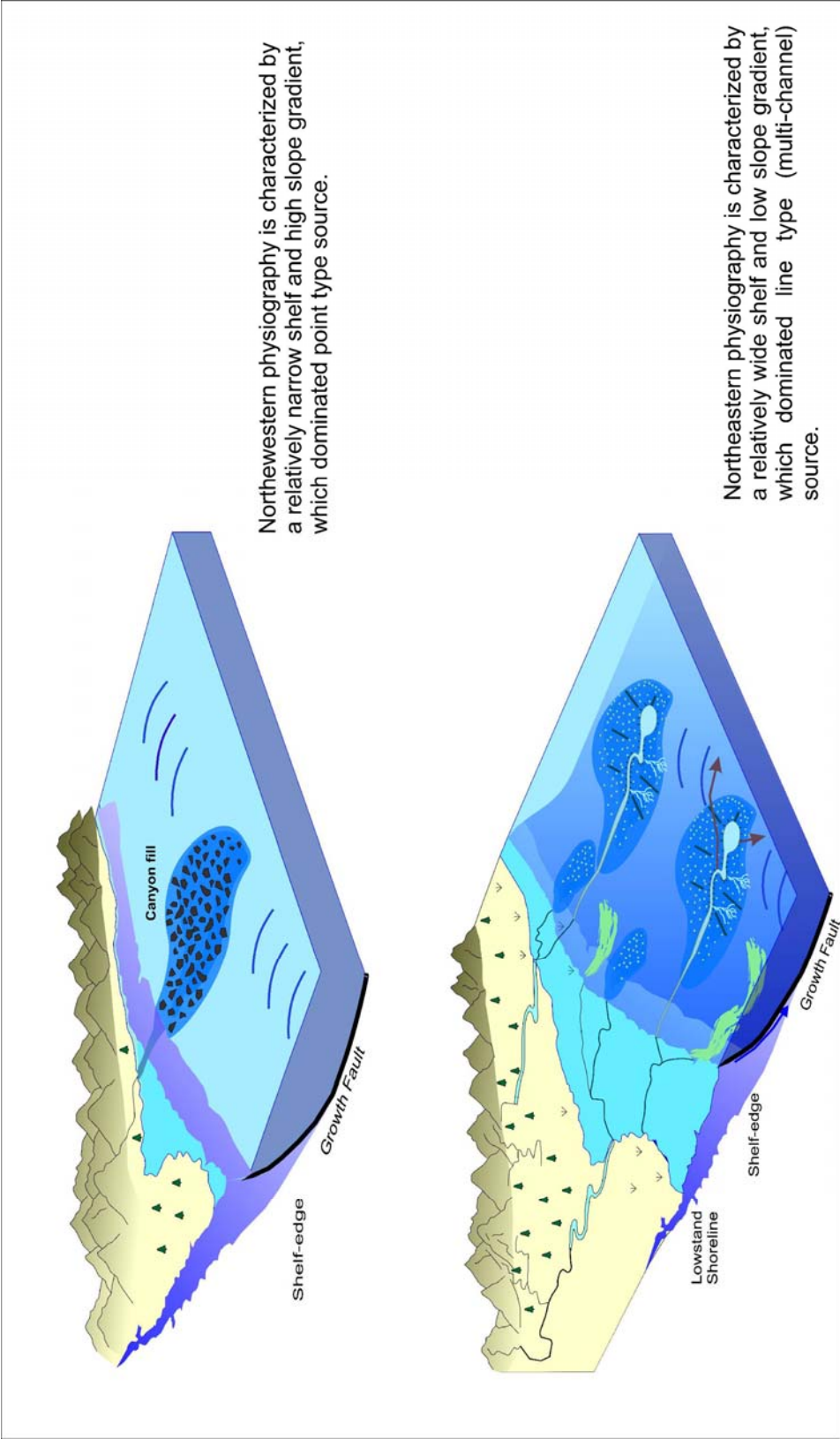


Figure 6.5 The Northwestern and the Northeastern depocenters exhibit different nature of depositional fill, which was mostly shaped by basin physiography.

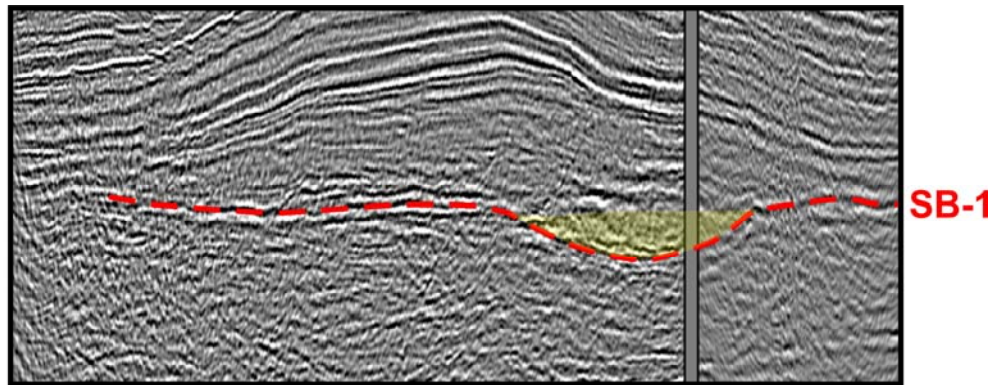
were bounded by the southeast to northwest oriented uplifted region between the YM-1 and AR-1 wells. In order to represent the changing sea-floor morphology, Line-WE-1 was flattened in Figure 6.6. The baselap surface (red color horizon) observed on seismic sections represented the basin physiography. Seismic line B demonstrated that the sea-floor morphology was uplifted towards the east of the seismic line.

Basin physiography in the following relative sea-level rise controlled the distribution of shallow marine carbonate facies (Figure 6.7). As the shelf setting is characterized by shallow marine carbonates and marl dominated intervals as response to relative sea-level fluctuations, the basinal setting is composed of pelagic limestone, marl and tuff alternations. Discrete shelf-slope boundary characterizes the distribution of shallow marine carbonates.

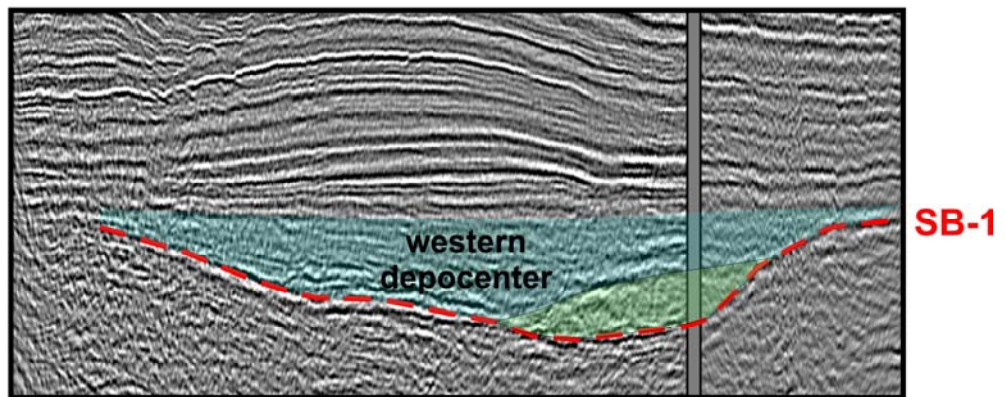
6.4 The Analysis of Mesozoic and Cenozoic Sequence Chronostratigraphic Chart of European Basins

“Mesozoic-Cenozoic Sequence Chronostratigraphic Framework of European Basins” project built a biochronostratigraphic record of depositional sequences in European Basins. The aim was to demonstrate the synchronicity of sequences in basins with different tectonic histories.

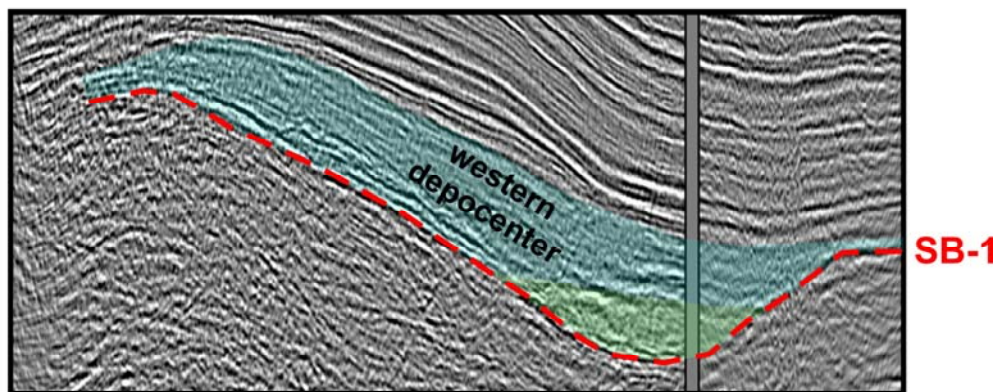
In Western European stratigraphic successions, 18 transgressive/regressive cycles, corresponding to second-order cycles have been identified. The building blocks of transgressive-regressive cycles are third-order depositional sequences. In their terminology, the term



A) Flatten to ponded phase of the Western depocenter



B) Flatten to filling phase of the Western depocenter



C) Present-day seismic representation of the Western depocenter, which was affected by post-Miocene strike-slip tectonic regime.

Figure 6.6 Three seismic lines represent the evolution of the Western depocenter by changing sea floor morphology. SB-1: Sequence Boundary-1.

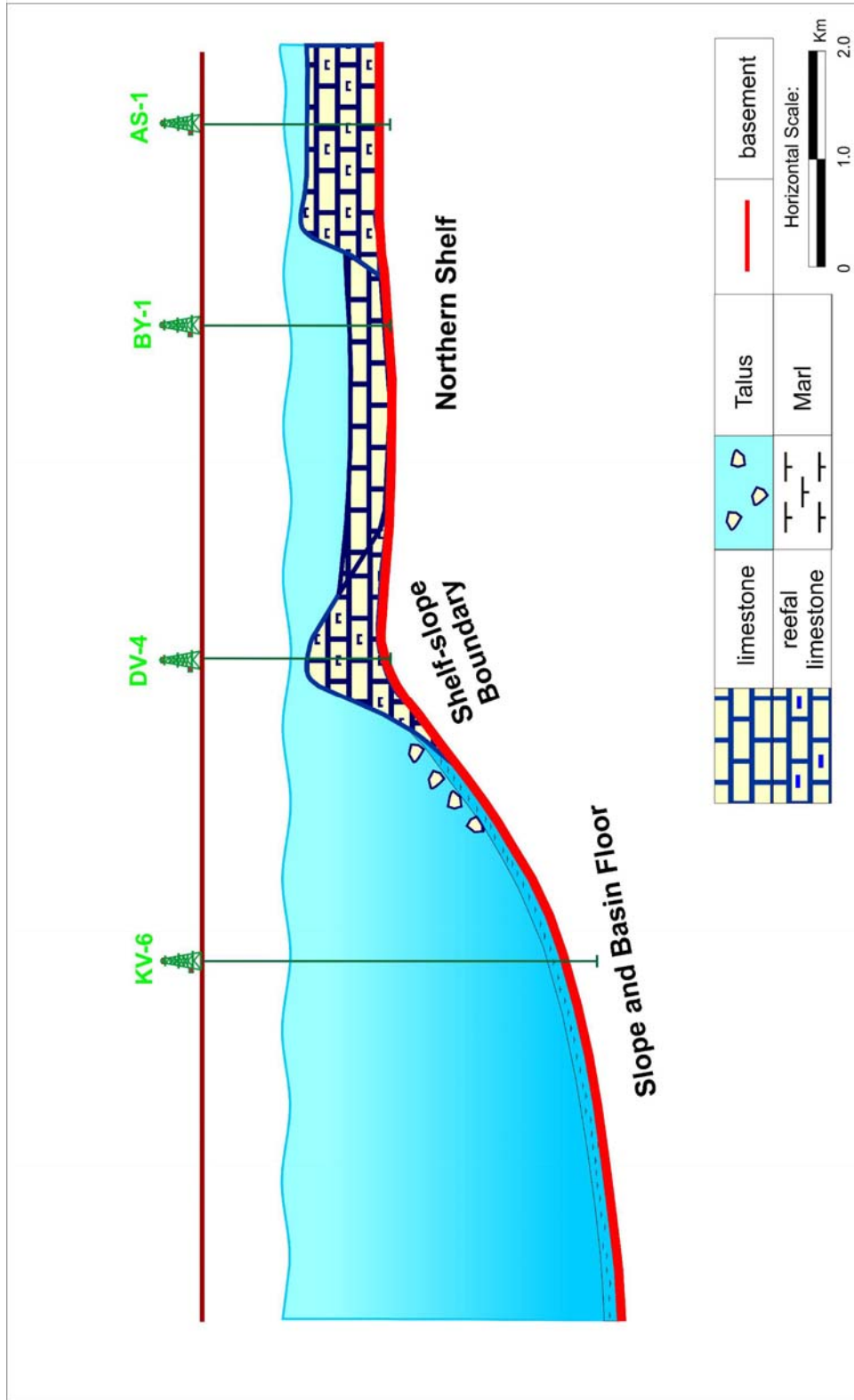


Figure 6.7 The figure shows a schematic cross-section in south to north direction, depicting major physiographic features of the basin in Late Eocene.

transgressive stands for stratal packages characterized by aggradationally or retrogradationally stacked depositional sequences. The term regressive defines stratal packages characterized by progradationally stacked depositional sequences. Their second-order cycles correspond best with the definition of post rift megasequences, which consist of successively stacked basinward stepping or landward stepping. Second-order transgressive-regressive cycles have a time duration ranging from 3 to 30 million years. Each regressive phase corresponds to a decrease in the rate of accommodation and each transgressive phase to an increasing rate of accommodation.

Within 18 transgressive/regressive cycles, some of them are synchronous with also Thrace sediments of Eocene age. This suggests the tectono-eustatic control with Thrace sedimentary package.

In their study, focusing on Eocene time interval (Figure 6.8), Lutetian is represented by a regressive cycle. On the other hand, Bartonian and Priabonian in Upper Eocene is represented by a transgressive cycle. My interpretations also suggest that the Late Eocene is characterized by shoreline transgression. In this time interval, the facies exhibits retrogradational stacking patterns. South to north oriented seismic lines and basinward well correlations demonstrate relative sea-level rise and landward shift in facies in the Late Eocene (Figure 6.9). Reflections onlapping onto metamorphic basement rocks of the Istranca Massif were used as an evidence of second-order transgressive facies cycle.

CENOZOIC SEQUENCE CHRONOSTRATIGRAPHY OF EUROPEAN BASINS

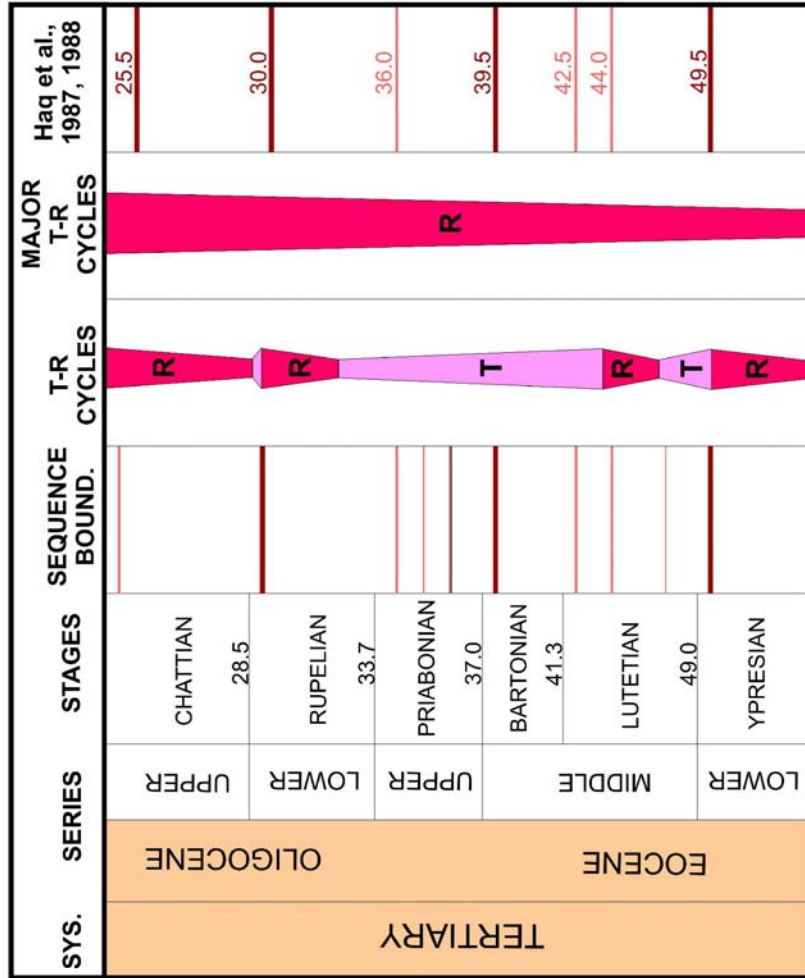


Figure 6.8 Cenozoic-Mesozoic Sequence Chronostratigraphic chart of European Basins. Transgressive-regressive cycles correspond to second-order cycles. The term transgressive (T) stands for stratal packages characterized by aggradationally or retrogradationally stacked depositional sequences. The term regressive (R) represents stratal packages characterized by progradationally stacked depositional sequences (modified from Hardenbol et al., 1998).

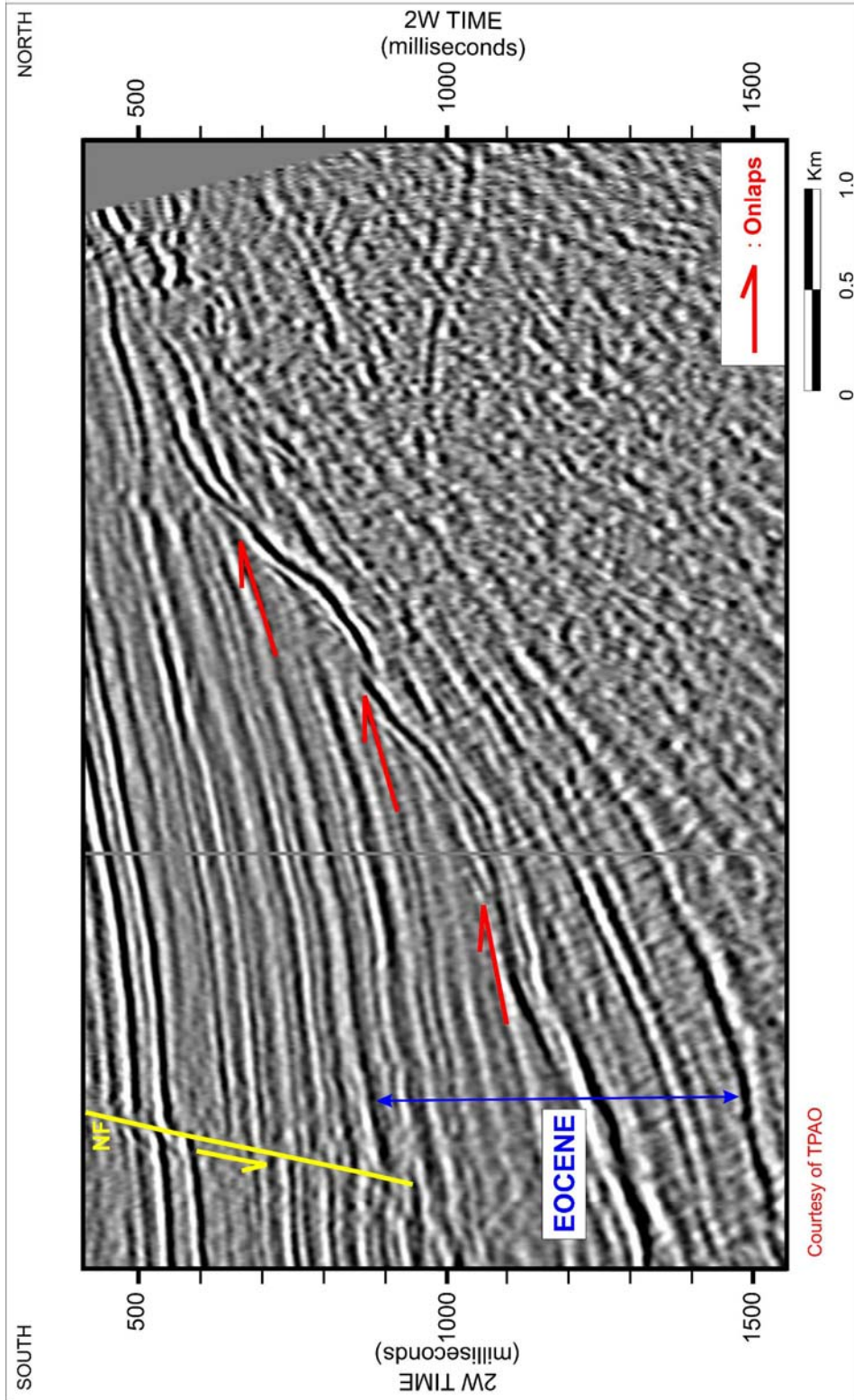


Figure 6.9 Seismic line is a south to north oriented seismic line. Onlapping reflections and backstepping of facies with well confirmation were used as an evidence of second-order transgressive facies cycle in the Thrace Basin. NF: Normal Fault.

These results confirmed with well data analysis. Shallow marine clastics are the first products of transgression of high energy shoreface and ravinement surface in the Late Eocene.

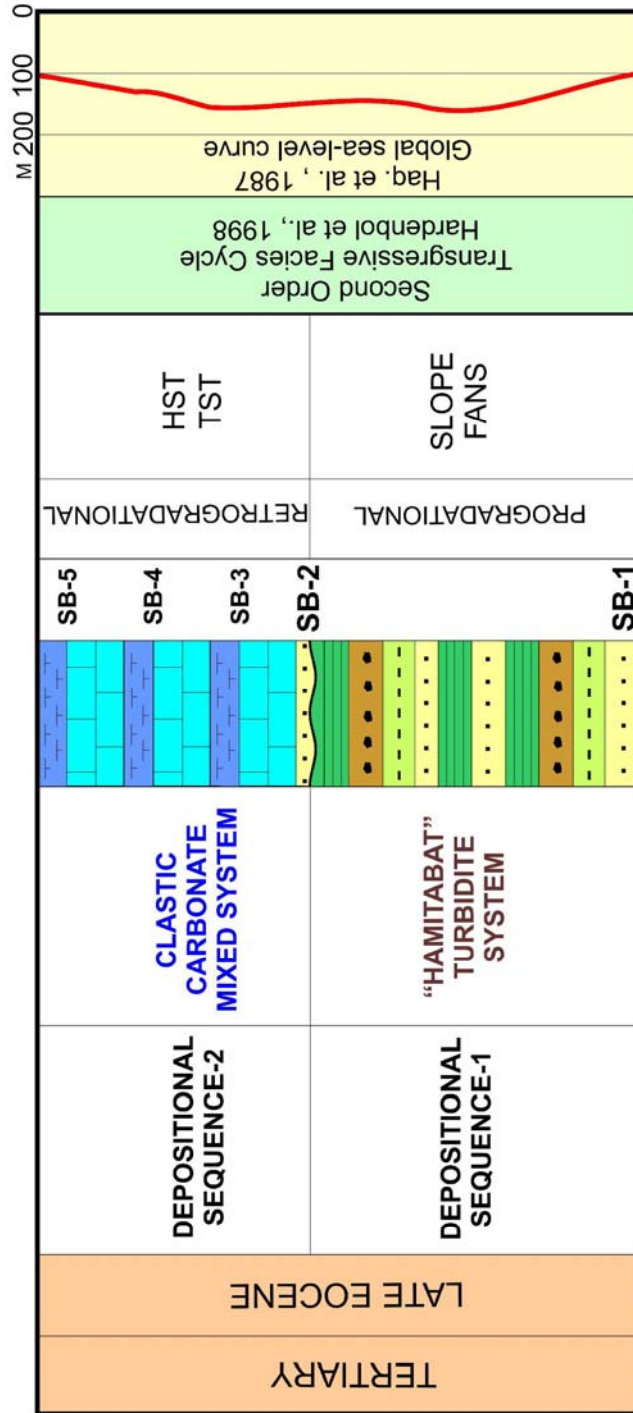
6.5 Results of the Analysis

In this study, Upper Eocene sedimentary succession was subdivided into third-order depositional sequences. Figure 6.10 and Figure 6.11 summarize major elements of two depositional sequences.

The comparison of my observations in the northern margin of the basin with various outcrop-based studies from southern part of the basin and the Gelibolu Peninsula (Sümengen and Terlemez, 1991; Yaltırak, 1995; Temel and Çiftçi, 2002; Siyako, 2006), suggested that the Thrace sedimentary succession was characterized by varying depositional environments as a consequence of different paleogeographic conditions.

Regional tectonics studies (Görür and Okay, 1996; Yılmaz et al., 1997) emphasized that the basin development during this time was affected by the rifting phase. This study proved that thick accumulations of slope fans were deposited during the early part of Late Eocene basin evolution. Tectonically induced canyons in rifting phase were formed as a result of high subsidence rate. This suggested that facies distribution in the early part of the Late Eocene in the Thrace Basin was mostly controlled by the sea floor subsidence instead of eustasy.

LATE EOCENE SEDIMENTARY SUCCESSION IN THRACE BASIN



SB-1 and SB-2: Third-Order Sequence Boundaries
 SB-3, SB-4 and SB-5: Higher-Order Sequence Boundaries
 TST: Transgressive Systems Tract, HST: Highstand Systems Tract

Figure 6.10 This study subdivides Upper Eocene sedimentary succession into two third-order depositional sequences. Depositional sequence-1 comprises "Hamitabat" turbidite system and Depositional Sequence-2 comprises clastic-carbonate mixed system.

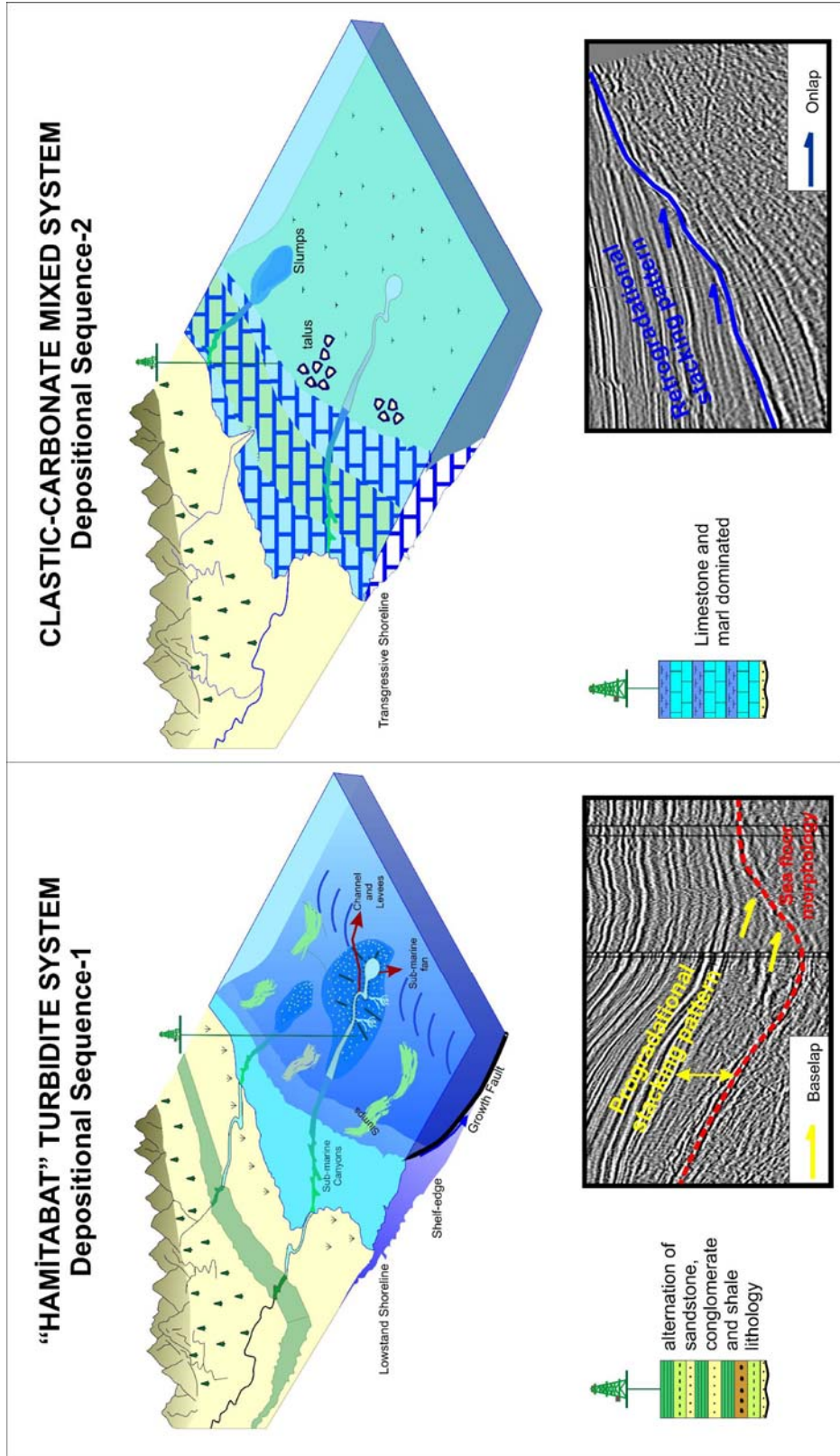


Figure 6.11 This study subdivides the Upper Eocene sedimentary succession into two-third order depositional sequences. The figure displays major elements of the Depositional Sequence-1 and Depositional Sequence-2.

The uppermost Eocene mostly exhibited retrogradational stacking patterns. The evolution of the carbonate platform was characterized by shoreline transgression and landward shift of the facies in Late Eocene. South to north oriented seismic lines and well data suggested that the reflections onlapping onto the metamorphic rocks of the Istranca Massif represented relative sea-level rise in the basin. In "Mesozoic-Cenozoic sequence chronostratigraphic framework of European basins" project, Bartonian and Priabonian epochs in Upper Eocene is also composed of a transgressive cycle, which corresponds to a second-order cycle. Reflections onlapping onto metamorphic basement rocks of the Istranca Massif and basinward well correlations were used as an evidence of second-order transgressive facies cycle in the Thrace Basin.

CHAPTER 7

SUMMARY AND CONCLUSIONS

1. Upper Eocene sedimentary succession of the northwestern part of the Thrace Basin was subdivided into two third-order sequences on the basis of well and seismic data sets.
2. Depositional Sequence-1 comprises a coarse-grained turbidite system and its landward equivalents, called the “Hamitabat” turbidite system. Depositional Sequence-2 comprises a clastic-carbonate mixed system. Shallow marine siliciclastics of the Koyunbaba Formation, shallow marine carbonates of the Soğucak Formation and coeval basinward pelagic limestones, and marl-tuff alternations of the Ceylan Formation are major lithologies of this system.
3. Early Late Eocene in the northwestern part of the Thrace Basin was dominantly represented by slope fan successions. The Sequence Boundary-1 corresponds to the boundary between Lower-Middle Eocene and Upper Eocene sediments. In the slope setting, this boundary was identified as the base of slope fan deposits. In the northern shelf setting, this boundary was placed to the base of the channel fill deposits.

4. "Hamitabat" turbidite system was analyzed in three major depocenters. They were named as Western, Northwestern and Northeastern depocenters respectively based on their geographic locations. Each depocenter was characterized by its own sediment delivery type, lithology, areal extent and facies architecture.
5. Western depocenter is restricted to the westernmost part of the study area. The areal extension of the Western depocenter was shaped by the enclosed sea-floor morphology. Seismic data revealed that the sediment flow direction is estimated from northwest to southeast by a submarine canyon geometry.
6. Northwestern depocenter, located between the KRK-1 and the DG-3 wells was classified as a canyon fill. The fill is composed of conglomerate and sandstone lithology. The basin physiography with the narrow shelf and steep slope gradient with high tectonic subsidence rate promoted the canyon formation.
7. Northeastern depocenter is extended in a larger area between the KY-2 well and Kavakdere Field. Relatively wider shelf and gentle slope gradient dominated a line type of source for the thick succession of mass flow and turbidity current deposits. Wide northern shelf is characterized by channelized continental to shallow marine deposits, which were used as sediment delivery pathways to the Northeastern depocenter.

8. This study proved that the characteristic features of the “Hamitabat” turbidite system were controlled by the interaction of regional tectonics, basin physiography and eustatic fluctuations in the Late Eocene.
9. Tectonically induced canyon developments, southeast to northwest trending basement-involved normal faults and fault controlled thickness changes suggested that facies distribution was controlled by a high subsidence rate of sea-floor dominantly instead of eustasy. The existence of the incised channel system in the northeastern shelf might be used as an evidence of the third-order lowstand sea-level, which may promote the slope deposition as a secondary factor.
10. The studies from different parts of the world (Bruhn and Walker, 1995; Clift, 1996; Trincardi et al., 1996) emphasized the role of the tectonic control on submarine canyons. They claimed that the tectonic control played an important role on sediment supply and local sea-level fluctuations instead of eustasy. This study highlighted the role of the both regional variables; tectonic influence and the basin physiography on the submarine canyon formation.
11. In Zink and Norris (2004) study, the facies diversity in the basin and submarine canyon formation were linked to the basin tectonism and related source area elevation as major parameters. They recorded an intense proximal sediment input in the rifting phase. On the contrary, during the transition to a more strike-slip dominated regime, they observed abundance of mud dominated distal sedimentary facies due

to the diminished topographic gradient of the source areas. In the following compressional tectonic regime, proximal deposits were again active. In my study, the integration of seismic, well-log and core data suggested that the formation of submarine canyons with proximal sediment fill were linked to the increased subsidence, related uplift and steepening of the margins in the rifting phase in the Basin.

12. Reading and Richards (1994) classified the depositional systems of the deepwater basin margins into twelve types regarding to their grain size (from mud to gravel dominated) and feeder systems (point source to multiple sources). The results of my study contribute to their study that even in a single basin varying basin morphology can shape the grain size distribution and the feeder system. In the northeast of the study area, the existence of shelf with gentle slope dominated the multi-channel source system. Whereas, the steep slope and the narrow shelf dominated the point source canyon formation with coarser fill.

Gervais et al. (2004) also made similar observations in the Corsica margin in the western Mediterranean Sea. They emphasized the Oligo-Miocene tectonic evolution and paleo-basin morphology of the Corsica margin in the western Mediterranean Sea. They observed different feeder systems in the eastern and the western margins. They indicated that the western Corsica margin was characterized by numerous deep canyons, which were developed in a steep slope

without a continental shelf. On the other hand, the eastern margin was characterized by a moderately developed continental shelf with shallower canyons and channels on a gentle slope. This study provided a case study, which concentrates on the role of the basin tectonics and varying morphology in the canyon formation.

13. The analysis of limestone and marl dominated intervals in the shelf setting indicated that the growth profile of carbonates was very sensitive to relative sea-level fluctuations in the paleo-shelf setting in the latest Eocene. During this time, tectonically induced subsidence rate diminished. Most of the synsedimentary basement-involved normal faults have lost their activities in a more stable tectonic regime.
14. Carbonate production and related drowning responded higher-order (fourth or fifth) of relative sea-level fluctuations than third-order sea-level fluctuations. Clastic-carbonate mixed system was subdivided into three higher-order (may be fourth or fifth) sequences. The absence of high resolution biostratigraphic data did not allow calibrating the chronostratigraphic position of the cycles.
15. The evolution of the carbonate platform was characterized by retrogradational stacking patterns. The boundaries of the sequences were defined as the base of transgressive deposits, which were induced by rapid relative sea-level rise.
16. Sequence-2 is represented by initial transgression in the Late Eocene. Shallow marine clastics were the first products of transgression of high

energy shoreface and ravinement surface. During this phase, carbonate production started depending on topography throughout the basin. Shallow marine clastics represent gradual upward into the limestone lithology. In the highstand position of the sea-level, carbonate production increased and a large platform has been developed.

17. Sequence-3 is characterized by partial drowning of the carbonate platform and backstepping of the shallow marine facies. Shallow marine carbonates are overlain by a marl dominated interval in the shelf setting. The base of the marl interval was set as the lower sequence boundary, which was induced by a rapid relative sea-level rise, shoreline transgression, partial drowning of the carbonate platform and backstepping of facies.
18. Sequence-4 is characterized by a rapid relative sea-level rise. Marl interval of the Sequence-3 is overlain by another marl dominated interval in a deep shelf setting. At the top of the sequence, highstand systems tract of Sequence-4 is represented by a limestone lithology in deep shelf environment. This interval exhibited retrogradational to progradational stacking patterns in the studied wells and shallower platform carbonates were deposited towards the land.
19. Many case studies stated in Kendall and Schlager, (1981); Handford and Loucks, (1993) emphasized that the lowstand sea-level contributes the slope deposition. Whereas basinwide subsurface

correlations in the Thrace Basin showed that most of the slope deposition in Late Eocene took place in the transgressive sea-level during the backstepping of carbonate production towards the land (corresponding to Sequence-2).

20. The comparison of my observations in the northern margin of the basin with outcrop-based studies from southern part of the basin and the Gelibolu Peninsula (Sümengen and Terlemez, 1991; Yaltırak, 1995; Temel and Çiftçi, 2002) suggested that the Thrace sedimentary succession was affected by a second-order transgressive cycle starting from the Middle Eocene. However, the study area (northwest of the Thrace), southern Thrace and the Gelibolu Peninsula were characterized by varying depositional environments as a consequence of different paleogeographic conditions. The northwest of the Thrace basin was represented by a slope fan succession of the “Hamitabat” turbidite system and the following clastic-carbonate mixed system and southern Thrace was represented by proximal turbidites of the Keşan Formation. Whereas, the Gelibolu Peninsula was characterized by shallow marine carbonates and their basinward equivalents in the Ceylan Formation.
21. In “Mesozoic-Cenozoic Sequence Chronostratigraphic Framework of European Basins” project, Bartonian and Priabonian epochs are represented by a second-order transgressive cycle. Late Eocene retrogradational stacking patterns, induced by the relative sea-level

rise were used as the products of the second-order transgressive cycle in the Thrace Basin.

REFERENCES

- Alişan, C., 1985, Trakya "I" Bölgesi'nde Umurca-1, Kaynarca-1, Delen-1 kuyularında kesilen formasyonların palinostratigrafisi ve çökeltme ortamlarının değerlendirilmesi: TPAO Research Center Archive, unpublished technical report, no: 386, 60 p.
- Alişan, C. and J.E. Gerhard, 1987, Kuzey Trakya havzasında açılan üç kuyunun palinostratigrafisi ve kaynak kaya özellikleri. Türkiye 7. Petrol Kongresi Bildiriler Kitabı, p. 461-474.
- Atalık, E., 1987, Trakya Havzası Soğucak Formasyonu çökel ortamları ve mikrofasiyes analizi: TPAO Exploration Group Archive, unpublished technical report, no: 2305, 92 p.
- Atalık, E., 1992, Depositional systems of the Osmancık Formation in the Thrace basin: METU, The Graduate School of Natural and Applied Sciences, Ph. D. Thesis, 366 p.
- Batı, Z., Erk, S., and N. Akça, 1993, Trakya Havzası Tersiyer birimlerinin palinomorf, foraminifer ve nannoplankton biyostratigrafisi: TPAO

Research Center Archive, unpublished technical report, no: 1947,
92 p.

Batı, Z., Alişan, C., Ediger, V.Ş., Teymur, S., Akça, N., Sancay, H., Ertuğ,
K., Kirici, S., Erenler, M., and Ö. Aköz, 2002, Kuzey Trakya
Havzası'nın Palinomorf, Foraminifer ve Nannoplankton
Biyostratigrafisi: Turkish Stratigraphic Committee Meeting
(Lithostratigraphic Nomenclature of Thrace Basin) Abstracts, 14 p.

Bertram , G., 1998, Seismic stratigraphy, in D. Emery and K.J. Myers ed.,
Sequence Stratigraphy, Blackwell Science, 297 p.

Boer, N.P. de, 1954, Report on a geological reconnaissance in Turkish
Thrace: September, December G.A. 25373.

Bouma, A.H., 1962, Sedimentology of some flysch deposits: Amsterdam,
Elsevier, 168 p.

Brown, L.F., Jr., and W.L. Fisher, 1977, Seismic stratigraphic interpretation
of depositional systems: examples from Brazilian rift and pull apart
basins, in, Payton, C.E., ed., Seismic Stratigraphy-Applications to
Hydrocarbon Exploration: American Association of Petroleum
Geologists Memoir 26, p. 213-248.

Brown, L.F., Jr., and W.L. Fisher, 1980, Seismic stratigraphic interpretation and petroleum exploration. American Association of Petroleum Geologists continuing education course note series. no: 16.

Bruhn, C.H.L. and R. Walker, 1995, High resolution stratigraphy and sedimentary evolution of coarse-grained canyon-filling turbidites from the Upper Cretaceous transgressive megasequence, Campos Basin, Offshore Brasil: *Journal of Sedimentary Research*, v. 65, no: 4, p. 426-442.

Cant, D.J., 1984, Subsurface facies analysis. In: *Facies Models* (ed. by R.G. Walker). Geoscience, Canada, 454 p.

Caron, V., Nelson, C.S. and P.J.J. Kamp, 2004, Transgressive surface of erosion as sequence boundary markers in cool water shelf carbonates: *Sedimentary Geology*, v. 164, p. 179-189.

Clift, P., 1996, Plume tectonics as a cause of mass wasting on the southeast Greenland continental margin: *Marine and Petroleum Geology*, v. 13, p. 771-780.

- Cloetingh, S.P., 1992, Lithospheric dynamics, the tectonics of sedimentary basins, reprinted from Proceedings of Koninklijke Nederlandse Akademie van Wetenschappen, Amsterdam, 95 (3), p. 349-369.
- Coleman, J.M. and D.B. Prior, 1982, Deltaic environments of deposition. In: Sandstone depositional environments (ed. by P.A. Scholle and D. Spearing): American Association of Petroleum Geologists Memoir 31, Tulsa, 410 p.
- Coşkun, B., 2000, Influence of the Istranca-Rodop massifs and strands of the North Anatolian fault on oil potential of Thrace basin, NW Turkey: Journal of Petroleum Science and Engineering, Elsevier, v. 27, p. 1-25.
- Çağlayan, A., M., Şengün, M. and A. Yurtsever, 1988, Main fault systems shaping the Istranca Massif, Turkey. Middle East Technical University, Journal of Pure and Applied Sciences, Series A "Geosciences", Tokay Volume, v. 21, p. 145-154.
- Çubukçu, A. and T. Erten, 1987, Petrography and sedimentology of the Thrace Basin: TPAO Exploration Group Archive, unpublished technical report, no: 2338, section-III, 37 p.

Dominguez, L. and H. Mullins, 1988, Cat Island Platform: An indiciptently drowned Holocene carbonate shelf: *Sedimentology*, v. 35, p. 805-819.

Doust, H., and Y. Arıkan, 1974, The geology of the Thrace Basin: Turkish Second Petroleum Congress Proceedings, p. 119-136.

Duval, C.B., Cramez, C., and P. Vail, 1998, Stratigraphic cycles and major marine source rocks, in *Mesozoic and Cenezoic Sequence Stratigraphy of European Basins: SEPM Special Publication*, no: 60, p. 43-51.

Ediger, V.Ş., and Z. Batı, 1987, Hamitabat-25 kuyusunda kesilen Hamitabat Formasyonu'nun detay stratigrafik, sedimantolojik ve palinolojik incelemesi: TPAO Research Center Archieve, unpublished technical report , no: 1185, 125 p.

Ediger, V.Ş. and C. Alişan, 1989, Tertiary fungal and algal palynomorph biostratigraphy of the northern Thrace basin, Turkey. *Review of Palaeobotany and Palynology*, v. 58, p. 139-161.

Ediger, V., Batı, Z., Uygur, E., Erenler, M and H. İztan, 1998, Hamitabat Formasyonu'nun stratigrafisi, çökeltme modeli ve hidrokarbon

olanakları (Kuzey Trakya Havzası): TPAO Research Center Archive, unpublished technical report , no: 2312, 165 p.

Eren, A., 1987, The analysis of depositional model and reservoir characteristics of the Koyunbaba Formation: TPAO Exploration Group Archive, no: 2246, 51 p.

Erenler, M., 1987, The foraminiferal biostratigraphy of the northern Thrace Basin: TPAO Exploration Group Archive, unpublished technical report, no: 2338, section-VI, 20 p.

Galloway, W.E., 1989, Genetic stratigraphic sequences in basin analysis, I. Architecture and genesis of flooding-surface bounded depositional units: American Association of Petroleum Geologists Bulletin, v. 73, p. 125-142.

Galloway, W.E., 1998, Siliciclastic slope and base of slope depositional systems: component facies, stratigraphic architecture, and classification: American Association of Petroleum Geologists Bulletin, v. 82, no: 4, p. 569-595.

Galloway, W.E. and D.K. Hobday, 1983, Terrigenous clastic depositional systems: applications to petroleum, coal, and uranium exploration: Springer-Verlag, New York, 413 p.

Gerhard, J.E. and C. Alişan, 1987, Palynostratigraphy, paleoecology, and visual organic geochemistry of the Turgutbey-2, Değirmencik-3 and Pancarköy-1 wells, Thrace Basin, Turkey: TPAO Research Center Archive, unpublished technical report, no: 983, 33 p.

Gervais, A., Savoye, B., Piper, D.J.W., Mulder, T., Cremer, M. and I. Pichevin, 2004, Present morphology and depositional architecture of a sandy confined submarine system: the Golo turbidite system: in Confined turbidite systems, Lomas, S.A. and Joseph, P. (ed) Geological Society, Special Publications 222, p. 59-89.

Gökçen, L.S., 1967, Keşan bölgesinde Eosen-Oligosen sedimantasyonu, Güneybatı Türkiye Trakyası: MTA Bulletin, v. 69, p. 1-10.

Görür, N. and A.I.Okay, 1996, A for-arc origin for the Thrace Basin: Geol Rundsch, v. 85, p. 662-668.

Haq, B.U., Hardenbol, J. and P.R. Vail, 1987, Chronology of fluctuating sea levels since the Triassic: Science, v. 235, p. 1156-1167.

Handford, R., and R.G. Loucks, 1993, Carbonate depositional sequences and systems tracts responses of carbonate platforms to relative sea-level change, in Loucks, R, G. and Sarg, Rick, eds., Carbonate sequence stratigraphy: recent advances and applications: American Association of Petroleum Geologists Memoir 57, p. 3-41.

Hardenbol, J., Thierry, J., Farley, M., Jacquin, T., Graciansky, P.C. and P. Vail, 1998, Mesozoic and Cenozoic sequence stratigraphic framework of European basins: SEPM Special Publication No: 60, p. 3-13.

Holmes, A.W., 1961, A stratigraphic review of Thrace: TPAO Exploration Group Archive, unpublished technical report, no: 368.

Kasar, S., 1987, Edirne-Kırklareli-Saray (Kuzey Trakya) Bölgesi'nin jeolojisi, Türkiye 7. Petrol Kongresi, s. 281-291.

Kasar, S. and A. Okay, 1992, Silivri-Kıyıköy-İstanbul Boğazı arasındaki alanın jeolojisi: TPAO Exploration Group Archive, unpublished technical report, no. 2208, 45 p.

Kendall, C.G.St.C., and W. Schlager, 1981, Carbonates and relative changes in sea-level: Marine Geology, v. 44, p. 181-212.

Kerans, C. and S.W. Tinker, 1997, Sequence stratigraphy and characterization of carbonate reservoirs: SEPM Short course notes no: 40, p. 307.

Keskin, C., 1974, Ergene Havzası kuzeyinin stratigrafisi: Türkiye 2. Petrol Kongresi Teb., s. 137-163.

Krausert, R., and Z. Malal, 1957, Measured cross-section of the Koyunbaba Member: TPAO Exploration Group Archive, unpublished technical report, no: 1433, 1 p.

Lebküchner, R.F., 1974, Orta Trakya Oligosen'inin jeolojisi hakkında. Maden Tetkik ve Arama Enstitüsü Dergisi, v. 83, p. 1-29.

Lomas, S and P. Joseph, 2004, Confined turbidite systems: Geological Society, Special Publication: 222, 328 p.

Millington, J.J., and J.D. Clark, 1995, The Charo/Arro canyon mouth sheet system, south central Pyrenees, Spain: a structurally influenced zone of sediment dispersal: Journal of Sedimentary Research, v. B65, p. 443-454.

Mitchum Jr., R. M., Vail, P.R. and S. Thompson, 1977, Seismic Stratigraphy and Global Changes of Sea Level: Part 11. Glossary of terms used in seismic stratigraphy: Section 2. Application of seismic reflection configuration to stratigraphic interpretation: American Association of Petroleum Geologists Memoir 26, p. 205-212.

Mitchum, R.M. and J.C. Van Wagoner, 1991, High frequency sequences and their stacking patterns: sequence stratigraphic evidence of high frequency eustatic cycles: *Sedimentary Geology*, v. 70, p. 131-160.

Mitchum, R.M., Sangree, J.B., Vail., P., and W.W. Wornardt, 1993, Recognizing sequences and systems tracts from well-logs, seismic data, and biostratigraphy: examples from the Late Cenozoic of the Gulf of Mexico, in Weimer, P. and Posamentier, H.W., ed., *Siliciclastic sequence stratigraphy: recent developments and applications*: American Association of Petroleum Geologists Bulletin Memoir 58, p. 163-197.

Mutti, E. and W.R. Normark, 1987, Comparing examples of modern and ancient turbidite systems: problems and concepts, in J.R. Leggett and G.G. Zuffa, eds., *Marine clastic sedimentology: concept and case studies*: London, Graham and Trotman, p. 1-38.

Mutti, E. and W.R. Normark, 1991, An integrated approach to the study of turbidite systems, in P. Weimer and M.H. Link, eds., Seismic facies and sedimentary processes of submarine fans and turbidite systems: New York, Springer-Verlag, p. 75-106.

Mörner, N.A., 1981, The Northwest European sea-level laboratory and regional Holocene: eustasy: Paleogeography, Paleoclimatology, Paleoecology, v. 29, p. 281-300.

Neumann, A.C., and I.G. McIntyre, 1985, Reef response to sea-level catch-up, keep-up, or give-up: in International 5th Coral Reef Congress, Morea, French Polynesia, Proceedings: Antenne Museum-Ephe, v. 3, p. 105-110.

Normark, W.R., 1978, Fan valleys, channels and depositional lobes on modern submarine fans: characters for recognition of sandy turbidite environments: American Association of Petroleum Geologists Bulletin, v. 62, p. 912-931.

N.V. Turkse Shell , 1972, I no'lu Marmara petrol bölgesinde AR/NTS/832, 833, 835, 836, 997, 998 hak sıra no'lu arama ruhsatlarına ait terk raporu: TPAO Exploration Group Archieve, unpublished technical report, no: 769.

Okay, A.I. and İ. Tansel, 1992, Pontid-İçi okyanusunun üst yaşı hakkında Şarköy kuzeyinden (Trakya) yeni bir bulgu: MTA Bulletin, v. 114, p. 21-24.

Okay A., İ. Tansel and O. Tüysüz, 2001, Obduction, subduction and collision as reflected in the Upper Cretaceous-Lower Eocene sedimentary record of western Turkey: Geol. Mag. v. 138, p. 117-142.

Okay, A.I. and A. Yurtsever, 2006, (eds.) Istranca masifinin metamorfik kaya birimleri ile metamorfizma sonrası Kretase kaya birimleri: Lithostratigraphic Units Series-2: General Directorate of Mineral Research and Exploration Publications, Ankara, p. 1-41.

Önal, M., 1985, Gelibolu (Çanakkale) kuzeybatısının jeolojisi: TPAO Exploration Group Archive, unpublished technical report, no: 2036, 200 p.

Özaydın, S. and V. Erol, 1981, Trakya havzasının tektonik oluşum modeli: TPAO Exploration Group Archive, unpublished technical report, no: 1613, 12 p.

Pamir, H. N. ve Baykal, F., 1947, Istranca Masifinin Jeolojik Yapısı, T.J.K.B.
Cilt I, sayı 1.

Perinçek, D., 1991, Possible strand of the North Anatolian Fault in the
Thrace Basin, Turkey: an interpretation: American Association of
Petroleum Geologists Bulletin, v. 75, p. 241-257.

Pickering, K.T. and R.N. Hiscott, 1985, Contained (reflected) turbidity
currents from the Middle Ordovician Cloridorme Formation, Quebec,
Canada: an alternative to the antidune hypothesis: Sedimentology, v.
32, p. 373-394.

Pigott, J.D., 1995, A seismic classification scheme for clastic shelf wedges
(deltas). In: Oti, M.N. and Postma (ed.), Geology of Deltas: p. 439-
453. A.A. Balkema Publishers, Rotterdam, Netherlands.

Pirson, S.J., 1983, Geological Well-Log Analysis: Gulf Publishing Co.,
Houston, TX, 476 p.

Pittet, B., Strasser, A. and E. Mattioli, 2000, Depositional sequences in
deep-shelf environments: A response to sea-level changes and
shallow-platform carbonate productivity (Oxfordian, Germany and

Spain): Journal of Sedimentary Research, Section B: Stratigraphy and Global Studies v. 70, no: 2, p. 392-407.

Posamentier, H.W., and G.P. Allen, 1999, Siliciclastic sequence stratigraphy; concepts and applications: Concepts in Sedimentology and Paleontology, SEPM Concepts in Sedimentology and Paleontology, v. 7, 204 p.

Prather, B.E., Booth, J.R., Steffens, G.S., and P.A. Craig, 1998, Classification, lithologic calibration, and stratigraphic succession of seismic facies of intraslope basins, deep water Gulf of Mexico: American Association of Petroleum Geologists Bulletin, v. 82, p. 701-728.

Reading H.G. and M. Richards, 1994, Turbidite systems in deep water basin margins classified by grain size and feeder system: American Association of Petroleum Geologists Bulletin, v. 78, p. 792-822.

Rich, J.L., 1951, Three critical environments of deposition and criteria for recognition of rocks deposited in each of them: American Association of Petroleum Geologists Bulletin, v. 62, p. 1-20.

Rider, M., 1986, The geological interpretation of well-logs: Blackie, London, 192 p.

Sabadini, R., Doglioni, C., and D.A. Yuen, 1990, Eustatic sea level fluctuations induced by polar wander: Nature, v. 345, p. 708-710.

Saner, S., 1980, Batı Pontidlerin ve komşu havzaların oluşumlarının levha tektoniği kuramıyla açıklanması: Kuzeybatı Türkiye: MTA Bulletin, v. 93-94, p. 1-26.

Sfodrini, C., 1961, Surface geological report on AR/TGO//538 and 537 (Eceabat and Çanakkale areas): TPAO Exploration Group Archive, unpublished technical report, no: 1429.

Shanmugam, G., 2000, 50 years of the turbidite paradigm (1950s-1990s): deep-water processes and facies models-a critical perspective: Marine and Petroleum Geology., v. 17, p. 285-342.

Sheriff, R.E., 2002, Encyclopedic dictionary of applied geophysics. IV. Edition. SEG, 429 p.

Sirel, E. and H. Gündüz, 1976, Kırklareli (Kuzey Trakya) denizel Oligosen'inin stratigrafisi ve nummulites türleri. Türkiye Jeoloji Kurumu Bülteni, v. 19, p. 155-158.

Siyako, M., 2006, Tertiary lithostratigraphic units of the Thrace Basin. in Siyako, A., Okay, A., Yurtsever, A., (eds), Lithostratigraphic units of the Thrace region, Lithostratigraphic Units Series-2. General Directorate of Mineral Research and Exploration Publications. Ankara, p. 43-83.

Siyako, M. and O. Huvaz, 2007, Eocene stratigraphic evolution of the Thrace Basin, Turkey: Sedimentary Geology, v. 198, p. 75-91.

Soreghan, G.S. and W.R. Dickinson, 1994, Generic types of stratigraphic cycles controlled by eustasy: Geology, v. 22, p. 759-761.

Sümengen, M., and İ. Terlemez, 1991, Güneybatı Trakya yöresi Eosen çökellerinin stratigrafisi: MTA Bulletin, v. 113, p. 15-29.

Şengör, A.M.C. and Y. Yılmaz, 1981, Tethyan evolution of Turkey: A plate tectonic approach: Tectonophysics, v. 75, p. 181-241 .

Şengör, A.M.C., 1984, The Cimmeride orogenic system and the tectonics of Euraisa: Geol. Soc. America Spec. Paper, v. 82, p. 195.

Temel, R.Ö., and N.B. Çiftçi, 2002, Gelibolu Yarımadası, Gökçeada ve Bozcaada Tersiyer çökellerinin stratigrafisi ve ortamsal özellikleri: The Association of Turkish Petroleum Geologists Bulletin, v. 14, p. 17-40.

Toker, V. and E. Erkan, 1985, Nannoplankton biostratigraphy of Eocene Formations, Gelibolu Peninsula: MTA Bulletin, v. 101-102, p. 72-91.

Trincardi, F., Correggiari, A., Field, M.E. and W.R. Normark, 1995, Turbidite deposition from multiple sources: Quaternary Paola Basin (eastern Tyrrhenian Sea): Journal of Sedimentary Research, v. B65, p. 469-483.

Turgut S., Siyako M. and A. Dilki, 1983, Trakya havzasının jeolojisi ve hidrokarbon olanakları: Turkish Geological Congress Bulletin, v. 4, p. 35-46.

Turgut, S., Kasar, S., Siyako, M., Bürkan, K.A., İvak, M., Yılmaz, İ., and Z. Aksoy, 1987, The geological evaluation of the Thrace basin,

northwestern Turkey. TPAO Exploration Group Archive, unpublished technical report, no: 2338, section-I, 42 p.

Turgut, S., Türkaslan, M., and D. Perinçek, 1991, Evolution of the Thrace sedimentary basin and its hydrocarbon prospectivity: Spencer AM (ed) Generation, accumulation, and production of Europe's hydrocarbons: Special Publication of European Association of Petroleum Geoscientists, v. 1, p. 415-437.

Turgut, S. , 1997, Depositional sequences and hydrocarbon potential of the Tertiary sediments of eastern Thrace basin, based on sequence stratigraphic concepts: METU, The Graduate School of Natural and Applied Sciences, Ph. D. Thesis.

Turgut, S. and G. Eseller, 1999, Sequence stratigraphy, tectonics and depositional history in eastern Thrace Basin, NW Turkey: Marine and Petroleum Geology, v.17, p.61-100.

Umut, M. Z. Kurt, M. İmik, I. Özcan, H. Sarıkaya and G. Saraç, 1983, Tekirdağ İli-Silivri (istanbul ili) - Pınarhisar (Kırklareli ili) Alanının jeolojisi: MTA Rap. v. 7349 (yayımlanmamış teknik rapor), Ankara.

Ünal, O. T., 1967, Trakya jeolojisi ve petrol imkanları: TPAO Exploration Group Archive, unpublished technical report, no: 391, 80 p, Ankara.

Üşümezsoy, Ş., 1990, Istranca orojeni; Karadeniz çevresi Kimmerid orojen kuşakları ve masif sülfid yatakları: Türkiye Jeol. Bült., 33/1, p. 17-28.

Vail, P.R., Mitchum, R.M., Jr., and S. Thompson, 1977, Seismic stratigraphy and global changes of sea-level, Part 4, global cycles of relative changes of sea-level: in C.E. Payton, (ed.), Stratigraphic interpretation of seismic data: American Association of Petroleum Geologists Memoir 26, p. 83-98.

Vail, P.R., Mitchum R.M., and S. Thompson, 1984, Jurassic unconformities, chronostratigraphy and sea-level changes from seismic stratigraphy and biostratigraphy, in SCHLEE, J.S. ed., Interregional unconformities and hydrocarbon accumulation: American Association of Petroleum Geologists Memoir 36, p. 129-144.

Van Andel, T. H. and P.D. Komar, 1969, Ponged sediment of the Mid-Atlantic Ridge between 22 and 23 degrees north latitude: Geological Society of America Bulletin, v. 80, p. 1163-1190.

Van Wagoner, J.C., Posamentier, H.W., Mitchum, R.M., Vail, P.R., Sarg, J.F., Loutit, T.S., and J. Hardenbol, 1988, An overview of the fundamentals of sequence stratigraphy and key definitions: *in* Wilgus, C.K., Hastings, B.S., Kendall, C.G.St.C., Posamentier, H.W., Ross, C.A., and Van Wagoner, J.C. (eds.), *Sea-level changes: an integrated approach*: SEPM Special Publication no: 42, p. 39-45.

Van Wagoner, J.C., Mitchum, R.M., Campion, K.M. and V.D. Rahmanian, 1990, Siliciclastic sequence stratigraphy in well logs, core and outcrop: Concepts for high-resolution correlation of time and facies: American Association of Petroleum Geologists, *Methods in Exploration*; no: 7, 55 p.

Yaltırak, C., 1995, Gaziköy - Mürefte (Tekirdağ) arasının sedimanter ve tektonik özellikleri: The Association of Turkish Petroleum Geologists Bulletin, v. 6, p. 93-112.

Yılmaz, Y., and A. Polat, 1998, Geology and evolution of the Thrace volcanism, Turkey: *Acta Volcanologica*, v. 10, p. 293-303.

Yılmaz, Y., Tüysüz, O., Yiğitbaş, E., Can Genç, S. and A.M.C. Şengör, 1997, Geology and tectonic evolution of the Pontides, in Robinson, A. G., ed., *Regional and Petroleum Geology of the Black Sea and*

Surrounding Region: American Association of Petroleum Geologists
Memoir 68, p. 183-226.

Zink, C. and R. Norris, 2004, Submarine fans within small basins: examples
from the Tertiary of New Zealand, in *Confined turbidite systems*,
Lomas, S.A. and Joseph, P. (ed), Geological Society, Special
Publications 222, p. 59-89.

CURRICULUM VITAE

PERSONAL INFORMATION

Surname, Name: Sünnetçioğlu, Mehmet Akif
Nationality: Turkish
Date and Place of Birth: 26 September 1974, Karabük
Marital Status: Single
Phone: +90 312 2072302
Fax: +90 312 2869049
email: msunnetci@tpao.gov.tr

EDUCATION

Degree	Institution	Year of Graduation
MS	Colorado School of Mines Department of Geophysics	2001
BS	İTU Faculty of Mines Department of Geophysical Engineering	1995
High School	Karabük Demir Çelik High School, Ankara	1991

WORK EXPERIENCE

Year	Place	Department
2001- Present	TPAO, Exploration Group	Thrace Basin Project
2006 Spring 2000 Summer	Chevron Energy Tech Co. Baker Hughes, Houston	Reservoir Properties Formation Evolution
1998-1999	Ministry of Public Works and Settlement	Geohazards

PAPERS

Sünnetçioğlu, M.A., A.Eroğlu and K.A. Gülek, 2005, Seismic Expression of the Strike-slip Thrace Fault System, Northwest of The Thrace Basin, Turkey: International Earthsciences Colloquium on the Aegean Regions, Izmir, Turkey.

Sunnetcioglu, M. and O. Sipahioglu, 2002, Supply and Network Integration in European Natural Gas Market. 14th International Natural Gas and Petroleum Congress and Exhibition, Ankara, Turkey.

MASTER OF SCIENCE THESIS

Sunnetcioglu, M., 2001, Borehole Image Log Interpretation, Barrel Springs Field, Carbon County, Wyoming. Master Thesis, Golden, Colorado.